ARRAY ANTENNA SYNTHESIS INCLUDING ELEMENT AND FEED COUPLING

by

Koichiro Takamizawa

Thesis submitted to the Faculty of the

Virginia Polytechnic Institute and State University

in partial fulfillment of the requirements for the degree of

Master of Science

in

Electrical Engineering

APPROVED:

W. L. Stutzman, Chairman

G. S. Brown

R. C. Robertson

August 1988

Blacksburg, Virginia

ARRAY ANTENNA SYNTHESIS INCLUDING ELEMENT AND FEED COUPLING

by

Koichiro Takamizawa

W. L. Stutzman, Chairman

Electrical Engineering

(ABSTRACT)

Precise radiation pattern control for an array antenna requires precise control of array element excitations. One application is that of low side lobe patterns. Classical synthesis methods for the desired pattern may not be realized in practice due to coupling effects. Coupling occurs in two forms: the mutual coupling between array elements and the coupling introduced by the feed networks. Ideally one could account for such coupling within the array architecture during the design process and alter the feed network parameters to adjust for such coupling. Unfortunately, this is a nonlinear problem requiring special solution techniques.

This report presents the solution techniques for determining feed network parameter values that compensate for antenna-feed network coupling. Scattering parameter representations of the antenna array and the feed networks are used. Examples of various array configurations for microstrip antenna arrays and for dipole arrays are included.

Acknowledgements

I would like to express my deep appreciation to Dr. Warren Stutzman for the constant advice in the preparation of this thesis and and in the entire course of graduate study. Thanks are also due to the members of my committee, Dr. Brown and Dr. Robertson, for their helpful suggestions.

Special thanks go to Joan for her understanding and encouragement during high and low times of this project.

Finally, I would like to thank my parents for their support in achieving my goal.

Table of Contents

I. Introduction

An array antenna is an assembly of radiating elements in one of many possible geometrical configurations with the outputs of the individual elements in the array combined to produce radiation of desired pattern shape and gain. The advantages of array antennas over a single antenna include the following: 1) high gain and high resolution without increasing the physical size of each element, 2) electronic control of radiation patterns, such as scanning of main beam and shaping of radiation pattern, and 3) graceful degradation.

Many techniques have been developed in the synthesis of array patterns. Most of the techniques, however, ignore mutual coupling between array elements. Mutual coupling is the electromagnetic interaction between array elements. In addition, unless the antenna elements are perfectly matched in impedance to the connected transmission lines and/or perfect isolation power dividers are used, there will be coupling through the feed network. The two fold coupling problem (element-to-element and feed network coupling) then becomes difficult for analysis and very difficult for synthesis. This is because coupling from one element to another can travel through the feed network and

reappear in other elements leading to further antenna coupling; this is an endless coupling effect.

The coupling effects are minimum in the synthesis of simple patterns such as sum and difference patterns since these patterns are not very sensitive to the element current variations. However, in cases of more complex patterns such as low side lobe patterns and shaped beams, mutual coupling can cause significant degradation of the radiation pattern from the desired pattern.

This report presents new methods to compensate for mutual coupling effects of both element and feed coupling. The techniques may be classified as synthesis methods since they lead to realization of specific current distributions across the array in the presence of practical coupling effects. The synthesis techniques described in this report use the scattering parameter representation of array antennas and were initially formulated by Smith and Stutzman [S-1]. Element currents can be calculated in the presence of mutual coupling (array analysis); also a network that compensates for mutual coupling effects cam be determined (array synthesis). A system of nonlinear equations was derived by Smith and solved numerically for a compensation network. Two approaches were used to compensate for mutual coupling: 1) the conventional feed network is unaltered and amplitude and phase shift devices are placed between it and the array at each port, 2) the parameters of the feed network are altered slightly in the design process to anticipate compensation for coupling.

This report marks the finish of a four-year project supported by the U.S. Army Research Office through the University of Massachusetts. Companion experiments were conducted at the Physical Science Laboratory of New Mexico State University by Russell P. Jedlicka and his colleagues. The problem attacked was very challenging, requiring analysis, numerical computations, and experimental verification. Some aspects of the experimental results are presented here as they relate to comparison with theory.

However, this report focuses on analytical and numerical methods of array synthesis. The first major document was Smith and Stutzman [S-1]. Our initial focus was on microstrip antenna arrays as a testbed (hence, the project title), but the formulation is completely general and both numerical computations and measurements involved both microstrip and wire antennas.

Chapter 2 reviews the network representations of array antennas and the general synthesis technique using network representations. Also in Chapter 2 the system of nonlinear equations derived by Smith will be reviewed. Chapter 3 reviews current literature and experiments on mutual coupling compensation. In Chapter 4 three types of compensation networks will be presented. Chapters 5, 6 and 7 modify the nonlinear equations for each type of compensation network so that the equations can be solved numerically. In Chapter 8 the compensation technique is applied to an eight-element microstrip array. Chapter 9 presents some numerical examples using a moment method computer program for wire antennas. Chapter 10 gives conclusions and recommendations for future study.

Reader note: This report and its predecessor [S-1] are lengthy and detailed. Chapter 10 of this report was written to aid the reader in extracting the contributions and technical results. For a comprehensive summary of the findings from the study refer to Chapter 10.

II. Overview of Array Modeling and Synthesis

2.1 Scattering Matrix Representation of Array Antennas

An array antenna in its most general form consists of N-elements connected to an N-way feed network and a generator as shown on Fig. 2.1-1. There are several ways to represent these multiport networks such as in terms of impedance, admittance and hybrid parameters. The mutual coupling in a network, however, is most easily represented by scattering parameters, or S-parameters. Unlike other parameters which are defined in terms of voltages and currents, S-parameters are defined in terms of incident waves $\{a_i\}$ and reflected waves $\{b_i\}$ as shown on Fig. 2.1-2. S-parameters are normalized reflection and transmission coefficients under the condition that all other ports are match loaded and undriven [G-1]:

$$S_{ij} = \frac{b_i}{a_j}\Big|_{a_k=0,\ k\neq j} \tag{2.1-1}$$

A network can be represented with S-parameters in matrix form as follows:

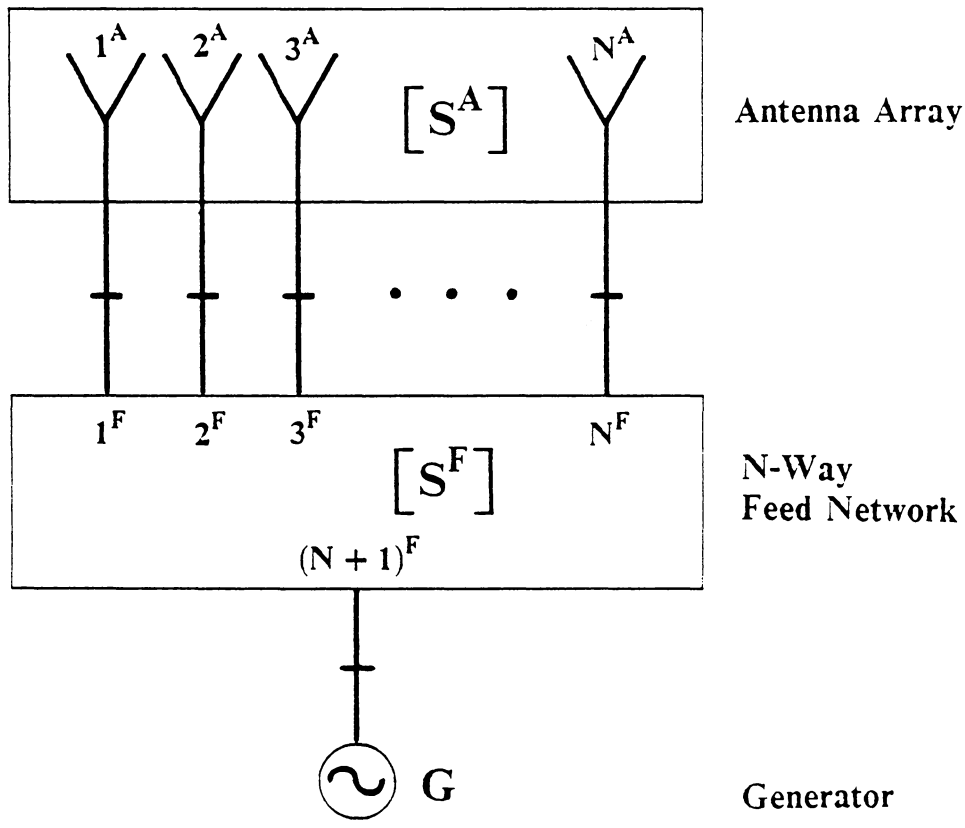

Figure 2.1-1. Network representation of an N-element array antenna.

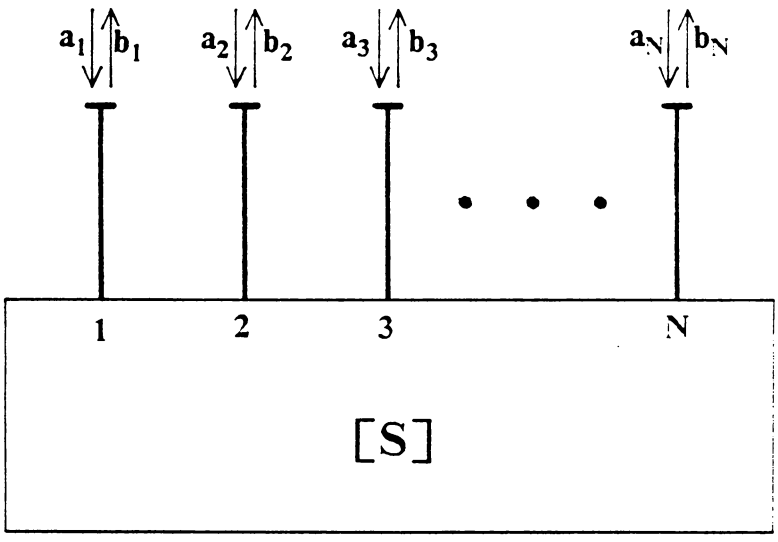

Figure 2.1-2. General N-port network as described by [b] = [S][a].

$$[b] = [S][a] \tag{2.1-2}$$

where [a] and [b] are vectors of incident waves and reflected waves at each port, and [S] is the S-matrix of the network. These wave variables are related to voltages and currents by

$$V_i = \sqrt{Z_{0i}}\,(a_i + b_i) \tag{2.1-3}$$

$$I_i = \frac{1}{\sqrt{Z_{0i}}}\,(a_i - b_i) \tag{2.1-4}$$

where Z_{0i} is the characteristic impedance of the port i. From (2.1-3) and (2.1-4) the average power flowing into port i is

$$\begin{aligned} P_i &= \frac{1}{2}\,\mathrm{Re}\{V_i I_i^*\} \\ &= \frac{1}{2}\left(a_i a_i^* - b_i b_i^*\right) \end{aligned} \tag{2.1-5}$$

It is often convenient to use normalized voltages and currents, where the voltage is normalized by dividing by the square root of the reference impedance Z_0 and the current is normalized by multiplying by the square root of the reference impedance. When normalized with $Z_0 = Z_{0i}$, (2.1-3) and (2.1-4) become

$$V_i = a_i + b_i \tag{2.1-6}$$

$$I_i = a_i - b_i \tag{2.1-7}$$

The power expression (2.1-5), however, remains the same. On the other hand, when the characteristic impedance of the port i and reference impedance are different ($Z_0 \neq Z_{0i}$) a step change in the characteristic impedance at port i must be assumed before the

voltages and currents can be normalized by Z_0. Throughout this report the normalized definition of currents and voltages are assumed.

When two or more networks represented by S-matrices are interconnected, a single S-matrix that describes the overall network can be formulated. In general, q ports of an M-port network A and an N-port network B may be connected as shown on Fig. 2.1-3. The combined network is described by the matrix equation

$$\begin{bmatrix} [b^A] \\ [b^B] \end{bmatrix} = \begin{bmatrix} [S^A] & [0] \\ [0] & [S^B] \end{bmatrix} \begin{bmatrix} [a^A] \\ [a^B] \end{bmatrix} \tag{2.1-8}$$

The order of the scattering matrix in the above equation can be reduced using the procedure discussed by Smith [S-1, Sec.3.1.2]. The resulting scattering matrix for the overall network is

$$[S^{A/B}] = [S_{PP} + S_{PC}(\Gamma - S_{CC})^{-1} S_{CP}] \tag{2.1-9}$$

where the matrix $[S^{A/B}]$ is a square matrix of the order $N + M - 2q$. The superscript A/B represents S-parameters for the combined network that consists of the network A and the network B. The S-parameters on the right hand side of (2.1-9) are submatrices of original S-matrix in (2.1-8) grouped in external (unconnected) and internal (interconnected) ports. These matrices are defined by Gupta [G-1] as

$$\begin{bmatrix} [b_P] \\ [b_C] \end{bmatrix} = \begin{bmatrix} [S_{PP}][S_{PC}] \\ [S_{CP}][S_{CC}] \end{bmatrix} \begin{bmatrix} [a_P] \\ [a_C] \end{bmatrix} \tag{2.1-10}$$

where $[a_P]$ and $[b_P]$ are the wave variables of the external ports, and $[a_C]$ and $[b_C]$ are wave variables of the internal ports. $[S_{PP}]$ and $[S_{CC}]$ are the S-parameters of external and internal ports, respectively, and $[S_{PC}]$ and $[S_{CP}]$ are the S-parameters from the external

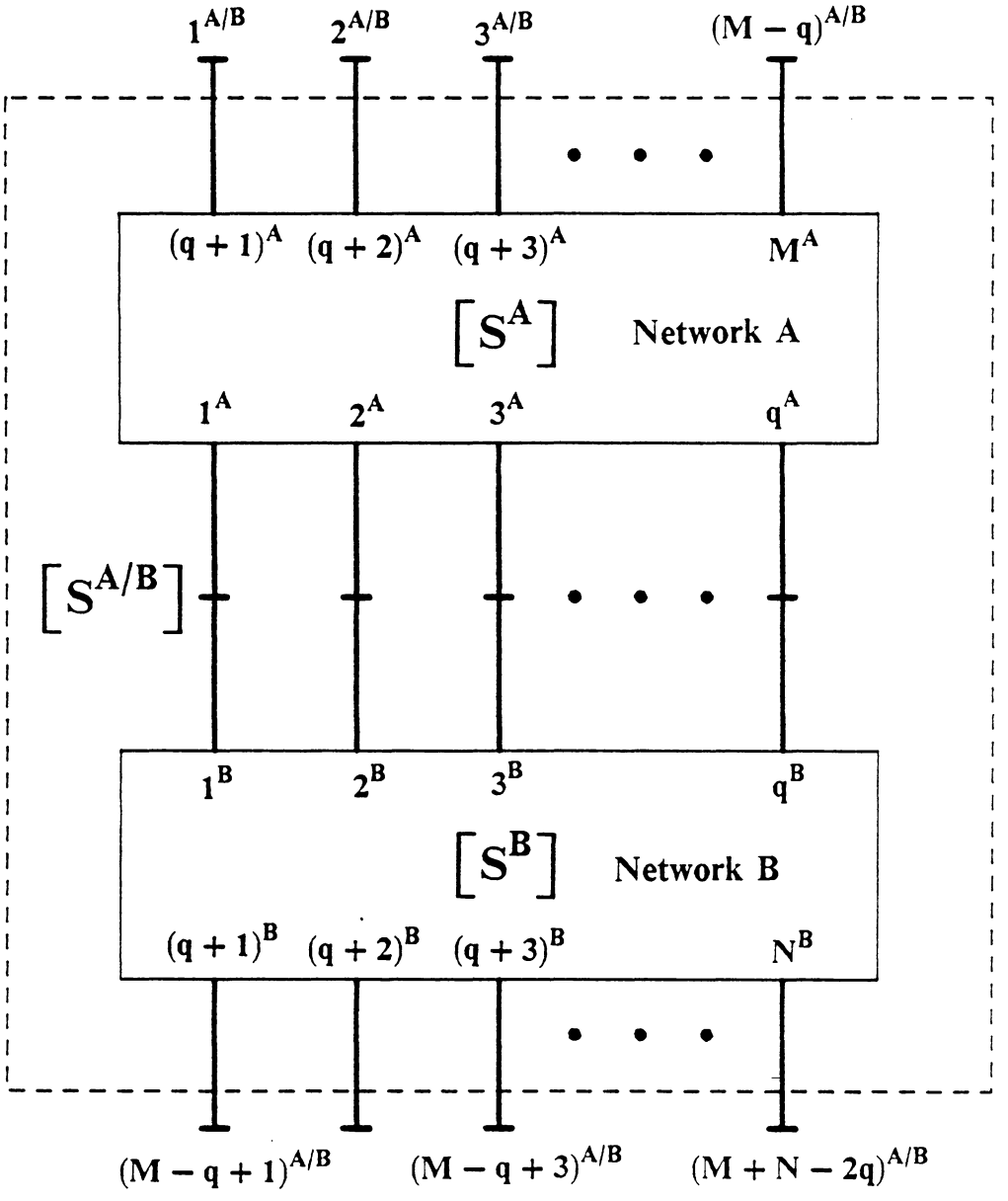

Figure 2.1-3. Arbitrary connection of M-port network A and N-port network B.

ports to the internal ports and vice versa. The matrix $[S_{PP}]$ is a square matrix of order $M + N - 2q$, and $[S_{CC}]$ is a square matrix of order 2q. The connection matrix $[\Gamma]$ is defined as $\Gamma_{ij} = 1$ if port i is connected to port j and $\Gamma_{ij} = 0$ otherwise. For example, the submatrices for the networks A and B in Fig. 2.1-3 can be written as

$$[S_{PP}] = \begin{bmatrix} S^A_{q+1,q+1} & S^A_{q+1,q+2} & \cdots & S^A_{q+1,M} & 0 & 0 & \cdots & 0 \\ \cdot & \cdot & \cdot & \cdot & \cdot & \cdot & \cdot & \cdot \\ S^A_{M,q+1} & S^A_{M,q+2} & \cdots & S^A_{M,M} & 0 & 0 & \cdots & 0 \\ 0 & 0 & \cdots & 0 & S^B_{q+1,q+1} & S^B_{q+1,q+2} & \cdots & S^B_{q+1,N} \\ \cdot & \cdot & \cdot & \cdot & \cdot & \cdot & \cdot & \cdot \\ 0 & 0 & \cdots & 0 & S^B_{N,q+1} & S^B_{N,q+2} & \cdots & S^B_{N,N} \end{bmatrix} \tag{2.1-11}$$

$$[S_{CC}] = \begin{bmatrix} S^A_{1,1} & S^A_{1,2} & \cdots & S^A_{1,q} & 0 & 0 & \cdots & 0 \\ \cdot & \cdot & \cdot & \cdot & \cdot & \cdot & \cdot & \cdot \\ S^A_{q,1} & S^A_{q,2} & \cdots & S^A_{q,q} & 0 & 0 & \cdots & 0 \\ 0 & 0 & \cdots & 0 & S^B_{1,1} & S^B_{1,2} & \cdots & S^B_{1,q} \\ \cdot & \cdot & \cdot & \cdot & \cdot & \cdot & \cdot & \cdot \\ 0 & 0 & \cdots & 0 & S^B_{q,1} & S^B_{q,2} & \cdots & S^B_{q,q} \end{bmatrix} \tag{2.1-12}$$

$$[S_{PC}] = \begin{bmatrix} S^A_{q+1,1} & S^A_{q+1,2} & \cdots & S^A_{q+1,q} & 0 & 0 & \cdots & 0 \\ \cdot & \cdot & \cdot & \cdot & \cdot & \cdot & \cdot & \cdot \\ S^A_{M,1} & S^A_{M,2} & \cdots & S^A_{M,q} & 0 & 0 & \cdots & 0 \\ 0 & 0 & \cdots & 0 & S^B_{q+1,1} & S^B_{q+1,2} & \cdots & S^B_{q+1,q} \\ \cdot & \cdot & \cdot & \cdot & \cdot & \cdot & \cdot & \cdot \\ 0 & 0 & \cdots & 0 & S^B_{N,1} & S^B_{N,2} & \cdots & S^B_{N,q} \end{bmatrix} \tag{2.1-13}$$

$$[S_{CP}] = \begin{bmatrix} S^A_{1,q+1} & S^A_{1,q+2} & \cdots & S^A_{1,M} & 0 & 0 & \cdots & 0 \\ \cdot & \cdot & \cdot & \cdot & \cdot & \cdot & \cdot & \cdot \\ S^A_{q,q+1} & S^A_{q,q+2} & \cdots & S^A_{q,M} & 0 & 0 & \cdots & 0 \\ 0 & 0 & \cdots & 0 & S^B_{1,q+1} & S^B_{1,q+2} & \cdots & S^B_{1,N} \\ \cdot & \cdot & \cdot & \cdot & \cdot & \cdot & \cdot & \cdot \\ 0 & 0 & \cdots & 0 & S^B_{q,q+1} & S^B_{q,q+2} & \cdots & S^B_{q,N} \end{bmatrix} \tag{2.1-14}$$

and the connection matrix is

$$[\Gamma] = \begin{bmatrix} 0 & 0 & \cdots & 0 & 1 & 0 & \cdots & 0 \\ 0 & 0 & \cdots & 0 & 0 & 1 & \cdots & 0 \\ \cdot & \cdot & \cdot & \cdot & \cdot & \cdot & \cdot & \cdot \\ 0 & 0 & \cdots & 0 & 0 & 0 & \cdots & 1 \\ 1 & 0 & \cdots & 0 & 0 & 0 & \cdots & 0 \\ 0 & 1 & \cdots & 0 & 0 & 0 & \cdots & 0 \\ \cdot & \cdot & \cdot & \cdot & \cdot & \cdot & \cdot & 0 \\ 0 & 0 & \cdots & 1 & 0 & 0 & \cdots & 0 \end{bmatrix} \tag{2.1-15}$$

where row/column i for i= 1...q in Γ represent ports 1 through q of the network A and row/column i for i=q+1...2q represent ports 1 through q of the network B. For example, $\Gamma_{1,q+1} = 1$ since port 1 of network A and port 1 of network B are connected as shown in Fig. 2.1-3.

When an external port is excited by a generator, (2.1-8) and (2.1-9) can be extended to allow calculation of wave variables impressed by the generator at the remaining port. Figure 2.1-4 shows a generator connected to port i of an N-port network. In general, a generator is expressed in S-parameters as

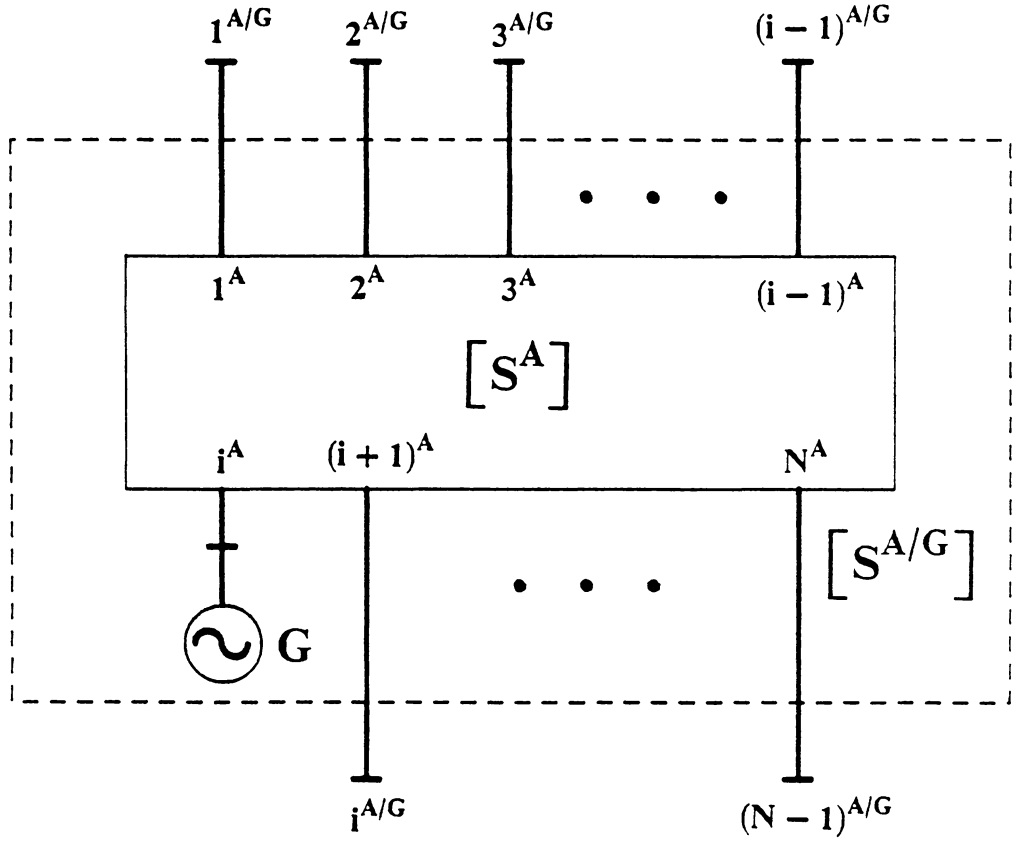

Figure 2.1-4. An N-port excited by a generator at port i.

$$b^G = S^G a^G + c^G \tag{2.1-16}$$

where S^G is reflection coefficient of the generator and c^G is the wave excited by the generator. The wave variable a^G is the incident wave into the generator from a network connected to the generator. Equation (2.1-16) is a statement of the fact that the signal that comes out of the generator, b^G, is a superposition of waves produced by the generator and waves reflected from the generator. Ideally, the reflection coefficient of a generator is small ($S^G = 0$). In this case the reflected wave from the generator is equal to the wave induced by the generator ($b^G = c^G$). The multiport combined with the generator (as in Fig. 2.1-4) can be expressed as

$$\left[\begin{array}{c} b_1^A \\ b_2^A \\ \cdot \\ \cdot \\ b_N^A \\ \hline b_i^A \\ b^G \end{array}\right] = \left[\begin{array}{cccc:cc} S_{1,1}^A & S_{1,2}^A & \cdots & S_{1,N}^A & S_{1,i}^A & 0 \\ S_{2,1}^A & S_{2,2}^A & \cdots & S_{2,N}^A & S_{2,i}^A & 0 \\ \cdot & \cdot & \cdot & \cdot & \cdot & \cdot \\ \cdot & \cdot & \cdot & \cdot & \cdot & \cdot \\ S_{N,1}^A & S_{N,2}^A & \cdots & S_{N,N}^A & S_{N,i}^A & 0 \\ \hline S_{i,1}^A & S_{i,2}^A & \cdots & S_{i,N}^A & S_{i,i}^A & 0 \\ 0 & 0 & \cdots & 0 & 0 & S^G \end{array}\right] \left[\begin{array}{c} a_1^A \\ a_2^A \\ \cdot \\ \cdot \\ a_N^A \\ \hline a_i^A \\ a^G \end{array}\right] + \left[\begin{array}{c} 0 \\ 0 \\ \cdot \\ \cdot \\ 0 \\ \hline 0 \\ c^G \end{array}\right] \tag{2.1-17}$$

If subscript P is used to denote external ports and subscript C to denote internal ports, (2.1-17) is of the form

$$\left[\begin{array}{c} [b_P] \\ [b_C] \end{array}\right] = \left[\begin{array}{cc} [S_{PP}] & [S_{PC}] \\ [S_{CP}] & [S_{CC}] \end{array}\right] \left[\begin{array}{c} [a_P] \\ [a_C] \end{array}\right] + \left[\begin{array}{c} [0] \\ [c_C] \end{array}\right] \tag{2.1-18}$$

The above equation can be reduced to two types of equations, one that relates the external ports and one that relates the internal ports. The relationship at the external

ports (for example, ports 1 through i-1 and i+1 through N in Fig. 2.1-4) can be described by

$$[b^{A/G}] = [S^{A/G}][a^{A/G}] + [c^{A/G}] \tag{2.1-19}$$

where $[S^{A/G}]$ is combined S-parameters for the network and the generator which is a square matrix of the order $N-1$ obtained using (2.1-9). The wave variables $[a^{A/G}]$ and $[b^{A/G}]$ are equivalent to $[a_P]$ and $[b_P]$ in (2.1-18), respectively. The waves induced by the generator at external ports of the combined networks are obtained from [G-1]

$$[c^{A/G}] = [S_{PC}][\Gamma - S_{CC}]^{-1}[c_C] \tag{2.1-20}$$

where Γ defines the connection between the generator and the feed network. The second relationship derived from (2.1-19) describes the incident waves and the reflected waves at the internal ports of the combined network (for example, port i and generator port of the network in Fig. 2.1-4) [G-1]:

$$[a_C] = [\Gamma - S_{CC}]^{-1}[c_C] \tag{2.1-21}$$

and

$$[b_C] = [\Gamma][a_C] \tag{2.1-22}$$

Suppose the network of Fig. 2.1-4 has 4 ports and port 3 is excited ($N=4$, $i=3$). The waves induced by the generator at external ports of the combined network (ports 1, 2, and 4) are obtained using (2.1-20) as follows:

$$
\begin{aligned}
[c^{A/G}] &= [S_{PC}][\Gamma - S_{CC}]^{-1}[c_C] \\
&= \begin{bmatrix} S^A_{1,3} & 0 \\ S^A_{2,3} & 0 \\ S^A_{4,5} & 0 \end{bmatrix} \begin{bmatrix} -S^A_{3,3} & -1 \\ -1 & -S^G \end{bmatrix}^{-1} \begin{bmatrix} 0 \\ c^G \end{bmatrix} \\
&= \frac{1}{S^A_{3,3}S^G - 1} \begin{bmatrix} -S^A_{1,3}c^G \\ -S^A_{2,3}c^G \\ -S^A_{4,3}c^G \end{bmatrix}
\end{aligned}
\tag{2.1-23}
$$

The incident waves at the internal ports of the combined network (ports 3 and 5) are obtained using (2.1-21)

$$
\begin{aligned}
[a_C] &= \begin{bmatrix} a^A_3 \\ a^G \end{bmatrix} \\
&= [\Gamma - S_{CC}]^{-1}[c_C] \\
&= \begin{bmatrix} -S^A_{3,3} & -1 \\ -1 & -S^G \end{bmatrix}^{-1} \begin{bmatrix} 0 \\ c^G \end{bmatrix} \\
&= \frac{1}{S^A_{3,3}S^G - 1} \begin{bmatrix} -c^G \\ -S^A_{3,3}c^G \end{bmatrix}
\end{aligned}
\tag{2.1-24}
$$

The reflected waves at the connected ports are obtained from the incident waves using (2.1-22)

$$
\begin{aligned}
[b_C] &= \begin{bmatrix} b^A_3 \\ b^G \end{bmatrix} \\
&= [\Gamma][a_C]
\end{aligned}
$$

$$= \begin{bmatrix} 0 & 1 \\ 1 & 0 \end{bmatrix} \begin{bmatrix} -c^G \\ -S^A_{3,3}c^G \end{bmatrix}$$
$$= \begin{bmatrix} -S^A_{3,3}c^G \\ -c^G \end{bmatrix} \qquad (2.1\text{-}25)$$

The above techniques can be used to analyze array antennas. In particular, the currents at each antenna element in the presence of mutual coupling can be calculated in five simple steps.

1. Find the S-parameters of the antenna array, S^A, the feed network, S^F, and the generator, S^G. This may be done by measurements, by using a mathematical model for the networks, or by using a CAD procedure such as MCAP (see Section 3.2).

2. Calculate the combined S-matrix for the feed network and a generator, $S^{F/G}$, using (2.1-9) and the waves induced by the generator at the output ports of the feed network, $c^{F/G}$, using (2.1-20).

3. Calculate S-parameters for the array/feed/generator network, $S^{A/F/G}$ using (2.1-9).

4. Calculate incident and reflected waves at antenna ports for the array/feed/generator network using (2.1-21) and (2.1-22).

5. Calculate the element currents with (2.1-7).

2.2 The Mutual Coupling Problem

Mutual coupling is the electromagnetic interaction between two antenna elements. Mutual coupling can significantly alter the performance of an array antenna. For instance, it can change the active impedance of the antenna elements (the input impedance of the elements when the array is fully excited), alter the element excitation currents, and lead to deterioration of the active element patterns. All of these changes lead to degradation of the radiation pattern from that obtained with no mutual coupling. The major effects on the radiation pattern are changes in sidelobe level, and shifting and filling of nulls. In addition, changes in gain and beamwidth of the main lobe, and other undesirable effects can occur due to mutual coupling. In general, these effects on the radiation pattern increase as the magnitude of coupling increases.

A comprehensive summary of mutual coupling studies is given by Smith [S-1]. In this section the mechanism of mutual coupling in an array antenna and the effect of mutual coupling on radiation pattern will be discussed. In particular, we will consider mutual coupling on microstrip array antennas. The basic theory, however, is applicable to any array antenna configuration.

2.2.1 The mechanism of mutual coupling in microstrip arrays

There are two types of mutual coupling that exist in an antenna array: the mutual coupling among antenna elements and the coupling through the feed network. Figure 2.2-1 shows the coupling mechanisms in a four element array antenna. The dominant mutual coupling among the antenna elements occurs through space waves. This type of coupling is strongly dependent upon the geometry of the array. The interelement

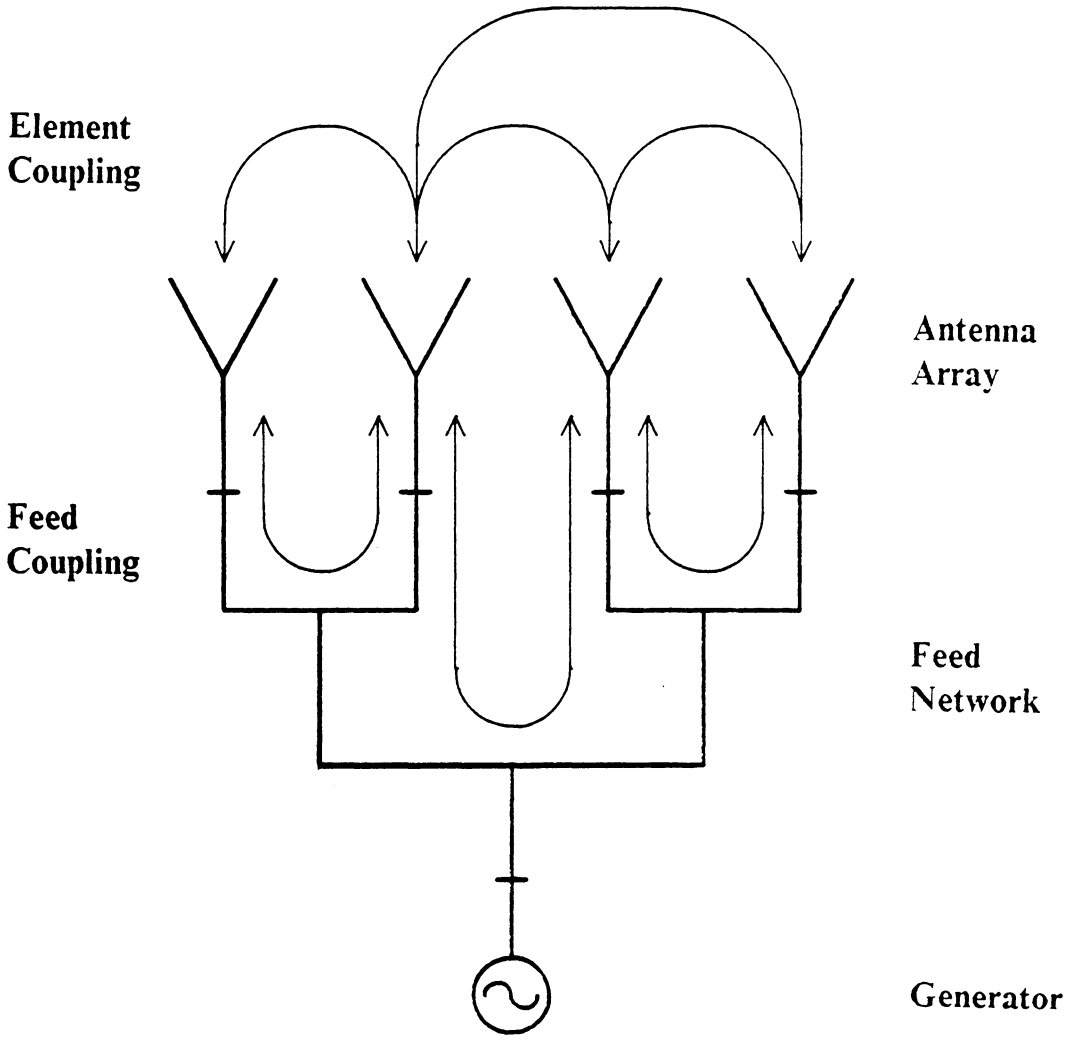

Figure 2.2-1 The mutual coupling in an N element array antenna.

spacing is the most important parameter in space wave coupling. The mutual coupling in an eight element microstrip array consisting of 0.312λ spaced quarter-wave patches which is used in one of the experiments performed for this project (described in Chapter 8) is shown in Fig. 2.2-2. The magnitude and phase of the scattering coefficients S_{1j} between element 1 and j are plotted versus element number j. Both magnitude and phase of the mutual coupling show strong correlation to the spacing between antenna elements. This result agrees with the mutual coupling studies conducted by Jedlicka and Carver [J-1,J-2]. In addition to the element spacing, the shape of antenna elements and their orientation are important in the space coupling [A-7,J-1].

Secondary mutual coupling in a microstrip array occurs through surface waves on the array substrate [J-1]. In this coupling the substrate acts as a dielectric waveguide permitting signals to propagate between antenna elements. The structure of the array board such as the thickness of substrate, the permittivity of dielectric material and the length of array are important variables in surface coupling. However, Jedlicka and Carver [J-1,J-2] have shown that a change in substrate thickness has little effect in mutual coupling. It implies that the degree of surface coupling is very small compared to space coupling. Surface wave coupling also occurs in a microstrip feed network as a secondary mutual coupling effect.

The third mutual coupling component among antenna elements is return loss represented by S_{ii}. This is reflection coefficient of an element when all other elements are match loaded. The return loss does not alter the element currents when there is no element to element coupling or when each element is driven by an independent generator. The most significant effect in these cases are loss of power efficiency. However, when mutual coupling exist among elements and in the feed network the return loss significantly changes element current distribution.

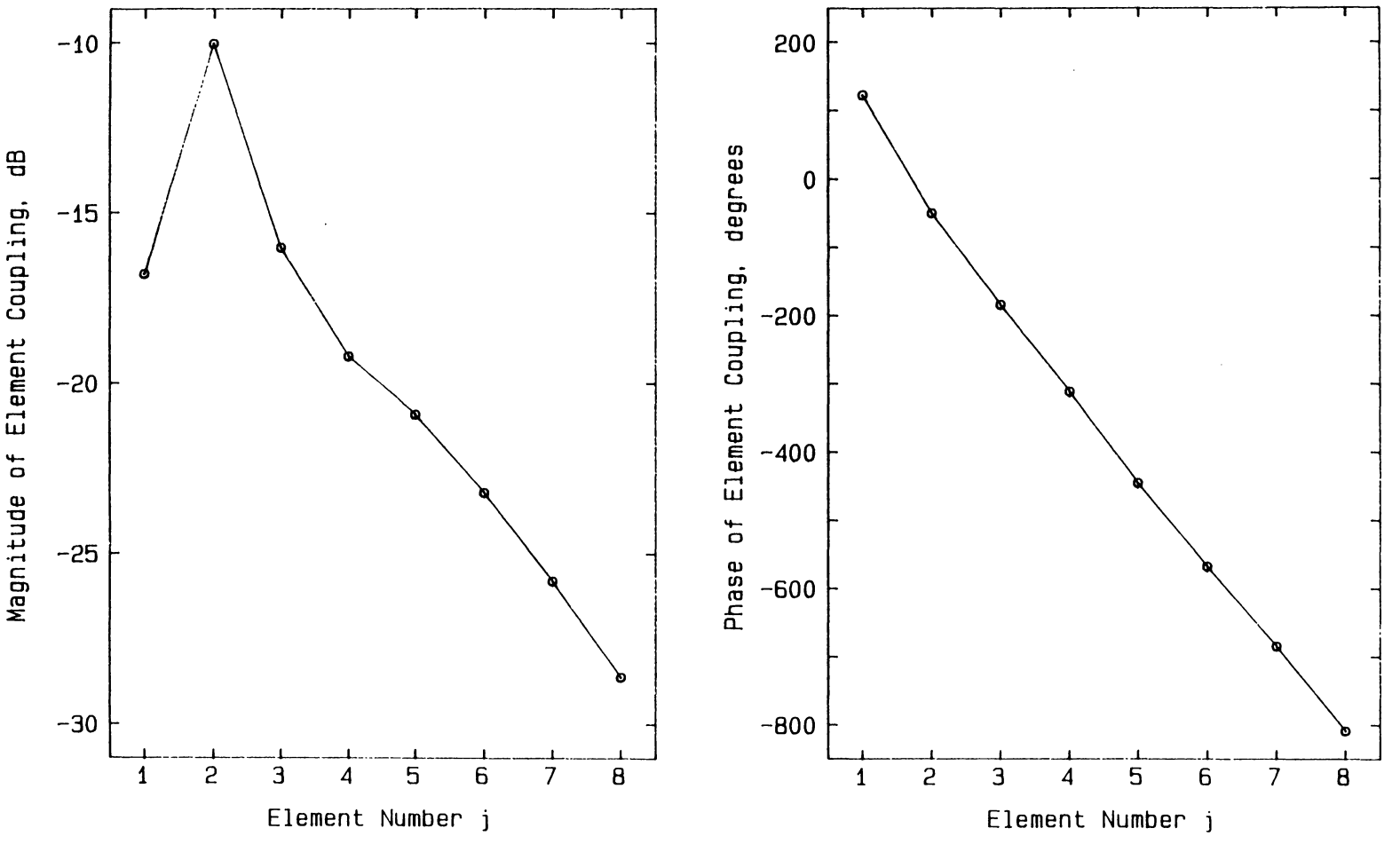

Figure 2.2-2. Measured magnitude and phase of mutual coupling as a function of element number for $0.312\lambda_0$ spaced quarter wave microstrip patches described in Section 8.1.

The primary coupling effect in the feed network occurs from the cross talk between two ports due to nonideal power dividers used in the network. In general, the cross talk in a power divider cannot be completely eliminated without use of active devices. It is also well known that passive multiport networks other than two port networks cannot be matched on all ports. This implies that any feed network for array antennas, even for a simple two element array, cannot have output ports matched to the antenna elements.

When mutual coupling in the antenna and the coupling in the feed network are combined very complex feedback loops are created. The overall effect of mutual coupling on the element excitation currents is nonlinear. This will be illustrated later in Section 5.4.

2.2.2 The effect of mutual coupling on the radiation pattern

The degradation of a radiation pattern due to mutual coupling in an array antenna includes increased side lobes and shifting and filling of nulls. These effects are especially severe when precise control of excitation currents is necessary as in the case of a low side lobe pattern. The effects on the radiation pattern will be illustrated here using numerical simulations.

Consider an eight element array with 0.312 wavelength interelement spacing. We will assume the measured mutual coupling in Fig. 2.2-2. An average element pattern of $\cos^{0.5}(0.9\theta)$ is assumed. Two types of excitations are considered: a sum pattern and a 35 dB Dolph-Chebyshev pattern.

The synthesis of the sum pattern requires equal magnitude and equal phase excitation on all antenna elements:

$$
\begin{aligned}
I_1 &= 1.0\underline{/0°} & I_5 &= 1.0\underline{/0°} \\
I_2 &= 1.0\underline{/0°} & I_6 &= 1.0\underline{/0°} \\
I_3 &= 1.0\underline{/0°} & I_7 &= 1.0\underline{/0°} \\
I_4 &= 1.0\underline{/0°} & I_8 &= 1.0\underline{/0°}
\end{aligned}
\qquad (2.2\text{-}1)
$$

This is the simplest form of array excitation. An 8-way corporate feed network consists of seven 3 dB power dividers as shown in Fig. 2.2-3 is assumed. The S-parameters of power divider feed networks are derived in Section 6.2. The element currents in the presence of mutual coupling are calculated using the Fortran program MCAP described in Section 4.2. Using MCAP the currents are obtained as

$$
\begin{aligned}
I_1 &= 1.14519\underline{/22.6°} & I_5 &= 0.90666\underline{/1.9°} \\
I_2 &= 0.62643\underline{/11.5°} & I_6 &= 1.14473\underline{/29.9°} \\
I_3 &= 0.96579\underline{/28.0°} & I_7 &= 0.84026\underline{/26.6°} \\
I_4 &= 0.82951\underline{/7.8°} & I_8 &= 1.16862\underline{/11.1°}
\end{aligned}
\qquad (2.2\text{-}2)
$$

The plot of normalized radiation patterns for the case with mutual coupling and for the case without mutual coupling are shown in Fig. 2.2-4. The figure shows that the major effect on the radiation pattern is filling of nulls. However, other effects such as change in side lobe levels are very small.

The 35 dB Dolph-Chebyshev array requires the following current distribution [S-2]:

$$
\begin{aligned}
I_1 &= 0.19154\underline{/0.0°} & I_5 &= 1.00000\underline{/0.0°} \\
I_2 &= 0.46362\underline{/0.0°} & I_6 &= 0.78425\underline{/0.0°} \\
I_3 &= 0.78425\underline{/0.0°} & I_7 &= 0.46362\underline{/0.0°} \\
I_4 &= 1.00000\underline{/0.0°} & I_8 &= 0.19154\underline{/0.0°}
\end{aligned}
\qquad (2.2\text{-}3)
$$

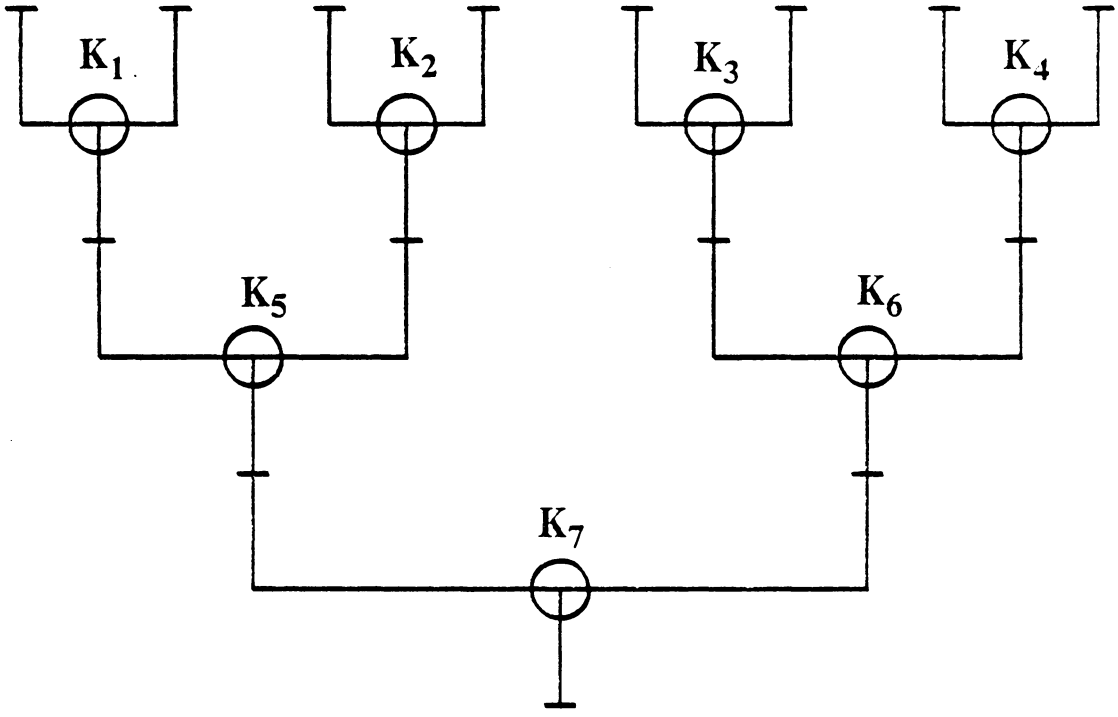

Figure 2.2-3. An 8-way corporate feed network consists of seven power dividers used in the calculation of the element currents.

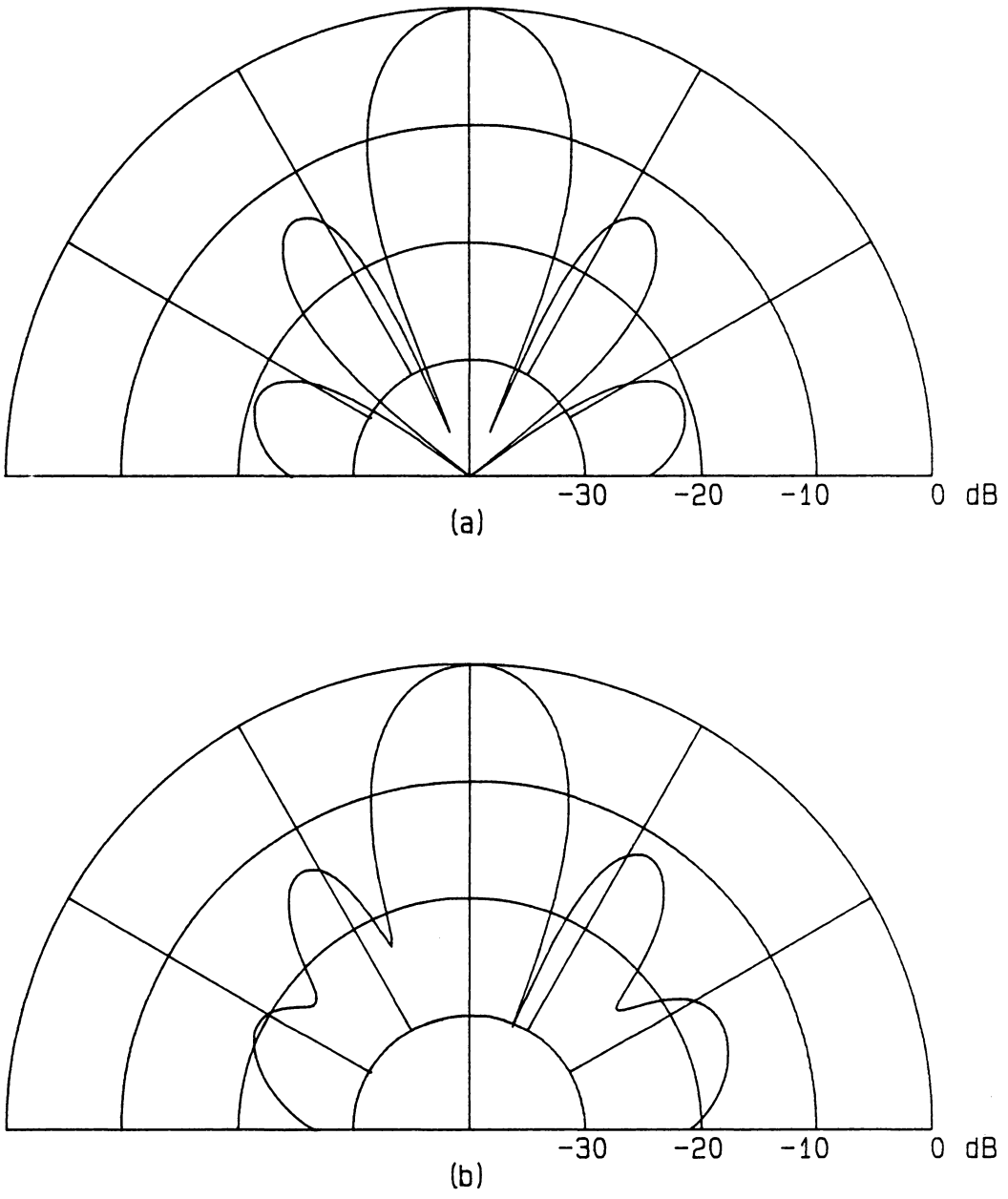

Figure 2.2-4. Normalized radiation patterns of sum array. a) without and b) with mutual coupling using currents from (2.2-1) and (2.2-2) and a $\cos^{0.5}(0.9\theta)$ element pattern.

The feed network consists of an 8-way corporate feed network consists of seven 2-way variable power dividers as shown in Fig. 2.2-3. The power split ratio K_i in the figure are set to yield desired currents when there is no coupling in the array. A detailed discussion on N-way power divider network is given in Section 6.2. The currents in the presence of mutual coupling obtained using MCAP are

$$\begin{aligned} I_1 &= 0.32639\angle -36.7^\circ & I_5 &= 0.63545\angle -75.3^\circ \\ I_2 &= 0.50824\angle -11.3^\circ & I_6 &= 0.99316\angle -71.4^\circ \\ I_3 &= 0.73737\angle -52.3^\circ & I_7 &= 0.27918\angle -113.9^\circ \\ I_4 &= 1.09558\angle -62.4^\circ & I_8 &= 0.11985\angle -71.7^\circ \end{aligned} \tag{2.2-4}$$

The calculated radiation pattern for both sets of currents (2.2-3) and (2.2-4) are shown in Fig. 2.2-5. The figure clearly shows that the side side lobes increase to approximatly -25dB for the array with mutual coupling. A change in the beamwidth is also apparent. Compared to the sum pattern this low side lobe pattern requires more precise control of excitation currents. It can be concluded from these results that an array that requires precise control of excitation currents is affected more by mutual coupling.

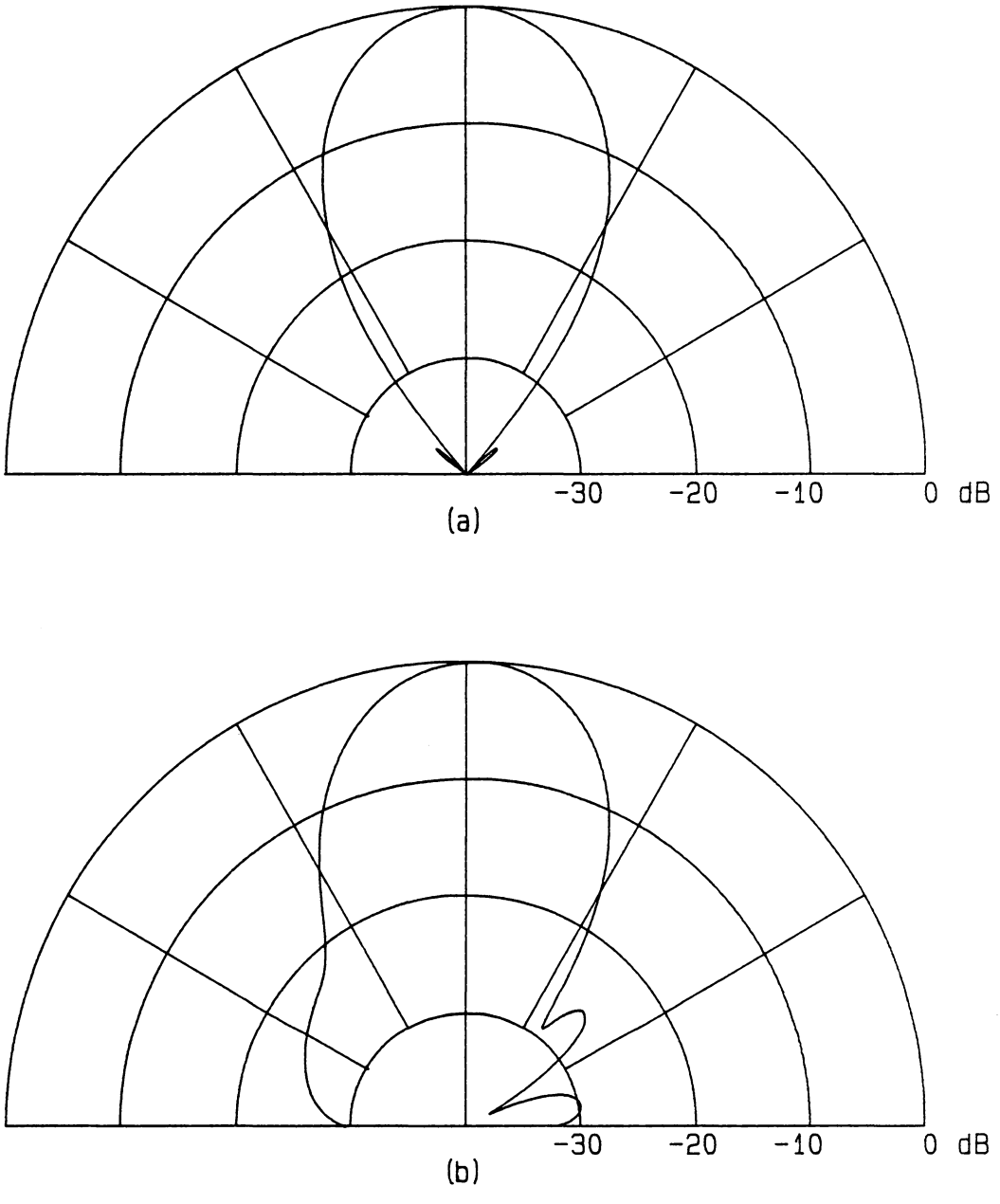

Figure 2.2-5. Normalized radiation patterns of 35dB Dolph-Chebyshev array with main beam steered to -10 degrees. a) without and b) with mutual coupling using currents from (2.2-3) and (2.2-4) and a $\cos^{0.5}(0.9\theta)$ element pattern.

2.3 Array Antenna Pattern Analysis Approaches Including Mutual Coupling

Most array analysis is based on the assumption that elements are connected to independent generators with either forced or free excitation [O-1]. However, array antennas are usually excited by a feed/generator network, in which case the above assumption is not applicable. We begin this section with a discussion of independent generator excitation methods, and follow it with a more general treatment that includes feed network effects.

2.3.1 Independent generator excitations

In the independent generator excitation case elements of the array are assumed to be identical and to be driven by independent generators. It is only necessary to consider the coupling among antenna elements.

Forced Excitation

In forced excitation, the antenna elements are fed by constant-voltage sources or constant-current sources. In practice it is difficult to create such sources to drive the elements, but they are convenient from a modeling standpoint. In the case of voltage sources, as shown in Fig. 2.3-1 the generator imposes constant voltages across the antenna elements. The element currents are then found from the voltage and the impedance matrices using

$$[i] = [Z]^{-1}[v] \tag{2.3-1}$$

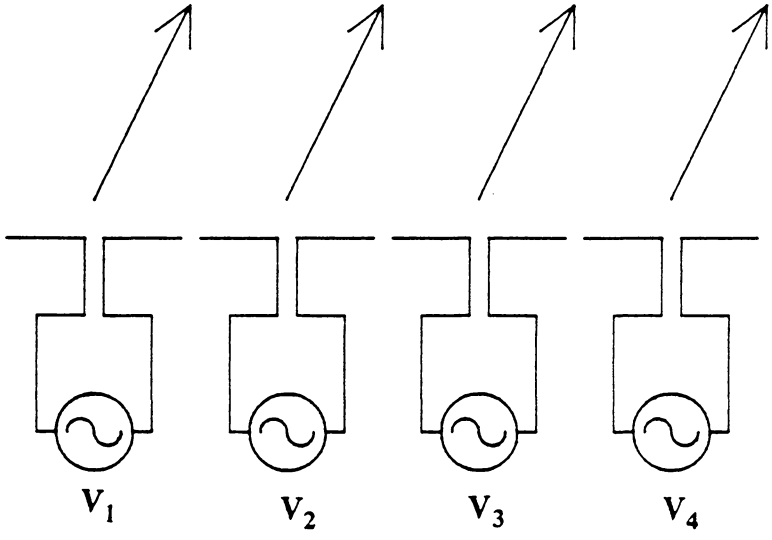

Figure 2.3-1. Array excited by constant-voltage sources (forced excitation).

where Z_{ii} represents self impedance of antenna element i and Z_{ij} for $i \neq j$ represents the mutual impedance between element i and element j. The radiation pattern for this array is given by [K-1,W-1]

$$F(\theta, \phi) = g_i(\theta, \phi) \sum_{n=1}^{N} i_n e^{j\xi_n} \tag{2.3-2}$$

where

$$\xi_n = x_n \sin\theta \cos\phi + y_n \sin\theta \sin\phi + z_n \cos\theta$$

for an array of identical elements with arbitrary locations (x_n, y_n, z_n). The coordinate system used here is defined in Fig. 2.3-2. The currents $\{i_n\}$ are obtained from (2.3-1) and may contain a linear phase that steers the beam to location (θ_0, ϕ_0). The isolated element pattern, $g_i(\theta, \phi)$, is obtained in the short circuited array environment where only one element is fed by a generator and all other elements are shorted. This is illustrated in Fig. 2.3-3.

Free Excitation

In the free excitation mode each antenna element is driven by constant incident power sources as shown in Fig. 2.3-4. This is a more realistic method of feeding array antennas than forced excitation method [O-1]. Because of the inclusion of the generator impedances, the change in input impedance of the elements alters both the voltage and current in each element. In this case the system can be described better with scattering parameters as

$$[b] = [S][a] \tag{2.3-3}$$

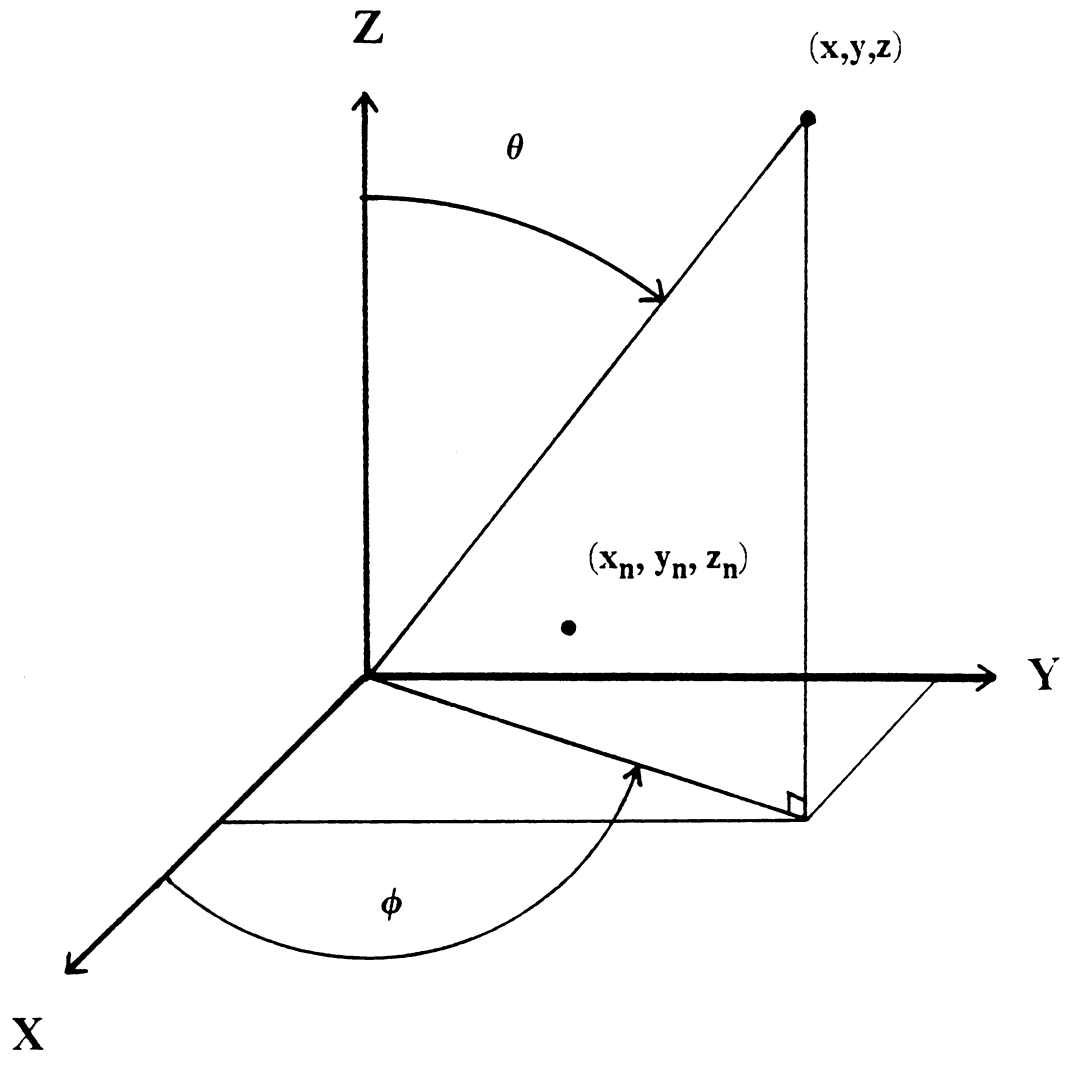

Figure 2.3-2. Geometry of an arbitrary array antenna

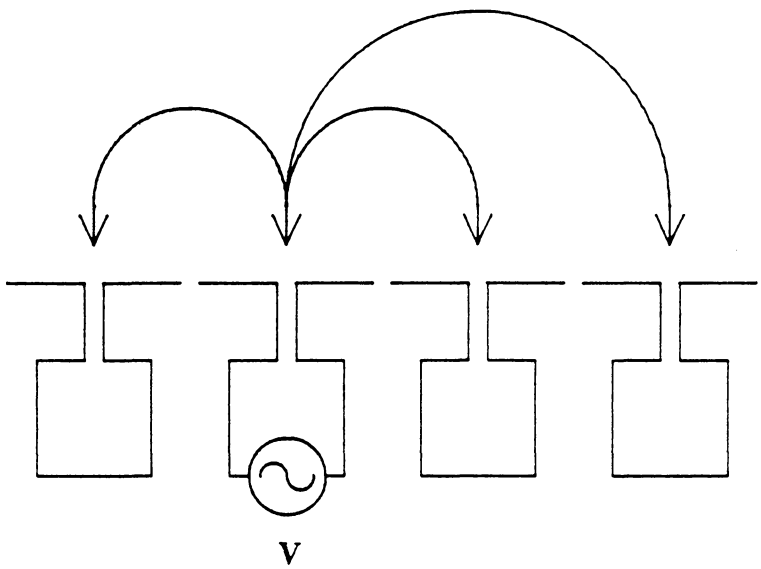

Figure 2.3-3. Array with all but one elements shorted (forced excitation).

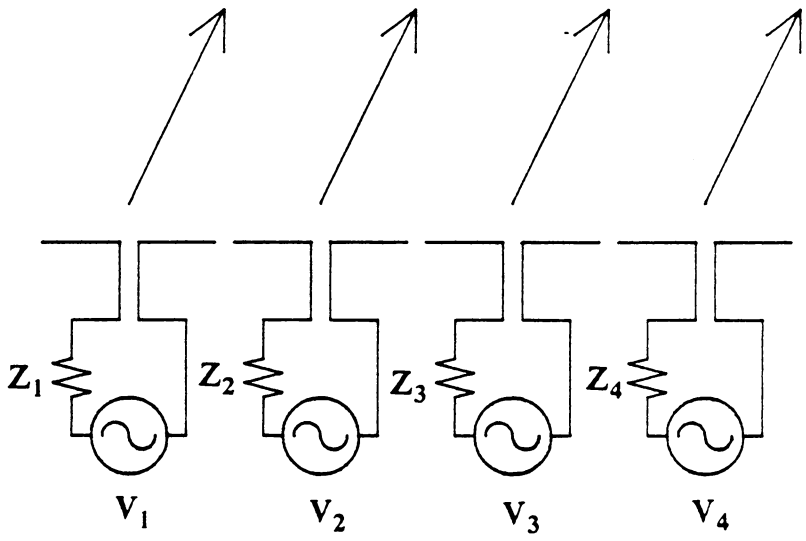

Figure 2.3-4. Array excited by constant incident power sources (free excitation).

where a's and b's represent incident and reflected waves for the array as discussed in Section 2.1. The elements of the scattering matrix [S] represent coupling coefficients between pairs of elements of the array with all others match loaded. The currents at each element can be calculated using (2.1-7) as

$$[i'] = [a] - [b] \tag{2.3-4}$$

The radiation pattern for free excitation is [A-1]

$$F(\theta, \phi) = g_i(\theta, \phi) \sum_{n=1}^{N} i'_n e^{j\xi_n} \tag{2.3-5}$$

where g_i is the isolated element pattern obtained as in the free excitation case. In (2.3-5) all mutual coupling effects are contained in the element currents $\{i'_n\}$.

Alternatively, the radiation pattern for the free excitation can be obtained from [A-1,W-1,J-3]

$$F(\theta, \phi) = \sum_{n=1}^{N} g_{a,n}(\theta, \phi) I'_n e^{j\xi_n} \tag{2.3-6}$$

where $g_{a,n}$ is the active element pattern for the n-th element which is obtained when only the n-th element is driven and all other elements are terminated with their generator impedance (see Fig. 2.3-5). I'_n is the current that would be flowing without coupling from other generators which is proportional to generator voltage V_n. In other words, the effect of mutual coupling is contained only in the active element pattern and not in the element currents [A-1,J-3]. The active element pattern of each element can be calculated from [P-3,P-4]

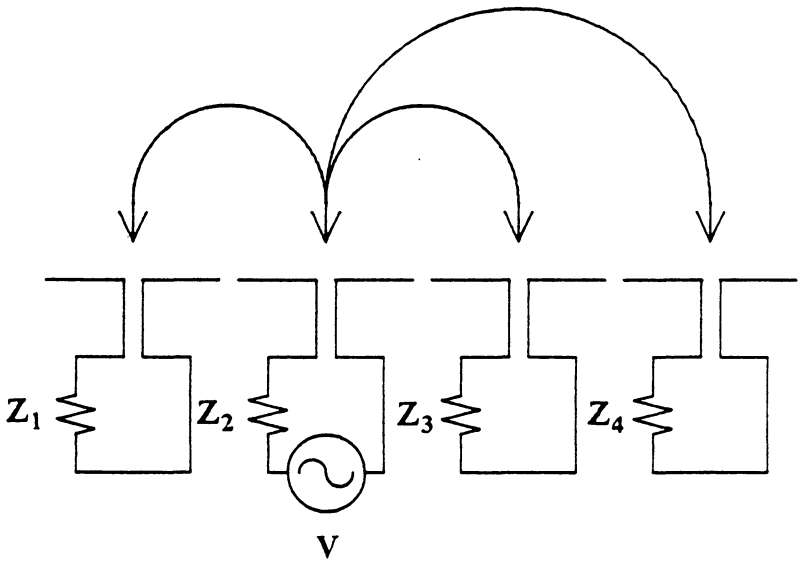

Figure 2.3-5. Array with all but one element match loaded. (free excitation).

$$g_{a,n}(\theta, \phi) = g_i(\theta, \phi) \sum_{m=1}^{N} i_m^{(n)} e^{j\xi_m} \tag{2.3-7}$$

where $i_m^{(n)}$ is the current in the m-th element induced by n-th generator when all other elements are match loaded.

The relationship in (2.3-6) is one of superposition and relies on linearity of the array environment, which is the usual case. The mutual coupling here arises only from scattering from the array elements. This is different from the fully excited array discussed next.

2.3.2 Full coupling array representation

Most arrays are fed by a feed/generator network which cannot be represented by independent generators. This general situation is shown in Fig. 2.3-6. The basic difference between the independently driven array and the feed network driven array is the existence of coupling through the feed network in the latter case as well as coupling between elements. To account for the element and feed coupling, the scattering parameter analysis discussed in Section 2.1 must be used. Specifically, the element and feed S-matrices must be combined using (2.1-9), and solved for the incident and reflected waves at the elements using (2.1-21) and (2.1-22), then solved for the element currents using (2.1-7). The radiation pattern can be obtained using (2.3-6) but with currents I_n:

$$F(\theta, \phi) = \sum_{n=1}^{N} g'_{a,n}(\theta, \phi) I_n e^{j\xi_n} \tag{2.3-8}$$

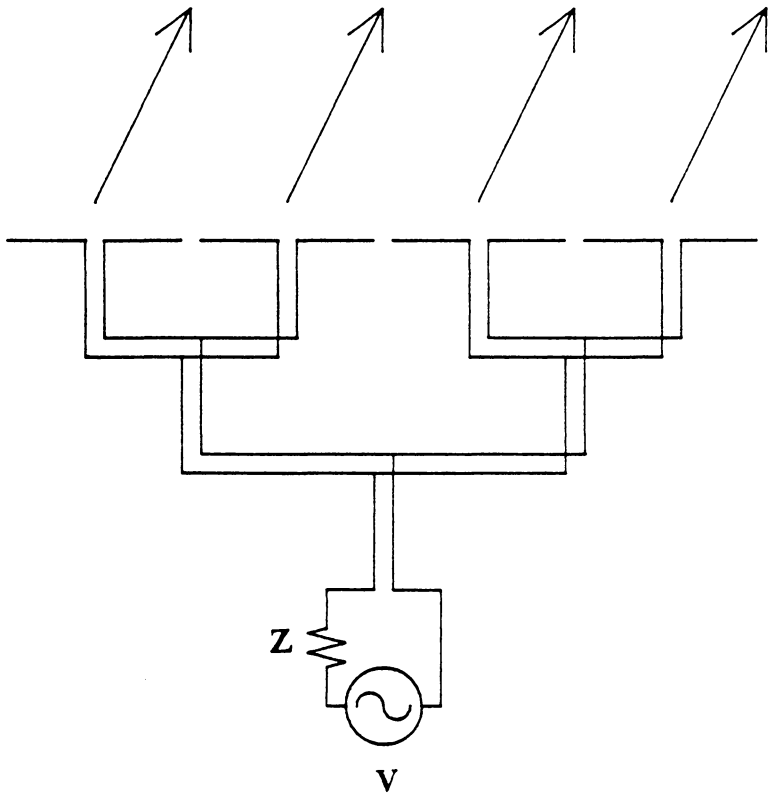

Figure 2.3-6. Full coupling array antenna.

Here $g'_{a,n}(\theta, \phi)$ is the pattern of each element in the array environment when the array is operating in a fully excited state. These element patterns cannot be measured directly, rendering (2.3-8) somewhat useless. It is, however, useful as a step in the process of accounting for all coupling effects in a fully excited array. The next section reveals this.

2.3.3 Approximate approaches to full coupling representation

The first level of approximation we introduce is to approximate the full array active element patterns in (2.3-8) by the active element pattern of (2.3-6) obtained by exciting elements one at a time. The current distribution on an element in the array is affected by neighboring elements. This includes element type, orientation, and position as well as the neighboring element current amplitude and phase. All these factors affect the current distribution. However, the current of an individual element is affected primarily by its own boundary conditions and secondarily by mutual coupling effects. Therefore, we assume that the element pattern is very well approximated by the case where it is excited and all other elements are match loaded (e.g. the active element pattern). Thus,

$$F(\theta, \phi) \simeq \sum_{n=1}^{N} g_{a,n}(\theta, \phi) I_n e^{j\xi_n} \tag{2.3-9}$$

The next level of approximation in array analysis is to factor the array pattern into a product of an array factor and an "element pattern" which we call the array element pattern $g_{ae}(\theta, \phi)$. The array element pattern is the pattern of a typical antenna element obtained by measuring its pattern with all other elements match loaded. The element

usually selected is a central element in the array. Then the array pattern of (2.3-9) is approximated using

$$F(\theta, \phi) \simeq g_{ae}(\theta, \phi) \sum_{n=1}^{N} I_n e^{j\xi_n} \tag{2.3-10}$$

where the summation is the classical array factor. The current I_n of (2.3-10) is obtained using the S-parameter array analysis technique discussed in Section 2.1. Employment of the principle of pattern multiplication requires that all elements be alike (in type and orientation), that coupling is not excessive (elements not extremely close together), and that array edge effects are not large.

Further study on derivation of (2.3-8) and approximations used to obtain (2.3-9) and (2.3-10) are necessary. In particular numerical experiments using computer programs such as ESP (described in Sec. 9.2) must be conducted to verify these equations.

2.4 The Synthesis Problem

As seen in Section 2.2, mutual coupling alters the radiation pattern of an array antenna. To compensate for mutual coupling a network can be placed between the elements and the feed network. The network is designed such that correct currents are obtained at the input to the antenna elements in the presence of mutual coupling. A more useful realization of a compensation effect is to not have a separate compensation network, but to include mutual coupling compensation into the design phase of the

conventional feed network which can be handled within the framework of the general approach introduced here.

In the most general form an array has N-elements, an M-way feed network connected to a generator, and an N+M port compensation network as shown on Fig. 2.4-1. This array can be fully described using S-parameters. The antenna elements and the compensation network are represented by matrices $[S^A]$ and $[S^C]$, respectively. The combined network of a feed network and a generator is described by a matrix $[S^{F/G}]$ and a vector $[c^{F/G}]$ obtained using (2.1-9) and (2.1-20), respectively.

In the synthesis of a compensation network, the matrix $[S^C]$ represents the unknowns, and the desired (design) element currents are denoted as $[I^A]$. The S-matrix of the elements, $[S^A]$, and the feed/generator network, $[S^{F/G}]$, are assumed to be known. The relationship between the incident and reflected waves of the compensation network is given by

$$\begin{bmatrix} b_1^C \\ b_2^C \\ \vdots \\ b_N^C \\ b_{N+1}^C \\ \vdots \\ b_{N+M}^C \end{bmatrix} = \begin{bmatrix} S_{1,1}^C & S_{1,2}^C & \cdots & S_{1,N}^C & \cdots & S_{1,N+M}^C \\ S_{2,1}^C & S_{2,2}^C & \cdots & S_{2,N}^C & \cdots & S_{2,N+M}^C \\ \vdots & \vdots & \vdots & \vdots & \vdots & \vdots \\ S_{N,1}^C & S_{N,2}^C & \cdots & S_{N,N}^C & \cdots & S_{N,N+M}^C \\ S_{N+1,1}^C & S_{N+1,2}^C & \cdots & S_{N+1,N}^C & \cdots & S_{N+1,N+M}^C \\ \vdots & \vdots & \vdots & \vdots & \vdots & \vdots \\ S_{N+M,1}^C & S_{N+M,2}^C & \cdots & S_{N+M,N}^C & \cdots & S_{N+M,N+M}^C \end{bmatrix} \begin{bmatrix} a_1^C \\ a_2^C \\ \vdots \\ a_N^C \\ a_{N+1}^C \\ \vdots \\ a_{N+M}^C \end{bmatrix} \quad (2.4\text{-}1)$$

where the notation used here is consistent with that in Fig. 2.4-1. In addition, it is clear from the figure that

$$b_i^C = a_i^A \quad (2.4\text{-}2)$$

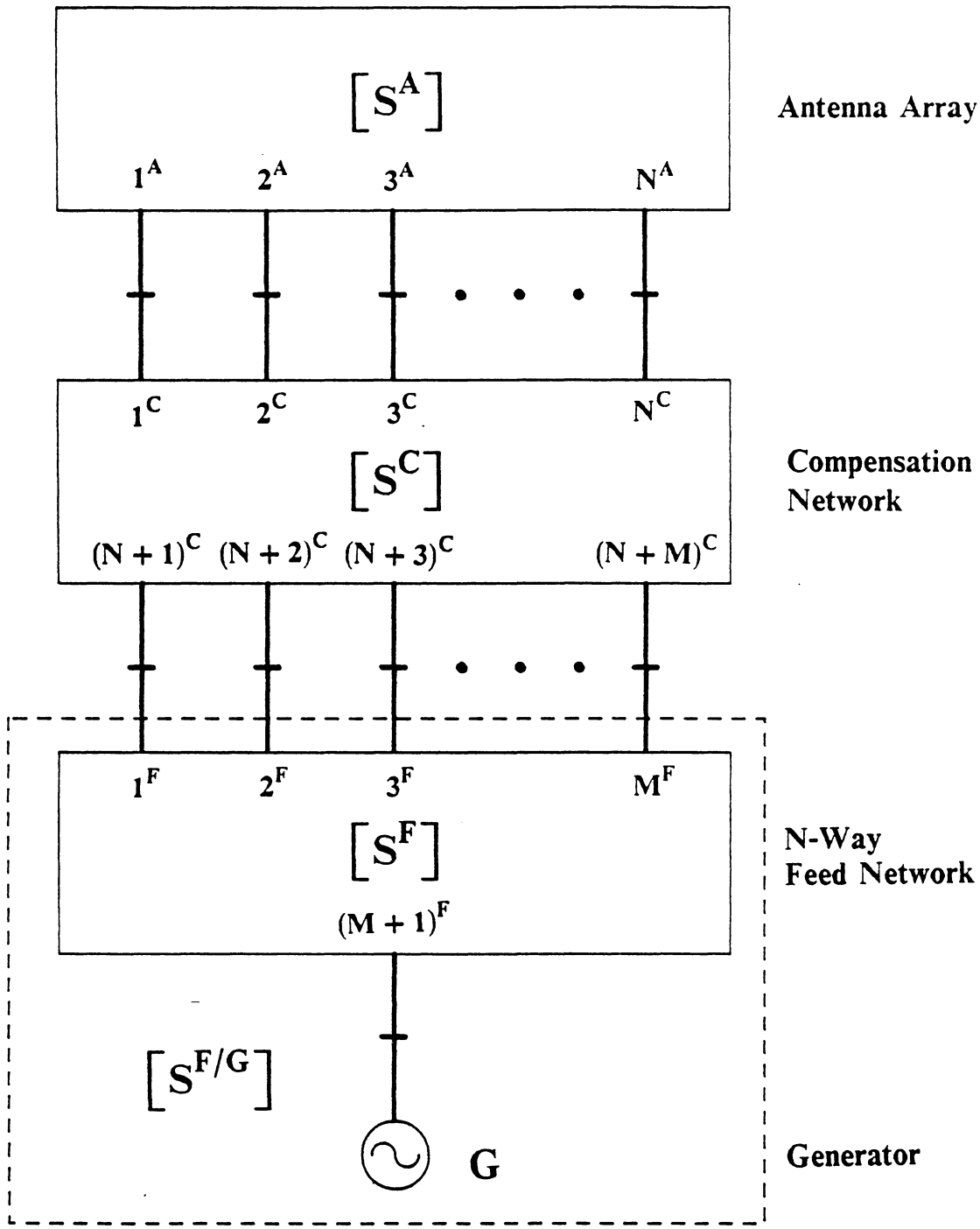

Figure 2.4-1. General form of an array antenna with a compensation network.

$$a_i^C = b_i^A \tag{2.4-3}$$

for $1 \leq i \leq N$. The wave variables $[a^A]$ and $[b^A]$ are related to the (specified) desired currents $[I^A]$ by

$$[I^A] = [a^A] - [b^A] \tag{2.4-4}$$

or

$$[a^A] = [I^A] + [b^A] \tag{2.4-5}$$

The wave variables are also related to the antenna S-matrix $[S^A]$ by

$$[b^A] = [S^A][a^A] \tag{2.4-6}$$

Substituting (2.4-5) into the above equation and solving for the vector $[b^A]$ proceeds as follows

$$[b^A] = [S^A][I^A - b^A]$$

$$[b^A] = [S^A][I^A] - [S^A][b^A]$$

$$[I - S^A][b^A] = [S^A][I^A]$$

$$[b^A] = [I - S^A]^{-1}[S^A][I^A] \tag{2.4-7}$$

where $[I]$ is the square identity matrix. It follows from (2.4-5) and (2.4-7) that wave variables $[a^A]$ can be represented as

$$[a^A] = [I^A] + [I - S^A]^{-1}[S^A][I^A] \tag{2.4-8}$$

Equations (2.4-7) and (2.4-8) or (2.4-5) relate the wave variables to the known S-matrix $[S^A]$ and the desired currents $[I^A]$.

At the junction between the feed/generator network and the compensation network (see Fig. 2.4-1),

$$a^C_{i+N} = b_i^{F/G} \tag{2.4-9}$$

$$b^C_{i+N} = a_i^{F/G} \tag{2.4-10}$$

for $1 \leq i \leq M$. Using (2.1-19), the wave variables at the feed network are related by

$$[b^{F/G}] = [S^{F/G}][a^{F/G}] + [c^{F/G}] \tag{2.4-11}$$

It should be noted that the incident wave vector from the compensation network into the feed/generator network $[a^{F/G}]$ is not a constant vector. Rather, it depends on the actual compensation network $[S^c]$. This vector is not necessary in the final solution. However, these variables play an important role as the intermediate unknowns in the solution process. To emphasize the fact that the incident waves need to be treated as unknowns, the vector entries are changed as follows:

$$U_i = a_i^{F/G} \quad \text{for} \quad 1 \leq i \leq M \tag{2.4-12}$$

Substituting (2.4-2), (2.4-3) and (2.4-9) through (2.4-12) into (2.4-1) gives

$$\begin{bmatrix} a_1^A \\ a_2^A \\ \vdots \\ a_N^A \\ U_1 \\ \vdots \\ U_M \end{bmatrix} = \begin{bmatrix} S_{1,1}^C & S_{1,2}^C & \cdots & S_{1,N}^C & \cdots & S_{1,N+M}^C \\ S_{2,1}^C & S_{2,2}^C & \cdots & S_{2,N}^C & \cdots & S_{2,N+M}^C \\ \vdots & \vdots & \vdots & \vdots & \vdots & \vdots \\ S_{N,1}^C & S_{N,2}^C & \cdots & S_{N,N}^C & \cdots & S_{N,N+M}^C \\ S_{N+1,1}^C & S_{N+1,2}^C & \cdots & S_{N+1,N}^C & \cdots & S_{N+1,N+M}^C \\ \vdots & \vdots & \vdots & \vdots & \vdots & \vdots \\ S_{N+M,1}^C & S_{N+M,2}^C & \cdots & S_{N+M,N}^C & \cdots & S_{N+M,N+M}^C \end{bmatrix} \begin{bmatrix} b_1^A \\ b_2^A \\ \vdots \\ b_N^A \\ c_1^{F/G} + \sum_{j=1}^{M} S_{1,j}^{F/G} U_j \\ \vdots \\ c_M^{F/G} + \sum_{j=1}^{M} S_{M,j}^{F/G} U_j \end{bmatrix}$$

(2.4-13)

From this the resulting system of nonlinear equations is

$$0 = -a_k^A + \sum_{i=1}^{N} S_{k,i}^C b_i^A + \sum_{i=1}^{M} S_{k,N+i}^C \left[c_i^{F/G} + \sum_{j=1}^{M} S_{i,j}^{F/G} U_j \right] \quad \text{for } 1 \le k \le N \tag{2.4-14}$$

which follow from the top portion of (2.4-13) and

$$0 = -U_{k-N} + \sum_{i=1}^{N} S_{k,i}^C b_i^A + \sum_{i=1}^{M} S_{k,N+i}^C \left[c_i^{F/G} + \sum_{j=1}^{M} S_{i,j}^{F/G} U_j \right] \quad \text{for } N+1 \le k \le N+M$$

(2.4-15)

which follow from the lower portion of (2.4-13). The system of equations (2.4-14) and (2.4-15) are in general form. The equations are solved for $S_{i,j}^C$ which are the scattering parameters of the compensation network. The variables a_i, b_i, $S_{i,j}^{F/G}$, and $c^{F/G}$ are known,

and U_i are intermediate unknowns. The nonlinear property in (2.4-14) and (2.4-15) arises from the the terms $S^C_{k,N+i}U_j$ where both $\{S^C_{ij}\}$ and $\{U_j\}$ depend on unknown variables $\{X_i\}$. When generator value G is treated as an unknown (for example, power divider compensation) the product $S^C_{k,N+i}c_i^{F/G}$ also contributes to the nonlinear property of the equations. These equations cannot be solved for a compensation network until the relationship between physical parameters and S-parameters of the compensation network is defined. In other words, we must define functions of the form

$$S^C_{ij} = f_{ij}(X_1, X_2, ..., X_N) \tag{2.4-16}$$

where $\{X_i\}$ are complex variables representing network parameters. Three different types of compensation networks considered in this report are discussed in Chapter 4. In Chapters 5 through 7 we proceed with solving for required compensation configurations for three networks.

The system of nonlinear equations are then solved for compensation network parameters using the Damped Newton's method [D-4] which is an iterative numerical technique. A review of the Newton's method and the Damped-Newton's method is given by Smith [S-1, Secs. 5.2-5.4]. The numerical technique is implemented in programs SANE and SANE-PODCON to solve for attenuator/phase shifter network and power divider network which are described in Appendix A and Appendix B, respectively.

2.5 Calculation of Element Currents at the Patch Edges

Microstrip arrays are usually fabricated with a section of transmission line attached between the antenna patches and the board input, which will be called the feed lines as indicated in Fig. 2.5-1. These feed lines should not be confused with the feed network

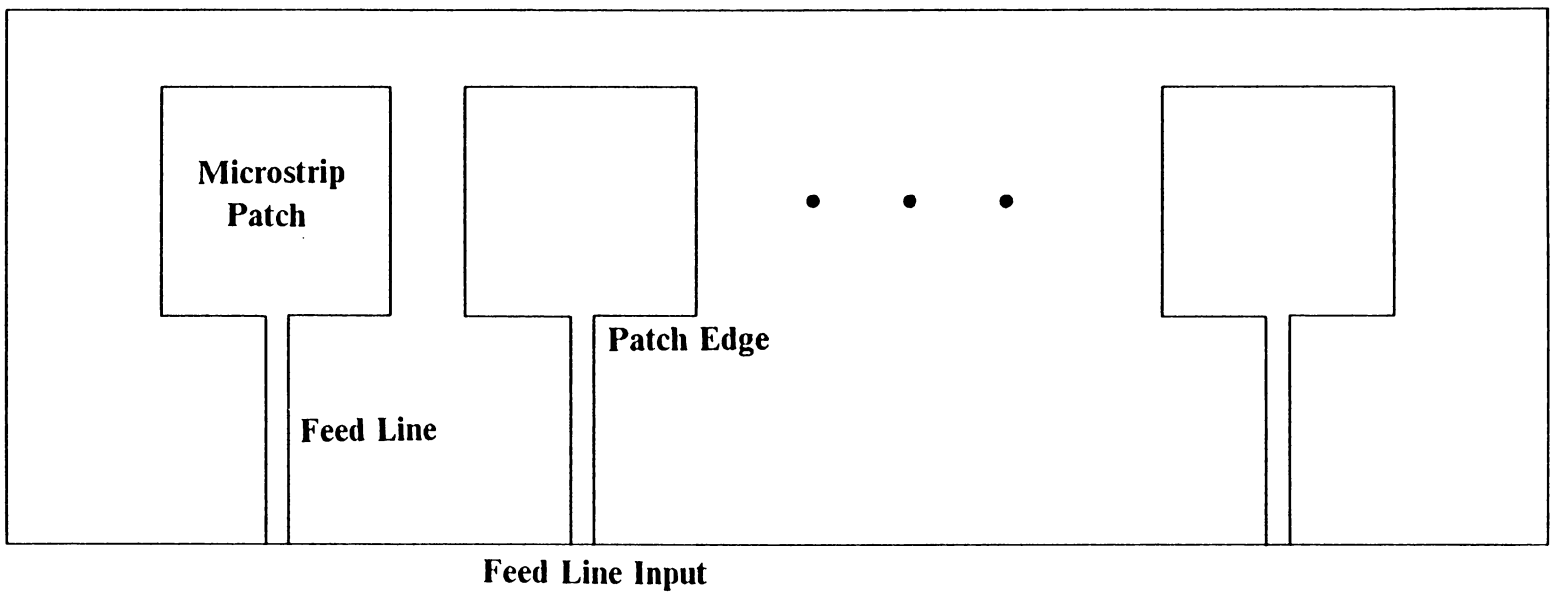

Figure 2.5-1. Definition of antenna patches and their feed lines.

that is fabricated on a separate substrate. The purpose of the feed lines are to excite the antenna patches with correct mode and polarization.

The S-parameters of the array board represent the combined network of antenna patches and their feed lines. The currents calculated from the antenna and feed network matrices using (2.1-7), (2.1-21) and (2.1-22) are the values at the feed line - feed network junction. In the absence of coupling these currents are equivalent to the array excitation coefficients. However, in the presence of mutual coupling each antenna element in an array has a different active impedance. As a result, the relative currents at the patch edges are different from that of the feed line input. To determine the correct currents at patch edges, the feed line currents need to be transformed.

Two types of current transformations are necessary for analysis and for synthesis. In the analysis case, the calculated currents at the board input need to be transformed to the currents at patch edges. In the synthesis case, on the other hand, the desired currents at patch edges need to be transformed to the board input currents to compute the compensation network.

In either case, it is necessary to assume that S-parameters of feed lines $[S^{FL}]$ are known. Since the feed lines cannot be separated from the antenna patches to measure S-parameters, an accurate mathematical model for the feed line is required. In this report the S-parameters obtained from MCAP are assumed to be accurate enough since the structure of feed line is simple. It is also necessary to assume that the currents at patch edges actually correspond to the excitation coefficients of the antenna patches. More rigorous analysis of the patch - feed line interaction can be accomplished using the method of moment as reported by Pozar [P-9].

In the analysis case the wave variables, the incident waves a and reflected waves b are known for the specified S-matrices of an antenna array, the feed network and

generator by (2.1-21) and (2.1-22). The wave variables at the patch edge can be obtained from the general S-parameter equation:

$$[b] = [S^{FL}][a] \tag{2.5-1}$$

or

$$\begin{bmatrix} b_{input} \\ b_{output} \end{bmatrix} = \begin{bmatrix} S_{11}^{FL} & S_{12}^{FL} \\ S_{21}^{FL} & S_{22}^{FL} \end{bmatrix} \begin{bmatrix} a_{input} \\ a_{output} \end{bmatrix} \tag{2.5-2}$$

where a_{input} and b_{input} are wave variables at board input which are known, and a_{output} and b_{output} are wave variables at the feed line near the patch edge. The matrix $[S^{FL}]$ represents S-parameters of a feed line which may include loss in the line. It is clear from Fig. 2.5-2 that the incident waves to the patches are the reflected waves from the feed line output and vice versa, i.e., $b_{output} = a_{patch}$ and $a_{output} = b_{patch}$. Using these relationships in (2.5-2) and solving for the wave variables at patches,

$$b_{patch} = \frac{b_{input} - S_{11}^{FL} a_{input}}{S_{12}^{FL}} \tag{2.5-3}$$

$$\begin{aligned} a_{patch} &= S_{21}^{FL} a_{input} + S_{22}^{FL} b_{patch} \\ &= S_{21}^{FL} a_{input} + \frac{S_{22}^{FL}}{S_{12}^{FL}} \left(b_{input} - S_{11}^{FL} a_{input} \right) \end{aligned} \tag{2.5-4}$$

Then, the current at the patch edge is

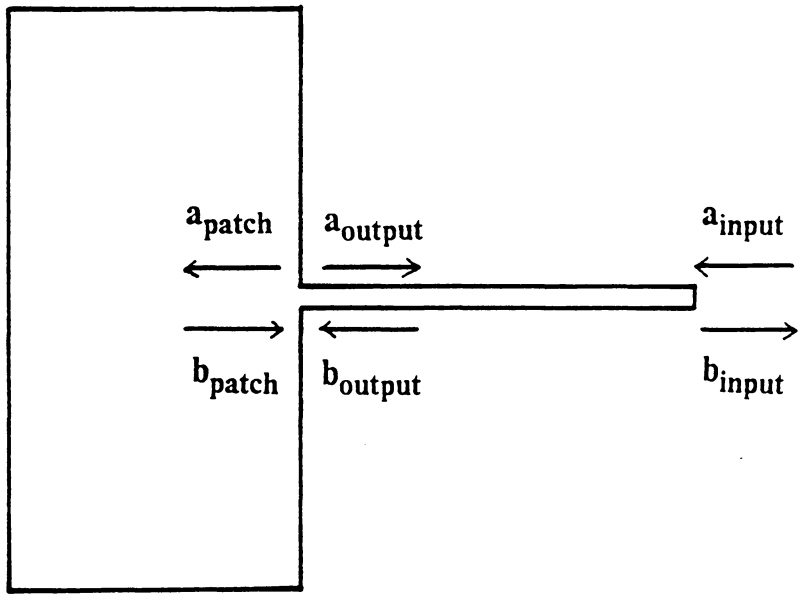

Figure 2.5-2. Definition of wave variables at the patch edge and the feed line input for a microstrip patch antenna.

$$
\begin{aligned}
I_{patch} &= a_{patch} - b_{patch} \\
&= S_{21}^{FL} a_{input} + \frac{S_{22}^{FL}}{S_{12}^{FL}} \left(b_{input} - S_{11}^{FL} a_{input} \right) - \frac{b_{input} - S_{11}^{FL} a_{input}}{S_{12}^{FL}} \\
&= S_{21}^{FL} a_{input} + \frac{S_{22}^{FL} - 1}{S_{12}^{FL}} \left(b_{input} - S_{11}^{FL} a_{input} \right)
\end{aligned}
\tag{2.5-5}
$$

In the synthesis case a similar transformation cannot be applied directly because only the desired currents and not wave variables are specified at the patch edges. It is clear from (2.1-7) that there is an infinite number of pairs of a_n and b_n which produce the specified value of currents I_n. To calculate wave variables at the patch edges, the scattering matrix for antenna patches without feed lines is necessary. This can be obtained by subtracting the feed line portion of S-parameters from the S-matrix of antenna patches with feed lines.

Consider the problem of removing a transmission line section of known S-parameters from the port 1 of a general N-port as indicated in Fig. 2.5-3. We will designate the original N-port scattering matrix by $[S^{(0)}]$ and the reduced N-port by $[S^{(1)}]$. The feed line section has an S-matrix of the form

$$
\left[S^{FL} \right] = \begin{bmatrix} S_{11}^{FL} & S_{12}^{FL} \\ S_{21}^{FL} & S_{22}^{FL} \end{bmatrix}
\tag{2.5-6}
$$

Using the interconnection matrix equation (2.1-9),

$$
\left[S^{(0)} \right] = \left[S_{PP} + S_{PC} (\Gamma - S_{CC})^{-1} \; S_{CP} \right]
\tag{2.5-7}
$$

where

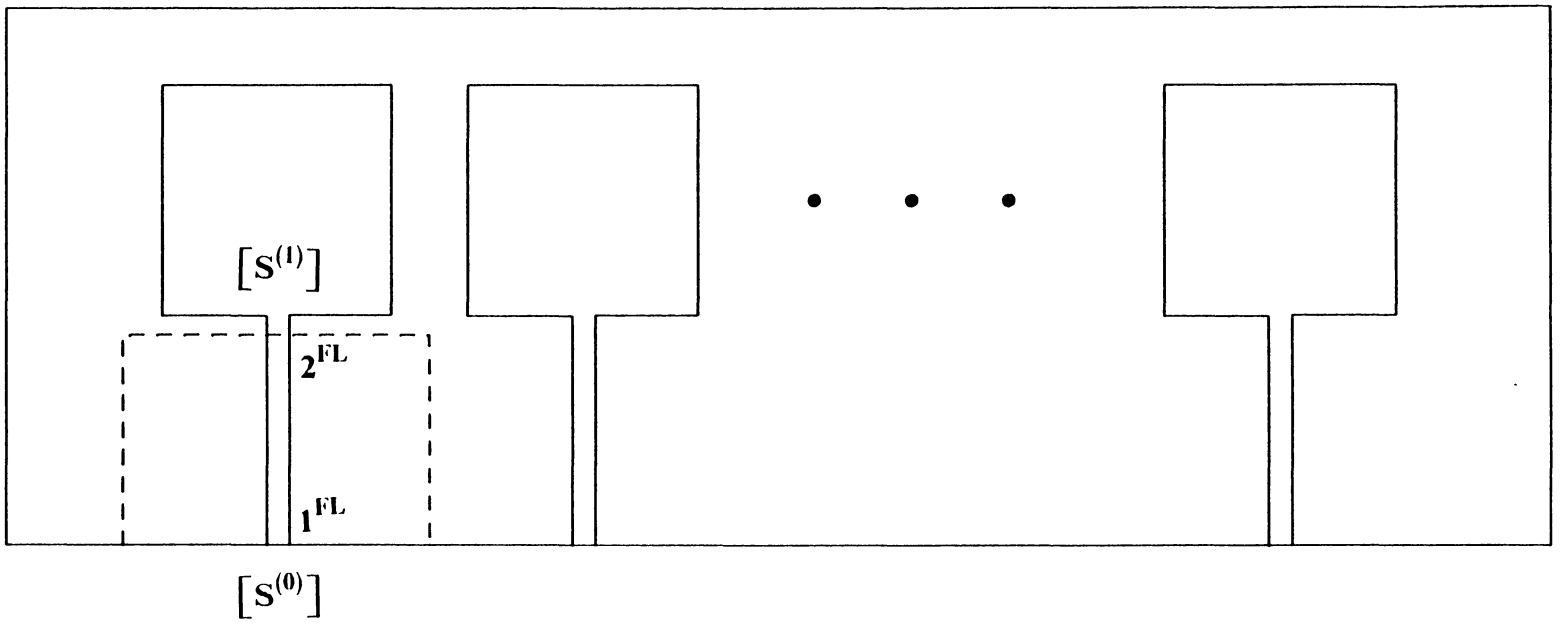

Figure 2.5-3. The procedure to remove a feed line from patch 1 in an array.

$$\begin{bmatrix} S_{PP} & S_{PC} \\ S_{CP} & S_{CC} \end{bmatrix} = \left[\begin{array}{ccccc:cc} S_{11}^{FL} & 0 & 0 & \dots & 0 & S_{12}^{FL} & 0 \\ 0 & S_{22}^{(1)} & S_{23}^{(1)} & \dots & S_{2N}^{(1)} & 0 & S_{21}^{(1)} \\ 0 & S_{32}^{(1)} & S_{33}^{(1)} & \dots & S_{3N}^{(1)} & 0 & S_{31}^{(1)} \\ . & . & . & . & . & . & . \\ 0 & S_{N2}^{(1)} & S_{N3}^{(1)} & \dots & S_{NN}^{(1)} & 0 & S_{N1}^{(1)} \\ \hdashline S_{21}^{FL} & 0 & 0 & \dots & 0 & S_{22}^{FL} & 0 \\ 0 & S_{12}^{(1)} & S_{13}^{(1)} & \dots & S_{1N}^{(1)} & 0 & S_{11}^{(1)} \end{array}\right] \tag{2.5-8}$$

S_{PP} represents the scattering matrix for the network with external ports 1,2,...,N and S_{CC} represents the connected ports. The connection of ports 2^{FL} and 1′ is expressed by

$$[\Gamma] = \begin{bmatrix} 0 & 1 \\ 1 & 0 \end{bmatrix} \tag{2.5-9}$$

Evaluation of the right hand side of (2.5-7) proceeds as follows:

$$\Gamma - S_{CC} = \begin{bmatrix} -S_{22}^{FL} & 1 \\ 1 & -S_{11}^{(1)} \end{bmatrix}$$

$$(\Gamma - S_{CC})^{-1} = \frac{1}{1 - S_{22}^{FL} S_{11}^{(1)}} \begin{bmatrix} S_{11}^{(1)} & 1 \\ 1 & S_{22}^{FL} \end{bmatrix}$$

$$S_{PC}(\Gamma - S_{CC})^{-1} = \begin{bmatrix} S_{12}^{FL} & 0 \\ 0 & S_{21}^{(1)} \\ 0 & S_{31}^{(1)} \\ . & . \\ . & . \\ 0 & S_{N1}^{(1)} \end{bmatrix} \frac{1}{1 - S_{22}^{FL} S_{11}^{(1)}} \begin{bmatrix} S_{11}^{(1)} & 1 \\ 1 & S_{22}^{FL} \end{bmatrix}$$

$$= \frac{1}{1 - S_{22}^{FL} S_{11}^{(1)}} \begin{bmatrix} S_{12}^{FL} S_{11} & S_{21}^{FL} \\ S_{21}^{(1)} & S_{22}^{FL} S_{21}^{(1)} \\ S_{31}^{(1)} & S_{22}^{FL} S_{31}^{(1)} \\ . & . \\ . & . \\ S_{N1}^{(1)} & S_{22}^{FL} S_{N1}^{(1)} \end{bmatrix}$$

$$S_{PC}(\Gamma - S_{CC})^{-1} S_{CP} = \frac{1}{1 - S_{22}^{FL} S_{11}^{(1)}} \begin{bmatrix} S_{12}^{FL} S_{11} & S_{21}^{FL} \\ S_{21}^{(1)} & S_{22}^{FL} S_{21}^{(1)} \\ S_{31}^{(1)} & S_{22}^{FL} S_{31}^{(1)} \\ . & . \\ . & . \\ S_{N1}^{(1)} & S_{22}^{FL} S_{N1}^{(1)} \end{bmatrix} \begin{bmatrix} S_{21}^{FL} & 0 & 0 & . . & 0 \\ 0 & S_{12}^{(1)} & S_{13}^{(1)} & . . & S_{1N}^{(1)} \end{bmatrix}$$

$$= \frac{1}{1 - S_{22}^{FL} S_{11}^{(1)}} \begin{bmatrix} S_{12}^{FL} S_{21}^{FL} S_{11}^{(1)} & S_{12}^{FL} S_{12}^{(1)} & S_{12}^{FL} S_{13}^{(1)} & \cdots & S_{12}^{FL} S_{1N}^{(1)} \\ S_{21}^{FL} S_{21}^{(1)} & S_{22}^{FL} S_{21}^{(1)} S_{12}^{(1)} & S_{22}^{FL} S_{21}^{(1)} S_{13}^{(1)} & \cdots & S_{22}^{FL} S_{21}^{(1)} S_{1N}^{(1)} \\ S_{21}^{FL} S_{31}^{(1)} & S_{22}^{FL} S_{31}^{(1)} S_{12}^{(1)} & S_{22}^{FL} S_{31}^{(1)} S_{13}^{(1)} & \cdots & S_{22}^{FL} S_{31}^{(1)} S_{1N}^{(1)} \\ \cdot & \cdot & \cdot & \cdot & \cdot \\ \cdot & \cdot & \cdot & \cdot & \cdot \\ S_{21}^{FL} S_{N1}^{(1)} & S_{22}^{FL} S_{N1}^{(1)} S_{12}^{(1)} & S_{22}^{FL} S_{N1}^{(1)} S_{13}^{(1)} & \cdots & S_{22}^{FL} S_{n1}^{(1)} S_{1N}^{(1)} \end{bmatrix}$$

And finally,

$$[S^{(0)}] = \left[S_{PP} + S_{PC}(\Gamma - S_{CC})^{-1} \; S_{CP} \right]$$

$$= \frac{1}{1 - S_{22}^{FL} S_{11}^{(1)}} \begin{bmatrix} (1 - S_{22}^{FL} S_{11}^{(1)}) S_{11}^{FL} + S_{12}^{FL} S_{21}^{FL} S_{11}^{(1)} & S_{12}^{FL} S_{12}^{(1)} \\ S_{21}^{FL} S_{21}^{(1)} & (1 - S_{22}^{FL} S_{11}^{(1)}) S_{22}^{(1)} + S_{22}^{FL} S_{21}^{(1)} S_{12}^{(1)} \\ S_{21}^{FL} S_{31}^{(1)} & (1 - S_{22}^{FL} S_{11}^{(1)}) S_{32}^{(1)} + S_{22}^{FL} S_{31}^{(1)} S_{12}^{(1)} \\ \cdot & \cdot \\ \cdot & \cdot \\ S_{21}^{FL} S_{N1}^{(1)} & (1 - S_{22}^{FL} S_{11}^{(1)}) S_{N2}^{(1)} + S_{22}^{FL} S_{N1}^{(1)} S_{12}^{(1)} \end{bmatrix}$$

$$\begin{bmatrix} S_{12}^{FL} S_{13}^{(1)} & \cdots & S_{12}^{FL} S_{1n}^{(1)} \\ (1 - S_{22}^{FL} S_{11}^{(1)}) S_{23}^{(1)} + S_{22}^{FL} S_{21}^{(1)} S_{13}^{(1)} & \cdots & (1 - S_{22}^{FL} S_{11}^{(1)}) S_{2N}^{(1)} + S_{22}^{FL} S_{21}^{(1)} S_{1N}^{(1)} \\ (1 - S_{22}^{FL} S_{11}^{(1)}) S_{33}^{(1)} + S_{22}^{FL} S_{31}^{(1)} S_{13}^{(1)} & \cdots & (1 - S_{22}^{FL} S_{11}^{(1)}) S_{3N}^{(1)} + S_{22}^{FL} S_{31}^{(1)} S_{1N}^{(1)} \\ \cdot & \cdot & \cdot \\ \cdot & \cdot & \cdot \\ (1 - S_{22}^{FL} S_{11}^{(1)}) S_{N3}^{(1)} + S_{22}^{FL} S_{N1}^{(1)} S_{13}^{(1)} & \cdots & (1 - S_{22}^{FL} S_{11}^{(1)}) S_{NN}^{(1)} + S_{22}^{FL} S_{N1}^{(1)} S_{1N}^{(1)} \end{bmatrix} \qquad (2.5\text{-}10)$$

Equating (2.5-10) to the original S-parameter matrix, we can obtain four relations.

$$S_{11}^{(0)} = S_{11}^{FL} + \frac{S_{12}^{FL} S_{21}^{FL} S_{11}^{(1)}}{1 - S_{22}^{FL} S_{11}^{(1)}} \tag{2.5-11}$$

$$S_{1j}^{(0)} = \frac{S_{12}^{FL} S_{1j}^{(1)}}{1 - S_{22}^{FL} S_{11}^{(1)}} \qquad j = 2 \ldots N \tag{2.5-12}$$

$$S_{j1}^{(0)} = \frac{S_{21}^{TL} S_{j1}^{(1)}}{1 - S_{22}^{FL} S_{11}^{(1)}} \qquad j = 2 \ldots N \tag{2.5-13}$$

$$S_{jk}^{(0)} = S_{jk}^{(1)} + \frac{S_{22}^{FL} S_{j1}^{(1)} S_{1k}^{(1)}}{1 - S_{22}^{FL} S_{11}^{(1)}} \qquad \begin{matrix} j = 2 \ldots N \\ k = 2 \ldots N \end{matrix} \tag{2.5-14}$$

Solving the above four equations for the S-parameters $S^{(0)}$ gives

$$S_{11}^{(1)} = \frac{S_{11}^{(0)} - S_{11}^{FL}}{S_{22}^{FL}\left(S_{11} - S_{11}^{FL}\right) + S_{12}^{FL} S_{21}^{FL}} \tag{2.5-15}$$

$$S_{1j}^{(1)} = \frac{S_{1j}^{(0)}\left(1 - S_{22}^{FL} S_{11}^{(1)}\right)}{S_{12}^{FL}} \qquad j = 2 \ldots N \tag{2.5-16}$$

$$S_{j1}^{(1)} = \frac{S_{j1}^{(0)}\left(1 - S_{22}^{FL} S_{11}^{(1)}\right)}{S_{21}^{FL}} \qquad j = 2 \ldots N \tag{2.5-17}$$

$$S_{jk}^{(1)} = S_{jk}^{(0)} - \frac{S_{22}^{FL} S_{j1}^{(1)} S_{1k}^{(1)}}{1 - S_{22}^{FL} S_{11}^{(1)}} \qquad \begin{matrix} j = 2 \ldots N \\ k = 2 \ldots N \end{matrix} \tag{2.5-18}$$

Generalizing (2.5-15) to (2.5-18) for i-th feed line,

$$S_{ii}^{(i)} = \frac{S_{ii}^{(i-1)} - S_{11}^{FL}}{S_{22}^{FL}\left(S_{ii}^{(i-1)} - S_{11}^{FL}\right) + S_{12}^{FL} S_{21}^{FL}} \tag{2.5-19}$$

$$S_{ij}^{(i)} = \frac{S_{ij}^{(i-1)}\left(1 - S_{22}^{FL} S_{ii}^{(i)}\right)}{S_{12}^{FL}} \qquad j \neq i \tag{2.5-20}$$

$$S_{ji}^{(i)} = \frac{S_{ji}^{(i-1)}\left(1 - S_{22}^{FL} S_{ii}^{(i)}\right)}{S_{21}^{FL}} \qquad j \neq i \tag{2.5-21}$$

$$S_{jk}^{(i)} = S_{jk}^{(i-1)} - \frac{S_{22}^{FL} S_{ji}^{(i)} S_{ik}^{(i)}}{1 - S_{22}^{FL} S_{ii}^{(i)}} \qquad \begin{matrix} j \neq i \\ k \neq i \end{matrix} \tag{2.5-22}$$

To obtain the S-matrix of antenna patches without feed lines, the above process must be applied sequentially to all feed lines; see Fig. 2.5-4. Thus, the S-matrix for the array shown at the bottom of Fig. 2.5-4 is $[S^{(N)}]$ with entries given by (2.5-19) to (2.5-22) and evaluated sequentially for $i = 1,...,N$. The wave variables can now be calculated for the antenna patches using (2.4-7) and (2.4-8), and desired currents referred to the board input are obtained from a process similar to the analysis case.

Subroutines were developed in the computer programs SANE (Appendix A) and SANE-PODCON (Appendix B) implementing the analysis and synthesis steps discussed in this section. In particular, equations (2.5-19) through (2.5-22) which calculate S-matrix of microstrip patches given S-matrix of an array board with feed lines are implemented in subroutine PREPRC in both SANE and SANE-PODCON.

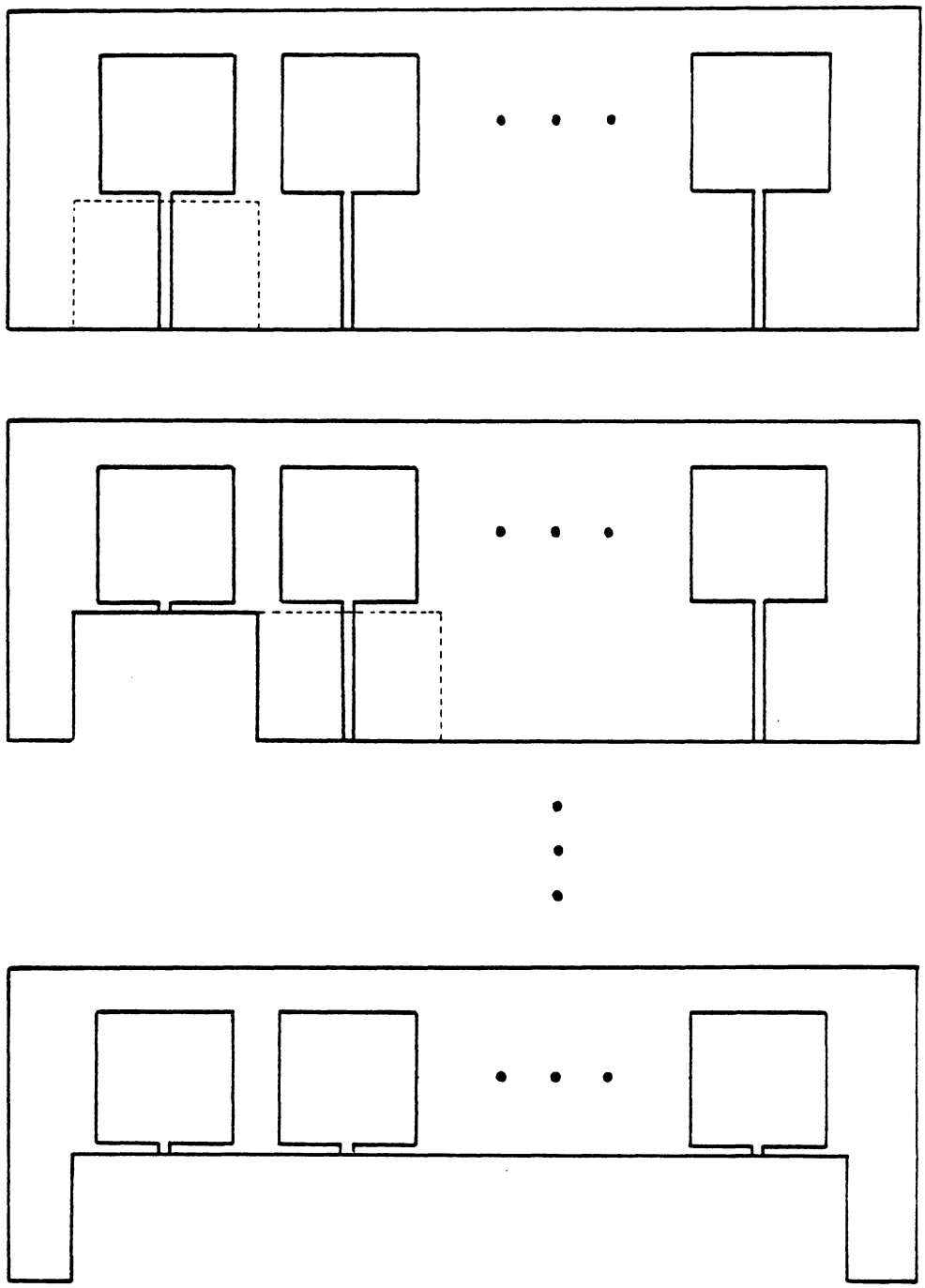

Figure 2.5-4. Steps to obtain S-matrix of antenna patches without feed lines.

III. Existing Methods to Compensate for Mutual Coupling

Many techniques have been developed to compensate or partially compensate for mutual coupling effects in array antennas. Most of these techniques, however, consider only the element coupling and neglect the second order effect of feed coupling. In addition, many techniques are applicable only for a specific array geometry or for specific radiating elements. This chapter presents a review of some existing compensation techniques.

3.1. Compensation by an Added Network

Perhaps the most popular method to compensate for mutual coupling is to place a network between the array element network and feed network. The simplest of such networks are circulators and isolaters [H-11]. However, these networks have power loss in reflection [H-4] and are non-reciprocal causing difference on transmit and receive.

They are also expensive components. A more practical method to compensate for mutual coupling is to place a matching network between the array and the feed network.

Hannan, et al. [H-4] developed a theory that accomplishes impedance matching using networks that connect feed lines. The theory was derived from the proof by Hannan [H-3] that for an infinite array it is possible to match all elements over all scan angles for a single frequency and polarization.

Andersen and Rasmussen [A-2] presented an example for synthesis of a connecting network applied to a finite array. Their technique uses a network that has the negative of the impedance matrix of the array elements. The network is connected in series with the elements which reduces the impedance matrix of the overall network to zero. For the connecting network to be lossless and passive it requires that the element impedance matrix be purely reactive. This is accomplished by changing the array geometry. A two element experiment showed a verification of the technique. However, for a three element array complete compensation was not achieved because reactive mutual impedance between two outer elements and adjacent elements cannot be obtained simultaneously.

Davies [D-3] presented an application of a matching network at the input ports of a Butler matrix network. He showed that for the case of small circularly symmetric planar arrays such as those used as feeds to reflector antennas, mutual coupling compensation can be accomplished by a set of fixed phase shifts. This is achieved by breaking down the array excitation into series of orthogonal circularly symmetric phase modes, and impedance matching phase mode ports with phase shifters. He claimed that these networks are independent of changes in the excitation which are necessary to scan the main beam.

The compensation techniques discussed above are all based on the knowledge of coupling coefficients between antenna elements. Another approach to mutual coupling

compensation is to use the radiation pattern of the array. Davis [D-9] showed that element currents in an N-element array can be approximately determined from the magnitude and phase of the radiation pattern at N points. This calculation assumes that active element patterns are similar for all elements. Using the calculated currents, attenuators and phase shifters are added between the elements and the feed network to correct for the error in the currents. As it will be shown later in Section 5.4 this process is nonlinear. Thus, the correction to the element currents must be done iteratively. Davis applied the pattern analysis technique to synthesize a 35 dB Dolph-Chebyshev pattern using an 8-element array. Using the technique the side lobe level were reduced from -26 dB to -31 dB after several iterations.

3.2. Compensation by Feed Network Modification

The methods treated in Section 3.1 compensated for mutual coupling by adding a network between the elements and feed network. In this section, we review methods which allows synthesis of feed networks that include mutual coupling compensation. Kang and Pozar [K-2] developed two techniques to determine terminal voltages required to produce the desired element currents using moment method impedance matrices of array antennas. Then, the calculated voltages and desired currents can be used to design a feed network. The first technique compensates for mutual coupling by point matching a desired pattern in a given plane. A more complicated second technique, on the other hand, corrects the pattern over all space. They show a numerical example of synthesis of a 30 dB Dolph-Chebyshev endfire pattern using an array of eight parallel dipoles. Application of these techniques, however, may be difficult for some radiating elements since the techniques require a moment method impedance matrix of the array. Also the

techniques neglect the feed network coupling effect which may be significant in a low side lobe pattern.

Another technique presented by Elliott and Stern [E-1] compensated for mutual coupling using microstrip dipoles which are fed with electromagnetically coupled feed lines. In this technique the spatial relation between the dipoles and the feed lines, the length of dipoles, and location of dipoles are design variables. The self impedance and mutual impedance of the dipoles are functions of the design variables which were determined by measurements. Using these functions, a multivariable equation can be solved for the design variables given a desired radiation pattern, and then realized by the geometry of the array. Experimental verification of the theory was achieved with a 32 element dipole array [S-3].

3.3. Other Mutual Coupling Compensation Techniques

There are many other compensation techniques that are specific to array architecture. For example, mutual coupling compensation can be accomplished by software for a digital beam forming (DBF) array [S-6,H-5]. In a DBF array, the received signals are detected and digitized at the element level. The digitized signals are then processed using digital computer to form a desired radiation pattern. Steyskal [S-6] showed that when the amplitude and phase of signals at each element in an array as well as coupling coefficients between elements are available such as in a DBF array, coupling effects can be cancelled by taking the inverse of the coupling coefficient matrix and then multiplying the inverted matrix with the signals at each element. Herd [H-5] used this technique for an eight element array to reduce the side lobe level from -20dB to -30dB.

IV. Feed Configurations

4.1 Introduction

To compensate for mutual coupling the system of nonlinear equations derived in Section 2.4 must be solved. These equations, however, cannot be solved until the form of the scattering matrix $[S^c]$ is specified for the physical configuration of the network. In this study we considered three types of feed network architectures that involve the following basic building blocks: attenuator/phase shifter network, variable power divider network, and transmission line network. This chapter develops the mathematical representations necessary to solve for compensation. In general, these networks will be considered as ideal in the sense that ohmic loss in transmission lines and phase shifters are ignored, and mismatch in the phase shifters and attenuators are also ignored. However, for the attenuator/phase shifter network, the non-ideal parameters of the device will also be discussed.

4.2 Using MCAP to Study Feed Components

The Microwave Circuit Analysis Program (MCAP) which was originally written at Indian Institute of Technology, Kanpur, is a general purpose program for microwave network analysis [G-1]. The program has been modified at New Mexico State University Physical Science Laboratory to enhance its capability. The modifications are discussed in detail by Henry and Jedlicka [H-1]. Many such microwave CAD codes exist, but this one is available at no cost and is documented in [G-1]. Access to the source code permitted the modifications.

MCAP evaluates the scattering matrix of an overall network given the S-parameters of individual components in the network. This is basically a computer implementation of the interconnected network equation in (2.1-9). The program is equipped with mathematical models of various stripline and microstrip components. These models evaluate the S-parameters of the components from their physical dimensions and their characteristic impedance. The standard components available in MCAP include transmission line section, step in the line width (impedance step), bend in a line at an arbitrary angle, T-junction, coupled lines, series impedance and admittance, and shunt impedance and admittance. In addition, user supplied S-matrices for networks with up to 10 ports can be specified as components. After the evaluation of the overall S-matrix, the program calculates the wave variables and corresponding currents at all internal ports when an external port is connected to a generator with the value $G = 1\underline{/0^\circ}$ and all other external ports are match loaded which is an implementation of (2.1-21) and (2.1-22).

MCAP was used extensively in our study to analyze antenna element currents from measured S-parameters of the antenna elements and feed networks. For example, an

eight element array can be treated as a combination of elements, a feed network and a generator. The internal ports for this network are the element input ports and the feed network output ports which are connected to each other. The element currents are calculated at the junctions between the element ports and feed network output ports using MCAP. The program was also used to investigate and verify the S-parameters of compensation networks.

4.3 The Attenuator/Phase Shifter Compensation Network

The basic configuration of the network consists of an attenuator in series with a phase shifter as shown on Fig. 4.3-1. The attenuator reduces the magnitude and the phase shifter alters the phase of the signal. The series combination of these two devices provides the required complex control of the signal flow to compensate for mutual coupling. The scattering matrix of an ideal attenuator/phase shifter is given as [S-1]

$$\left[S^{A/P}\right] = \begin{bmatrix} 0 & Ae^{-j\phi} \\ Ae^{-j\phi} & 0 \end{bmatrix} \tag{4.3-1}$$

where A is the attenuation and ϕ is the phase delay. This equation assumes that both the attenuator and phase shifter are matched, so that no reflection occurs ($S_{ii} = 0$). It also assumes that the attenuator provides only attenuation and no phase delay, and that the phase shifter provides only phase shift. In the subsequent analysis, the ideal performance via (4.3-1) is assumed. However, representation of non-ideal performance is discussed next for completeness.

In practice, neither the attenuators nor the phase shifters are ideal devices. The attenuator introduces some phase shift and mismatch. Similarly, the phase shifter has

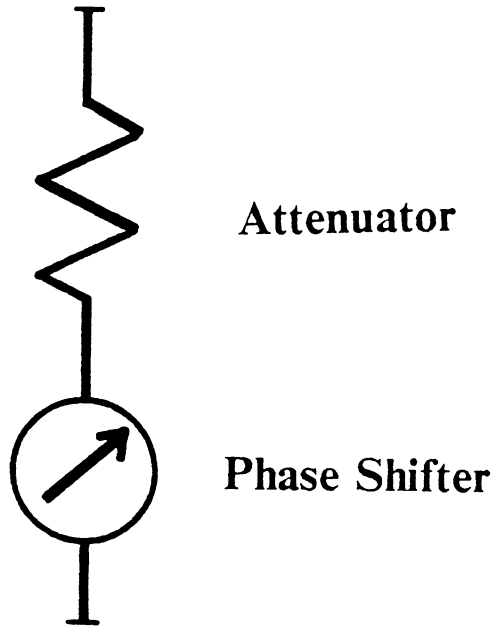

Figure 4.3-1. Graphical representation of attenuator/phase shifter compensation network.

some attenuation and mismatch. The S-matrix of attenuator/phase shifter which includes these non-ideal parameters was derived by Smith [S-1] as follows

$$\left[S^{A/P}_{\text{non-ideal}}\right] = \begin{bmatrix} \left[\Gamma_p - \dfrac{\Gamma_a B^2 e^{-j2\phi_p}}{\Gamma_p\Gamma_a - 1}\right] & \dfrac{-ABe^{-j(\phi_a+\phi_p)}}{\Gamma_p\Gamma_a - 1} \\ \dfrac{-ABe^{-j(\phi_a+\phi_p)}}{\Gamma_p\Gamma_a - 1} & \left[\Gamma_a - \dfrac{\Gamma_p A^2 e^{-j2\phi_a}}{\Gamma_p\Gamma_a - 1}\right] \end{bmatrix} \tag{4.3-2}$$

where A is the attenuation, ϕ_a is the phase shift and Γ_a is the reflection coefficient of the attenuator. Similarly, B is the attenuation, ϕ_p is the phase shift and Γ_p is the reflection coefficient of the phase shifter. When mismatches of these devices are small enough such that they can be neglected ($\Gamma_a = \Gamma_b = 0$), the S-matrix reduces to

$$\left[S^{A/P}_{\text{no mismatch}}\right] = \begin{bmatrix} 0 & ABe^{-j(\phi_a+\phi_p)} \\ ABe^{-j(\phi_a+\phi_p)} & 0 \end{bmatrix} \tag{4.3-3}$$

From this we see that phase shifter loss can be lumped with the attenuator and attenuator phase shift can be lumped with the phase shifter. Interconnecting transmission loss and phase shift can be handled similarly.

In the experiment associated with this project, the S-matrix of the form (4.3-3) was utilized to realize required attenuation and phase shift by the combination of an attenuator and a section of coaxial cable. It is usually difficult to obtain an attenuator with the exact value required for the compensation. One can use precision variable attenuators to obtain exact values. However, they are not practical in a permanent configuration. In the compensation experiment associated with this project a fixed attenuator was chosen to approximate the required attenuation. Then a section of coaxial cable was cut to realize the required phase shift and remaining attenuation.

4.4 Variable Power Divider Network

The variable power divider network compensates for the mutual coupling in a very different way from the other two methods discussed in this report. Unlike the attenuator/phase shifter (Sec. 4.3) or transmission line (Sec. 4.5) networks, the power divider network is itself a feed network. In this compensation technique, the feed network and the compensation network are synthesized simultaneously. Only a knowledge of the S-matrix of the antenna elements is required to solve for the compensation network.

A general representation of a 2-way variable power divider network is shown in Fig. 4.4-1. The network consists of two parts, a variable power divider and a section of transmission line. The amplitude control of the output signal is achieved through power division instead of attenuation. A separate control of phase is necessary since the power dividers are phase balanced. This network has a definite advantage over the attenuator/phase shifter network from an efficiency standpoint since power dividers are ideally lossless.

4.4.1 S-matrix representation of power divider network

In order to solve for the power divider compensation network parameters, it is necessary to know the S-parameters of the network in terms of K, the fraction of input power transmitted to output port 2. We will assume that all input power is split between the two output ports as follows:

$$\begin{aligned} P_1 &= (1 - K)P_{in} \\ P_2 &= KP_{in} \end{aligned} \tag{4.4-1}$$

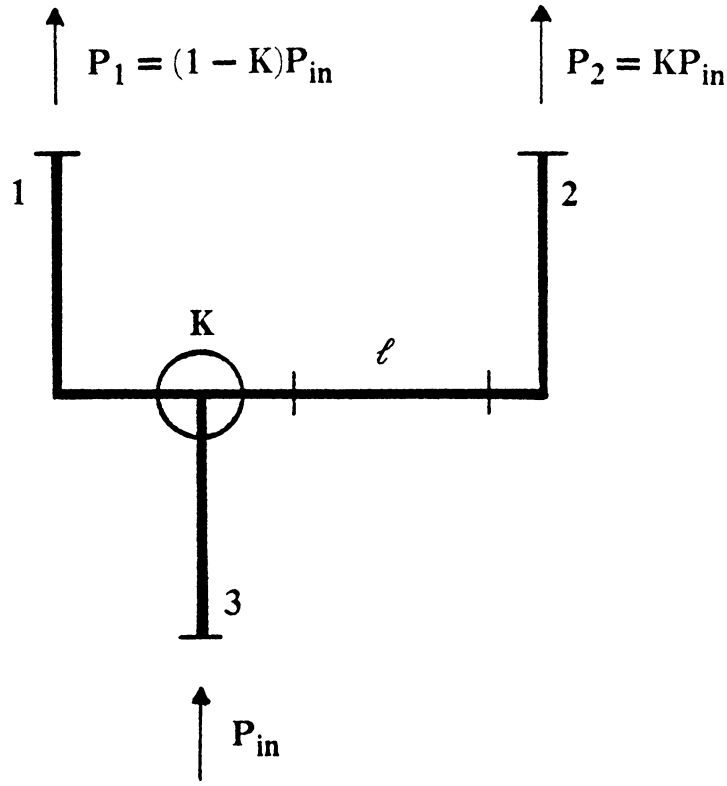

Figure 4.4-1. Graphical representation of the 2-way power divider network.

where P_1 and P_2 are the output powers from port 1 and 2, respectively, and P_{in} is the input power to port 3. The power flowing into port i is related to the wave variables as

$$P_i = a_i a_i^* - b_i b_i^* \tag{4.4-2}$$

Then (4.4-1) can be expressed as

$$\begin{aligned} b_1 b_1^* - a_1 a_1^* &= (1 - K)(a_3 a_3^* - b_3 b_3^*) \\ b_2 b_2^* - a_2 a_2^* &= K(a_3 a_3^* - b_3 b_3^*) \end{aligned} \tag{4.4-3}$$

In general, a three port device such as a 2-way power divider has an S-matrix of the form

$$[S^{PD}] = \begin{bmatrix} S_{11} & S_{12} & S_{13} \\ S_{21} & S_{22} & S_{23} \\ S_{31} & S_{32} & S_{33} \end{bmatrix} \tag{4.4-4}$$

where $[b] = [S^{PD}][a]$. We assume that port 3, the input port, is matched so that $S_{33} = 0$. When port 1 and port 2 are match loaded, $a_1 = 0$ and $a_2 = 0$, (4.4-4) becomes

$$\begin{bmatrix} b_1 \\ b_2 \\ b_3 \end{bmatrix} = \begin{bmatrix} S_{11} & S_{12} & S_{13} \\ S_{21} & S_{22} & S_{23} \\ S_{31} & S_{32} & 0 \end{bmatrix} \begin{bmatrix} 0 \\ 0 \\ a_3 \end{bmatrix} \tag{4.4-5}$$

and (4.4-3) becomes

$$\begin{aligned} b_1 b_1^* &= (1 - K) a_3 a_3^* \\ b_2 b_2^* &= K a_3 a_3^* \end{aligned} \tag{4.4-6}$$

since $b_3 = 0$ from (4.4-5). Using (4.4-6) equation (4.4-5) can be expanded as

$$S_{13} = \frac{b_1}{a_3} = \sqrt{1-K}\, e^{j\phi_{13}}$$
$$S_{23} = \frac{b_2}{a_3} = \sqrt{K}\, e^{j\phi_{23}} \tag{4.4-7}$$

With these results and the application of the reciprocal property of power dividers, (4.4-4) becomes

$$[S^{PD}] = \begin{bmatrix} S_{11} & S_{12} & \sqrt{1-K}\, e^{j\phi_{13}} \\ S_{12} & S_{22} & \sqrt{K}\, e^{j\phi_{23}} \\ \sqrt{1-K}\, e^{j\phi_{13}} & \sqrt{K}\, e^{j\phi_{23}} & 0 \end{bmatrix} \tag{4.4-8}$$

The remaining four S-parameters can be solved for using the unitary property of lossless networks which is

$$\sum_{i=1}^{N} S_{ji} S_{ki}^{*} = \begin{cases} 1 & \text{for } j = k \\ 0 & \text{for } j \neq k \end{cases} \tag{4.4-9}$$

For $j = 1$ and $k = 3$,

$$S_{11}\sqrt{1-K}\, e^{j\phi_{13}} + S_{12}\sqrt{K}\, e^{j\phi_{23}} = 0 \tag{4.4-10}$$

Solving for S_{12} gives

$$S_{12} = -\frac{S_{11}\sqrt{1-K}}{\sqrt{K}}\, e^{j(\phi_{13} - \phi_{23})} \tag{4.4-11}$$

Next, for $j = k = 1$ in (4.4-9),

$$S_{11}S_{11}^{*} + S_{12}S_{12}^{*} + 1 - K = 1 \tag{4.4-12}$$

Substituting (4.4-11) into this gives

$$S_{11}S_{11}^* + \left[-\frac{S_{11}\sqrt{1-K}}{\sqrt{K}} \; e^{j(\phi_{13}-\phi_{23})} \right] \left[-\frac{S_{11}^*\sqrt{1-K}}{\sqrt{K}} \; e^{-j(\phi_{13}-\phi_{23})} \right] = K$$

$$S_{11}S_{11}^* + \frac{1-K}{K} S_{11}S_{11}^* = K$$

$$KS_{11}S_{11}^* + (1-K)S_{11}S_{11}^* = K^2$$

$$S_{11}S_{11}^* = K^2$$

$$S_{11} = Ke^{j\phi_{11}} \tag{4.4-13}$$

Using this in (4.4-11),

$$S_{12} = -\sqrt{K(1-K)}\, e^{j(\phi_{13}+\phi_{11}-\phi_{23})} \tag{4.4-14}$$

Similarly, for $j = k = 2$,

$$S_{12}S_{12}^* + S_{22}S_{22}^* + K = 1 \tag{4.4-15}$$

Using (4.4-14) in this and solving for S_{22},

$$S_{22}S_{22}^* = 1 - K - S_{12}S_{12}^*$$

$$= 1 - K - K(1-K)$$

$$= 1 - 2K + K^2$$

$$= (1-K)^2$$

$$S_{22} = (1-K)e^{j\phi_{22}} \tag{4.4-16}$$

Finally, for j = 2 and k = 3 in (4.4-9) and using (4.4-7) and (4.4-14),

$$S_{21}S_{31}^{*} + S_{22}S_{32}^{*} = 0$$

$$-\sqrt{K}\,(1-K)e^{j(\phi_{11}-\phi_{23})} + (1-K)\sqrt{K}\,e^{j(\phi_{22}-\phi_{23})} = 0$$

$$\phi_{11} - \phi_{23} = \phi_{22} - \phi_{23}$$

$$\phi_{11} = \phi_{22} \tag{4.4-17}$$

Combining the forgoing results of (4.4-13), (4.4-14), (4.4-16) and (4.4-17), the scattering matrix of the 2-way power divider of (4.4-8) becomes

$$[S^{PD}] = \begin{bmatrix} Ke^{j\phi_{11}} & -\sqrt{K(1-K)}\,e^{j(\phi_{11}+\phi_{13}-\phi_{23})} & \sqrt{1-K}\,e^{j\phi_{13}} \\ -\sqrt{K(1-K)}\,e^{j(\phi_{11}+\phi_{13}-\phi_{23})} & (1-K)e^{j\phi_{11}} & \sqrt{K}\,e^{j\phi_{23}} \\ \sqrt{1-K}\,e^{j\phi_{13}} & \sqrt{K}\,e^{j\phi_{23}} & 0 \end{bmatrix} \tag{4.4-18}$$

Adding a section of transmission line of length ℓ to port 2 of the power divider for phase control as indicated in Fig. 4.4-1 yields the complete S-matrix for the variable power divider network

$$[S^{PD}] = \begin{bmatrix} Ke^{j\phi_{11}} & -\sqrt{K(1-K)}\,e^{j(\phi_{11}+\phi_{13}-\phi_{23}-\beta\ell)} & \sqrt{1-K}\,e^{j\phi_{13}} \end{bmatrix}$$

$$\begin{bmatrix} -\sqrt{K(1-K)}\, e^{j(\phi_{11}+\phi_{13}-\phi_{23}-\beta\ell)} & \sqrt{1-K}\, e^{j\phi_{13}} \\ (1-K)e^{j(\phi_{11}-2\beta\ell)} & \sqrt{K}\, e^{j(\phi_{23}-\beta\ell)} \\ \sqrt{K}\, e^{j(\phi_{23}-\beta\ell)} & 0 \end{bmatrix} \tag{4.4-19}$$

4.4.2 Physical realization of the variable power divider

Many types of power dividers using microstrip technology have been discussed in the literature and have been implemented. These power dividers can be categorized into two groups. In 1960 Wilkinson [W-4] implemented an N-way power divider using strip line. Unfortunately, this device provides only equal power split among the output ports. For mutual coupling compensation variable power dividers must be used. Hanna [H-6,H-7] has designed an N-way variable power divider by using a Wilkinson power divider and attenuators. This design has inherent power loss in the network due to attenuators and, thus, is not practical as a power divider compensation network. A general N-way variable power divider does not seem to be practical.

Variable 2-way power dividers, on the other hand, are physically realizable. Branch guide couplers and in-line power dividers discussed by House [H-2], and hybrid ring and modified hybrid ring power dividers [A-8,A-9] are some of the common designs for variable power dividers. In general, these power dividers realize the unequal output power split by the ratio of characteristic impedances of transmission lines in the device. These devices are adequate when the power ratio required is relatively small. In the case of large power split ratio the narrow line width required for the high characteristic impedance or the wide line width required for the low characteristic impedance would be impractical to implement.

The quadrature hybrid power divider discussed by Bailey [B-2] uses the ratio of the length of transmission lines for control of power division. See Fig. 4.4-2. In this device an unequal output power ratio is obtained by exciting the input ports of the quadrature hybrid with signals of equal amplitude but different phases. The phase adjustment is made by varying input line length ℓ_a . Then, the signal at the output ports are the superposition of two input signals. Any desired output signal amplitude ratio can be achieved by selecting the proper phase difference as we now discuss.

Bailey has shown that the transmission line length ℓ_a is related to the output power ratio by

$$\ell_a = \frac{2\ell_b}{\pi} \arctan\sqrt{\frac{P_1}{P_2}} \tag{4.4-20}$$

The output powers at each port are related to the fraction K by (4.4-1). Thus, the length of the line required is expressed in terms of K as

$$\ell_a = \frac{2\ell_b}{\pi} \arctan\sqrt{\frac{1-K}{K}} \tag{4.4-21}$$

When a $\lambda/4$ quadrature hybrid is used ($\ell_b = \lambda/4$), the equation simplifies to

$$\ell_a = \frac{\lambda}{2\pi} \arctan\sqrt{\frac{1-K}{K}} \tag{4.4-22}$$

The value for ℓ_c is discussed in the next subsection.

4.4.3 Verification of power divider network by MCAP

Before we can proceed to synthesis using power divider networks, it is necessary to confirm that the network has acceptable bandwidth. Also, the three phase variables in

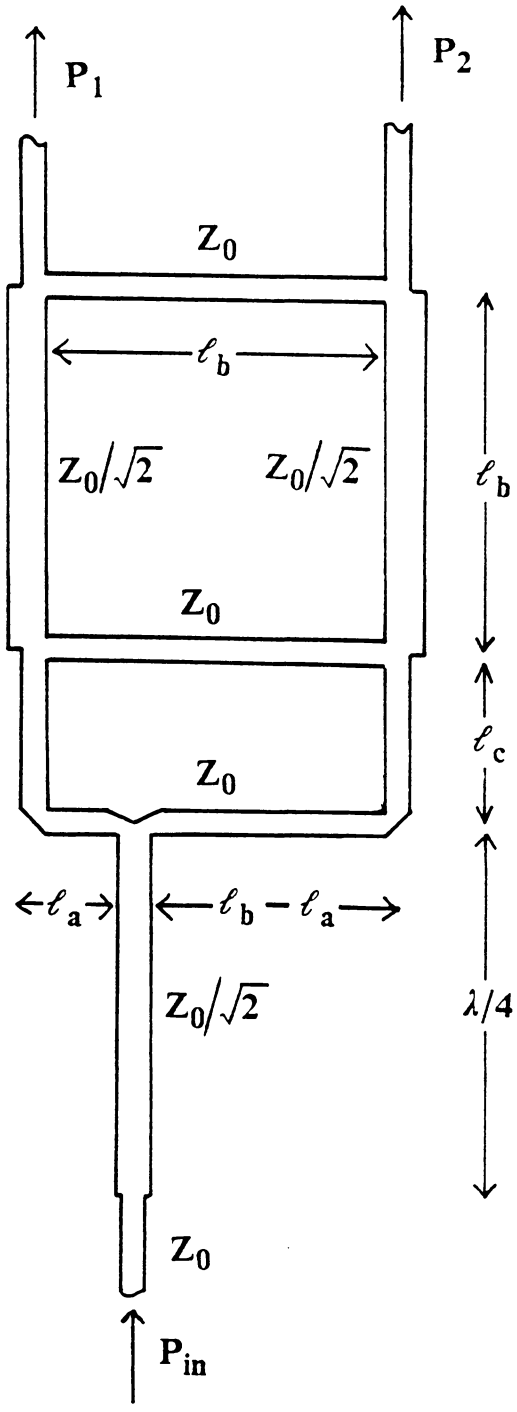

Figure 4.4-2. The quadrature hybrid power divider discussed by Bailey [B-2].

(4.4-18), ϕ_{11}, ϕ_{13} and ϕ_{23}, which depend on the physical configuration of the network must be obtained. We investigated these points using MCAP.

Figures 4.4-3 and 4.4-4 plot the magnitude and phase response of quadrature hybrid power dividers as a function of frequency calculated with MCAP. These power dividers are designed for 2733 MHz center frequency using 1/16 inch substrate with relative dielectric constant $\varepsilon_r = 2.5$. Four cases are considered: 1) K = 0.4, 2) K = 0.25, 3) K = 0.1 and 4) K = 0.01. The magnitude of the computed output power ratio plotted in Fig. 4.4-3 shows that the output remains close to the design values of K over about 10 % bandwidth. One the other hand, the phase plot in Fig. 4.4-4 shows that for the extreme case of K = 0.01 the phase difference between the two output ports deviates from zero for operation off of the design frequency. Thus, some caution must be used when a large power ratio is required for the compensation network.

Next, the phase variables must be determined. In the case of the quadrature hybrid power divider, the length ℓ_c in Fig. 4.4-2 is the only variable undefined. It would be reasonable to assume that the phase variables depend on the line length. Indeed, this is confirmed by MCAP as we now show.

From (4.4-18) the S-matrix for the variable power divider has the following phase components

$$\left[\underline{/S^{PD}}\right] = \begin{bmatrix} \phi_{11} & \pi - \phi_{11} + \phi_{13} - \phi_{23} & \phi_{13} \\ \pi - \phi_{11} + \phi_{13} - \phi_{23} & \phi_{11} & \phi_{23} \\ \phi_{13} & \phi_{23} & 0 \end{bmatrix} \tag{4.4-23}$$

For the case $\beta\ell_c = 0$, the phase of S-parameters are calculated by MCAP as

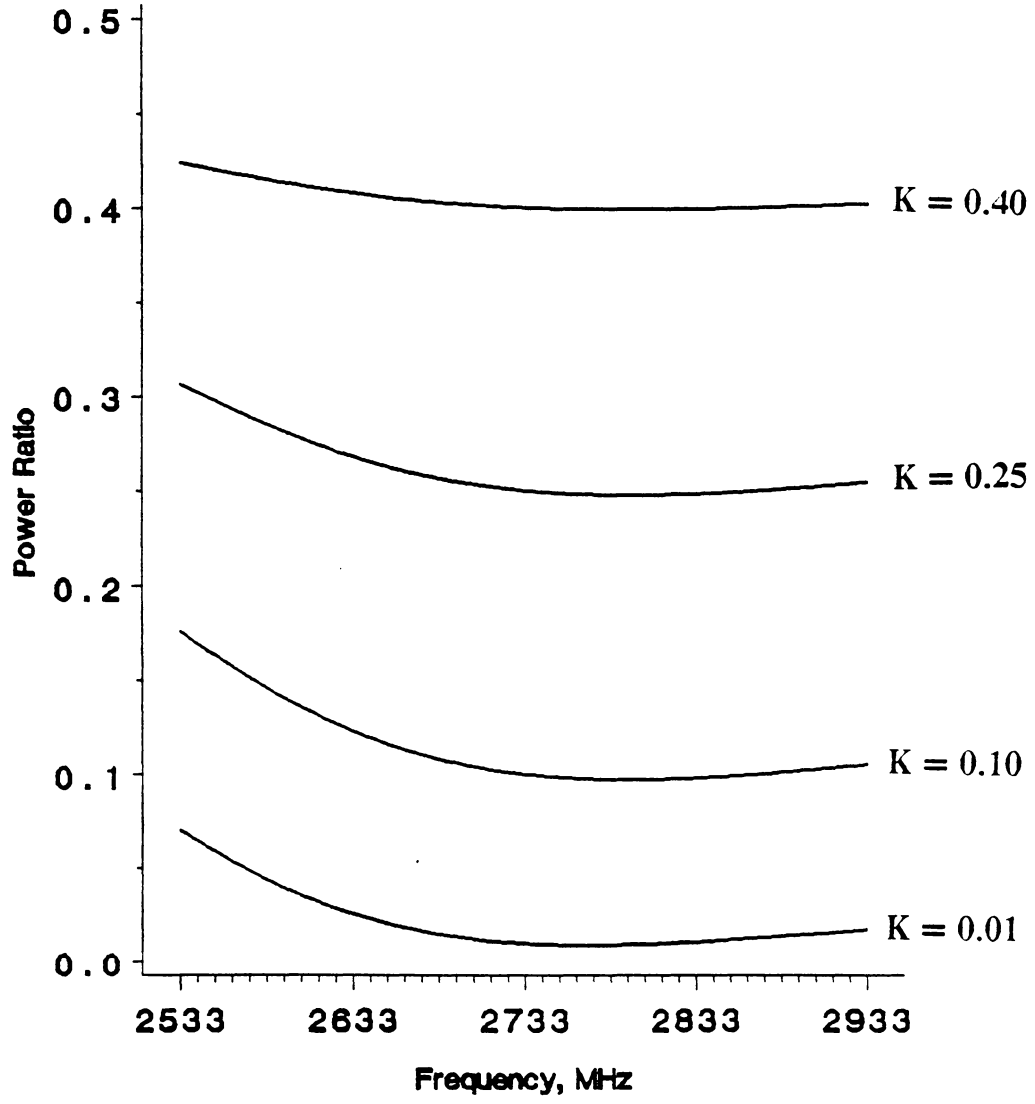

Figure 4.4-3. Magnitude response of the 2-way variable power divider in Fig. 4.4-2 for K = 0.4, K = 0.25, K = 0.1 and K = 0.01 designed for 2733 MHz as a function of frequency. The substrate is 1/16 inch with $\varepsilon_r = 2.5$.

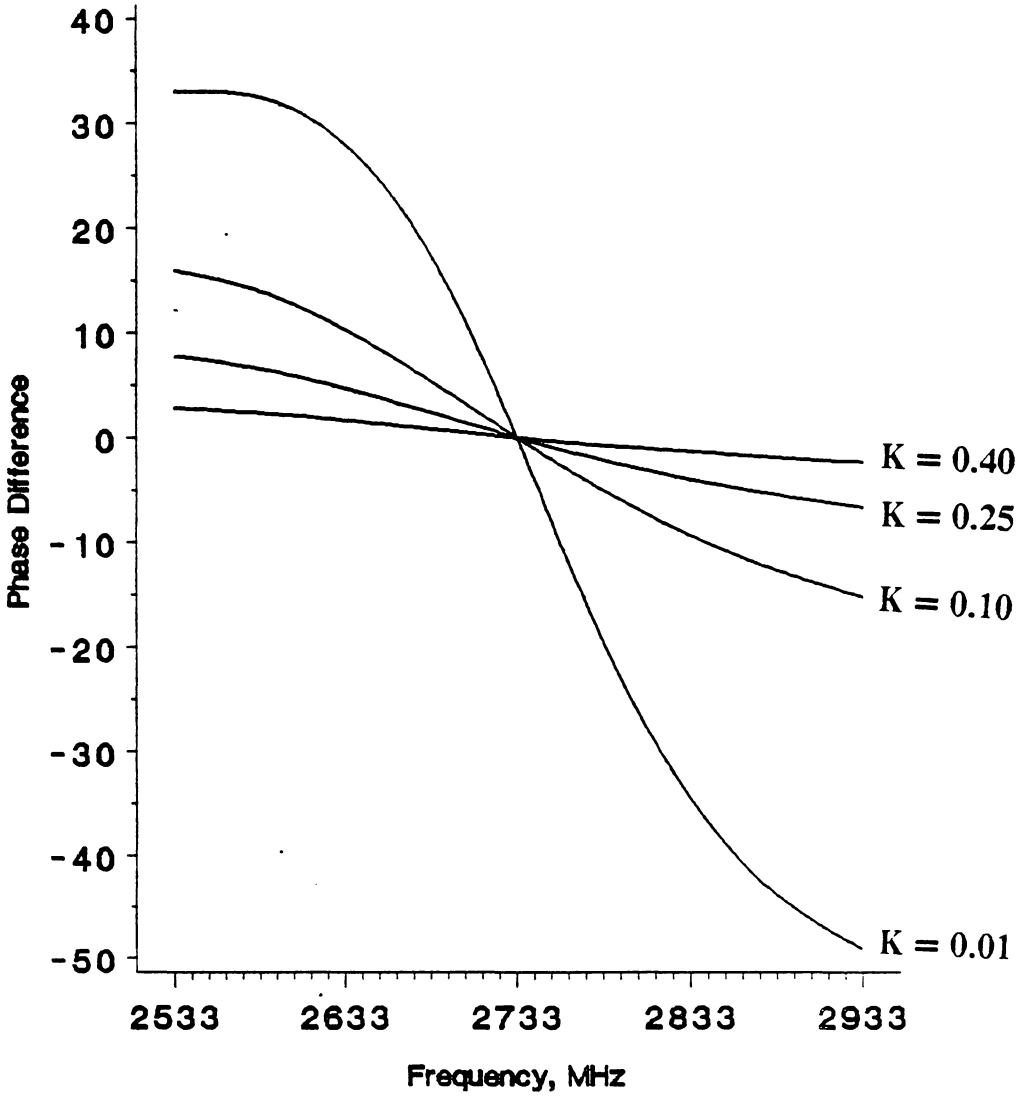

Figure 4.4-4. Phase response of the 2-way variable power divider in Fig. 4.4-2 for $K = 0.4$, $K = 0.25$, $K = 0.1$ and $K = 0.01$ designed for 2733 MHz as a function of frequency. The substrate is 1/16 inch with $\varepsilon_r = 2.5$.

$$\left[\underline{/S^{PD}}\right]_{\beta\ell_c=0} = \begin{bmatrix} 0 & \pi & \frac{\pi}{2} \\ \pi & 0 & \frac{\pi}{2} \\ \frac{\pi}{2} & \frac{\pi}{2} & 0 \end{bmatrix} \tag{4.4-24}$$

Equating (4.4-24) with (4.4-23) it is seen that

$$\begin{aligned} \phi_{11} &= 0 \\ \phi_{13} &= \pi/2 \qquad \text{for } \beta\ell_c = 0 \\ \phi_{23} &= \pi/2 \end{aligned} \tag{4.4-25}$$

For $\beta\ell_c = \frac{\pi}{2}$,

$$\left[\underline{/S^{PD}}\right]_{\beta\ell_c=\frac{\pi}{2}} = \begin{bmatrix} -\pi & 0 & 0 \\ 0 & -\pi & 0 \\ 0 & 0 & 0 \end{bmatrix} \tag{4.4-26}$$

and

$$\begin{aligned} \phi_{11} &= -\pi \\ \phi_{13} &= 0 \qquad \text{for } \beta\ell_c = \frac{\pi}{2} \\ \phi_{23} &= 0 \end{aligned} \tag{4.4-27}$$

Comparing between (4.4-25) and (4.4-27) it is seen by inspection that

$$\begin{aligned} \phi_{11} &= -2\beta\ell_c \\ \phi_{13} &= \frac{\pi}{2} - \beta\ell_c \\ \phi_{23} &= \frac{\pi}{2} - \beta\ell_c \end{aligned} \tag{4.4-28}$$

Using the above result in (4.4-19), the S-matrix for the variable power divider network can be rewritten as

$$[S^{PD}] = \begin{bmatrix} Ke^{-j2\beta\ell_c} & -\sqrt{K(1-K)}\,e^{-j\beta(2\ell_c+\ell)} & \sqrt{1-K}\,e^{j(\frac{\pi}{2}-\beta\ell_c)} \\ -\sqrt{K(1-K)}\,e^{-j\beta(2\ell_c+\ell)} & (1-K)e^{-j2\beta(\ell_c+\ell)} & \sqrt{K}\,e^{j(\frac{\pi}{2}-\beta(\ell_c+\ell))} \\ \sqrt{1-K}\,e^{j(\frac{\pi}{2}-\beta\ell_c)} & \sqrt{K}\,e^{j(\frac{\pi}{2}-\beta(\ell_c+\ell))} & 0 \end{bmatrix} \quad (4.4\text{-}29)$$

We see from this result that ℓ_c acts to control the phase at both output ports 1 and 2.

4.5 Transmission Line Network

The third device considered for the mutual coupling compensation network was a section of transmission line. In this technique the transmission line is placed between the feed and the array networks as in attenuator/phase shifter compensation. The form of the S-matrix, however, is quite different in the two cases. Unlike the attenuator/phase shifter case, a section of transmission line cannot be matched to the array network and the feed network unless its characteristic impedance is the same as that of the networks. Thus, for this technique both the transmission coefficient and the reflection coefficient must be considered, even for an ideal line.

Figure 4.5-1 shows a typical microstrip line with characteristic impedance Z and length ℓ. Smith [S-1] has shown that this general line has the S-matrix

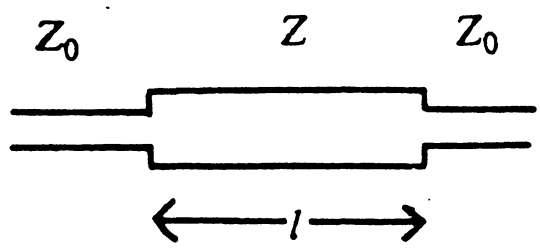

Figure 4.5-1. Transmission line characteristic impedance network.

$$[S^{TL}] = \begin{bmatrix} \Gamma & T \\ T & \Gamma \end{bmatrix} \tag{4.5-1}$$

where

$$\Gamma = \text{reflection coefficient} = \frac{j \sin \beta\ell (Z^2 - Z_0^2)}{2ZZ_0 \cos \beta\ell + j(Z^2 + Z_0^2) \sin \beta\ell} \tag{4.5-2}$$

and

$$T = \text{transmission coefficient} = \frac{2ZZ_0}{2ZZ_0 \cos \beta\ell + j(Z^2 + Z_0^2) \sin \beta\ell} \tag{4.5-3}$$

Z_0 in the above equations is the normalization impedance of the feed network and the antenna array. In microstrip networks $Z_0 = 50\Omega$ is usually used.

There are many empirical equations that relate the characteristic impedance of a microstrip line to the physical dimensions of the line. The expressions given by Wheeler [W-5] and Schneider [S-11] are

$$Z_0 = \begin{cases} \dfrac{60}{\sqrt{\varepsilon_{re}}} \ln\left(\dfrac{8h}{W} + \dfrac{W}{4h}\right) & \text{for } W/h \le 1 \\ \dfrac{120\pi}{\sqrt{\varepsilon_{re}}} \left[\dfrac{W}{h} + 1.393 + 0.667 \ln\left(\dfrac{W}{h} + 1.444\right)\right]^{-1} & \text{for } W/h > 1 \end{cases} \tag{4.5-4}$$

where W is the microstrip line width and h is the substrate height as illustrated on Fig. 4.5-2. The effective relative dielectric constant is given by [W-5]

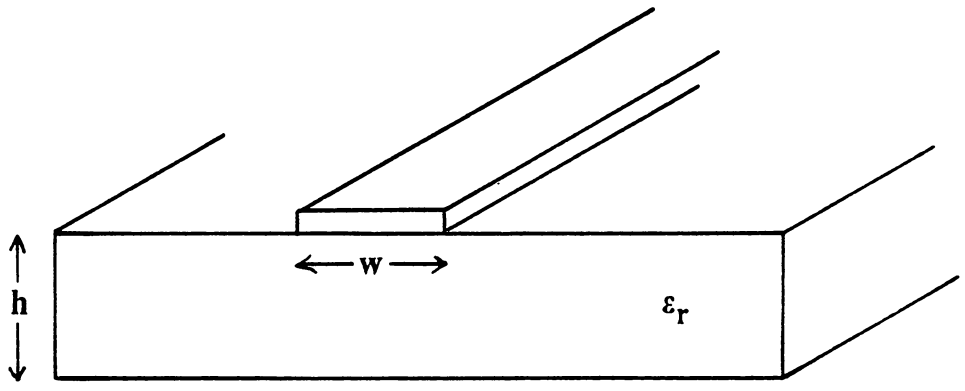

Figure 4.5-2. The geometry of a microstrip line.

$$\varepsilon_{re} = \frac{\varepsilon_r + 1}{2} + \frac{\varepsilon_r - 1}{2}\left(1 + \frac{10h}{W}\right)^{-1/2} \tag{4.5-5}$$

These two expressions are reported to have a relative error of less than two percent [G-1].

There are many other two port networks which can be used in place of the transmission line as a compensation network. We have considered four other passive networks: series impedance network, shunt admittance network, shunt connected open ended stub network and shunt connected short circuited stub network. These networks are shown in Fig. 4.5-3. The expressions for the transmission coefficients and the reflection coefficients of these networks are given by Gupta [G-1]. For the series impedance network,

$$\Gamma^{SI} = \frac{Z}{Z + 2Z_0} \tag{4.5-6}$$

and

$$T^{SI} = \frac{2Z_0}{Z + 2Z_0} \tag{4.5-7}$$

Where Z is the impedance of a component connected in series. The shunt admittance network has very similar expressions as the above two:

$$\Gamma^{SA} = \frac{-Y}{Y + 2Y_0} \tag{4.5-8}$$

$$T^{SA} = \frac{2Y_0}{Y + 2Y_0} \tag{4.5-9}$$

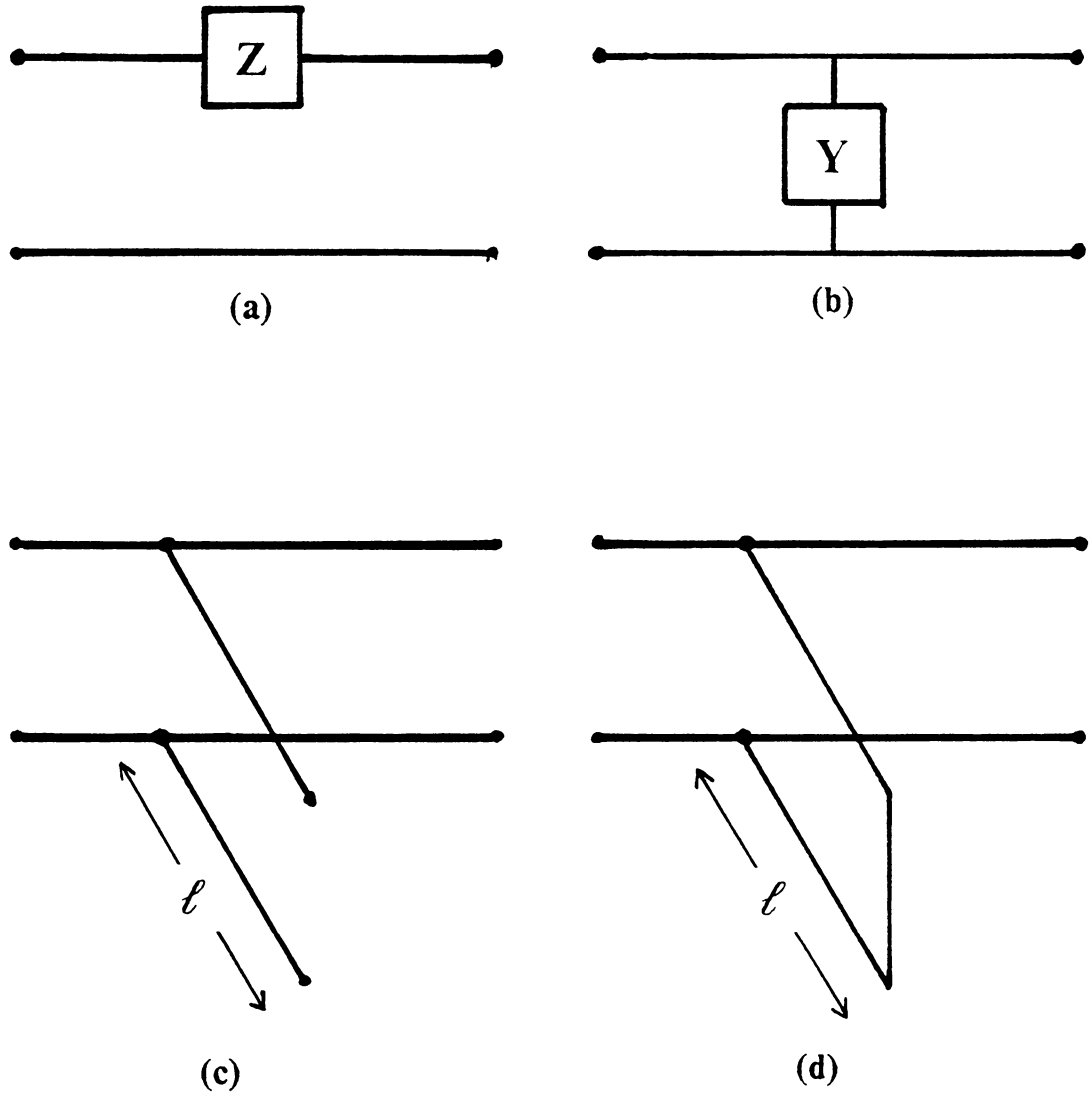

Figure 4.5-3. Four other networks considered: a) a series impedance network, b) a shunt admittance network, c) a shunt connected open ended stub and d) a shunt connected short circuited stub.

where Y is the admittance of a component connected in shunt with the ports. As in the case of first two networks the shunt connected open ended stub and the shunt connected short circuited stub have similar expressions for the reflection coefficients and the transmission coefficients. For the former network the coefficients are given by

$$\Gamma^{OS} = \frac{Z_0 \tan \beta\ell}{-Z_0 \tan \beta\ell + j2Z} \tag{4.5-10}$$

and

$$T^{OS} = \frac{j2Z}{-Z_0 \tan \beta\ell + j2Z} \tag{4.5-11}$$

where the stub has the characteristic impedance Z and the length ℓ . For the latter network,

$$\Gamma^{SS} = \frac{Z_0}{Z_0 + jZ \tan \beta\ell} \tag{4.5-12}$$

$$T^{SS} = \frac{j2Z \tan \beta\ell}{Z_0 + j2Z \tan \beta\ell} \tag{4.5-13}$$

where Z and ℓ are defined as before.

V. Compensation with an Attenuator/Phase Shifter Network

5.1 Introduction

In this chapter the system of nonlinear equations derived in Section 2.4 will be solved for a specific compensation network using the S-matrices obtained in the previous chapter. The first type of compensation network considered uses the attenuator/phase shifter network. This technique was discussed extensively by Smith [S-1]. He has successfully solved the equations using computer program Synthesis of Array with Network and Element Coupling (SANE).

In the first stage of a companion experiment at New Mexico State University the attenuator/phase shifter network was used to verify the mutual coupling compensation technique. This network was selected because it is simple to implement and the S-parameters of the compensation network can be easily measured. The attenuator phase shifter network is also the simplest to deal with theoretically.

We begin this chapter with the derivation of nonlinear equations specific to the attenuator/phase shifter compensation network, followed by a discussion of the physical constraints imposed on compensation network variables. Then, the relationship between the generator phase and power efficiency of the attenuator/phase shifter network is shown. Finally, the nonlinear property of attenuator/phase shifter compensation network is demonstrated.

5.2 Nonlinear Equations for an Attenuator/Phase Shifter Network

This section develops a reduced set of nonlinear equations for the attenuator/phase shifter network. The scattering matrix for a single attenuator/phase shifter combination was derived in Section 4.3. The S-matrix of an N element array, $[S^A]$, and the S-matrix of N-way feed network, $[S^F]$, are assumed to be known. Thus, in Fig. 2.4-1 and (2.4-14) and (2.4-15) we are assuming $M = N$. Figure 5.2-1 shows the structure of the compensation network for the N element array. The complex variable X_i represents the combined effect of an attenuator and a phase shifter between port i and port $N+i$. When ideal devices are assumed, the magnitude and the phase of X_i represent an attenuator and a phase shifter, respectively. The S-matrix of this network is given as

$$[S^C] = \begin{bmatrix} [0] & [X^N] \\ [X^N] & [0] \end{bmatrix} \tag{5.2-1}$$

where

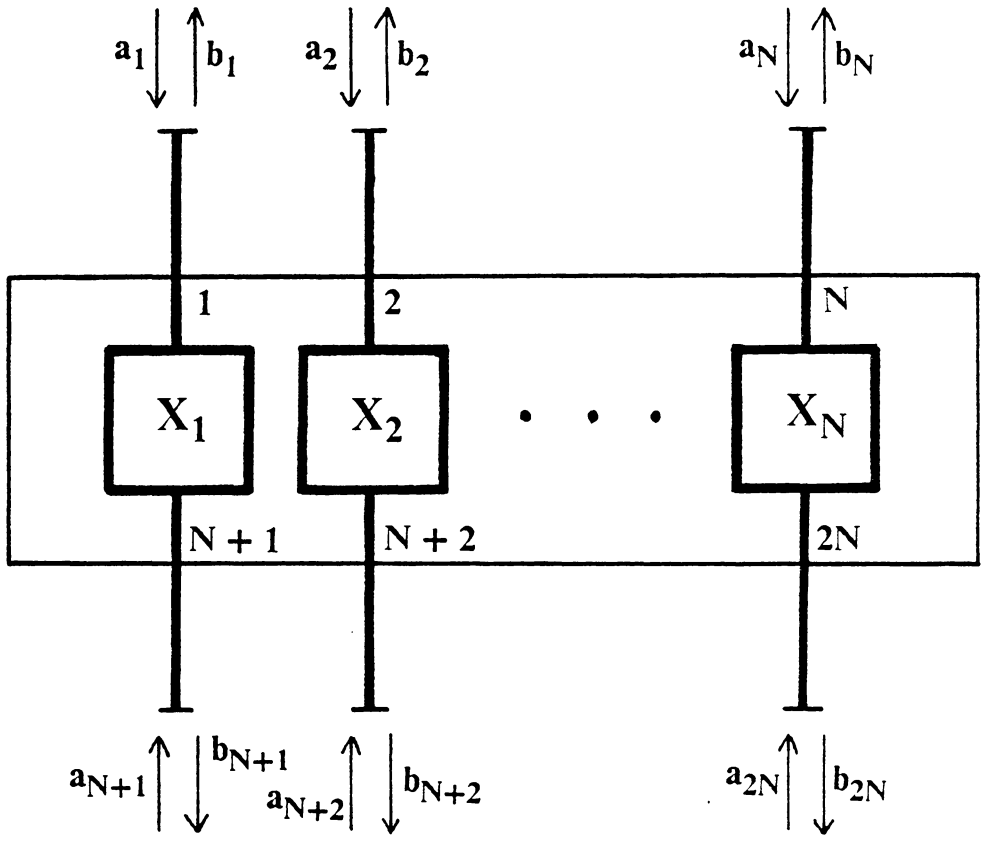

Figure 5.2-1. Attenuator/phase shifter compensation network for an N-element array.

$$[X^N] = \begin{bmatrix} X_1 & 0 & 0 & \dots & 0 \\ 0 & X_2 & 0 & \dots & 0 \\ 0 & 0 & X_3 & \dots & 0 \\ . & . & . & . & . \\ 0 & 0 & 0 & \dots & X_N \end{bmatrix} \tag{5.2-2}$$

Substituting $[S^C]$ into (2.4-15) the equations reduce to

$$\begin{aligned} 0 &= -U_1 + X_1 b_1^A \\ 0 &= -U_2 + X_2 b_2^A \\ &\vdots \\ 0 &= -U_N + X_N b_N^A \end{aligned} \tag{5.2-3}$$

Remember that $\{U_i\}$ are intermediate unknowns representing reflected waves from the compensation network to the feed/generator network. It is clear from the above equations that the variables $\{U_j\}$ are related to the unknowns $\{X_j\}$ by

$$U_j = X_j b_j^A \quad \text{for } j = 1 \dots N \tag{5.2-4}$$

Substituting (5.2-1), (5.2-2) and (5.2-4) into (2.4-14) and noting that $S^C_{k,N+i} = X_i$ for $k = i$ and zero for $k \neq i$ the nonlinear equations become

$$0 = -a_i^A + X_i c_i^{F/G} + \sum_{j=1}^{N} S_{i,j}^{F/G} X_i X_j b_j^A \qquad \text{for } i = 1 \dots N \tag{5.2-5}$$

In the essence, $N + M = 2N$ nonlinear equations have been reduced to N equations due to specific structure of the attenuator/phase shifter scattering matrix $[S^c]$. This result can now be solved using numerical techniques.

Since (5.2-5) imposes no constraint on the range of X_i, it is possible that a solution represents a physically impractical network such as an attenuator with a value greater than unity. Such a network represents gain that requires the use of active components, which increases the complexity of compensation network.

The use of active components can be avoided by reducing the magnitude of attenuators. It is tempting to correct this situation by normalizing the variables. However, this cannot be done because of nonlinear nature of the system of equations [S-1, Sec. 6.2]. Smith has solved this problem in SANE by varying the magnitude of generator G until the largest magnitude of $\{X_i\}$ becomes close to unity within a specified margin. This is accomplished by adding a constraint to the nonlinear equations which can be written as

$$1.0 - \varepsilon < \max\{|X_i|\} \leq 1.0 \tag{5.2-6}$$

where $\varepsilon << 1$. This ensures that the variables $\{X_i\}$ represent attenuation. The left hand side of the inequality eliminates one attenuator from the compensation network by an appropriately small ε . In other words, at most $N - 1$ attenuators and N phase shifters are required to compensate for mutual coupling in an N element array and N-way feed network.

5.3 Relation Between Compensation Parameters and the Generator Phase

The nonlinear equations contain one more variable which can be varied to optimize the compensation network for power efficiency. The variable is the absolute phase of desired element currents. Equivalently, the phase of generator G can be varied to give the same effect. Unlike relative phase differences among element currents which steer main beam, the absolute phase of the currents have no effect on the radiation pattern. However, the solution values for $\{X_i\}$ to (5.2-5) change with the absolute phase, as we now illustrate with an example.

The change in the solution vector with respect to the absolute current phase can be illustrated with a two element array antenna. Consider a two element array with $d = 0.4\lambda_0$ element spacing. Also assume that the elements have -10 dB mutual coupling with $-\beta d$ phase shift, -17 dB mismatch with -90° phase shift, and are fed by an ideal tee as shown in Fig. 5.3-1. The S-matrices of the elements and the feed network are

$$[S^A] = \begin{bmatrix} 0.00000 - j0.14142 & -0.25583 - j0.18587 \\ -0.25583 - j0.18587 & 0.00000 - j0.14142 \end{bmatrix} \tag{5.3-1}$$

$$[S^F] = \begin{bmatrix} -0.50000 & 0.50000 & 0.70711 \\ 0.50000 & -0.50000 & 0.70711 \\ 0.70711 & 0.70711 & 0.00000 \end{bmatrix} \tag{5.3-2}$$

Suppose the desired currents for the array are

$$\begin{aligned} I_1 &= 1.0\underline{/0.0} \\ I_2 &= 1.0\underline{/-90.0} \end{aligned} \tag{5.3-3}$$

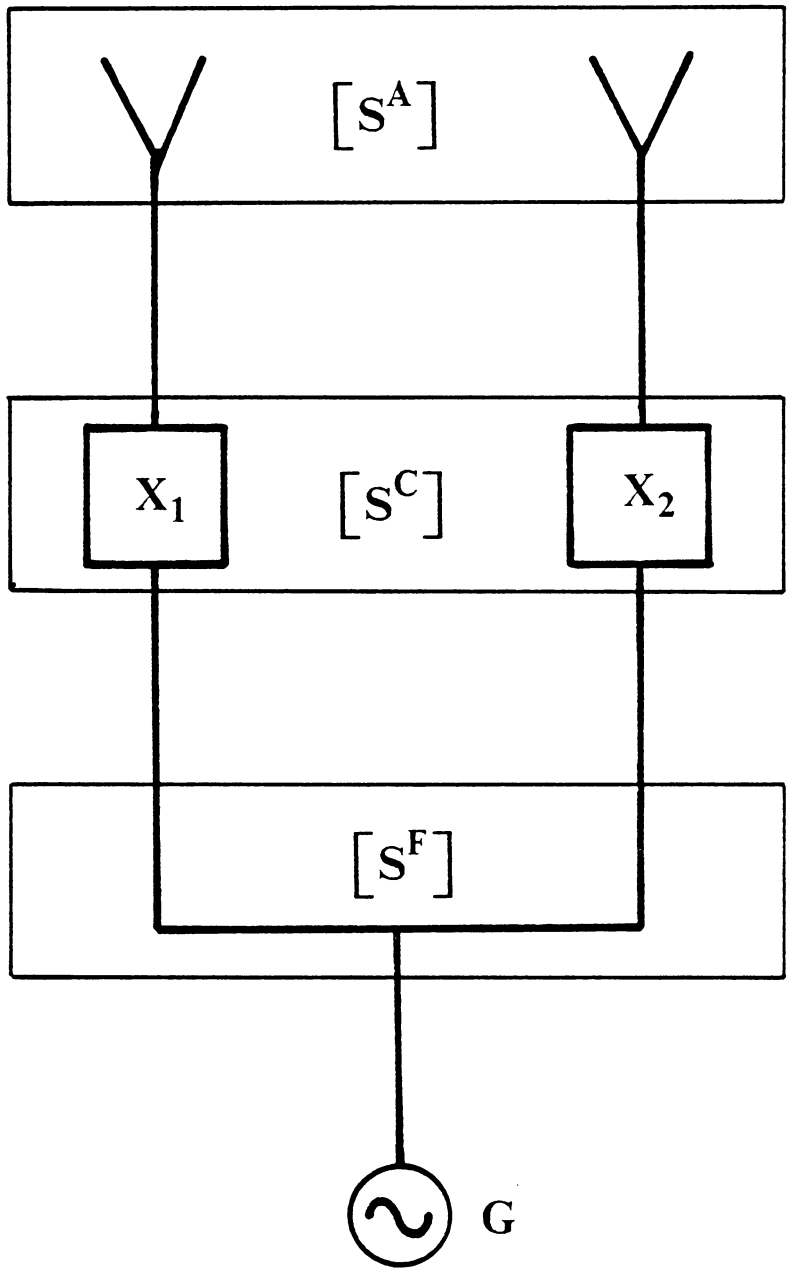

Figure 5.3-1. Two element array antenna example with -10 dB mutual coupling with $-\beta d$ phase shift between antenna elements and -17 dB mismatch with -90° phase shift.

This excitation gives a sum pattern with main beam steered to 51.3° off broadside.

The required compensation network variables were solved using SANE for the generator phase between 0° and 180° for every 5°. Figure 5.3-2 shows the magnitude and phase of variables $\{X_i\}$ with respect to the generator phase. The plots clearly show the variations of $\{X_i\}$ with generator phase. Figure 5.3-3 shows the generator magnitude required to excite the elements at the desired currents while keeping the peak $|X_i|$ at unity; this generator magnitude with the generator phase of Fig. 5.3-2 produces the required element currents (5.3-3). The generator magnitude can be interpreted as being a measure of the efficiency of compensation network, the lowest generator magnitude being most desireable. In the array considered, the compensation network is most efficient at $\underline{/G} \simeq 120°$ because it requires the minimum generator magnitude. On the other hand, the compensation network is least efficient at $\underline{/G} \simeq 45°$. Comparison of Figs. 5.3-2 and 5.3-3 shows that the lowest generator value and the lowest attenuator setting occur together (at the same $\underline{/G}$). This property is seen only for certain 2-element arrays and cannot be generalized for N-element arrays.

The calculated difference in gain from the most efficient to the least efficient compensation networks is 1.9 dB. The difference is small in this case. However, for an array with large number of elements the difference can be significant. For example, an eight element 35 dB Dolph-Chebyshev array used in the experiment (described in Chapter 8) has 4.5 dB difference in gain from the least efficient compensation network to the most efficient.

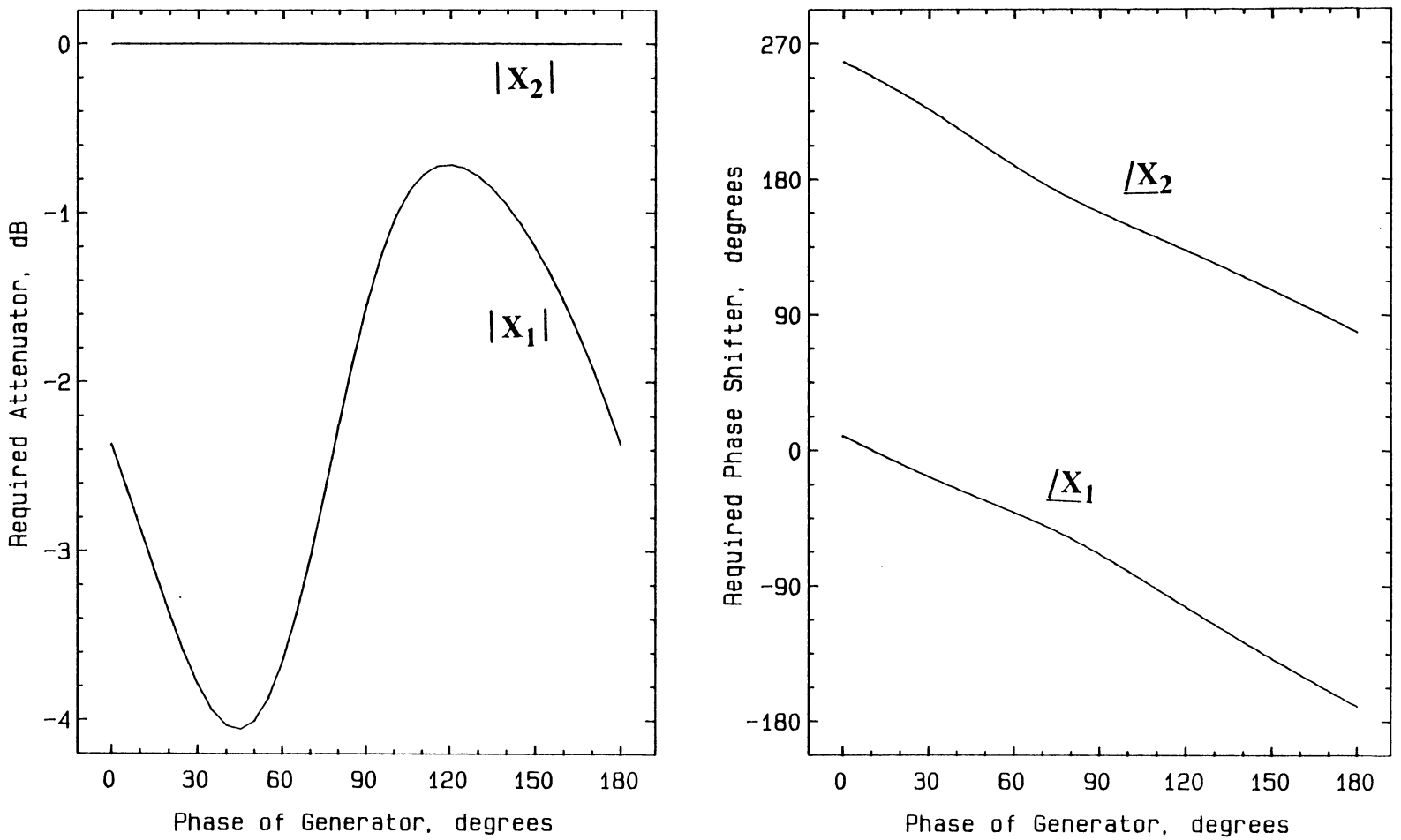

Figure 5.3-2. The magnitude and the phase of compensation network value with respect to the absolute phase of generator for two element array example of Fig. 5.3-1.

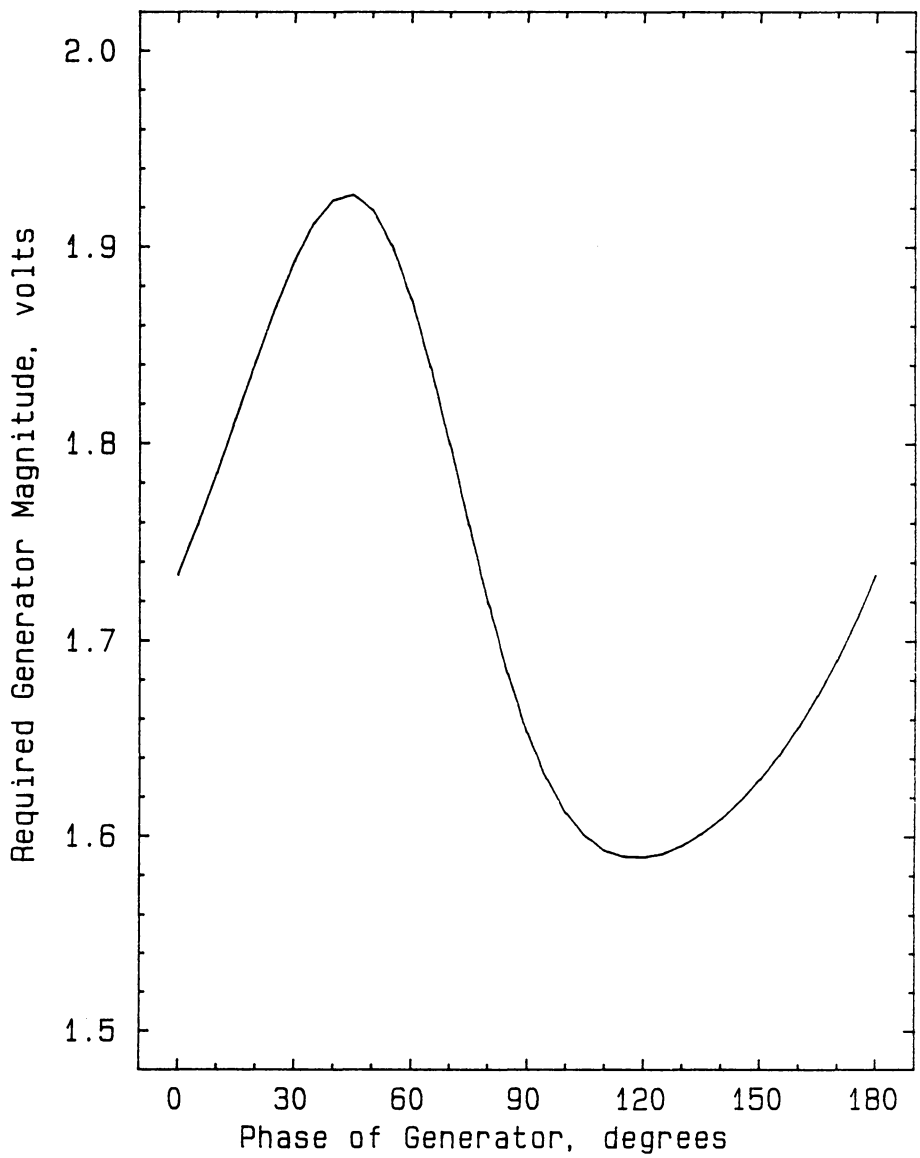

Figure 5.3-3. The required generator magnitude with respect to the absolute phase of the generator for the two element array example of Fig. 5.3-1.

5.4 The Nonlinear Property of Attenuator/Phase Shifter Compensation

In attenuator/phase shifter compensation, the value of compensation variables required for a given antenna array are unpredictable and are often surprising. This phenomenon was shown with a simple numerical example by Smith [S-1, Sec.6.2] and is demonstrated here with a similar example. Consider the array used in the previous section (shown in Fig. 5.3-1) which is represented by the S-matrices (5.3-1) and (5.3-2). Analysis of the array/feed combination using MCAP gives the following element currents:

$$\begin{aligned} I_1 &= 0.91767 \angle 14.61° \\ I_2 &= 0.91767 \angle 14.61° \end{aligned} \tag{5.4-1}$$

These excitations have equal magnitude and equal phase because both the feed and the element coupling are symmetric. Now suppose the desired currents for the array are

$$\begin{aligned} I_1 &= 1.00000 \angle 0.0° \\ I_2 &= 1.00000 \angle -90.0° \end{aligned} \tag{5.4-2}$$

which are the same as in the previous section. This excitation is not symmetric and if realized would give a main beam at $\theta_0 = 51.318°$ from broadside.

Intuitively, one would think that the compensation network requires only $-90°$ phase shift for element 2 since the magnitudes of the uncompensated currents are identical for both elements. According to the plots in Fig. 5.3-2 calculated using SANE, however, an attenuator and a phase shifter are required for the element 1 whereas only a phase shifter is required for the element 2. In addition, the difference in the required

phase shifts between element 1 and element 2 is not 90° . For example, the required compensation variables for $\underline{/G} = 0°$ obtained using SANE are

$$\begin{aligned} X_1 &= 0.76154 \ \underline{/\ 9.80°} \\ X_2 &= 1.00000 \ \underline{/\ 258.32°} \end{aligned} \tag{5.4-3}$$

Clearly, an attenuator is required only for element 1. It is also apparent that the difference in phase shifts is not 90.0° .

The above example demonstrates how the unexpected can happen even for simple arrays. Since this property is not directly apparent, we present a treatment of how the compensation network affects the currents in the antenna element in a step by step fashion for the various coupling mechanism.

In general, the S-matrices of two element array, feed and attenuator/phase shifter compensation networks (see Fig. 5.4-1) can be represented as

$$[S^A] = \begin{bmatrix} S_{11}^A & S_{12}^A \\ S_{21}^A & S_{22}^A \end{bmatrix} \tag{5.4-4}$$

$$[S^F] = \begin{bmatrix} S_{11}^F & S_{12}^F & S_{13}^F \\ S_{21}^F & S_{22}^F & S_{23}^F \\ S_{31}^F & S_{32}^F & S_{33}^F \end{bmatrix} \tag{5.4-5}$$

$$[S^C] = \begin{bmatrix} 0 & 0 & X_1 & 0 \\ 0 & 0 & 0 & X_2 \\ X_1 & 0 & 0 & 0 \\ 0 & X_2 & 0 & 0 \end{bmatrix} \tag{5.4-6}$$

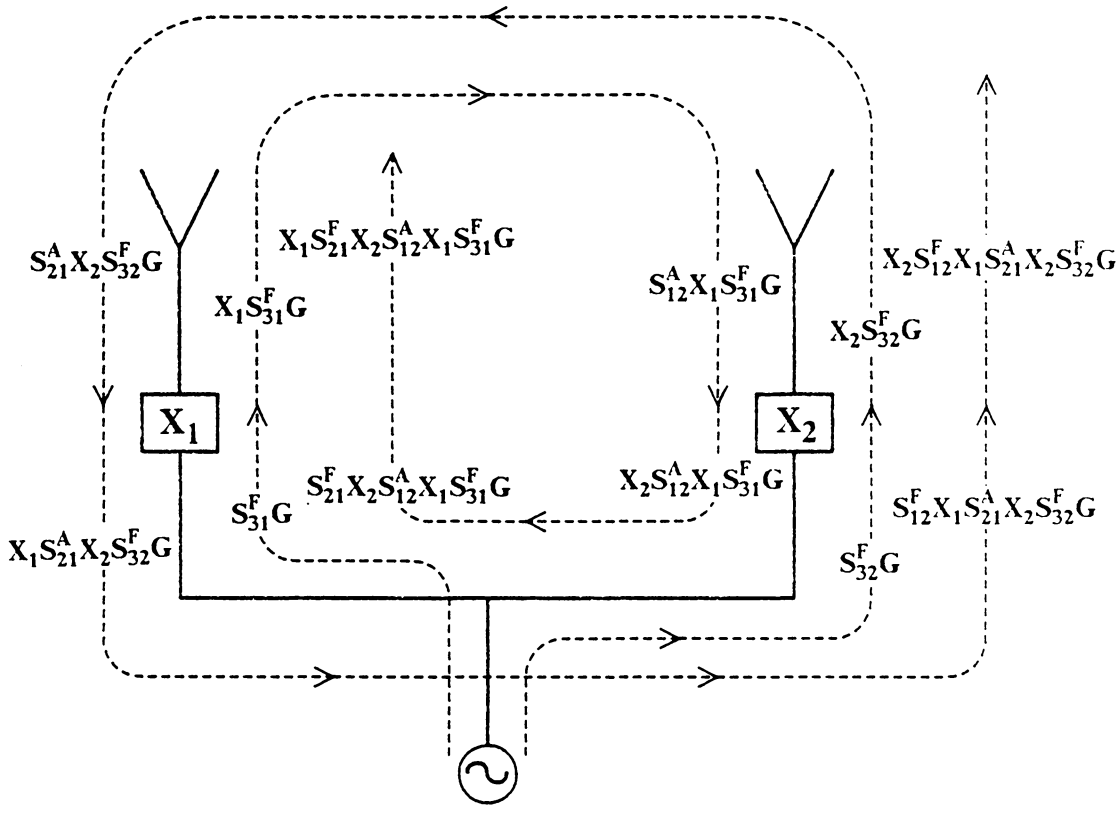

Figure 5.4-1. Current components in a two element array with matched array and feed network.

5.4.1 Matched Case

The nonlinear effect can be demonstrated without including mismatches. In fact, even for the two element case tracing individual signals becomes very involved with reflections present, so we neglect them for this discussion. The compensation network is assumed to be matched to the antenna and to the feed at the respective ports. The generator is also assumed to be matched to the feed. Thus, $S^A_{11} = S^A_{22} = 0$ and $S^F_{11} = S^F_{22} = S^F_{33} = 0$. It is physically impossible for multiport networks other than two port networks to have all ports matched. However, this constraint is neglected in the feed network assumptions to simplify the analysis. Under these assumptions, there will be no reflected waves generated at the junctions between antenna elements and feed, and between feed and generator.

Using the above S-parameters, the current in antenna element 1 can be represented as an infinite sum of circulating currents that are shown in Fig. 5.4-1:

$$\begin{aligned} I_1 &= X_1 S^F_{31} G - S^A_{21} X_2 S^F_{32} G + X_1 S^F_{21} X_2 S^A_{12} X_1 S^F_{31} G - S^A_{21} X_2 S^F_{12} X_1 S^A_{21} X_2 S^F_{32} G + \cdots \\ &= \sum_{n=0}^{\infty} \left(X_1 S^F_{21} X_2 S^A_{12}\right)^n X_1 S^F_{31} G - \left(S^A_{21} X_2 S^F_{12} X_1\right)^n S^A_{21} X_2 S^F_{32} G \end{aligned} \tag{5.4-7}$$

Assume that the antenna and the feed are reciprocal networks.

$$\begin{aligned} S^A_{12} &= S^A_{21} \\ S^F_{12} &= S^F_{21} \end{aligned} \tag{5.4-8}$$

Then, (5.4-7) can be rewritten as

$$
\begin{aligned}
I_1 &= \sum_{n=0}^{\infty}\left(X_1 S_{12}^F X_2 S_{12}^A\right)^n X_1 S_{31}^F G - \left(X_1 S_{12}^F X_2 S_{12}^A\right)^n S_{12}^A X_2 S_{32}^F G \\
&= \sum_{n=0}^{\infty}\left(X_1 S_{12}^F X_2 S_{12}^A\right)^n \left(X_1 S_{31}^F G - S_{12}^A X_2 S_{32}^F G\right) \\
&= \left(X_1 S_{31}^F - X_2 S_{12}^A S_{32}^F\right) G \sum_{n=0}^{\infty}\left(X_1 X_2 S_{12}^F S_{12}^A\right)^n
\end{aligned}
\tag{5.4-9}
$$

Showing the first term of the summation explicitly,

$$
\begin{aligned}
I_1 &= \left(X_1 S_{31}^F - X_2 S_{12}^A S_{32}^F\right) G \left[1 + \sum_{n=1}^{\infty}\left(X_1 X_2 S_{12}^F S_{12}^A\right)^n\right] \\
&= X_1 S_{31}^F G - X_2 S_{12}^A S_{32}^F G + \left(X_1 S_{31}^F - X_2 S_{12}^A S_{32}^F\right) G \sum_{n=1}^{\infty}\left(X_1 X_2 S_{12}^F S_{12}^A\right)^n
\end{aligned}
\tag{5.4-10}
$$

The current at element 2 can also be expressed in similar way.

$$
I_2 = X_2 S_{32}^F G - X_1 S_{21}^A S_{31}^F G + \left(X_2 S_{32}^F - X_1 S_{21}^A S_{31}^F\right) G \sum_{n=1}^{\infty}\left(X_1 X_2 S_{12}^F S_{12}^A\right)^n \tag{5.4-11}
$$

These current expressions consist of three terms:

$$
I = I_{\text{ideal}} - I_{\text{antenna coupling}} + I_{\text{full coupling}} \tag{5.4-12}
$$

where

$$
I_{1\ \text{ideal}} = X_1 S_{31}^F G \tag{5.4-13}
$$

$$
I_{1\ \text{antenna coupling}} = X_2 S_{12}^A S_{32}^F G \tag{5.4-14}
$$

$$I_{1\ \text{full coupling}} = (X_1 S_{31}^F - X_2 S_{12}^A S_{32}^F) G \sum_{n=1}^{\infty} (X_1 X_2 S_{12}^F S_{12}^A)^n \tag{5.4-15}$$

for the current in element 1.

The first term I_{ideal} is the current (in the case of element 1) that would be present in element 1 if no mutual coupling were present anywhere in the system. This current is directly proportional to the coupling from input to output of the feed network (represented by S_{31}^F for element 1 and S_{32}^F for the element 2), and to the magnitude of generator, G. This ideal current can be changed by the attenuator and phase shifter values in a linear fashion (i.e. 1 dB increase in attenuation reduces the output currents by 1 dB).

$I_{\text{antenna coupling}}$ is the contribution to the current (in the case of element 1) from antenna element 2 through antenna coupling. It is the current contribution when there is mutual coupling between antenna elements but no coupling exists in the feed. This is similar to the case of independent generator excitation as discussed in Sec. 2.3.1. The actual element current in such a system is the sum of I_{ideal} and $-I_{\text{antenna coupling}}$. $I_{\text{antenna coupling}}$ is a negative current because it circulates in the opposite direction from I_{ideal}. In this case, the equations (5.4-13) and (5.4-14) show a linear dependence on unknown $\{X_i\}$. Thus, the compensation network can be calculated by simply solving a system of linear equations.

For the third component, $I_{\text{full coupling}}$, to be nonzero the two output ports of the feed network must not be isolated from each other; i.e., $S_{12}^F = S_{21}^F \neq 0$. The coupling between these two ports introduces a feedback loop in the system which makes the current a nonlinear function of compensation variables. This is seen in (5.4-15) by the presence

of the products X_1X_2. Obviously this term is not present if either antenna coupling,$S^A_{12,}$ or feed coupling,$S^F_{12,}$ is zero.

5.4.2 Comment on generator excitation dependence

It should be noted that the required attenuator variation with respect to the generator phase as discussed in the previous section does not occur in this particular array. For example, suppose the two element array in Fig. 5.3-1 has matched feed and element ports. The desired element currents are those of (5.3-1). The requireed compensation variables as with respect to generator phase calculated from SANE are shown in Fig. 5.4-2. Clearly, the required attenuators values remain constant as the generator phase is varied. The required phase shifters, on the other hand, show the dependence to the generator phase similar to the case in the previous section. The efficiency of the compensation network also varies with respect the generator phase. This is demonstrated in a plot of the required generator magnitude versas the generator phase shown in Fig. 5.4-3.

This phenomena, however, cannot be generalized to array with larger number of elements. In the case of a N-element array, the generator phase effect on the attenuator values can be observed even when all the elements and feed ports are matched.

5.4.3 Mismatched case

The preceding current analysis assumed that all network components are matched. When mismatches are introduced, the incident waves at each junction will be split to two components; reflected and transmitted waves. Thus, the current expression cannot be written in simple summation form. However, it can be generalized from the matched case

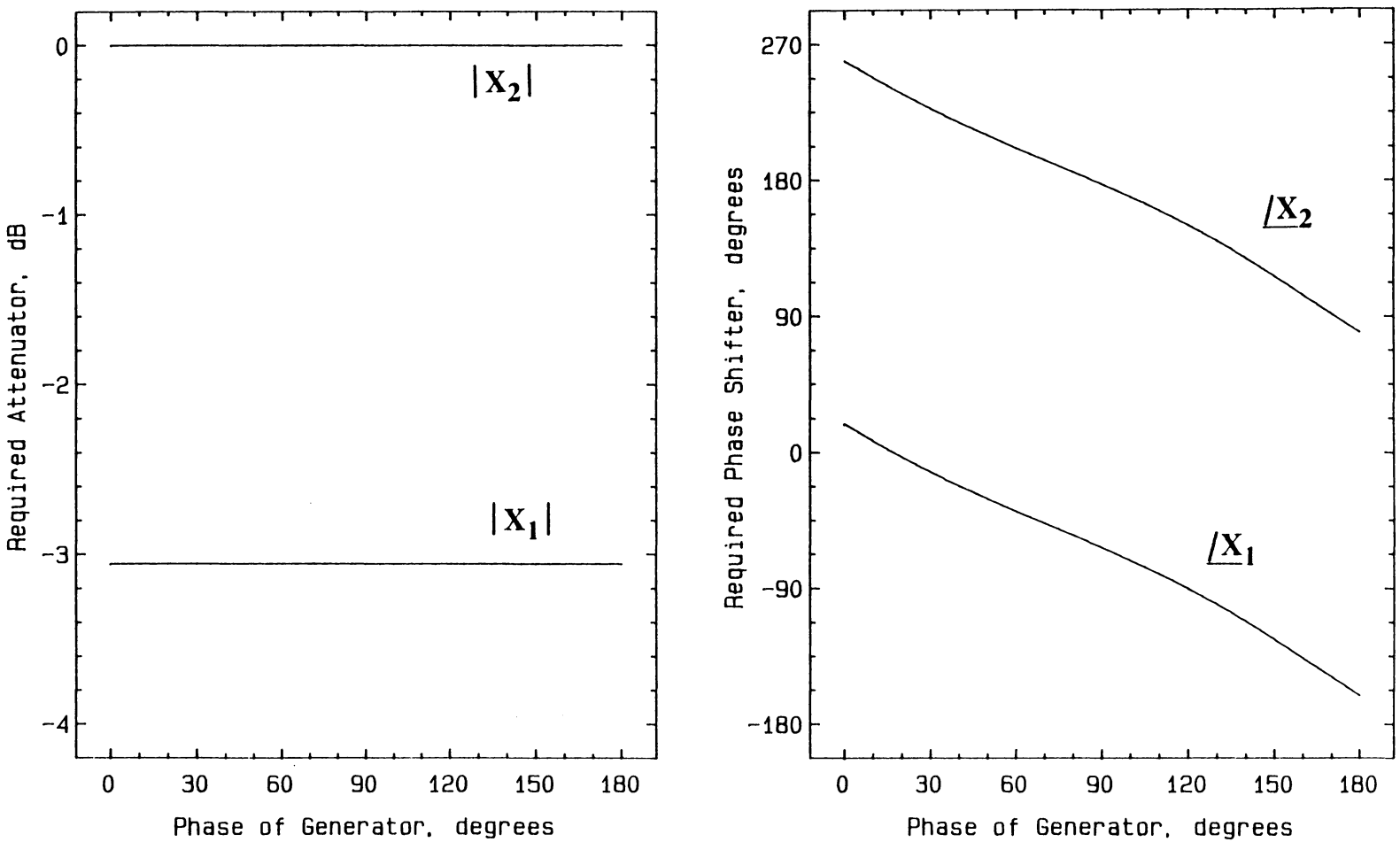

Figure 5.4-2. The magnitude and the phase of compensation network value with respect to the absolute phase of generator for two element array with matched elements and feed ports.

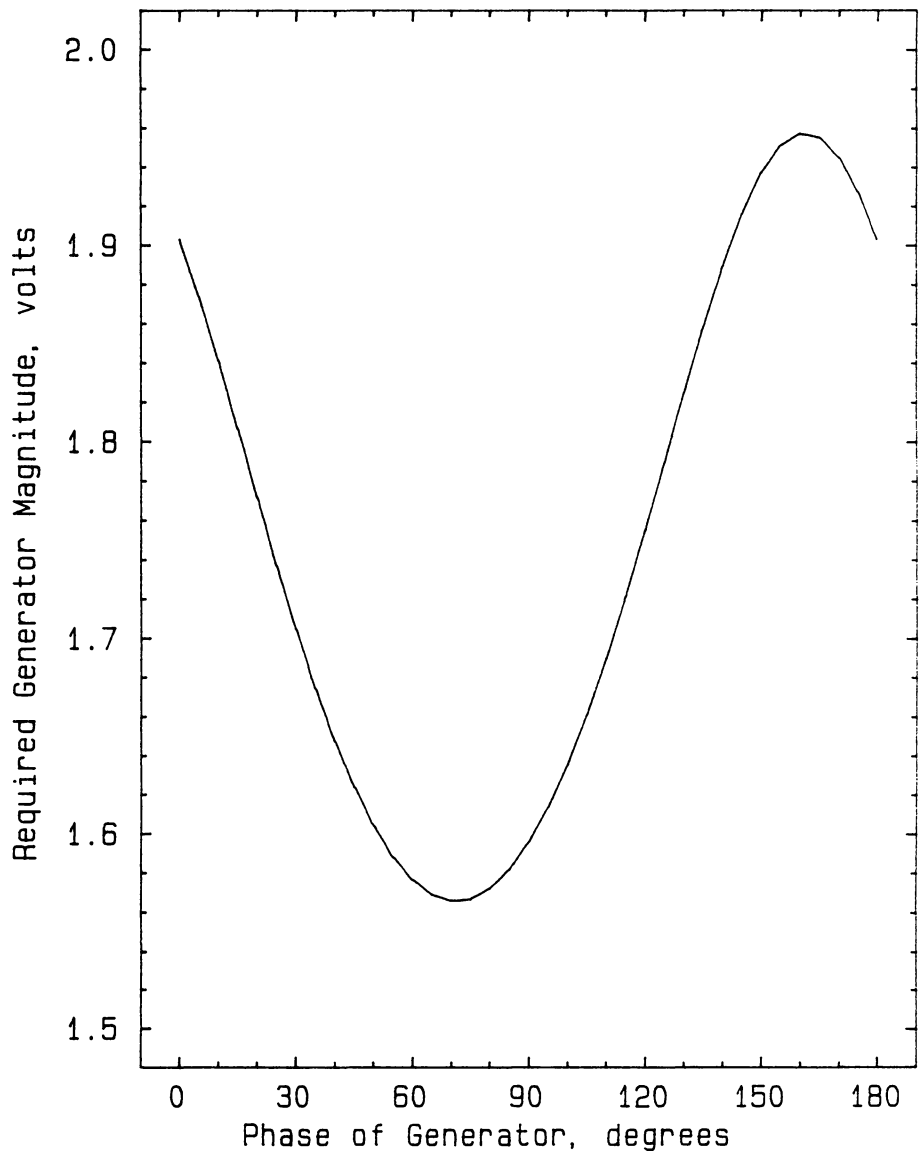

Figure 5.4-3. The required generator magnitude with respect to the absolute phase of the generator for the two element array with matched element and feed ports.

that even in the unmatched case nonlinearly will occur when feed network coupling is present.

VI. Synthesis with a Power Divider Network

6.1 Introduction

The second type of compensation technique considered uses a variable power divider network. Smith [S-1] has originally treated this problem using the general nonlinear equations of (2.4-14) and (2.4-15). These equations were solved by Smith using computer program SANE-GECON, Synthesis of Array with Network and Element Coupling for General Compensation Network [S-1]. Though the solution vectors were found for different cases of mutual coupling and desired element excitation, the program converged with difficulty. Convergence problems are common in the solution of nonlinear equations. As we found with the attenuator/phase shifter compensation network in Chapter 5, a general solution technique cannot be applied directly to solve the nonlinear equations. We must include the specific nature and the physical constraints of the compensation network before solution is attempted.

In this chapter we first present three preparatory steps necessary to solve for the power divider compensation network using numerical techniques. First, the

S-parameters of an N-way power divider are derived. Then the nonlinear equations are simplified for the power divider network. Finally, the initial guess for the solution vector which plays important role in the numerical technique is discussed.

The steps described in this chapter were used to develop the computer program SANE-PODCON, Synthesis of Array with Network and Element Coupling for Power Divider Compensation Network; see Appendix B for the details. This program converges much faster than SANE-GECON for various cases of mutual coupling.

6.2 N-way Power Divider

Before we can proceed with the synthesis of the power divider network, it is necessary to look at the implementation of an N-way power divider. We choose a power divider built up from 2-way power dividers. This is done because only 2-way variable power dividers are available (see Sec. 4.4.2). In this section, the S-matrix of a 4-way power divider is derived from known results for 2-way power dividers. Then, the result is generalized to the S-matrix for N-way power dividers.

6.2.1 S-matrix representation of a 4-way power divider

The 4-way power divider is modeled from three 2-way power dividers as shown on Fig. 6.2-1. S-matrix representation of a 4-way power divider can be obtained from the S-matrices of 2-way power dividers using the matrix connection technique discussed in Section 2.1. The 2-way power dividers are represented by $[S^{(2)L}]$, $[S^{(2)R}]$ and $[S^{(2)C}]$ for the left, the right and the center power divider, respectively. The superscript (2) in the

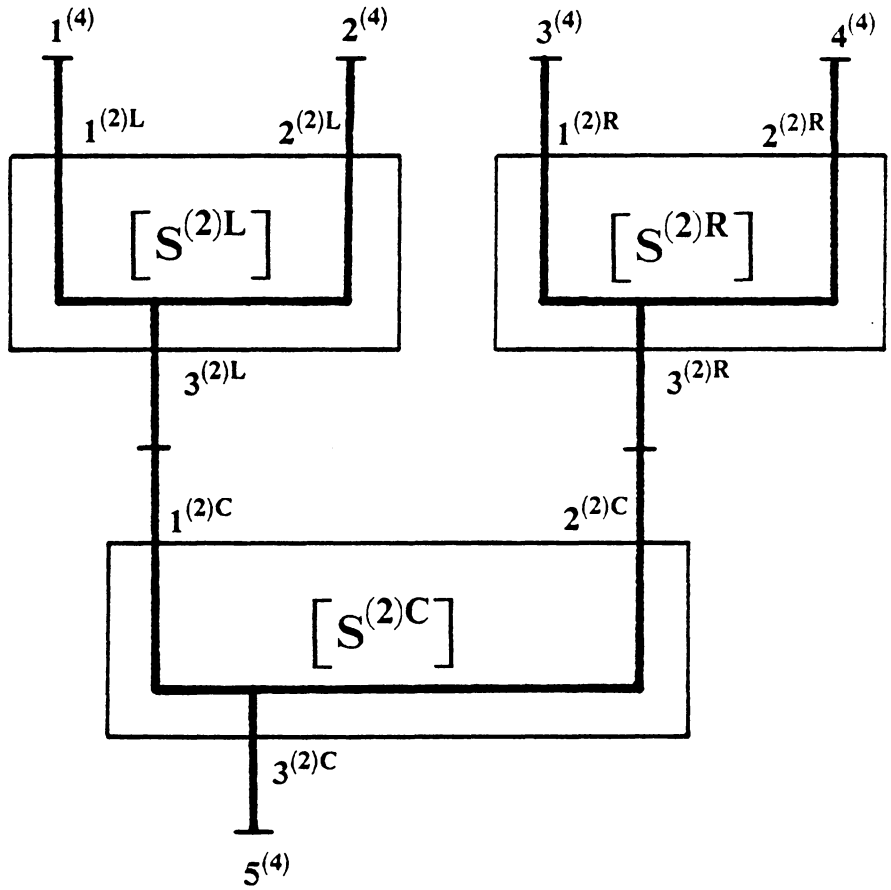

Figure 6.2-1. Implementation of a 4-way power divider network from three 2-way power divider networks.

notation indicates a 2-way power divider. These matrices are of the form (4.4-18) and they can be realized as discussed in Section. 4.4.2.

The combined S-matrix for the 4-way power divider is

$$[S^{(4)}] = \begin{bmatrix} [S^{(2)L}] & 0 & 0 \\ 0 & [S^{(2)R}] & 0 \\ 0 & 0 & [S^{(2)C}] \end{bmatrix} \tag{6.2-1}$$

Rearranging the S-parameters for the internal and external ports gives

$$[S^{(4)}] = \begin{bmatrix} S_{PP} & S_{PC} \\ S_{CP} & S_{CC} \end{bmatrix}$$

$$= \left[\begin{array}{ccccc|cccc} S_{11}^{(2)L}S_{21}^{(2)L} & 0 & 0 & 0 & 0 & S_{13}^{(2)L} & 0 & 0 & 0 \\ S_{21}^{(2)L}S_{22}^{(2)L} & 0 & 0 & 0 & 0 & S_{23}^{(2)L} & 0 & 0 & 0 \\ 0 & 0 & S_{11}^{(2)R}S_{12}^{(2)R} & 0 & & 0 & S_{13}^{(2)R} & 0 & 0 \\ 0 & 0 & S_{21}^{(2)R}S_{22}^{(2)R} & 0 & & 0 & S_{23}^{(2)R} & 0 & 0 \\ 0 & 0 & 0 & 0 & S_{33}^{(2)C} & 0 & 0 & S_{31}^{(2)C}S_{32}^{(2)C} & \\ \hline S_{31}^{(2)L}S_{32}^{(2)L} & 0 & 0 & 0 & 0 & S_{33}^{(2)L} & 0 & 0 & 0 \\ 0 & 0 & S_{31}^{(2)R}S_{32}^{(2)R} & 0 & & 0 & S_{33}^{(2)R} & 0 & 0 \\ 0 & 0 & 0 & 0 & S_{13}^{(2)C} & 0 & 0 & S_{11}^{(2)C}S_{12}^{(2)C} & \\ 0 & 0 & 0 & 0 & S_{23}^{(2)C} & 0 & 0 & S_{21}^{(2)C}S_{22}^{(2)C} & \end{array}\right] \tag{6.2-2}$$

Using the connection technique discussed in Section 2.1, the reduced S-matrix for the 4-way power divider can be calculated from

$$[S^{(4)}] = [S_{PP} + S_{PC}(\Gamma - S_{CC})^{-1}S_{CP}] \tag{6.2-3}$$

where the connection matrix is

$$\Gamma = \begin{bmatrix} 0 & 0 & 1 & 0 \\ 0 & 0 & 0 & 1 \\ 1 & 0 & 0 & 0 \\ 0 & 1 & 0 & 0 \end{bmatrix} \tag{6.2-4}$$

The port numbers corresponding to row/column numbers in Γ are the same as the definition used in the submatrix S_{cc} in (6.2-2). For example, row/column number 1 corresponds to port 3 of the left 2-way power divider. Note from (4.4-18) that a 2-way power divider has a matched input port, so that $S_{33}^{(2)L} = S_{33}^{(2)R} = S_{33}^{(2)C} = 0$. Evaluation of the right hand side of (6.2-3) proceeds as follows:

$$(\Gamma - S_{CC}) = \begin{bmatrix} 0 & 0 & 1 & 0 \\ 0 & 0 & 0 & 1 \\ 1 & 0 & -S_{11}^{(2)C} & -S_{21}^{(2)C} \\ 0 & 1 & -S_{21}^{(2)C} & -S_{22}^{(2)C} \end{bmatrix}$$

$$(\Gamma - S_{CC})^{-1} = \begin{bmatrix} S_{11}^{(2)C} & S_{12}^{(2)C} & 1 & 0 \\ S_{21}^{(2)C} & S_{22}^{(2)C} & 0 & 1 \\ 1 & 0 & 0 & 0 \\ 0 & 1 & 0 & 0 \end{bmatrix}$$

$$S_{PC}(\Gamma - S_{CC})^{-1} = \begin{bmatrix} S_{13}^{(2)L} & 0 & 0 & 0 \\ S_{23}^{(2)L} & 0 & 0 & 0 \\ 0 & S_{13}^{(2)R} & 0 & 0 \\ 0 & S_{23}^{(2)R} & 0 & 0 \\ 0 & 0 & S_{31}^{(2)C} & S_{32}^{(2)C} \end{bmatrix} \begin{bmatrix} S_{11}^{(2)C} & S_{12}^{(2)C} & 1 & 0 \\ S_{21}^{(2)C} & S_{22}^{(2)C} & 0 & 1 \\ 1 & 0 & 0 & 0 \\ 0 & 1 & 0 & 0 \end{bmatrix}$$

$$= \begin{bmatrix} S_{13}^{(2)L}S_{11}^{(2)C} & S_{13}^{(2)L}S_{12}^{(2)C} & S_{13}^{(2)L} & 0 \\ S_{23}^{(2)L}S_{11}^{(2)C} & S_{23}^{(2)L}S_{12}^{(2)C} & S_{23}^{(2)L} & 0 \\ S_{13}^{(2)R}S_{21}^{(2)C} & S_{13}^{(2)R}S_{22}^{(2)C} & 0 & S_{13}^{(2)R} \\ S_{23}^{(2)R}S_{21}^{(2)C} & S_{23}^{(2)R}S_{22}^{(2)C} & 0 & S_{23}^{(2)R} \\ S_{31}^{(2)C} & S_{32}^{C} & 0 & 0 \end{bmatrix}$$

$$S_{PC}(\Gamma - S_{CC})^{-1}S_{CP}$$

$$= \begin{bmatrix} S_{13}^{(2)L}S_{11}^{(2)C} & S_{13}^{(2)L}S_{12}^{(2)C} & S_{13}^{(2)L} & 0 \\ S_{23}^{(2)L}S_{11}^{(2)C} & S_{23}^{(2)L}S_{12}^{(2)C} & S_{23}^{(2)L} & 0 \\ S_{13}^{(2)R}S_{21}^{(2)C} & S_{13}^{(2)R}S_{22}^{(2)C} & 0 & S_{13}^{(2)R} \\ S_{23}^{(2)R}S_{21}^{(2)C} & S_{23}^{(2)R}S_{22}^{(2)C} & 0 & S_{23}^{(2)R} \\ S_{31}^{(2)C} & S_{32}^{(2)C} & 0 & 0 \end{bmatrix} \begin{bmatrix} S_{31}^{(2)L} & S_{32}^{(2)L} & 0 & 0 & 0 \\ 0 & 0 & S_{31}^{(2)R} & S_{32}^{(2)R} & 0 \\ 0 & 0 & 0 & 0 & S_{13}^{(2)C} \\ 0 & 0 & 0 & 0 & S_{23}^{(2)C} \end{bmatrix}$$

$$= \begin{bmatrix} S_{13}^{(2)L}S_{11}^{(2)C}S_{31}^{(2)L} & S_{13}^{(2)L}S_{11}^{(2)C}S_{32}^{(2)L} & S_{13}^{(2)L}S_{12}^{(2)C}S_{31}^{(2)R} & S_{13}^{(2)L}S_{12}^{(2)C}S_{32}^{(2)R} & S_{13}^{(2)L}S_{13}^{(2)C} \\ S_{23}^{(2)L}S_{11}^{(2)C}S_{31}^{(2)L} & S_{23}^{(2)L}S_{11}^{(2)C}S_{32}^{(2)L} & S_{23}^{(2)L}S_{12}^{(2)C}S_{31}^{(2)R} & S_{23}^{(2)L}S_{12}^{(2)C}S_{32}^{(2)R} & S_{23}^{(2)L}S_{13}^{(2)C} \\ S_{13}^{(2)R}S_{21}^{(2)C}S_{31}^{(2)L} & S_{13}^{(2)R}S_{21}^{(2)C}S_{32}^{(2)L} & S_{13}^{(2)R}S_{22}^{(2)C}S_{31}^{(2)R} & S_{13}^{(2)R}S_{22}^{(2)C}S_{32}^{(2)R} & S_{13}^{(2)R}S_{23}^{(2)C} \\ S_{23}^{(2)R}S_{21}^{(2)C}S_{31}^{(2)L} & S_{23}^{(2)R}S_{21}^{(2)C}S_{32}^{(2)L} & S_{23}^{(2)R}S_{22}^{(2)C}S_{31}^{(2)R} & S_{23}^{(2)R}S_{22}^{(2)C}S_{32}^{(2)R} & S_{23}^{(2)R}S_{23}^{(2)C} \\ S_{13}^{(2)L}S_{13}^{(2)C} & S_{23}^{(2)L}S_{13}^{(2)C} & S_{13}^{(2)R}S_{23}^{(2)C} & S_{23}^{(2)R}S_{23}^{(2)C} & 0 \end{bmatrix}$$

$$
\begin{aligned}
\left[S^{(4)}\right] &= \left[S_{PP} + S_{PC}(\Gamma - S_{CC})^{-1}S_{CP}\right] \\
&= \begin{bmatrix}
S_{11}^{(2)L} + S_{13}^{(2)L}S_{11}^{(2)C}S_{31}^{(2)L} & S_{12}^{(2)L} + S_{13}^{(2)L}S_{11}^{(2)C}S_{32}^{(2)L} & S_{13}^{(2)L}S_{12}^{(2)C}S_{31}^{(2)R} \\
S_{21}^{(2)L} + S_{23}^{(2)L}S_{11}^{(2)C}S_{31}^{(2)L} & S_{22}^{(2)L} + S_{23}^{(2)L}S_{11}^{(2)C}S_{32}^{(2)L} & S_{23}^{(2)L}S_{12}^{(2)C}S_{31}^{(2)R} \\
S_{13}^{(2)R}S_{21}^{(2)C}S_{31}^{(2)L} & S_{13}^{(2)R}S_{21}^{(2)C}S_{32}^{(2)L} & S_{11}^{(2)R} + S_{13}^{(2)R}S_{22}^{(2)C}S_{31}^{(2)R} \\
S_{23}^{(2)R}S_{21}^{(2)C}S_{31}^{(2)L} & S_{23}^{(2)R}S_{21}^{(2)C}S_{32}^{(2)L} & S_{21}^{(2)R} + S_{23}^{(2)R}S_{22}^{(2)C}S_{31}^{(2)R} \\
S_{31}^{(2)L}S_{31}^{(2)C} & S_{32}^{(2)L}S_{31}^{(2)C} & S_{31}^{(2)R}S_{32}^{(2)C}
\end{bmatrix} \\
&\qquad \begin{bmatrix}
S_{13}^{(2)L}S_{12}^{(2)C}S_{32}^{(2)R} & S_{13}^{(2)L}S_{13}^{(2)C} \\
S_{23}^{(2)L}S_{12}^{(2)C}S_{32}^{(2)R} & S_{23}^{(2)L}S_{13}^{(2)C} \\
S_{12}^{(2)R} + S_{13}^{(2)R}S_{22}^{(2)C}S_{32}^{(2)R} & S_{13}^{(2)R}S_{23}^{(2)C} \\
S_{22}^{(2)R} + S_{23}^{(2)R}S_{22}^{(2)C}S_{32}^{(2)R} & S_{23}^{(2)R}S_{23}^{(2)C} \\
S_{32}^{(2)R}S_{32}^{(2)C} & 0
\end{bmatrix}
\end{aligned}
\tag{6.2-5}
$$

The matrix equation (6.2-5) represents S-parameters of a general 4-way power divider network. This matrix is used as a building block for the S-matrix of an N-way power divider network.

6.2.2 Derivation of the N-way power divider S-matrix

The results of previous section can be extended to that for an N-way power divider. In this and subsequent sections the N-way power divider will be represented by $[S^{(N)}]$. The network consists of two $N/2 = M$ power dividers and a 2-way power divider as shown on Fig. 6.2-2. Each M-way power divider is, in turn, made of 2-way power dividers also. We must have then $N - 1$ 2-way dividers to realize an N-way power divider. The matrix $[S^{(N)}]$ can be written by generalization of (6.2-5) as

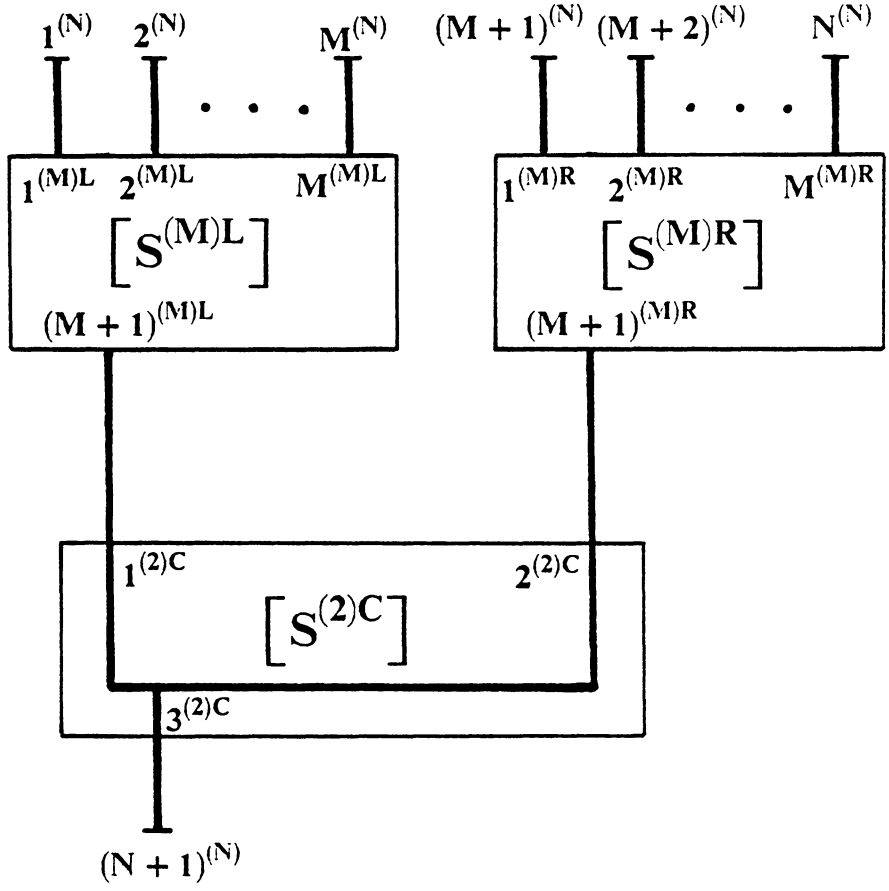

Figure 6.2-2. Implementation of an N-way power divider network from two M-way power divider networks and a 2-way power divider network.

$$[S^{(N)}] = \begin{bmatrix} [S_I^{(N)}][S_{II}^{(N)}] \begin{bmatrix} \\ S_V^{(N)} \\ \\ \end{bmatrix} \\ [S_{III}^{(N)}][S_{IV}^{(N)}] \\ \begin{bmatrix} \quad S_{VI}^{(N)} \quad \end{bmatrix} \quad 0 \end{bmatrix} \tag{6.2-6}$$

where

$$[S_I^{(N)}] = \begin{bmatrix} S_{1,1}^{(M)L} + S_{1,M+1}^{(M)L} S_{1,1}^{(2)C} S_{M+1,1}^{(M)L} & S_{1,2}^{(M)L} + S_{1,M+1}^{(M)L} S_{1,1}^{(2)C} S_{M+1,2}^{(M)L} & \cdots \\ S_{2,1}^{(M)L} + S_{2,M+1}^{(M)L} S_{1,1}^{(2)C} S_{M+1,1}^{(M)L} & S_{2,2}^{(M)L} + S_{2,M+1}^{(M)L} S_{1,1}^{(2)C} S_{M+1,2}^{(M)L} & \cdots \\ \vdots & \vdots & \vdots \\ \vdots & \vdots & \vdots \\ S_{M,1}^{(M)L} + S_{M,M+1}^{(M)L} S_{1,1}^{(2)C} S_{M+1,1}^{(M)L} & S_{M,2}^{(M)L} + S_{M,M+1}^{(M)L} S_{1,1}^{(2)C} S_{M+1,2}^{(M)L} & \cdots \end{bmatrix}$$

$$\begin{bmatrix} \cdots & S_{1,M}^{(M)L} + S_{1,M+1}^{(M)L} S_{1,1}^{(2)C} S_{M+1,M}^{(M)L} \\ \cdots & S_{2,M}^{(M)L} + S_{2,M+1}^{(M)L} S_{1,1}^{(2)C} S_{M+1,M}^{(M)L} \\ & \vdots \\ & \vdots \\ \cdots & S_{M,M}^{(M)L} + S_{M,M+1}^{(M)L} S_{1,1}^{(2)C} S_{M+1,M}^{(M)L} \end{bmatrix}$$

$$[S_{II}^{(N)}] = \begin{bmatrix} S_{1,M+1}^{(M)L} S_{1,2}^{(2)C} S_{M+1,1}^{(M)R} & S_{1,M+1}^{(M)L} S_{1,2}^{(2)C} S_{M+1,2}^{(M)R} & \cdots & S_{1,M+1}^{(M)L} S_{1,2}^{(2)C} S_{M+1,M}^{(M)R} \\ S_{2,M+1}^{(M)L} S_{1,2}^{(2)C} S_{M+1,1}^{(M)R} & S_{2,M+1}^{(M)L} S_{1,2}^{(2)C} S_{M+1,2}^{(M)R} & \cdots & S_{2,M+1}^{(M)L} S_{1,2}^{(2)C} S_{M+1,M}^{(M)R} \\ \vdots & \vdots & \vdots & \vdots \\ \vdots & \vdots & \vdots & \vdots \\ S_{M,M+1}^{(M)L} S_{1,2}^{(2)C} S_{M+1,1}^{(M)R} & S_{M,M+1}^{(M)L} S_{1,2}^{(2)C} S_{M+1,2}^{(M)R} & \cdots & S_{M,M+1}^{(M)L} S_{1,2}^{(2)C} S_{M+1,M}^{(M)R} \end{bmatrix}$$

$$[S_{III}^{(N)}] = \begin{bmatrix} S_{1,M+1}^{(M)R} S_{2,1}^{(2)C} S_{M+1,1}^{(M)L} & S_{1,M+1}^{(M)R} S_{2,1}^{(2)C} S_{M+1,2}^{(M)L} & \cdots & S_{1,M+1}^{(M)R} S_{2,1}^{(2)C} S_{M+1,M}^{(M)L} \\ S_{2,M+1}^{(M)R} S_{2,1}^{(2)C} S_{M+1,1}^{(M)L} & S_{2,M+1}^{(M)R} S_{2,1}^{(2)C} S_{M+1,2}^{(M)L} & \cdots & S_{2,M+1}^{(M)R} S_{2,1}^{(2)C} S_{M+1,M}^{(M)L} \\ \vdots & \vdots & \vdots & \vdots \\ \vdots & \vdots & \vdots & \vdots \\ S_{M,M+1}^{(M)R} S_{2,1}^{(2)C} S_{M+1,1}^{(M)L} & S_{M,M+1}^{(M)R} S_{2,1}^{(2)C} S_{M+1,2}^{(M)L} & \cdots & S_{M,M+1}^{(M)R} S_{2,1}^{(2)C} S_{M+1,M}^{(M)L} \end{bmatrix}$$

$$[S_{IV}^{(N)}] = \begin{bmatrix} S_{1,1}^{(M)R} + S_{1,M+1}^{(M)R} S_{2,2}^{(2)C} S_{M+1,1}^{(M)R} & S_{1,2}^{(M)R} + S_{1,M+1}^{(M)R} S_{2,2}^{(2)C} S_{M+1,2}^{(M)R} & \cdots \\ S_{2,1}^{(M)R} + S_{2,M+1}^{(M)R} S_{2,2}^{(2)C} S_{M+1,1}^{(M)R} & S_{2,2}^{(M)R} + S_{2,M+1}^{(M)R} S_{2,2}^{(2)C} S_{M+1,2}^{(M)R} & \cdots \\ \vdots & \vdots & \vdots \\ \vdots & \vdots & \vdots \\ S_{M,1}^{(M)R} + S_{M,M+1}^{(M)R} S_{2,2}^{(2)C} S_{M+1,1}^{(M)R} & S_{M,2}^{(M)R} + S_{M,M+1}^{(M)R} S_{2,2}^{(2)C} S_{M+1,2}^{(M)R} & \cdots \end{bmatrix}$$

$$\begin{bmatrix} \cdots & S_{1,M}^{(M)R} + S_{1,M+1}^{(M)R} S_{2,2}^{(2)C} S_{M+1,M}^{(M)R} \\ \cdots & S_{2,M}^{(M)R} + S_{2,M+1}^{(M)R} S_{2,2}^{(2)C} S_{M+1,M}^{(M)R} \\ \vdots & \vdots \\ \vdots & \vdots \\ \cdots & S_{M,M}^{(M)R} + S_{M,M+1}^{(M)R} S_{2,2}^{(2)C} S_{M+1,M}^{(M)R} \end{bmatrix}$$

$$[S_V^{(N)}] = \begin{bmatrix} S_{1,M+1}^{(M)L} S_{1,3}^{(2)C} \\ S_{2,M+1}^{(M)L} S_{1,3}^{(2)C} \\ \vdots \\ S_{M,M+1}^{(M)L} S_{1,3}^{(2)C} \\ S_{1,M+1}^{(M)R} S_{2,3}^{(2)C} \\ S_{2,M+1}^{(M)R} S_{2,3}^{(2)C} \\ \vdots \\ S_{M,M+1}^{(M)R} S_{2,3}^{(2)C} \end{bmatrix}$$

$$[S_{VI}^{(N)}] = [S_{M+1,1}^{(M)L} S_{3,1}^{(2)C} \quad S_{M+1,2}^{(M)L} S_{3,1}^{(2)C} \quad \cdots \quad S_{M+1,M}^{(M)L} S_{3,1}^{(2)C} \quad S_{M+1,1}^{(M)R} S_{3,2}^{(2)C} \quad S_{M+1,2}^{(M)R} S_{3,2}^{(2)C} \quad \cdots \quad S_{M+1,M}^{(M)R} S_{3,2}^{(2)C}]$$

A complete S-matrix for an N-way power divider in terms of the S-parameters of 2-way power dividers is obtained by solving the above equations iteratively. This is done by letting M for iteration i be N for the succeeding iteration i + 1, and solving for the new matrix using (6.2-6). This process is continued until M = 2; in other words, until the entire S-matrix is represented in terms of 2-way power divider S-parameters.

Example: An 8-way power divider

As an example of the use of (6.2-6), let us solve for $S_{4,4}^{(8)}$, the mismatch at port 4 of an 8-way power divider. The initial network consists of two 4-way power dividers and a 2-way power divider as shown on Fig. 6.2-3. First, we let N = 8 and M = N/2 = 4 in (6.2-6). $S_{4,4}^{(8)}$ corresponds to the bottom right element in $[S_I^{(N)}]$:

$$S_{4,4}^{(8)} = S_{4,4}^{(4)L} + S_{4,5}^{(4)L} S_{1,1}^{(2)C} S_{5,4}^{(4)L} \tag{6.2-7}$$

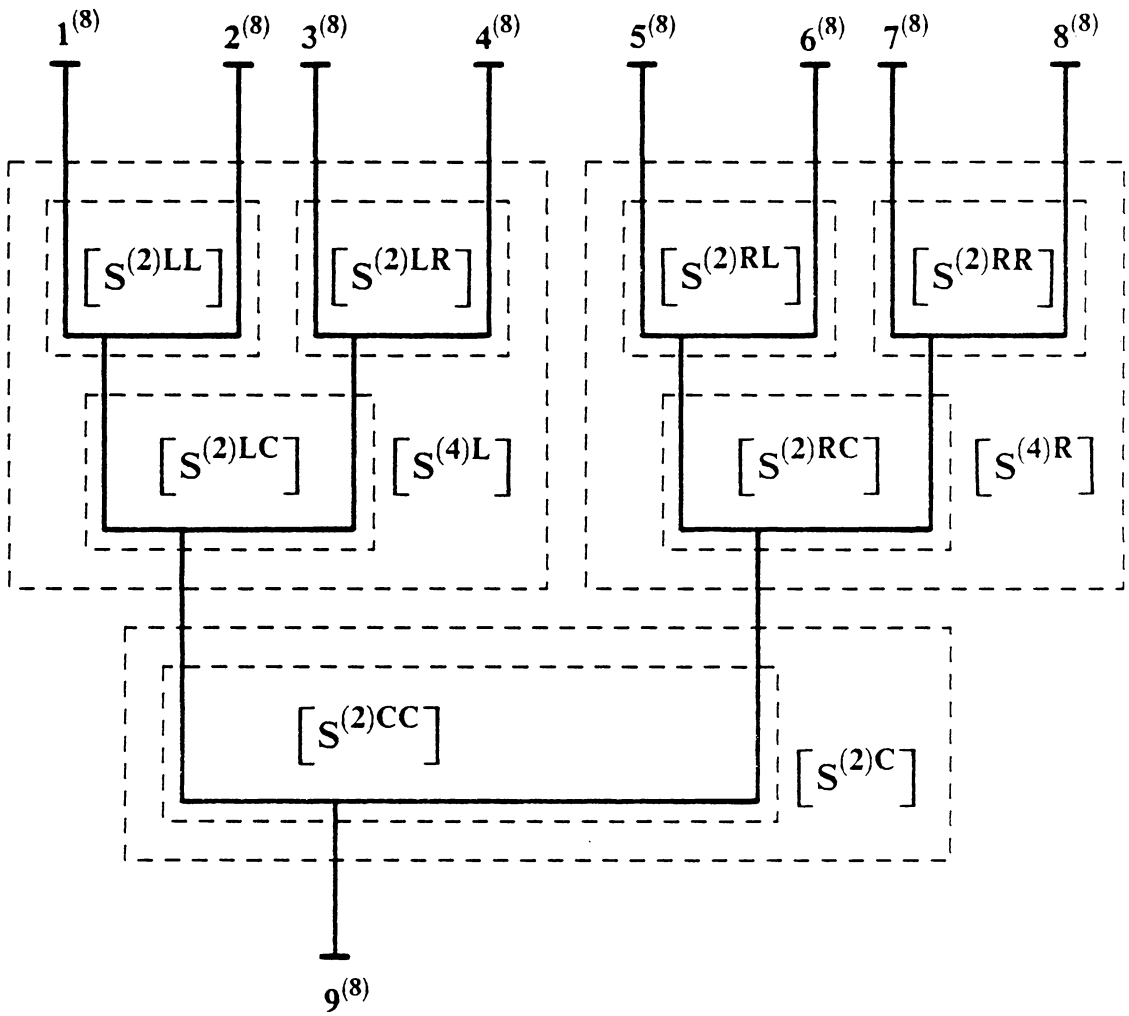

Figure 6.2-3. An 8-way power divider network example.

The 4-way power divider on the left is constructed from three 2-way power dividers as in Section 6.2.1 (LL, LC and LR in Fig. 6.2-3). The S-parameters for the 4-way power divider in (6.2-7) are obtained from (6.2-5) or equivalently from (6.2-6) for N = 4 and M = 2.

$$S_{4,4}^{(4)L} = S_{2,2}^{(2)LR} + S_{2,3}^{(2)LR} S_{2,2}^{(2)LC} S_{3,2}^{(2)LR} \tag{6.2-8}$$

$$S_{4,5}^{(4)L} = S_{2,3}^{(2)LR} S_{2,3}^{(2)LC} \tag{6.2-9}$$

$$S_{5,4}^{(4)L} = S_{3,2}^{(2)LR} S_{3,2}^{(2)LC} \tag{6.2-10}$$

To illustrate the notation, $S_{i,j}^{(2)LR}$ is used to represent S-parameter for the right 2-way power divider which is contained in the left hand side 4-way power divider. Substituting (6.2-8) to (6.2-10) into (6.2-7),

$$S_{4,4}^{(8)} = S_{2,2}^{(2)LR} + S_{2,3}^{(2)LR} S_{2,2}^{(2)LC} S_{3,2}^{(2)LR} + S_{2,3}^{(2)LR} S_{2,3}^{(2)LC} S_{1,1}^{(2)CC} S_{3,2}^{(2)LR} S_{3,2}^{(2)LC} \tag{6.2-11}$$

where $S_{i,j}^{(2)C} = S_{i,j}^{(2)CC}$ which is apparent from Fig. 6.2-3. Using the reciprocity property, the above expression simplifies to

$$S_{4,4}^{(8)} = S_{2,2}^{(2)LR} + \left\{S_{2,3}^{(2)LR}\right\}^2 S_{2,2}^{(2)LC} + \left\{S_{2,3}^{(2)LR} S_{2,3}^{(2)LC}\right\}^2 S_{1,1}^{(2)CC} \tag{6.2-12}$$

Finally, the S-parameters in (6.2-12) can be written in terms of the power ratio and phase shift at each power divider network using (4.4-19).

$$S_{2,2}^{(2)LR} = (1 - K^{(2)LR}) e^{j(\phi_{11}^{(2)LR} - 2\beta\ell^{(2)LR})} \tag{6.2-13}$$

$$S_{2,3}^{(2)LR} = \sqrt{K^{(2)LR}}\, e^{j(\phi_{23}^{(2)RR} - \beta\ell^{(2)LR})} \tag{6.2-14}$$

$$S_{2,2}^{(2)LC} = (1 - K^{(2)LC}) e^{j(\phi_{11}^{(2)LC} - 2\beta\ell^{(2)LC})} \tag{6.2-15}$$

$$S_{2,3}^{(2)LC} = \sqrt{K^{(2)LC}}\, e^{j(\phi_{23}^{(2)RC} - \beta\ell^{(2)RC})} \tag{6.2-16}$$

$$S_{1,1}^{(2)CC} = K^{(2)CC} e^{j\phi_{11}^{(2)CC}} \tag{6.2-17}$$

Substituting (6.2-13) through (6.2-17) into (6.2-12) gives

$$\begin{aligned} S_{4,4}^{(8)} &= (1 - K^{(2)LR}) e^{j(\phi_{11}^{(2)LR} - 2\beta\ell^{(2)LR})} \\ &+ \{\sqrt{K^{(2)LR}}\, e^{j(\phi_{23}^{(2)LR} - \beta\ell^{(2)LR})}\}^2 (1 - K^{(2)LC}) e^{j(\phi_{11}^{(2)LC} - 2\beta\ell^{(2)LC})} \\ &+ \{\sqrt{K^{(2)LR}}\, e^{j(\phi_{23}^{(2)LR} - \beta\ell^{(2)LR})} \sqrt{K^{(2)LC}}\, e^{j(\phi_{23}^{(2)LC} - \beta\ell^{(2)LC})}\}^2 K^{(2)CC} e^{j\phi_{11}^{(2)CC}} \end{aligned} \tag{6.2-18}$$

The procedure similar to this example is implemented in SANE-PODCON to solve for S-matrix of an N-way power divider network.

6.3 The System of Nonlinear Equations

The S-matrix developed in the last section can be substituted to the nonlinear equations of (2.4-14) and (2.4-15) to solve for the compensation network using power divider networks. The important practical feature of this design is that compensation network is contained within the feed network. By incorporating compensation at the design stage no new elements or layouts are needed. The difference in the network with compensation for coupling included is that the individual 2-way power dividers have different power split ratio and phase shift values from the conventional 3 dB equal phase approach.

For the power divider implementation the feed network as defined in Fig. 2.4-1 reduces to a transmission line that connects to the network C as shown in Fig. 6.3-1. The S-matrix for the feed network is then

$$[S^F] = \begin{bmatrix} 0 & 1 \\ 1 & 0 \end{bmatrix} \tag{6.3-1}$$

It follows that $M = 1$ for this compensation technique. Thus, for power divider compensation the network C in Figs. 2.4-1 and 6.3-1 containes the conventional feed junctions with compensation imbedded. The network is excited by a generator G with reflection coefficient S^G where wave induced by the generator, c^G , is treated as an unknown variable. Using (2.1-9) and (2.1-20), the feed/generator network is described by

$$S^{F/G} = S^G \tag{6.3-2}$$

$$c^{F/G} = c^G \tag{6.3-3}$$

There is one intermediate variable in the nonlinear equation since $M = 1$. Then, (2.4-15) becomes

$$0 = -U_1 + S^C_{N+1,1} b^A_1 + \cdots + S^C_{N+1,N} b^A_N + S^C_{N+1,N+1}\left[c^{F/G} + S^{F/G} U_1\right] \tag{6.3-4}$$

The S-matrix for the power divider network derived in the previous section assumes that the network has a matched input port ($S^C_{N+1,N+1} = 0$). Then, (6.3-4) simplifies to a linear equation of the form

$$U_1 = S^C_{N+1,1} b^A_1 + S^C_{N+1,2} b^A_2 + \cdots + S^C_{N+1,N} b^A_N = \sum_{i=1}^{N} S^C_{N+1,i} b^A_i \tag{6.3-5}$$

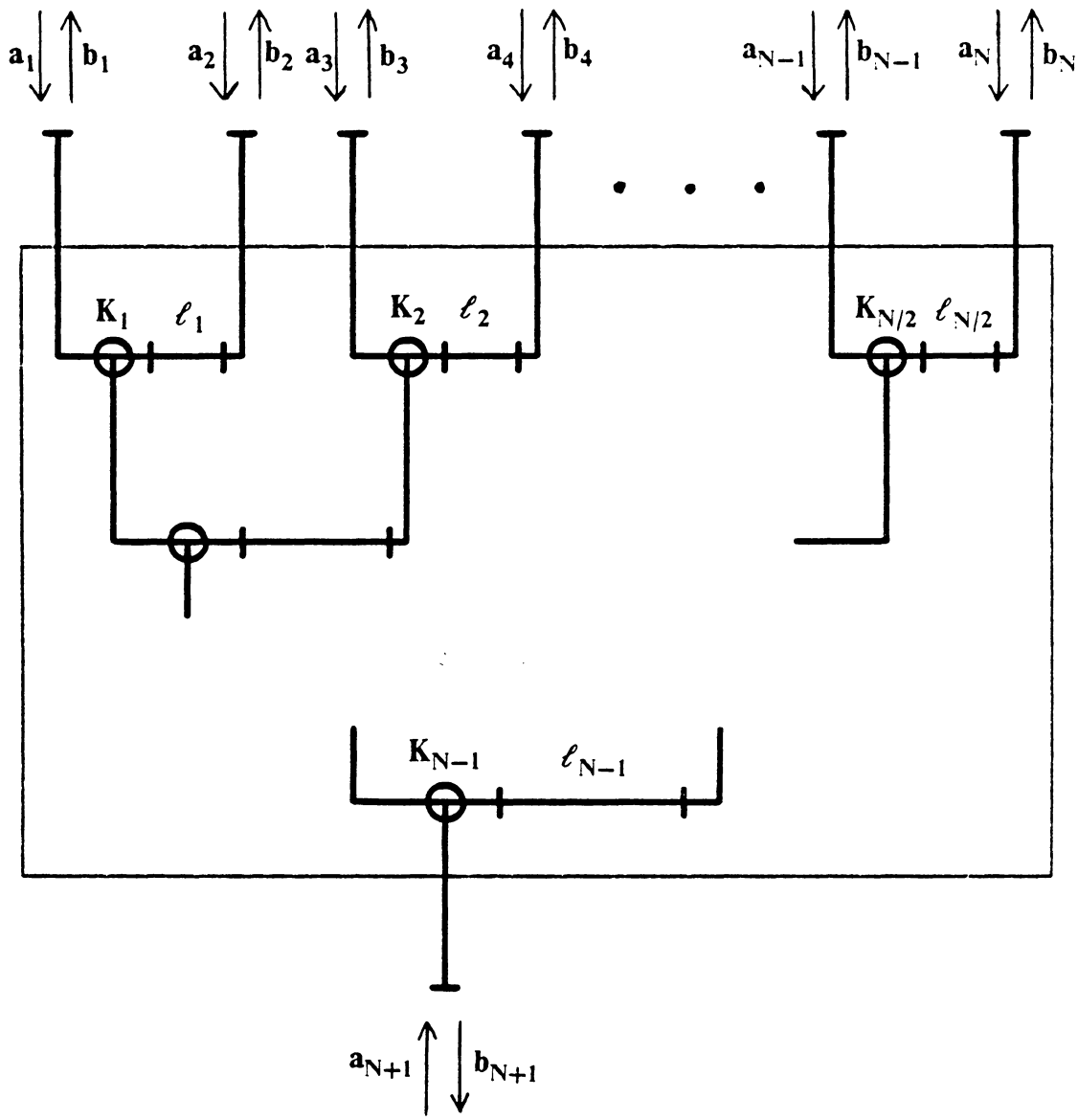

Figure 6.3-1. Variable power divider compensation network for an N-element array.

Substituting (6.3-2), (6.3-3) and (6.3-5) into (2.4-14) results

$$0 = -a_i^A + \sum_{j=1}^{N} S_{i,j}^C b_j^A + S_{i,N+1}^C \left[c^G + S^G \sum_{k=1}^{N} S_{N+1,k}^C b_k^A \right] \qquad \text{for } i = 1 \ldots N \qquad (6.3\text{-}6)$$

Thus, $N + M = N + 1$ nonlinear equations are reduced to N equations. However, (6.3-6) is not as simple as the attenuator/phase shifter equations because the S-parameters of the compensation network, $S_{i,j}^C$, are related to physical parameters in more complicated fashion as was illustrated in (6.2-18) for an 8-element array. The nonlinear property in (6.3-6) arises from the products of unknowns $S_{i,N+1}^C S_{N+1,k}^C$. In addition, for power divider compensation, the generator value G is treated as an unknown. Thus, the term $S_{i,N+1}^C c^G$ also contributes to the nonlinear property of the equation. The nonlinear equations are solved numerically by the program SANE-PODCON using the Damped Newton's method [D-4]. A detailed description of SANE-PODCON is given in Appendix B.

6.4 Initial Guess to the Solution Vector

In the modified Newton's method (which is the numerical technique used to solve for the system of nonlinear equations) the initial guess for the solution vector is one of the most important parameters the user must supply. Generally, a good choice of initial guess greatly increases the probability of convergence to a solution. It has also been proven that Newton's method converges quadratically, so an initial guess which is close to the solution also increases the convergence speed [D-4,J-4,J-5]. On the other hand,

a poor initial guess could, at worst, lead to divergence from the actual solution. It is obvious that the initial guess cannot be left to chance.

There are two requirements that the initial guess must satisfy in addition to being relatively close to the actual solution. First, the initial power split ratio K at each power divider must be between zero and one. This is necessary so that the power divider would remain a passive device. The other requirement is the unitary property of a S-matrix, which is required for the network to be lossless. Thus, the initial guess must be selected such that the matrix $[S^c]$ satisfies these requirements.

A possible choice for the initial guess is to set the variables such that the power divider network would produce the required element currents when there is no mutual coupling in the antenna elements. Clearly, this choice meets the requirements discussed above. Also, in the case where mutual coupling among antenna elements is small, the initial network will be close to the required compensation network. In the small coupling environment the effect on the element currents would also be small. Thus, the required compensation network should not be very different from the initial network.

The SANE-PODCON program, which was developed at Va Tech and is described in Appendix B, is implemented with a routine to give an initial guess using the above procedure. In all cases tested the program converged to a solution. The program has even converged for the experimental array described in Chapter 8 which employed tight element spacings to intentionally increase mutual coupling between elements. In most antenna arrays mutual coupling would be less than that of the experimental array. This initial guess procedure, therefore, should be adequate for most antenna arrays.

VII. Synthesis with a Transmission Line Network

7.1 Introduction

The third technique considered uses the characteristic impedance of transmission lines to compensated for mutual coupling. Smith treated this problem by solving the nonlinear equations (2.4-14) and (2.4-15) using SANE-GECON [S-1]. The program converged to a solution for two element array cases. However, convergence was never achieved for higher element number.

Initially, we anticipated that the convergence problem arose from general treatment of the nonlinear equations by SANE-GECON since similar problems were found for the power divider compensation network. Thus, we modified the nonlinear equations specifically for the transmission line network (this is discussed in next section). Then a computer program SANE-TRACON (Synthesis of Array with Network and Element coupling for TRansmission line COmpensation Network) was developed using the modified nonlinear equations. However, we could not achieve convergence for the cases other than two element arrays. Although there is no mathematical proof, we speculate

that the lack of convergence is due to a physical limitation of the network rather than the numerical technique used to solve the equations. This remains an open question. Since the approach used is simple and implementation is straight forward, future attempts to find a solution are warranted. Also, an attempt to prove in general a necessary condition for a feed network to yield a solvable compensation network would be valuable.

7.2 The System of Nonlinear Equations

The S-matrices of a single transmission line network (discussed in Section 4.5) can be substituted into the system of nonliner equations (2.4-14) and (2.4-15) to develop a simplified set of nonlinear equations. As in the case of the attenuator/phase shifter network, this is a compensation technique using an added network between the element and feed network. The modified nonlinear equations, however, are not as simple due to inherent existence of reflection coefficients at all ports of the compensation network.

The S-matrix of an N-element array, $[S^A]$, and the S-matrix of N-way feed network, $[S^F]$, are assumed to be known. Thus, we are assuming $N = M$ in Fig. 2.4-1 and (2.4-14) and (2.4-15). The compensation network consists of N transmission lines as shown in Fig. 7.2-1. The magnitude and phase of the complex variable X_i represent characteristic impedance and length of the transmission line between port i and $i+N$, respectively. The S-matrix of this network is given by

$$[S^C] = \begin{bmatrix} [\Gamma] & [T] \\ [T] & [\Gamma] \end{bmatrix} \tag{7.2-1}$$

where

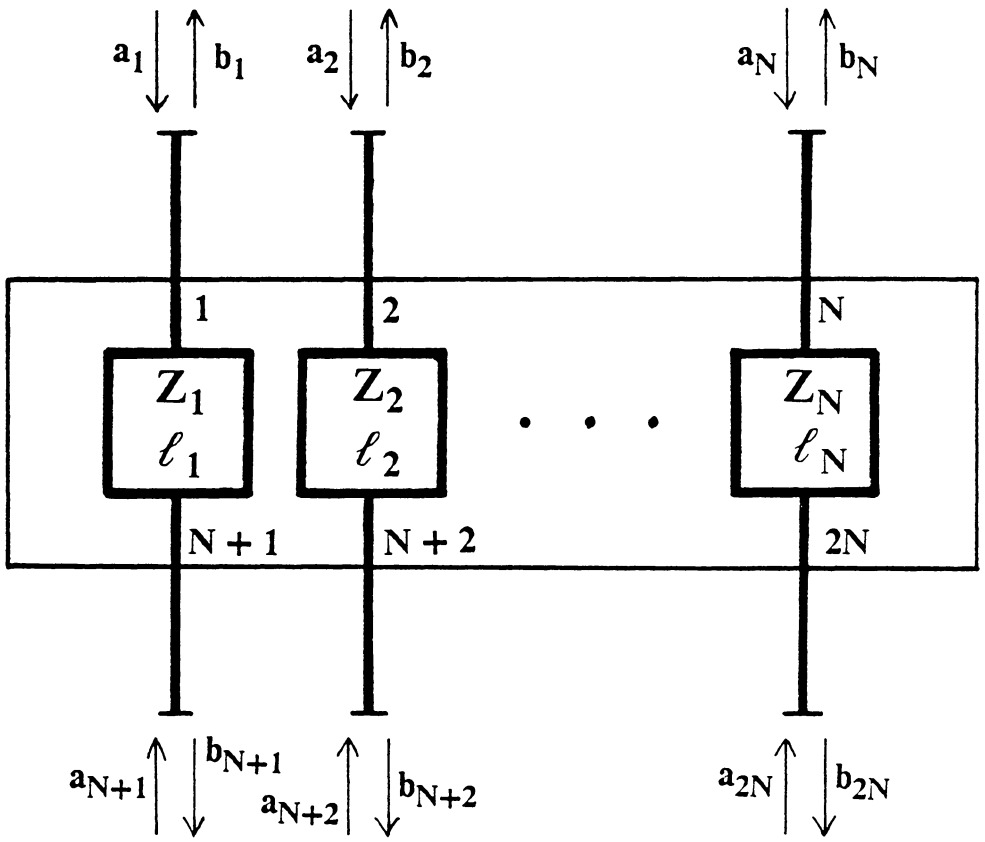

Figure 7.2-1. Transmission line characteristic impedance compensation network for an N-element array.

$$[\Gamma] = \begin{bmatrix} \Gamma_1 & 0 & 0 & \dots & 0 \\ 0 & \Gamma_2 & 0 & \dots & 0 \\ 0 & 0 & \Gamma_3 & \dots & 0 \\ . & . & . & . & . \\ 0 & 0 & 0 & \dots & \Gamma_N \end{bmatrix}$$

and

$$[T] = \begin{bmatrix} T_1 & 0 & 0 & \dots & 0 \\ 0 & T_2 & 0 & \dots & 0 \\ 0 & 0 & T_3 & \dots & 0 \\ . & . & . & . & . \\ 0 & 0 & 0 & \dots & T_N \end{bmatrix}$$

Γ_i and T_i are the reflection coefficient and the transmission coefficient of i-th transmission line, respectively. These coefficients are calculated from the characteristic impedance Z_i and and the length of the transmission line ℓ_i using (4.5-2) and (4.5-3). Substituting $[S^c]$ into (2.4-14) and (2.4-15) yields

$$0 = -a_i + \Gamma_i + T_i \left[c_i^{F/G} + \sum_{j=1}^{N} S_{i,j}^{F/G} U_j \right] \tag{7.2-2}$$

and

$$0 = -U_i + T_i + \Gamma_i \left[c_i^{F/G} + \sum_{j=1}^{N} S_{i,j}^{F/G} U_j \right] \tag{7.2-3}$$

for i = 1,...,N. It is clear that these equations are not as simple as other two cases. In particular, there are N intermediate unknowns, $\{U^i\}$ and N unknown variables in (7.2-2) and (7.2-3). Hence, it is necessary to solve for 2N unknowns in order to determine compensation network values.

VIII. Microstrip Array Antenna Experiments

8.1 Description of Experimental Hardware

The microstrip array used to investigate the mutual coupling compensation is composed of two sections: a board containing the array of radiating elements (the array board) and a feed network board. The hardware which was constructed and tested at New Mexico State University Physical Science Laboratory was operated at a center frequency of 2733 MHz [J-9]. Both the array board and feed network board were fabricated on 1/16 inch thick teflon fiberglass substrate with relative dielectric constant $\varepsilon_r = 2.55$.

The array board consists of eight quarter-wavelength wide patches with 3.43 cm (0.312 λ_0) interelement spacings. At the center frequency of 2733 MHz the wavelength is $\lambda_0 = 10.98$ cm in air and $\lambda_d = \lambda_0/\sqrt{\varepsilon_{eff}} = 7.706$ cm in the substrate where the effective dielectric constant is $\varepsilon_{eff} = 2.03$. The geometry of the array board is shown in Fig. 8.1-1. The quarter-wavelength patches are used to obtain closer than one half-wavelength element spacing in order to increase the element coupling. This was done intentionally

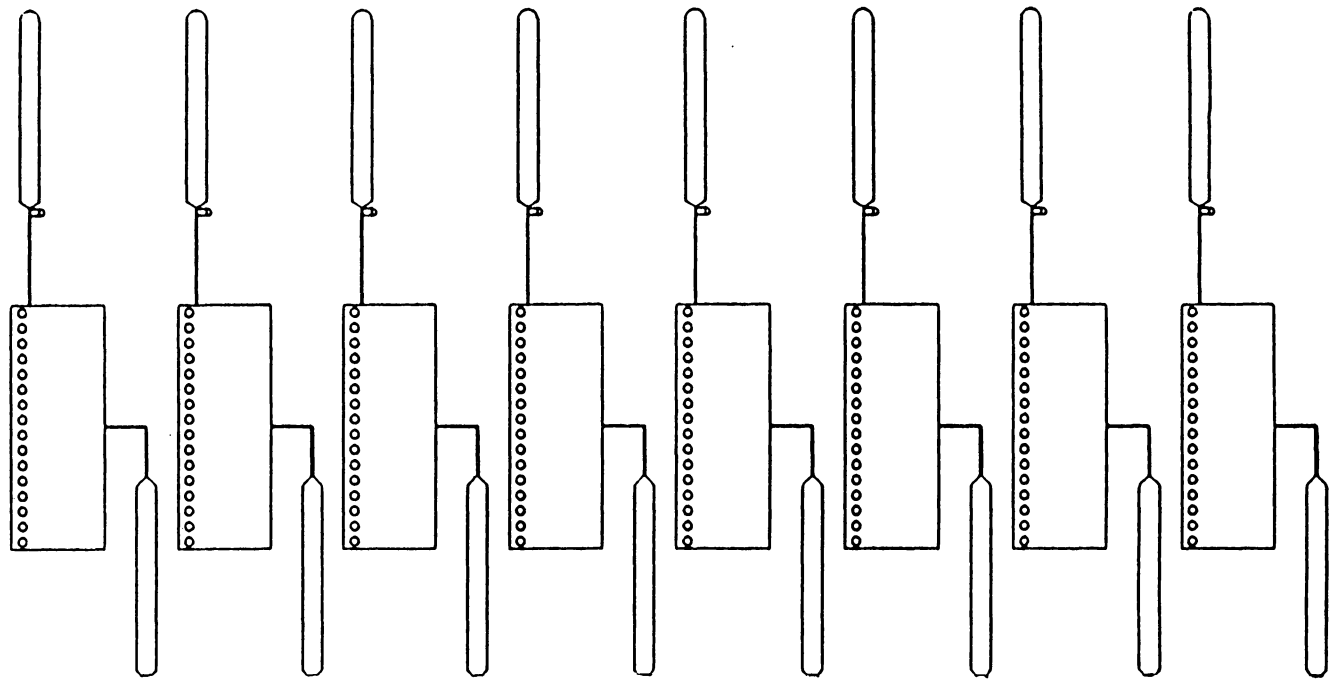

Figure 8.1-1 Experimental array of eight quarter-wavelength microstrip patches. This board is refered to as the array board. The left most input port is No. 1.

in an attempt to make mutual coupling effects more readily measurable. The individual elements are 5.08cm by 1.89cm rectangular patches with sixteen shorting pins placed approximately 1.68cm ($0.25\lambda_d$) from the opposite radiating edges. A detailed sketch of a patch is shown in Fig. 8.1-2. The elements are fed by 50 Ω transmission lines which are matched to the patches with a 132 Ω quarter-wavelength transformer at the center of radiating edges.

The transmission lines attached to non-radiating edges of the patches are probe circuits intended for measurements of active element excitation coefficients. The probe circuits are made of 158 Ω quarter-wavelength transmission lines and 50 Ω chip resistors. The input impedance of the probe circuits looking in from the patches are kept high (approximately 1 KΩ) with the quarter-wavelength transformers so that the probes would not load the patches which have low input impedance because of shorting pins. The chip resistors are added because the probe circuits have high input impedance looking in from detector ports.

Two feed network boards were fabricated to test different cases of array excitation: a sum/difference feed (Fig. 8.1-3) and an ordinary endfire feed (Fig. 8.1-4). A sum pattern requires equal magnitude and equal phase excitation, while a difference pattern requires one half of the array to be excited 180° out of phase from the other half. The sum feed and the difference feed are integrated and constructed on the same substrate. The combined sum/difference network uses a quarter-wavelength hybrid with two input ports attached to a corporate feed network. Depending on the input port chosen, the sum pattern or the difference pattern excitation is obtained.

An ordinary endfire pattern, on the other hand, requires equal magnitude and progressive phase shift $\phi_n = \pm n\beta d$ where d is the inter-element spacing. The endfire feed is constructed with seven 3 dB power dividers connected in the form of a corporate feed with additional transmission lines on the right branch of the power dividers. The

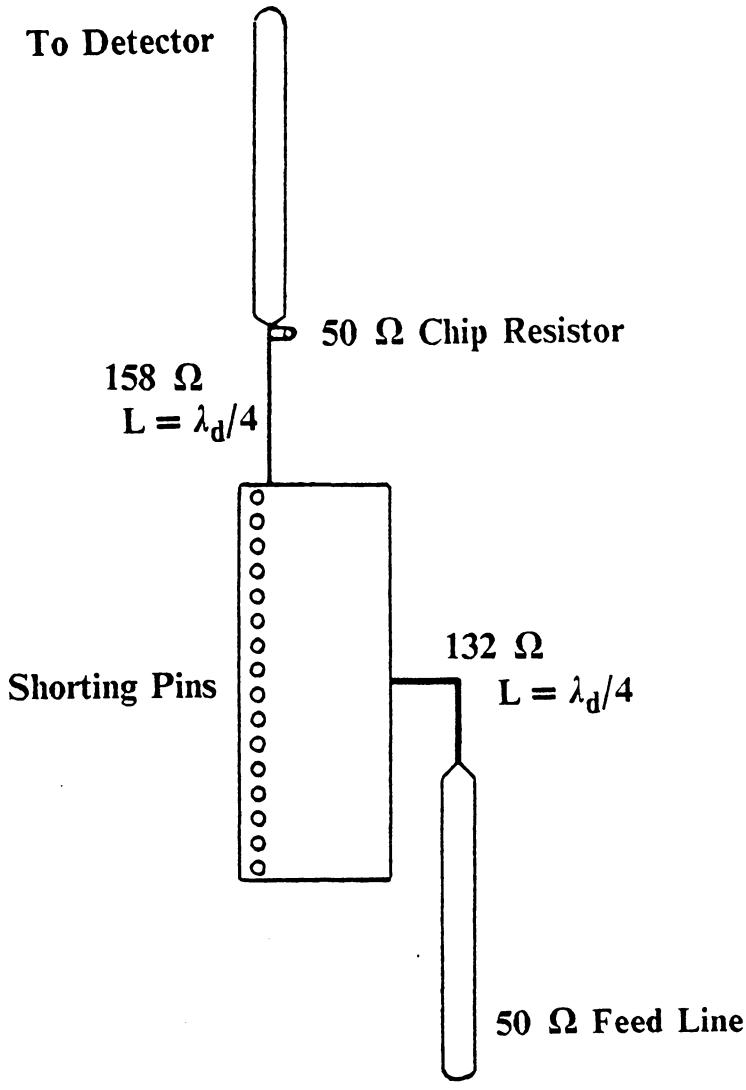

Figure 8.1-2. Geometry of the quarter-wavelength radiating element with feed line and probe circuit used in the experimental array.

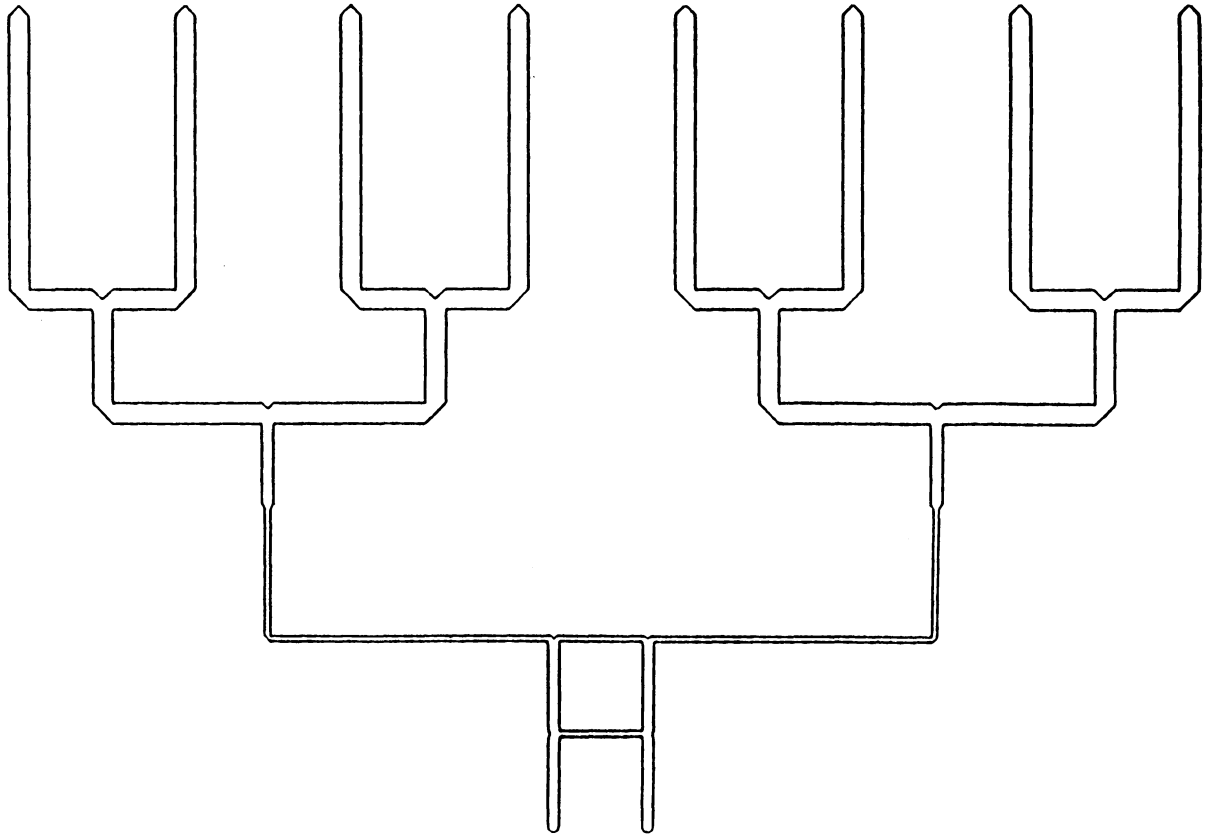

Figure 8.1-3. Sum/difference feed network. The left most output port is No. 1.

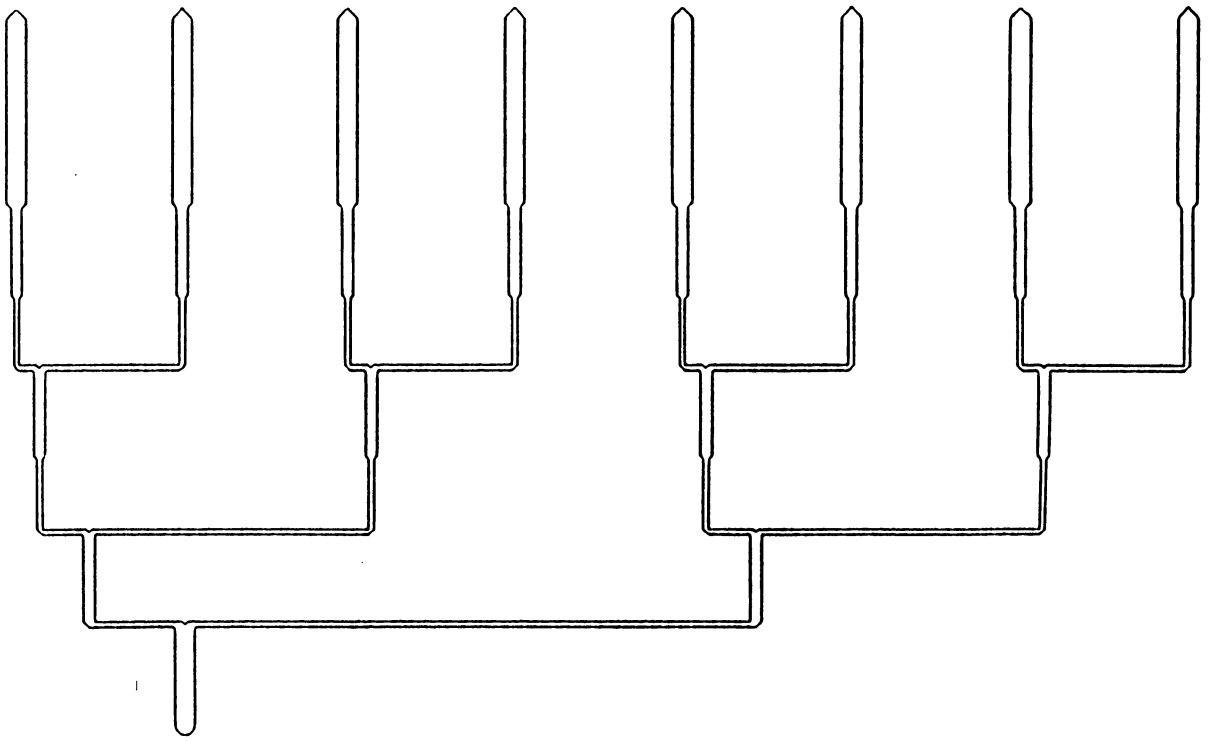

Figure 8.1-4. Endfire feed network. The left most output port is No. 1.

transmission lines are designed to provide 113°(0.312 λ_0) phase shift between elements at 2733 MHz. For example, the difference in the length of transmission lines between port 1 and port 2 is $d_g = 2.432$ cm as shown in Fig. 8.1-4. The interelement phasing between two adjacent ports, α , is obtained as follows:

$$\alpha = \beta_g d_g = \frac{360°}{\lambda_g} d_g = \frac{360°}{7.706\text{cm}} 2.432\text{cm} \\ = 113° \tag{8.1-1}$$

where β_g and λ_g are propagation constant and wavelength in the substrate, respectively.

The array board and the feed networks are connected using coaxial cables between the feed output ports and the antenna element ports. This design allows measurement of S-parameters as well as placement of a compensation network between the array and the feed network (the compensation network was discussed in Section 2.4). In addition to the above three microstrip networks, two other boards were constructed, one containing both the array network and an endfire feed and the other containing both the array and the sum/difference feed. These boards were built to verify that the coaxial cables between the array and the feed do not affect the radiation pattern.

8.2 Measurements with the Uncompensated Microstrip Arrays

This section presents measured and predicted radiation patterns for the uncompensated experimental array consisting of the array board connected to a feed network board (these boards were described in the previous section). All measurements (S-parameters and far-field patterns) which were conducted at PSL were taken at the design frequency 2733 MHz and at side frequencies 2723 MHz and 2743 MHz to study frequency variation effects. Element patterns were measured only at 2733 MHz because

the element patterns do not change appreciably with frequency. The individual element patterns of the experimental array when operating in array environment are shown in Fig. 8.2-1. These element patterns are measured by feeding one element while all others were 50 Ω loaded. Figure 8.2-1 shows that the element patterns are significantly different. This suggests that an average element pattern cannot be used to calculate predicted radiation patterns for the entire array as in (2.3-10). For the complete accuracy the difference in the element patterns must be incorporated in far-field calculations. This was not done and proved to limit the achievable compensation. Assuming that the measured element patterns are close to that of active element pattern in fully excited array, the radiation pattern can be approximated using (2.3-9).

Before proceeding to actual compensation it is desireable to see how well array behavior can be predicted; i.e. we first study analysis (uncompensated) before synthesis (compensated). Figures 8.2-2 to 8.2-4 show the measured and predicted E-plane radiation patterns of the uncompensated array for sum, difference and endfire excitation at 2733 MHz. The predicted patterns are calculated from element currents which are obtained from measured array and feed network S-parameters using MCAP. The currents are given in Table 8.2-1. The element patterns used in these predicted patterns are those of Fig. 8.2-1. In addition, the uncompensated radiation patterns shown in Figs. 8.2-2(a) to 8.2-4(a) are compared to predicted patterns calculated from ideal excitation currents which are shown in Figs. 8.2-2(c) to 8.2-4(c). The ideal patterns are obtained when array elements are excited with the desired currents. These patterns, thus, represent what can be achieved through mutual coupling compensation. The excitations for the ideal patterns are given in Table 8.2-2. The endfire patterns (Fig. 8.2-4) have the main beams away from the endfire direction ($\theta = 90°$). This is due to non-omnidirectional element pattern in E-plane of the microstrip array.

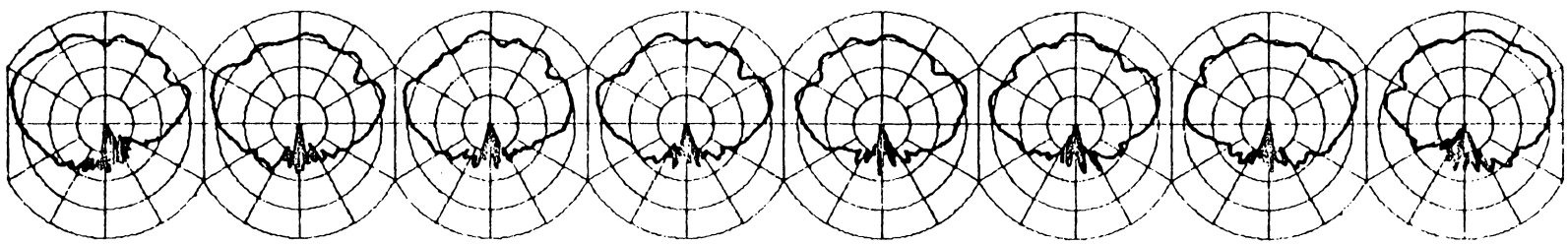

Figure 8.2-1. Measured individual element patterns of experimental array of Fig. 8.1-1. Each pattern was measured with the remaining seven elements 50 Ω loaded.

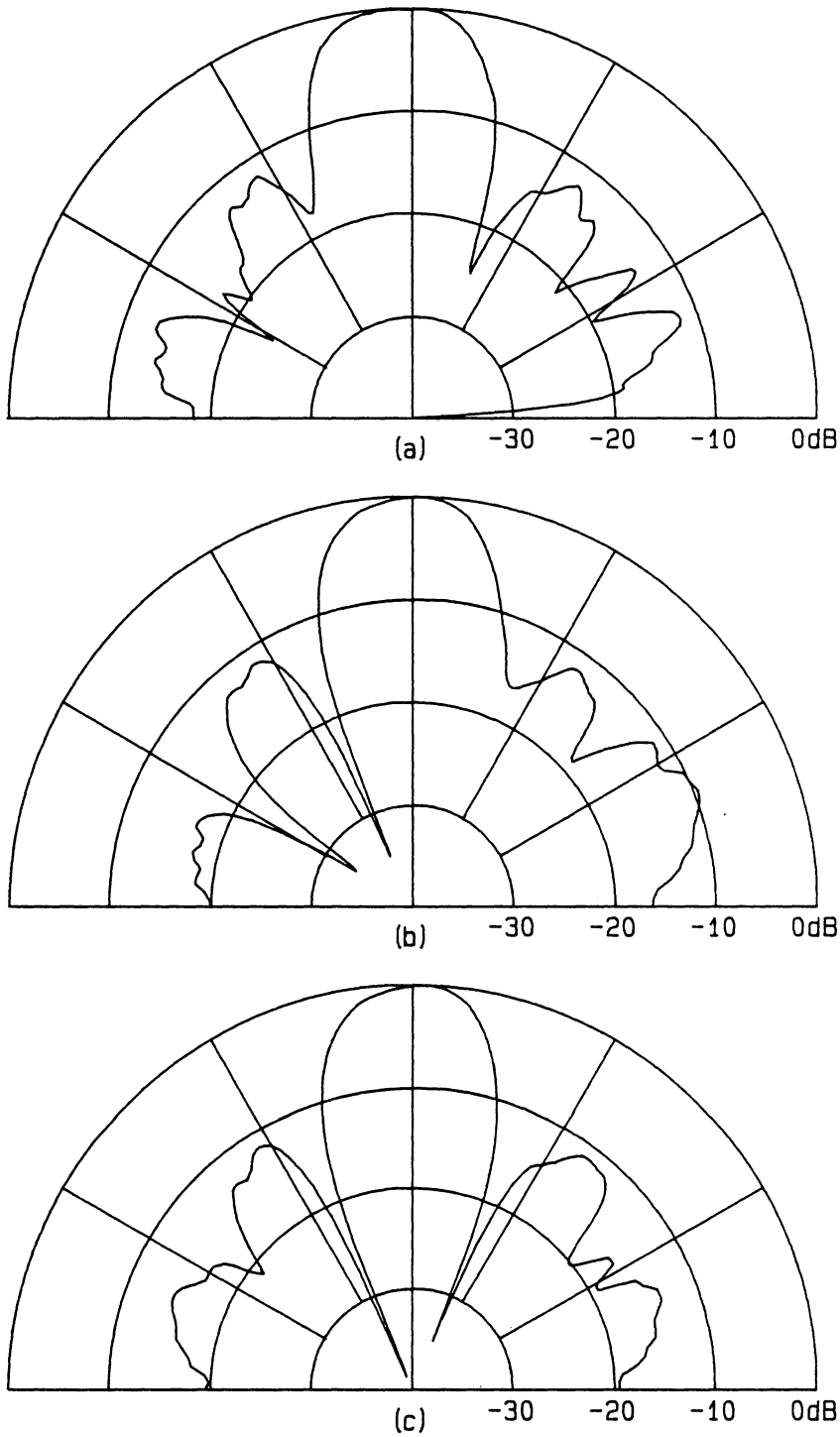

Figure 8.2-2. Comparison of measured and calculated radiation patterns for the array with sum pattern feed network. a) measured, b) calculated and c) ideal patterns.

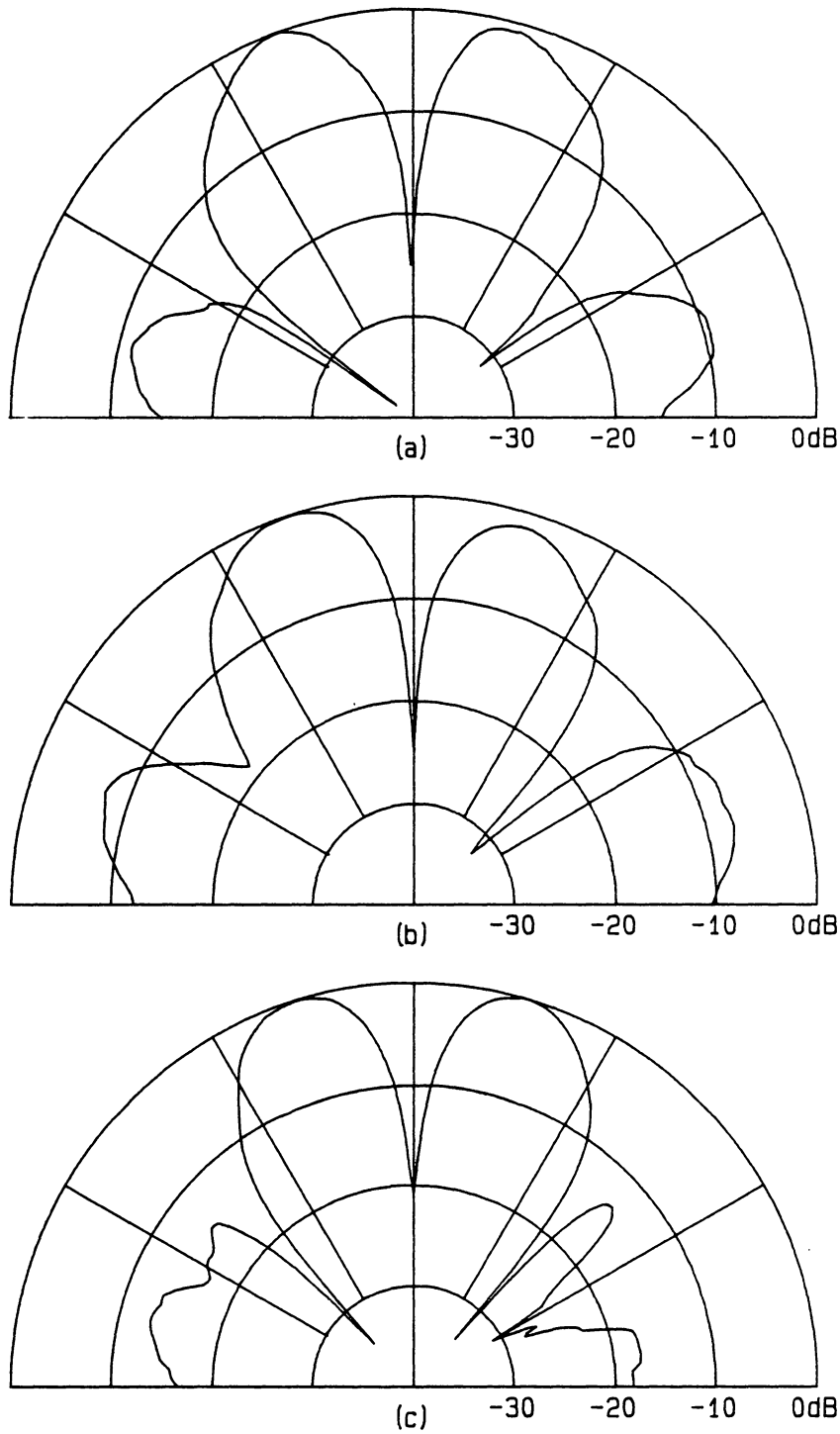

Figure 8.2-3. Comparison of measured and calculated radiation patterns for the array with difference pattern feed network. a) measured, b) calculated and c) ideal patterns.

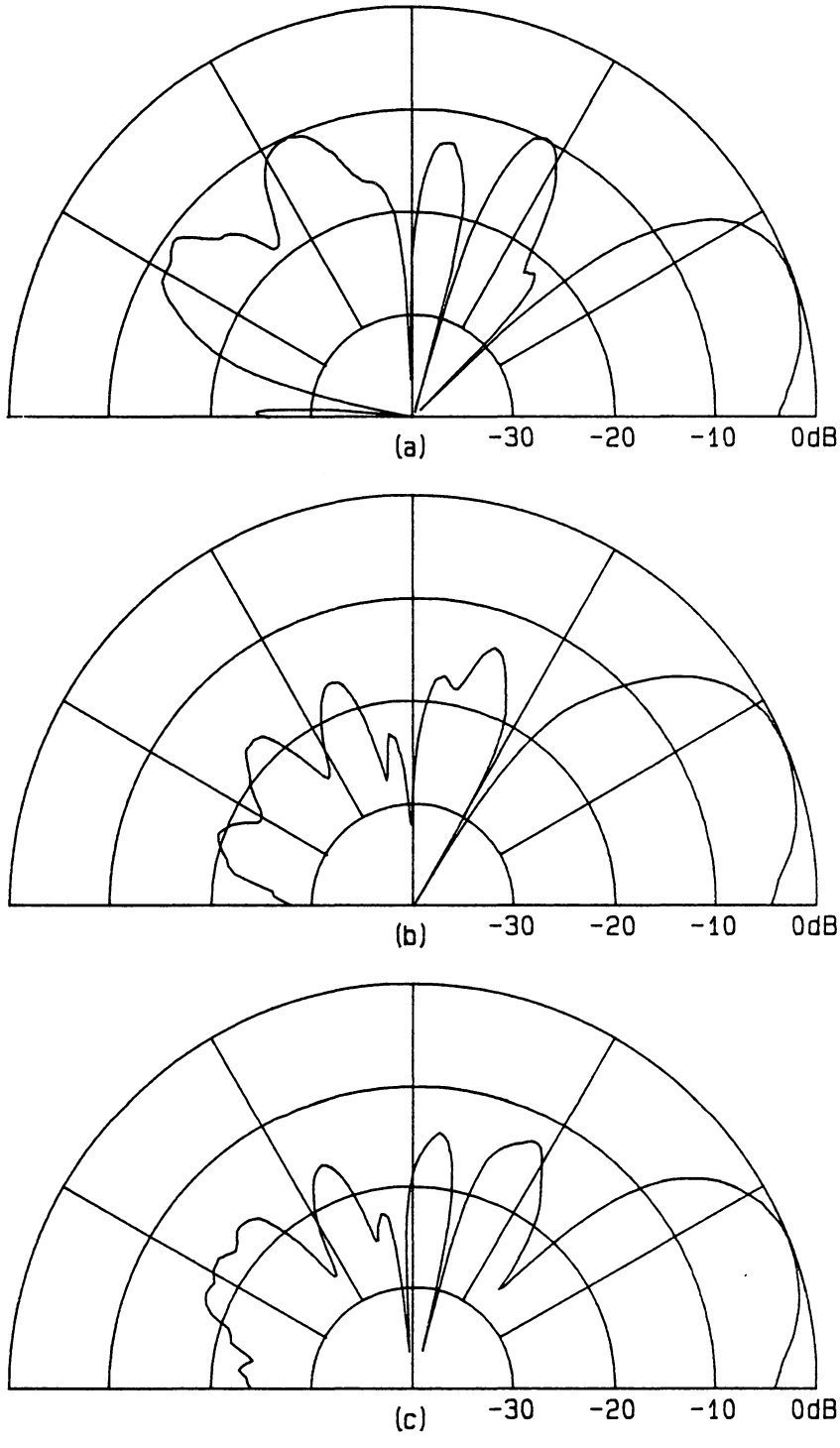

Figure 8.2-4. Comparison of measured and calculated radiation patterns to for the array with endfire feed network. a) measured, b) calculated and c) ideal patterns.

Table 8.2-1. Calculated currents for the predicted patterns of Figs. 8.2-2 through 8.2-4.

Element Number	Sum Array	Difference Array	Endfire Array
1	0.68664/60.74°	0.45911/132.37°	0.34980/221.87°
2	0.66823/42.03°	0.40396/115.25°	0.46687/81.22°
3	0.96257/60.61°	0.84871/140.52°	0.89593/-28.68°
4	1.00000/59.25°	1.00000/156.20°	0.68871/238.61°
5	0.71603/35.55°	0.80937/-29.02°	1.00000/129.15°
6	0.69268/30.96°	0.69511/-54.34°	0.78323/11.80°
7	0.60754/63.25°	0.40664/-41.27°	0.77976/267.39°
8	0.74779/67.59°	0.56739/-34.52°	0.85398/152.65°

Table 8.2-2. Excitation for "Ideal" patterns for Figs. 8.2-2 through 8.2-4.

Element Number	Sum Array	Difference Array	Endfire Array
1	1.0000/0.00°	1.00000/0.00°	1.0000/0.00°
2	1.0000/0.00°	1.00000/0.00°	1.0000/-112.32°
3	1.0000/0.00°	1.00000/0.00°	1.0000/-224.64°
4	1.0000/0.00°	1.00000/0.00°	1.0000/-336.96°
5	1.0000/0.00°	1.00000/180.00°	1.0000/-89.28°
6	1.0000/0.00°	1.00000/180.00°	1.0000/-201.60°
7	1.0000/0.00°	1.00000/180.00°	1.0000/-313.92°
8	1.0000/0.00°	1.00000/180.00°	1.0000/-66.24°

Figures 8.2-2 to 8.2-4 clearly show that the order of error between measured and predicted patterns are close to the difference between measured patterns and ideal patterns. The deviation of predicted patterns from measured patterns apparently comes from errors in measured S-parameters. This suggests that compensation for mutual coupling in the experimental array may be difficult to demonstrate in microstrip. The small improvements seen in the ideal radiation patterns from the uncompensated patterns are due to variation in the element patterns as shown in Fig. 8.2-1. For example, there are up to 8 dB differences in the element patterns at 60° off broadside which is close to the location of the main beam in the endfire array. The element pattern variation occurs primarily from ground plane edge effects.

8.3 Compensation Networks for the Experimental Arrays

Both attenuator/phase shifter and power divider compensation networks have been calculated for the experimental array in all three cases of excitations. The compensation network values were calculated from measured S-parameters using SANE for attenuator/phase shifter network and SANE-PODCON for power divider network. Since the accuracy of the S-parameters was shown in the previous section to be questionable, the compensation networks calculated here may be somewhat inaccurate. However, the S-parameters represent typical mutual coupling phenomena in an array. Thus, the networks obtained are representative of the mutual coupling compensation technique.

8.3.1 Attenuator/phase shifter compensation networks

This section presents attenuator/phase shifter compensation networks for the sum, difference and endfire array. The compensation networks are calculated from measured S-parameters of the sum/difference and the endfire feed networks and measured S-parameters of the microstrip elements. The variables for this example are defined as follows:

$$\begin{aligned} &\text{Attenuation[dB]} = -20\log(|X|) \\ &\text{Phase Shift [°]} = \underline{/X} \end{aligned} \tag{8.3-1}$$

The results are shown in Table 8.3-1 which are the most efficient compensation networks when phase of generator G is varied for every 10°. The relationship between the generator excitation and the efficiency of attenuator/phase shifter compensation network was discussed in Section 5.3. The predicted patterns for the compensated array for the three cases of excitations are equivalent to patterns with the ideal excitation currents. The ideal patterns are shown in Figs. 8.2-2(c), 8.2-3(c), and 8.2-4(c) for the sum, difference and endfire array, respectively.

8.3.2 Power divider compensation network

Similar to the attenuator/phase shifter compensation, the power divider compensation networks are calculated from measured S-parameters of the microstrip array for the synthesis of a sum, a difference and an endfire pattern. The variable power divider networks are defined in terms of complex variables as shown below

Table 8.3-1. Attenuator/phase shifter compensation networks for the microstrip array.

case	Sum		Difference		Endfire	
Element	Attenuator	Ph.Shift	Attenuator	Ph.Shift	Attenuator	Ph.Shift
X_1	2.201 dB	243.91°	2.536 dB	213.53°	0.000 dB	257.34°
X_2	1.075 dB	272.19°	0.631 dB	226.19°	2.468 dB	258.62°
X_3	2.372 dB	254.09°	1.210 dB	220.40°	5.206 dB	254.51°
X_4	2.628 dB	258.00°	6.193 dB	184.24°	5.636 dB	275.04°
X_5	2.041 dB	255.82°	6.299 dB	193.81°	2.532 dB	273.71°
X_6	0.302 dB	258.91°	0.000 dB	224.01°	2.756 dB	281.55°
X_7	0.000 dB	266.99°	0.004 dB	218.41°	5.401 dB	261.24°
X_8	2.199 dB	239.67°	3.482 dB	206.21°	6.401 dB	286.36°
G	5.55346	40.00°	5.23843	0.00°	4.64400	240.00°

$$\begin{aligned} &\text{Fraction of power to left branch } = 1 - K = 1 - |X| \\ &\text{Fraction of power to right branch } = K = |X| \\ &\text{Phase Shift } [^\circ] = \underline{/X} \end{aligned} \tag{8.3-2}$$

The results are shown on Table 8.3-2. The compensation networks were calculated using quadrature hybrid power dividers discussed in Section 4.4 with transmission line length $\ell_c = \lambda/8$ (see Figure 4.4-2). The calculated patterns for the compensated arrays are equivalent to the ideal patterns which are shown in Figs. 8.2-2(c), 8.2-3(c) and 8.2-4(c).

Table 8.3-2. Results of power divider compensation networks for the microstrip array.

case	Sum		Difference		Endfire	
	K	Ph.Shift	K	Ph.Shift	K	Ph.Shift
X_1	0.55230	38.17°	0.60849	19.01°	0.40649	-113.56°
X_2	0.49141	8.11°	0.10034	-11.66°	0.29009	-159.83°
X_3	0.56489	3.02°	0.84312	45.89°	0.43559	-151.01°
X_4	0.29576	-17.47°	0.28341	-14.03°	0.01106	-150.50°
X_5	0.43517	19.76°	0.30678	23.92°	0.04399	142.75°
X_6	0.52865	-5.92°	0.64275	38.63°	0.14548	145.97°
X_7	0.48339	28.27°	0.49484	160.83°	0.21778	-70.76°
G	4.35587	116.86°	4.11564	124.33°	3.04167	-138.73°

8.4 Synthesis of a 35 dB Dolph-Chebyshev Pattern

As shown in Section 8.2, the differences between the uncompensated patterns and the compensated patterns are small. A better way to demonstrate the effect of the mutual coupling compensation on the microstrip array is to synthesize a low side lobe pattern. A 35 dB Dolph-Chebyshev pattern was chosen for this purpose. The required element currents are [S-2]

$$\begin{aligned} I_1 &= 0.19154 \angle 0.0^\circ & I_5 &= 1.00000 \angle 0.0^\circ \\ I_2 &= 0.46362 \angle 0.0^\circ & I_6 &= 0.78425 \angle 0.0^\circ \\ I_3 &= 0.78425 \angle 0.0^\circ & I_7 &= 0.46362 \angle 0.0^\circ \\ I_4 &= 1.00000 \angle 0.0^\circ & I_8 &= 0.19154 \angle 0.0^\circ \end{aligned} \qquad (8.4\text{-}1)$$

A feed network for the above current distribution that does not include mutual coupling compensation (blind design feed) was constructed from the sum/difference feed network (using sum pattern input port) with six attenuators corresponding to the magnitude of required currents attached to the output ports. See Table 8.4-1. The resulting element currents calculated using measured S-parameters of the feed network and the array elements are shown in Table 8.4-2. The measured and predicted patterns are shown in Fig, 8.4-1. The predicted patterns were again computed using individual element patterns of Fig. 8.2-1.

To demonstrate that a feed network that is tuned to produce the desired currents does not compensate for mutual coupling effect, a network which corrects the magnitude and phase error of the feed network was designed. This is designated as partial blind design. The attenuators and phase shifters required by partial blind design are shown in Table 8.4-1. These parameters are calculated using SANE with measured S-parameters

Table 8.4-1. Attenuator/phase shifter compensation network for a 35 dB Dolph Chebyshev array using the eight element microstrip array and the sum feed network.

Design	Blind		Partial Blind		Compensated	
Element	Attenuator	Ph.Shift	Attenuator	Ph.Shift	Attenuator	Ph.Shift
X_1	14.355 dB	0.00°	14.271 dB	-0.95°	11.540 dB	-135.57°
X_2	6.667 dB	0.00°	6.178 dB	0.00°	3.053 dB	-125.10°
X_3	2.111 dB	0.00°	2.516 dB	-6.08°	2.768 dB	-144.95°
X_4	0.000 dB	0.00°	0.405 dB	-6.07°	0.261 dB	-142.68°
X_5	0.000 dB	0.00°	0.000 dB	-2.96°	0.000 dB	-137.71°
X_6	2.111 dB	0.00°	1.209 dB	-3.98°	1.259 dB	-134.74°
X_7	6.667 dB	0.00°	6.095 dB	-6.97°	1.602 dB	-132.37°
X_8	14.355 dB	0.00°	13.857 dB	-4.00°	12.013 dB	-134.48°
G	2.82843	0.00°	3.19917	0.00°	3.94536	80.00°

of the sum feed network while setting all S-parameters of the elements to zero. The predicted radiation pattern for the blind design array is shown in Fig. 8.4-2. It clearly shows that mutual coupling among elements cannot be neglected in design of an array.

An attenuator/phase shifter compensation network was calculated from the S-parameters of the sum feed network measured at PSL. The results of the calculation using SANE for the required compensation network parameters are summarized in Table 8.4-1. The compensation network was constructed at PSL using attenuators and coaxial cables. Attenuators which closely approximate required values were chosen first. Then, coaxial cables were cut to achieve the required phase shifts and the difference in required and actual attenuation using the loss introduced by the cables. The normalized E-plane radiation pattern of the compensated array is presented in Fig. 8.4-3. The currents used in the calculation of predicted pattern are shown in Table 8.4-2.

Comparison of measured patterns between the blind design array (Fig. 8.4-1) and the compensated array (Fig. 8.4-3) shows some improvement in sidelobe level and main beam shape. However, the sidelobes of the compensated array are not as low as we have predicted due to variation in the individual element pattern. Nevertheless, the result offers encouragement that experimental verification may be possible for an array with small element pattern variations.

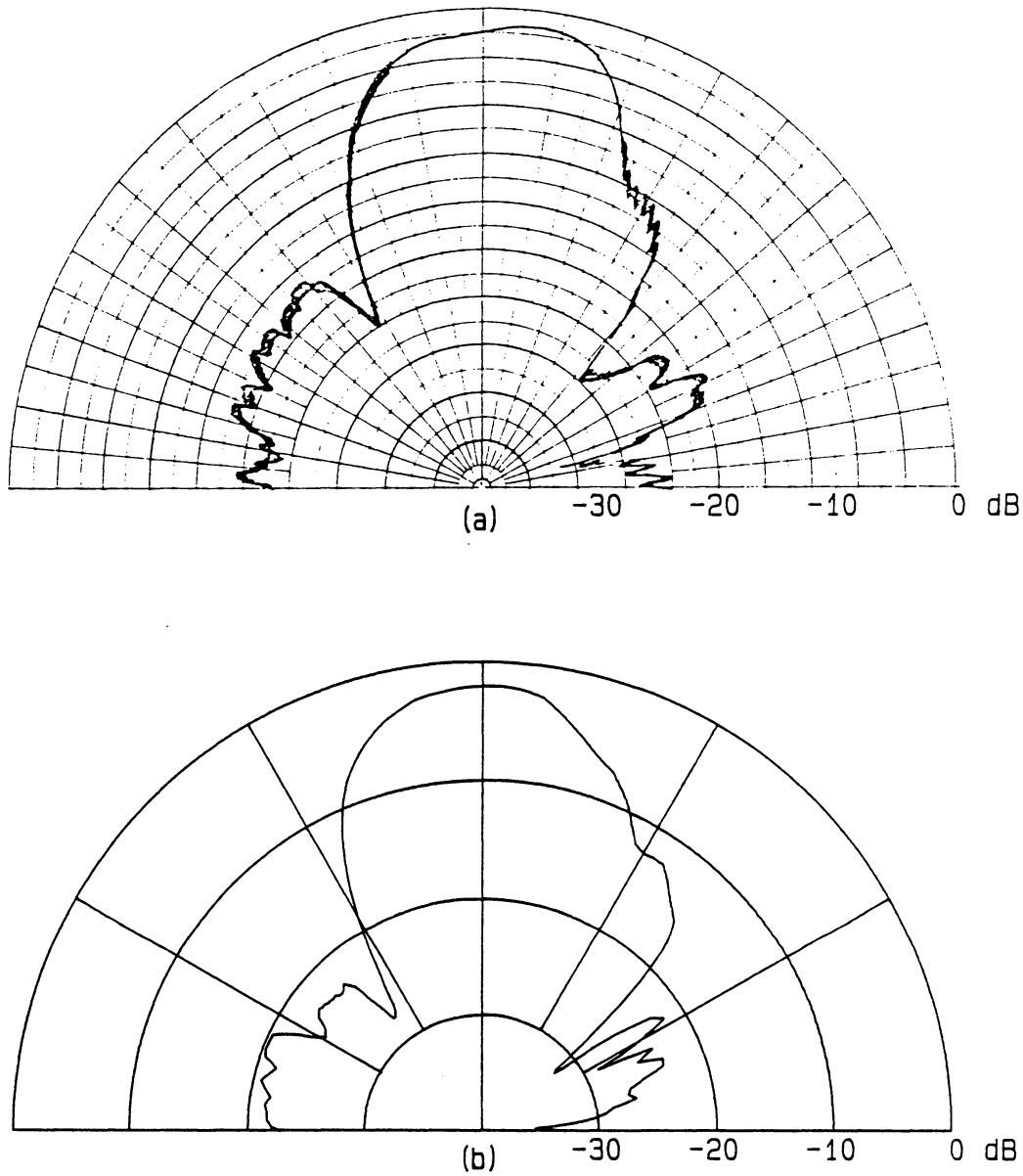

Figure 8.4-1. Comparison of measured and calculated radiation patterns of a blind design 35 dB Dolph-Chebyshev array. a) measured, b) calculated.

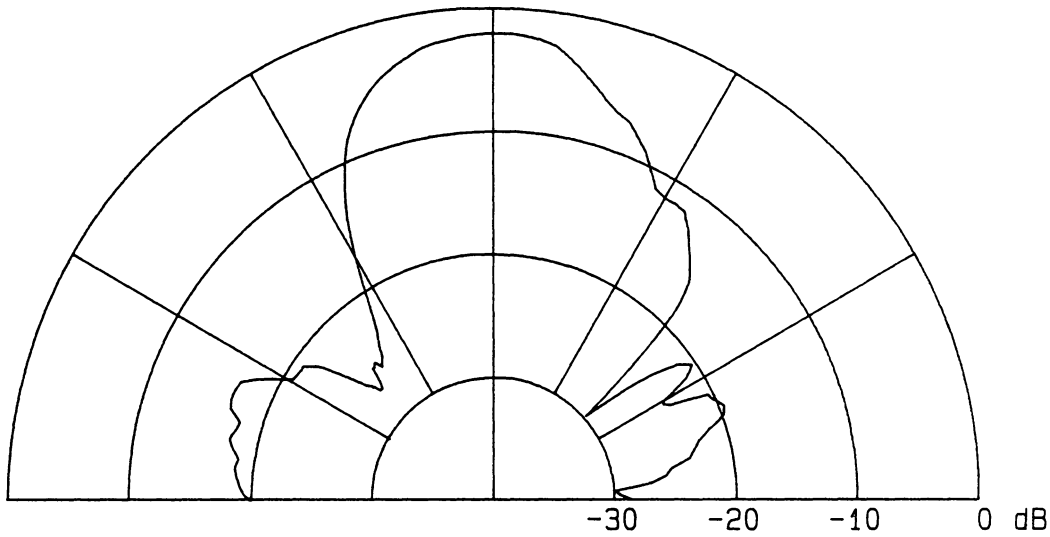

Figure 8.4-2. Calculated radiation patterns of a partial blind design 35 dB Dolph-Chebyshev array.

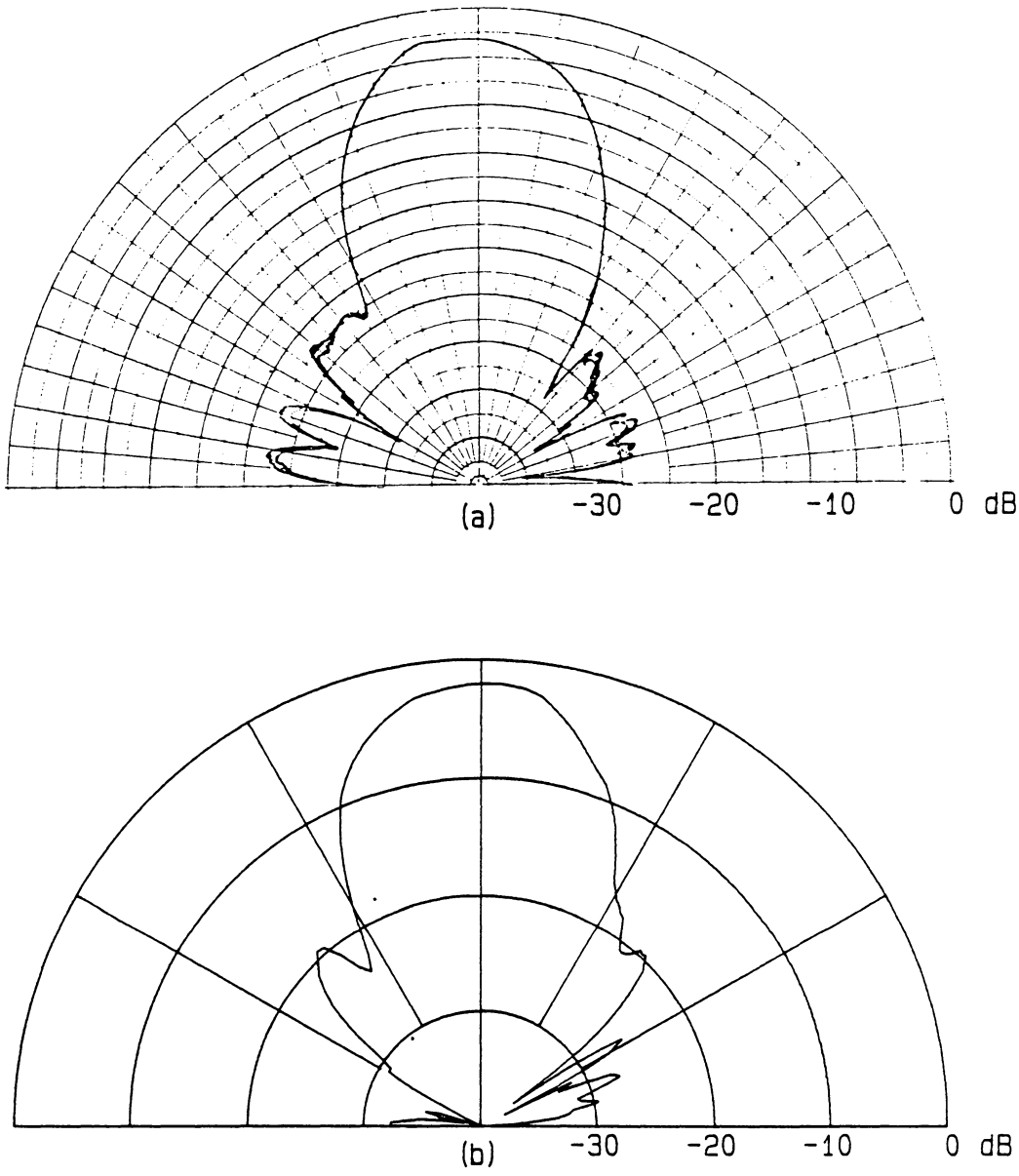

Figure 8.4-3. Comparison of measured and calculated radiation patterns of a compensated 35 dB Dolph-Chebyshev array. a) measured, b) calculated.

Table 8.4-2. Calculated element currents of the blind designs and compensated 35 dB Dolph-Chebyshev array using the eight element microstrip array and the sum feed network with G = 1/0.0°

Element	Blind	Partial Blind	Compensated
1	0.03537/77.20°	0.03655/77.76°	0.05359/-79.13°
2	0.08540/61.26°	0.06978/53.85°	0.11785/-80.03°
3	0.18667/57.07°	0.18699/49.96°	0.20661/-83.62°
4	0.22160/56.08°	0.22419/53.31°	0.25848/-84.59°
5	0.17864/40.42°	0.18456/40.35°	0.26881/-89.37°
6	0.14962/44.91°	0.15711/32.09°	0.21686/-86.16°
7	0.07063/61.41°	0.05719/66.48°	0.12240/-83.22°
8	0.03916/68.61°	0.04427/71.86°	0.04994/-88.44°

IX. Numerical Studies with Wire Antennas

9.1 Introduction

In order for the synthesis techniques developed here to work, accurate knowledge of all coupling effects is required. This is an obvious restriction; coupling effects must be quantified before compensation values can be determined. In Chapter 8 experimental means were used to characterize the coupling (both array and feed coupling). The results did not adequately demonstrate the improvements possible with the synthesis methods. Another approach which offers knowledge of the antenna array mutual coupling is to use moment methods with wire antennas. The results of such a study are presented in this chapter. The array is modeled using a moment method program discussed fully in Section 9.2 and the feed is modeled using SANE and SANE-PODCON. Details of the procedure are presented in Section 9.3. Both arrays of parallel dipoles and parallel monopoles over a finite ground plane are studied. Dipole array synthesis and monopole array synthesis are discussed in Section 9.4 and Section 9.5, respectively. In both cases the compensation process is successfully demonstrated.

9.2 Using Moment Methods in Numerical Experiments

The method of moments is a general technique used to approximately solve equations of the form

$$F(g) = h \tag{9.2-1}$$

where F is a known linear operator, h is a given excitation function, and g is an unknown response function. Expansion of the unknown functions in a linear combination of known basis function allows (9.2-1) to be expanded to a system of N linear equations [B-9]:

$$\sum_{n=1}^{N} c_n < w_m, F(g_n) > = < w_m, h > \qquad m = 1,2,...,N \tag{9.2-2}$$

where $\{g_n\}$ are expansion functions for the unknown function g with coefficients $\{c_n\}$, $\{w_m\}$ are weighting functions, and $< a,b >$ represents the inner product of a and b. The system of N equations can be written in matrix form as

$$[F_{mn}][c_n] = [h_m] \tag{9.2-3}$$

where

$$F_{ij} = < w_i, F(g_j) >$$
$$h_i = < w_i, h >$$

Equation (9.2-3) can be solved for the unknowns $\{c_n\}$ using matrix inversion:

$$[c_n] = [F_{mn}]^{-1}[h_m] \tag{9.2-4}$$

The unknown response function g in (9.2-1) can now be approximated by

$$g \simeq \sum_{n=1}^{N} c_n g_n \tag{9.2-5}$$

Using the method of moments the electric field integral equation of the form

$$\int I(s')K(s, s')ds' = -E^i(s) \tag{9.2-6}$$

can be solved for unknown current I(s') where kernel K(s, s') is specified by the geometry of the antennas and the incident electric field $E^i(s)$ is specified by the given excitation. For example, one of the common integral equations used in treatment of thin wire structures was derived by Pocklington. His integral equation for a z-directed wire is given as [S-2]

$$\frac{1}{j\omega\varepsilon_0}\int_{-L/2}^{L/2} I(z')\left[\frac{\partial^2\psi(z, z')}{\partial z^2} + \beta^2\psi(z, z')\right]dz' = -E_z^i(z) \tag{9.2-7}$$

The function $\psi(z, z')$ is the free space Green's function

$$\psi(z, z') = \frac{e^{-j\beta R}}{4\pi R} \tag{9.2-8}$$

where R is distance between the observation point z and the source location z'. Once the induced currents on the wires are determined using the method of moment the radiated electric fields are computed by

$$E_\theta = \frac{j\eta\beta e^{-j\beta r}}{4\pi r} \sin\theta \int_{-L/2}^{L/2} I(z')e^{j\beta z' \cos\theta} dz' \qquad (9.2\text{-}9)$$

There are numerous computer programs implementing method of moments for various antenna structures. In this study two programs are used. The Electromagnetic Surface Patch code (ESP), which was developed at the Ohio State University Electroscience Laboratory, is a computer implementation of the moment method technique for solving geometries consisting of thin wires and perfectly conducting polygonal plates [N-2]. ESP uses piecewise sinusoidal functions as both expansion function and weighting function [N-2]. The procedure is known as the piecewise sinusoidal Galerkin's method which is computationally more efficient than other pairs of expansion and weighting functions [S-2]. The program approximates the excitation by delta gap voltage generators which can be located anywhere on the wires or at the attachment points between plates and wires [N-2]. Then the excitation function $E^i(s)$ is zero everywhere (since tangential electric field must be along a wire) except across the feed points.

The second moment method program used in this study, MININEC II written by Davis [D-10], is an improved version of the Mini-Numerical Electromagnetics Code (MININEC). MININEC is a personal computer version of more extensive Numerical Electromagnetics Code (NEC). MININEC II determines the current distribution and far field pattern of wire geometries in free space and wire geometries over an infinite ground plane. The program uses pulse function as both expansion and weighting function [D-10].

Before ESP is used in numerical experiments to calculate coupling coefficients of array antennas it is necessary to verify that the mutual impedance values obtained from

the program are reasonable. Figure 9.2-1 compares the mutual impedance between two parallel half wavelength dipoles for various element spacings. The dotted curves represent the values calculated by ESP for dipoles with radius $a = 0.005\lambda_0$. The solid curves represent the mutual impedance between two ideal parallel dipoles of length $L = \lambda_0/2$ which are obtained from [B-9]

$$\begin{aligned} R_{12} &= \frac{\eta}{4\pi \sin^2(\beta L/2)} [2Ci(u_0) - Ci(u_1) - Ci(u_2)] \\ X_{12} &= \frac{\eta}{4\pi \sin^2(\beta L/2)} [2Si(u_0) - Si(u_1) - Si(u_2)] \end{aligned} \tag{9.2-10}$$

where

$$\begin{aligned} u_0 &= \beta d \\ u_1 &= \beta(\sqrt{d^2 + L^2} + L) \\ u_2 &= \beta(\sqrt{d^2 + L^2} - L) \end{aligned}$$

R_{12} and X_{12} are real and imaginary parts of the mutual impedance Z_{12}, respectively. The functions Ci and Si are cosine and sine integrals. The differences between ideal dipole results and the values calculated by ESP for close element spacings are due to the finite radius of dipoles accounted for with the ESP model.

The programs ESP and MININEC II are also used to predict S-parameters of an array of eight monopoles over a ground plane. The monopoles have length $L = 0.2375\lambda_0$, radius $a = 0.011\lambda_0$ and are spaced $d = 0.5\lambda_0$ apart. The ground plane is a $5.55\lambda_0 \times 5.55\lambda_0$ rectangular conductor. In the MININEC calculation, the finite ground plane was replaced with an infinite ground plane.

Figure 9.2-2 shows comparison of the calculated to measured S-parameters of the array. The S-parameters of the array are calculated from the outputs of ESP and

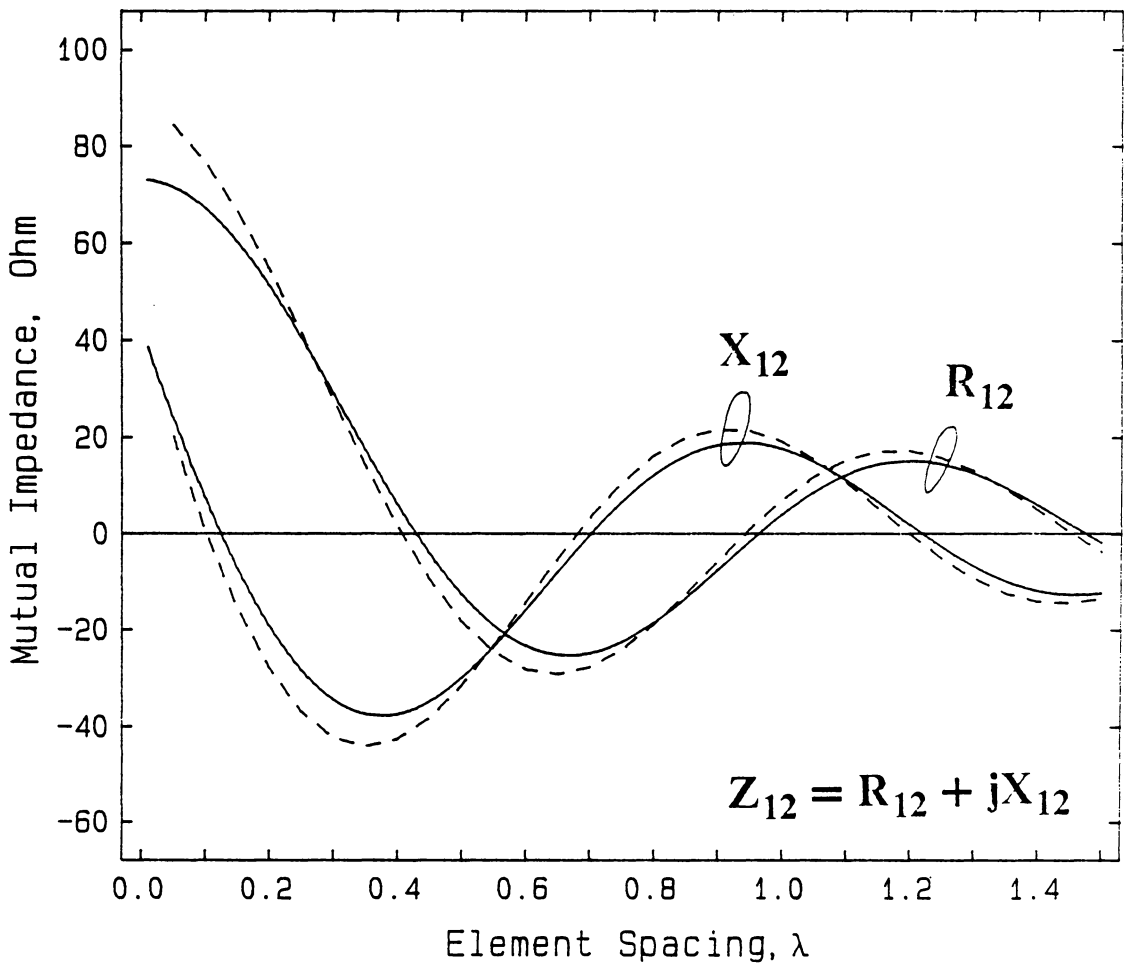

Figure 9.2-1. Comparison of mutual impedance between two parallel $\lambda_0/2$ dipoles. Ideal dipoles (solid curves). Calculated using ESP (dotted curves).

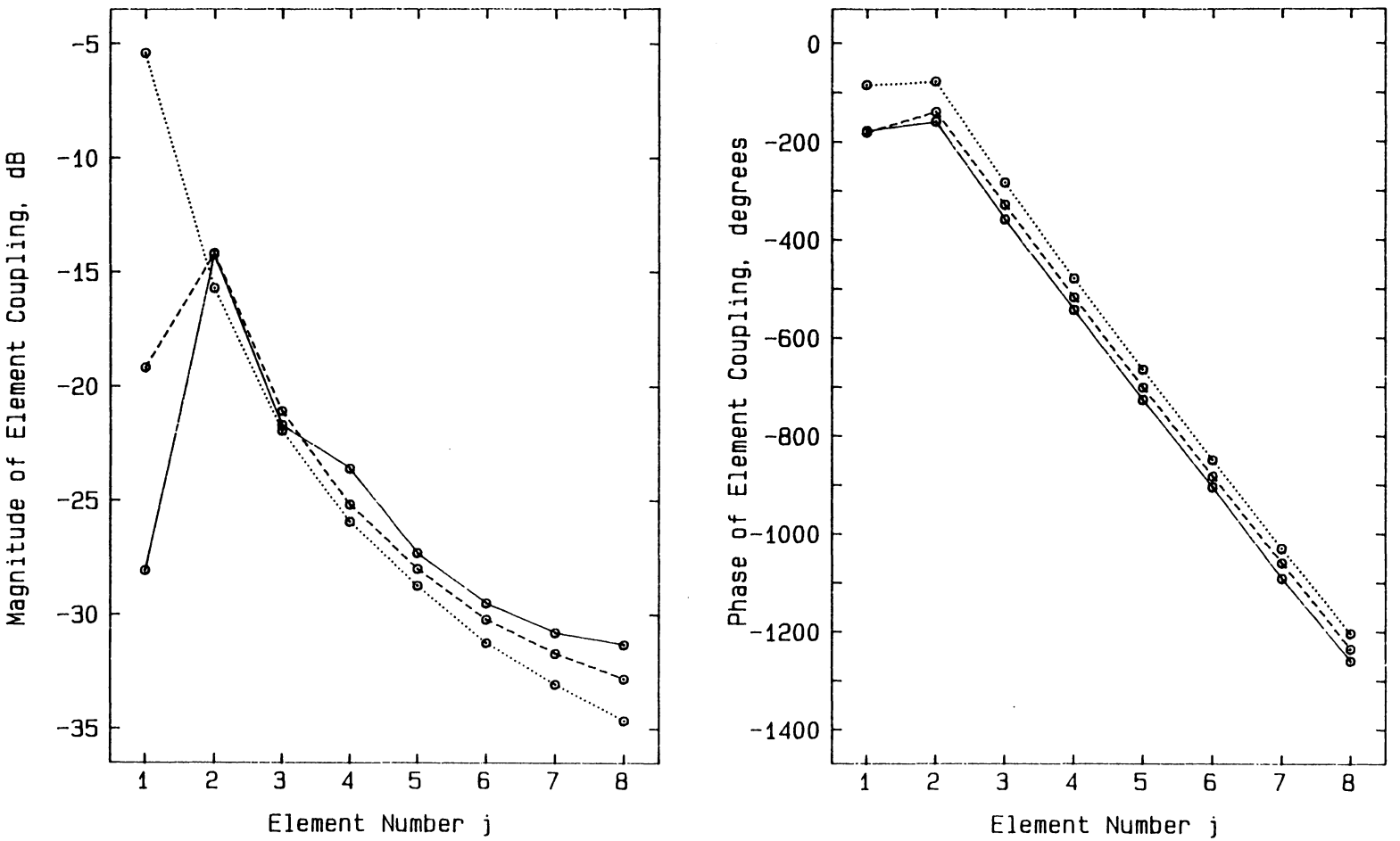

Figure 9.2-2. Comparison of the calculated to the measured S-parameters of an eight element monopole array. Measured (solid curves). Calculated using ESP (dotted curves). Calculated using MININEC II (dashed curves).

MININEC II using steps 1) and 2) of the numerical experiment procedures described in next section. It is apparent from the plots that MININEC II predicts measured results more closely than ESP. ESP is especially poor at predicting the return loss, S_{ii}, of the monopole array. This result suggest that the uncompensated patterns of a monopole array calculated in the numerical experiments in Section 9.5 may be worse than the actual radiation patterns of the array.

9.3 Numerical Experiment Procedures

The numerical experiments in the next two sections were performed using the following steps.

1). The port to port mutual admittance of array antennas are calculated using ESP. The admittance parameters are obtained by exciting one element and shorting all other elements in an array:

$$Y_{mn} = \frac{I_m}{V_n} \quad \text{where } V_j = 0 \text{ for } j \neq n \tag{9.3-1}$$

where I_m is the appropriate port current obtained from the moment method solution. The calculation must be repeated N times for an N element array to obtain the complete Y-matrix.

2). The admittance matrix of the array is converted to S-matrix by [G-1]

$$[S] = [\sqrt{Z_0}][Y_0 - Y][Y_0 + Y]^{-1}[\sqrt{Y_0}] \tag{9.3-1}$$

where $[Y_0]$, $[\sqrt{Y_0}]$ and $[\sqrt{Z_0}]$ are diagonal matrices with elements given by Y_{0i} , $\sqrt{Y_{0i}}$ and $\sqrt{Z_{0i}} = 1/\sqrt{Y_{0i}}$, respectively. Y_{0i} represents the characteristic admittance of the transmission line attached to port i of the network.

3) Calculate the required element currents using an ordinary array synthesis technique.

4). Calculate the S-matrix of the initial feed network that does not include mutual coupling compensation using MCAP for the element currents obtained in step 3 (blind design).

5). Calculate the actual element currents and voltages using MCAP for the array and the feed network obtained in the previous steps. Then calculate blind design far-field pattern using ESP with the voltages as excitation (in place of a feed network).

6). Compute a compensation network using SANE or modify the feed network using SANE-PODCON to compensate for mutual coupling.

7). Calculate the element voltages using MCAP.

8). Compute the compensated far-field patterns using ESP with the voltages of step 7 as excitations (in place of a compensated feed network).

9.4 An Eight Element Dipole Array Example

The eight element linear array considered in this section consists of z-directed parallel dipoles of length $L = 0.466\lambda_0$ and radius $a = 0.005\lambda_0$. The elements are spaced $d = 0.500\lambda_0$ apart along x-axis and are fed at the center of the dipoles. The geometry and the orientation of the array is shown in Fig. 9.4-1. An operating frequency of 300 MHz was chosen for the ease of calculation ($\lambda_0 = 1$ m). A 30 dB Dolph-Chebyshev pattern with the main beam steered to 30° off broadside is the design objective. The required element currents found using the step 3 in Section 9.3 are [S-2]

$$\begin{aligned} I_1 &= 0.26222/\underline{315°} & I_5 &= 1.00000/\underline{-45°} \\ I_2 &= 0.51875/\underline{225°} & I_6 &= 0.81196/\underline{-135°} \\ I_3 &= 0.81196/\underline{135°} & I_7 &= 0.51875/\underline{-225°} \\ I_4 &= 1.00000/\underline{45°} & I_8 &= 0.26222/\underline{-315°} \end{aligned} \qquad (9.4\text{-}1)$$

The feed network for the above current distribution that does not include mutual coupling compensation (blind design) consists of seven 2-way variable power divider networks with the required phase shift to steer the main beam. The required power dividers and phase shifters are listed in Table 9.4-2. The element currents that result from the blind design feed network and the corresponding E-plane and H-plane radiation patterns are shown in Table 9.4-3 and Figure 9.4-5, respectively.

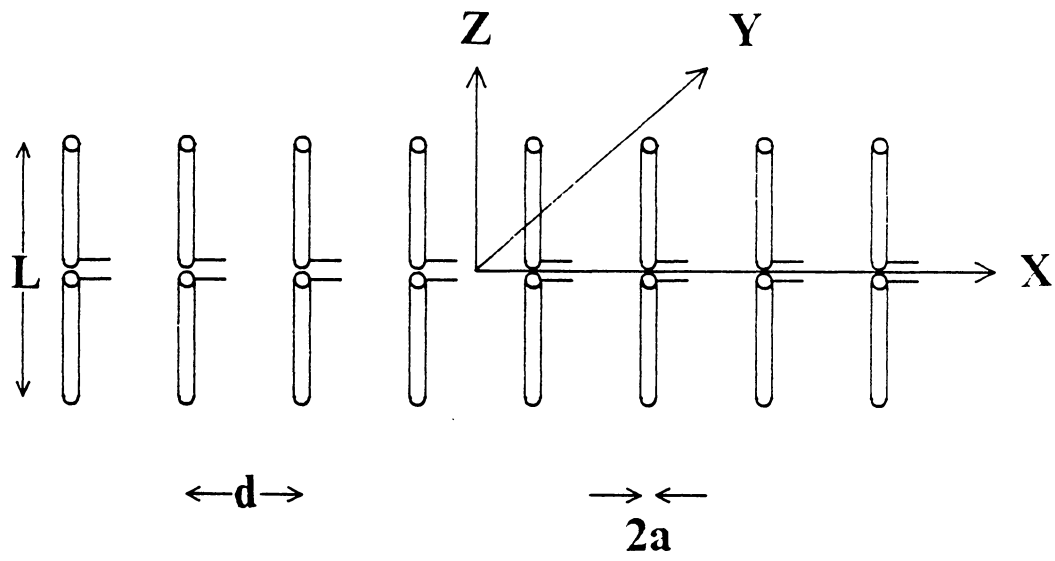

Figure 9.4-1. Geometry of eight $\lambda_0/2$ dipole array with $d = \lambda_0/2$ element spacing.

9.4.1 Attenuator/phase shifter compensation

In the attenuator/phase shifter compensation network an attenuator in series with a phase shifter was placed between the feed and each element (see Fig. 9.4-2). In this compensation technique the generator phase was changed at 10° increment to find the most efficient network. (See discussion in Section 5.3). The required compensation network parameters and other results using SANE are summarized in Table 9.4-1. The normalized E-plane and H-plane radiation patterns of the compensated array are plotted in Fig. 9.4-5. The radiation patterns of the blind design array are also plotted for comparison.

9.4.2 Power divider compensation

For variable power divider network compensation the power ratio and phase shifts are modified from those of the blind design to achieve mutual coupling compensation. The power dividers and phase shifters are formed in the corporate feed network configuration as shown in Fig. 9.4-3. The required power divider and phase shifter values are given in Table 9.4-2. The radiation patterns of the array with the modified feed network along with those of blind design array are shown in Fig. 9.4-8.

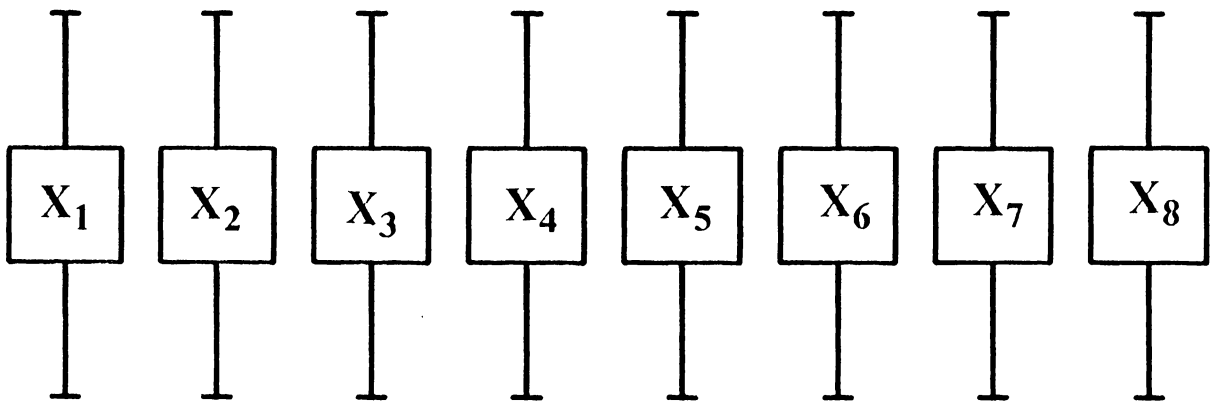

Figure 9.4-2. Attenuator/phase shifter compensation network for an eight element dipole array.

Table 9.4-1. Required attenuators and phase shifters for the 30 dB Dolph-Chebyshev 8-element dipole array example.

No.	Attenuation	Phase Shift
1	3.119 dB	31.94°
2	2.425 dB	29.81°
3	1.509 dB	34.53°
4	1.080 dB	18.70°
5	0.000 dB	26.04°
6	0.831 dB	0.36°
7	0.329 dB	18.64°
8	2.307 dB	-12.84°
G	2.51264	150.00°

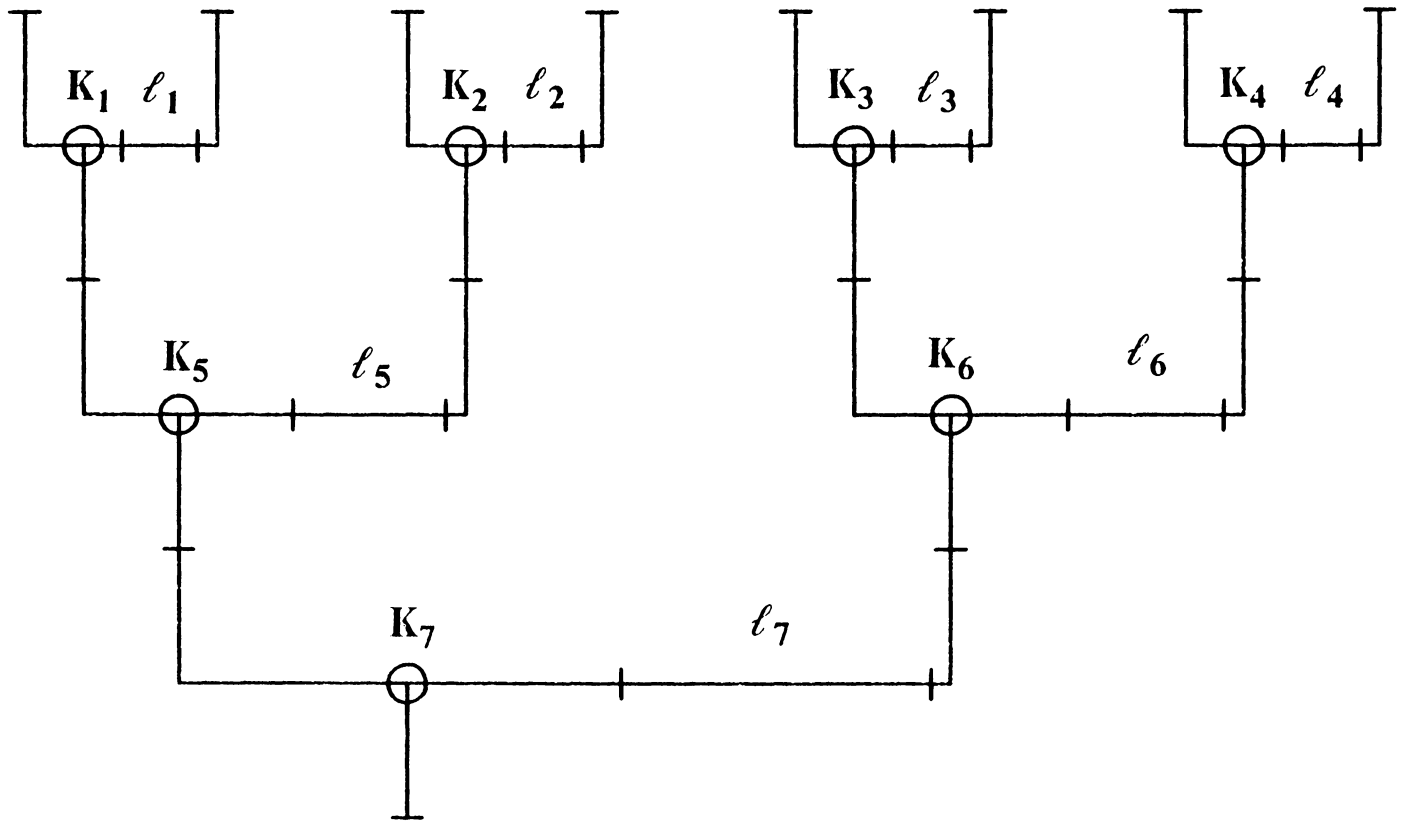

Figure 9.4-3. Variable power divider network for an eight element dipole array.

Table 9.4-2. Required variable power dividers and phase shifters for 30dB Dolph-Chebyshev 8-element dipole array example.

	Blind Design		Compensated Design	
No.	K	Ph. Shift	K	Ph. Shift
1	0.79649	-90.00°	0.81382	-80.76°
2	0.60267	-90.00°	0.47938	-100.79°
3	0.39733	-90.00°	0.22670	-105.57°
4	0.20351	-90.00°	0.06047	-112.71°
5	0.83083	180.00°	0.85703	-170.25°
6	0.16917	180.00°	0.15481	-179.89°
7	0.50000	0.00°	0.49279	-2.37°
G	1.99857	-135.00°	2.23865	171.65°

9.4.3 The frequency sensitivity of the compensation networks

The compensation networks derived in the previous subsections are of no practical value if they are very sensitive to changes in the frequency. Thus, it is necessary to test the frequency sensitivity of the networks. In this section the radiation patterns using the compensation networks in the previous two sections are calculated at 294 MHz and 306 MHz.

In the attenuator/phase shifter network, the compensation variables are kept constant while S-parameters of the blind design feed network array are modified according to their frequency behavior. The array S-matrices are also recomputed at each frequency using ESP. In the case of the variable power divider compensation network, the S-matrices of the modified feed network are calculated at three frequencies using MCAP to include the frequency variation effects of the power dividers discussed in Section 4.4.3. The array S-matrices are the same as those used for the attenuator/phase shifter case.

Figures 9.4-4 through 9.4-6 show the normalized E-plane and H-plane patterns of the blind design array and the array with attenuator/phase shifter compensation at 294 MHz, 300 MHz and 306 MHz, respectively; these represent a 4% frequency swing. Figures 9.4-7 through 9.4-9 show the compensated patterns using variable power divider networks at the three frequencies. The figures show that though the compensated patterns deviate from the desired pattern, they are still closer to the desired pattern than the blind design radiation patterns.

The frequency sensitivity investigation in this section showed that the synthesis techniques are not so sensitive that a slight frequency change eliminates the improvements achieved at the design frequency.

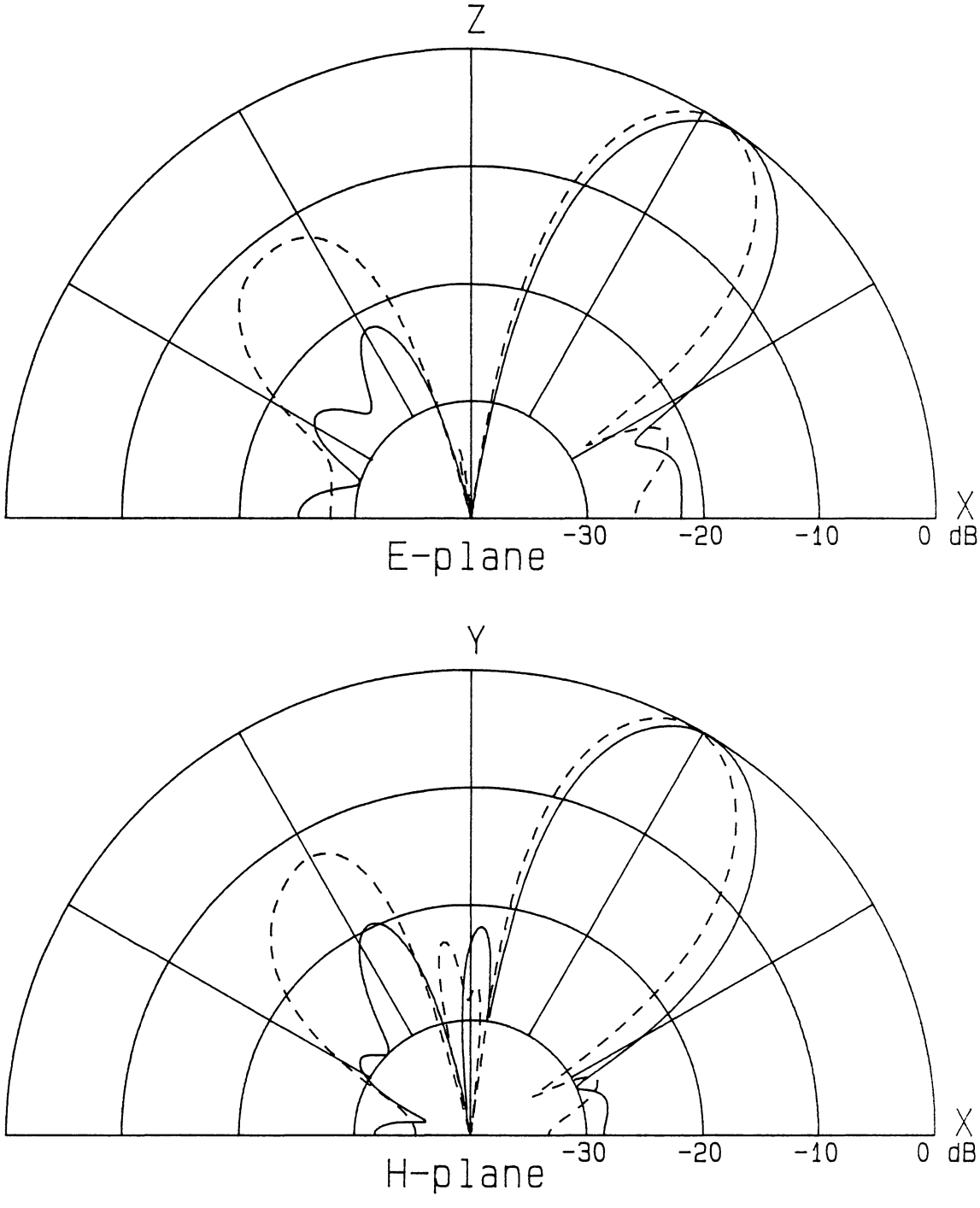

Figure 9.4-4. Comparison of E-plane and H-plane radiation patterns of the array of Fig. 9.4-1 for blind design (dotted) and the attenuator/phase shifter network compensation (solid) at 294 MHz.

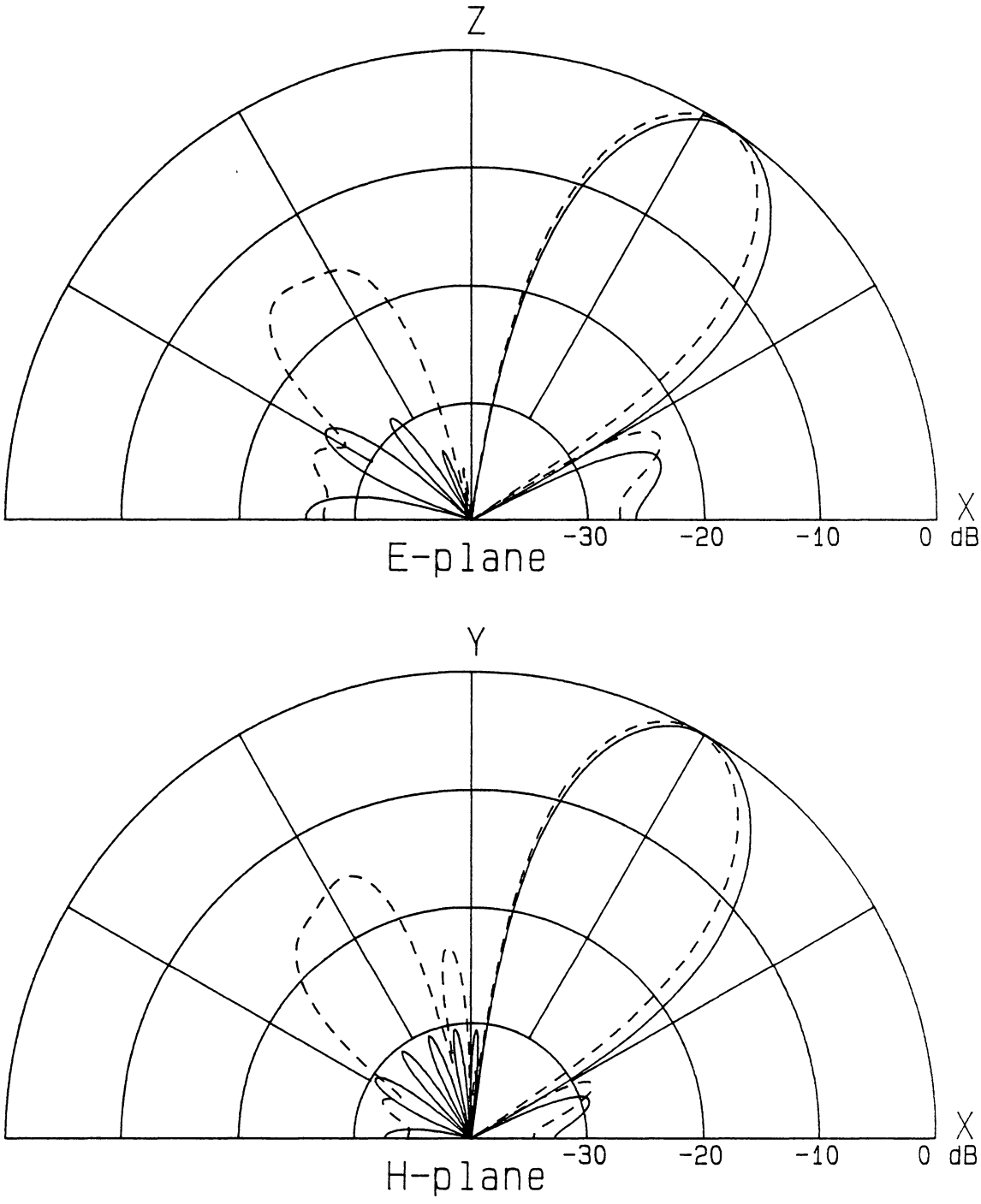

Figure 9.4-5. Comparison of E-plane and H-plane radiation patterns of the array of Fig. 9.4-1 for blind design (dotted) and the attenuator/phase shifter network compensation (solid) at 300 MHz the design frequency.

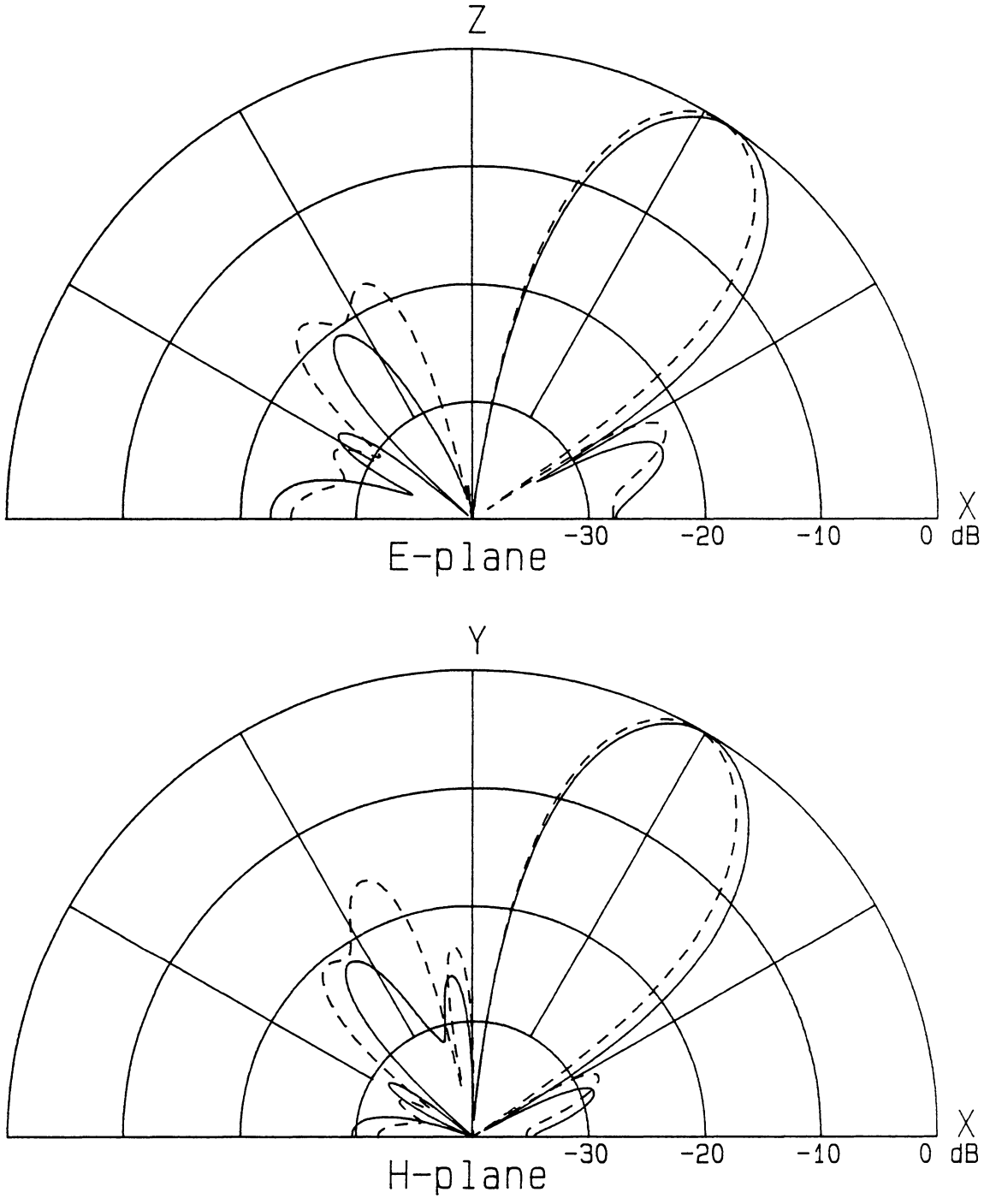

Figure 9.4-6. Comparison of E-plane and H-plane radiation patterns of the array of Fig. 9.4-1 for blind design (dotted) and the attenuator/phase shifter network compensation (solid) at 306 MHz.

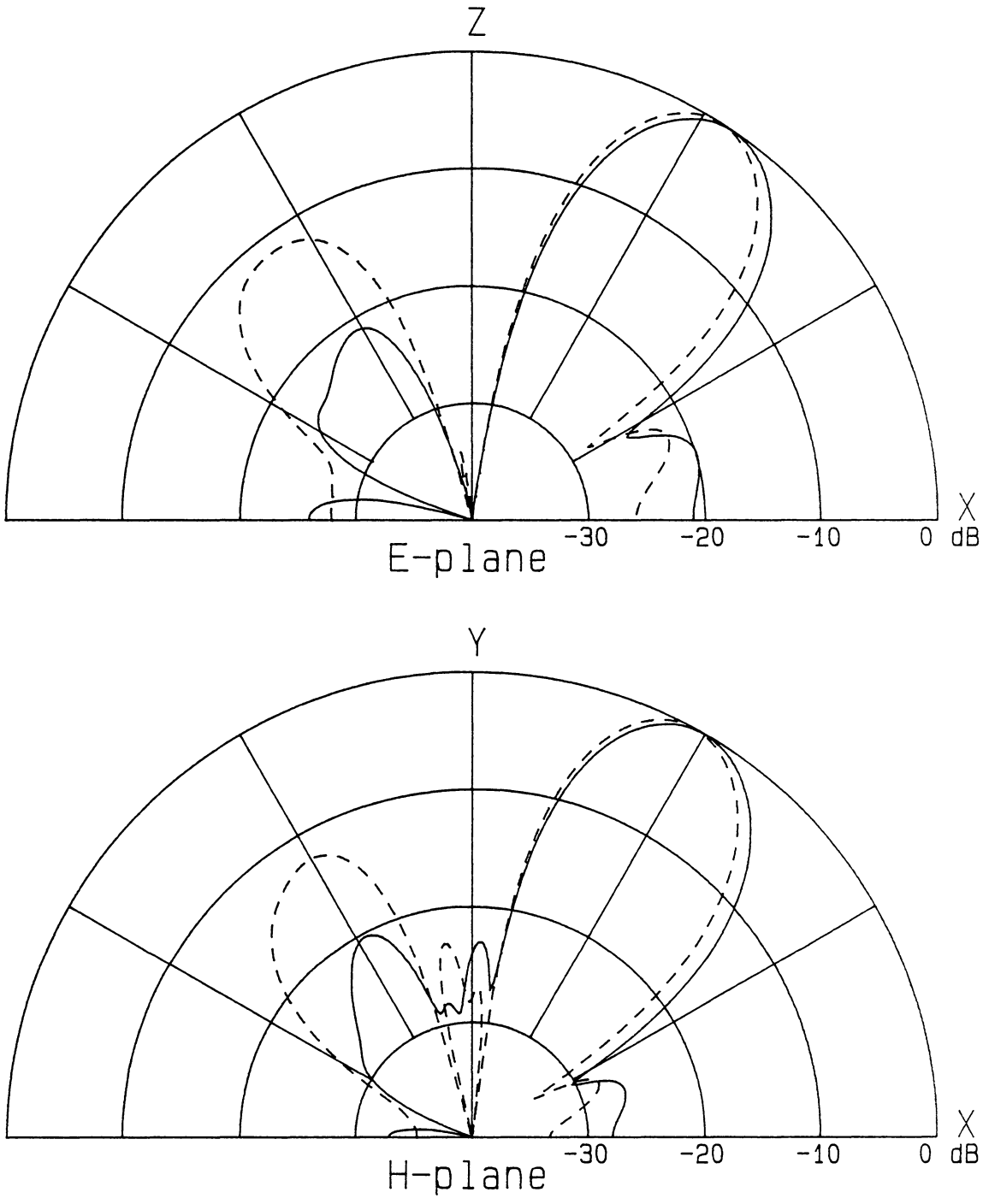

Figure 9.4-7. Comparison of E-plane and H-plane radiation patterns of the array of Fig. 9.4-1 for the blind design (dotted) and the variable power divider network compensation (solid) at 294 MHz.

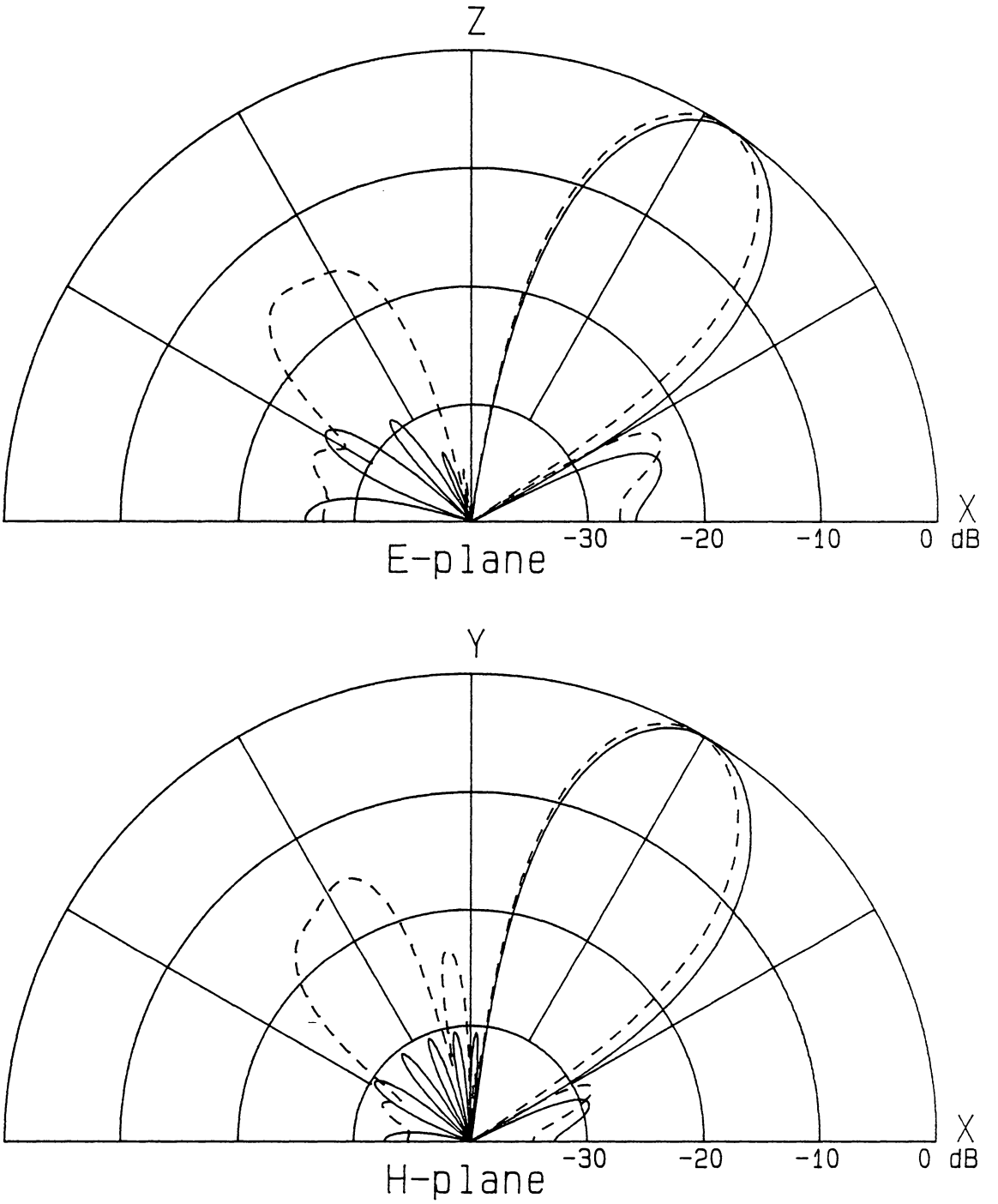

Figure 9.4-8. Comparison of E-plane and H-plane radiation patterns of the array of Fig. 9.4-1 for the blind design (dotted) and the variable power divider network compensation (solid) at 300 MHz the design frequency.

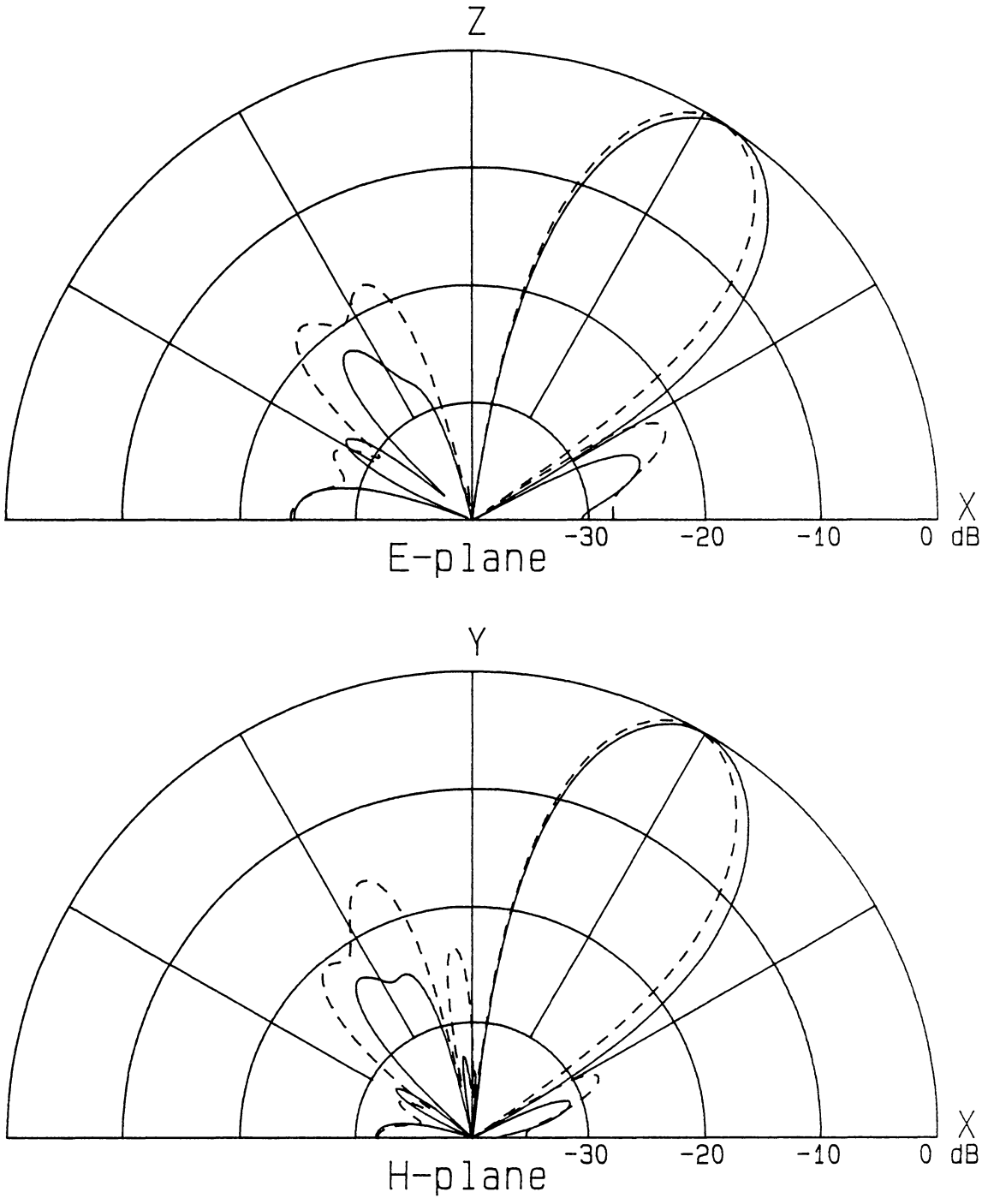

Figure 9.4-9. Comparison of E-plane and H-plane radiation patterns of the array of Fig. 9.4-1 for the blind design (dotted) and the variable power divider network compensation (solid) at 306 MHz.

Table 9.4-3 Element currents used to produce Figs. 9.4-4 through 9.4-9.

294 MHz			
Element No.	Blind Design	Atten./Ph. Shifter	Power Divider
1	0.12656/157.46°	0.11161/189.7°	0.10979/162.02°
2	0.25370/77.99°	0.22646/109.57°	0.26891/81.99°
3	0.32176/-22.37°	0.36830/16.09°	0.37959/-12.15°
4	0.51418/-88.75°	0.39167/-65.89°	0.50272/269.90°
5	0.36823/168.92°	0.38359/189.18°	0.39586/174.04°
6	0.43171/107.68°	0.30566/110.95°	0.37092/91.76°
7	0.21874/-7.11°	0.20139/13.16°	0.23050/-1.59°
8	0.19632/-51.16°	0.08812/-65.90°	0.12030/-76.34°

300 MHz			
Element No.	Blind Design	Atten./Ph. Shifter	Power Divider
1	0.13054/137.22°	0.10436/165.00°	0.11712/143.35°
2	0.23044/50.02°	0.20646/75.00°	0.23171/53.35°
3	0.31110/-45.47°	0.32315/-15.00°	0.36269/-36.65°
4	0.47433/236.12°	0.39799/255.00°	0.44671/233.35°
5	0.39349/140.01°	0.39799/165.00°	0.44669/143.35°
6	0.43402/69.29°	0.32315/75.00°	0.36271/53.35°
7	0.20806/-40.61°	0.20646/-15.00°	0.23173/-36.65°
8	0.19572/260.94°	0.10436/255.00°	0.11713/233.35°

306 MHz			
Element No.	Blind Design	Atten./Ph. Shifter	Power Divider
1	0.14284/105.88°	0.10290/138.08°	0.13260/111.71°
2	0.21113/18.36°	0.18571/40.18°	0.20781/21.75°
3	0.33308/-78.09°	0.31038/-45.03°	0.38278/-69.47°
4	0.44560/201.40°	0.37339/216.76°	0.41316/199.86°
5	0.40143/107.98°	0.41354/134.50°	0.45570/109.74°
6	0.40001/33.83°	0.30791/39.11°	0.33384/19.68°
7	0.19011/-73.65°	0.20078/-49.51°	0.20793/-70.22°
8	0.17099/220.02°	0.10378/214.10°	0.09783/192.50°

9.4.4 Power and efficiency

Table 9.4-4 summarizes the power distribution and the efficiency of the attenuator/phase shifter compensation and the power divider compensation for the dipole array considered. The notation as defined by Smith [S-2] is used in the table.

P_{inc} = incident power produced by the generator

$= G^2$

where G is the generator voltage magnitude.

P_{ref} = reflected power back into the generator

$= (S^N G)^2$

where S^N is the reflection coefficient of the compensated array looking into the input port.

P_{dis} = power dissipated by the compensation network

P_{rad} = power radiated

$= P_{inc} - P_{ref} - P_{dis}$

The efficiency is defined as

$$\text{Eff.} = \frac{P_{rad}}{P_{inc}} \times 100\%$$

The power distributions are calculated from the results of MCAP analysis of the compensated arrays.

Table 9.4-4. The power distribution in the attenuator phase shifter compensation network and power divider compensation network for a 30 dB Dolph-Chebyshev dipole array (all powers in Watts).

	Atten./Ph. Shifter	Power Divider
P_{inc}	6.31335	5.01155
P_{ref}	0.00455	0.00590
P_{dis}	1.30290	0.00000
P_{rad}	5.00590	5.00590
Efficiency	79.3 %	99.8 %

In Table 9.4-4 the power divider networks are assumed to be lossless. Thus, no power is lost in the blind design feed network and the power divider compensated feed network. In other words, P_{dis} only represents the power lost in the attenuators. The high efficiency shown in Table 9.4-4 for the power divider compensation results from this. When line losses due to finite conductivity and other nonideal effects are considered in the S-matrix calculation of the compensation network, the power divider network would be somewhat less efficient.

9.4.5 Computational efficiency

Figure 9.4-10 shows plots of CPU time and number of iterations required by SANE and SANE-PODCON as functions of interelement phasing, α, in desired currents. The calculations are based on the array of eight dipoles shown in Fig. 9.4-1. The magnitude of desired currents are the same as (9.4-1) while the interelement phasing is changed from $\alpha = 0°$ which produces a broadside pattern to $\alpha = 180°$ which scans the main beam to endfire direction.

In the case of SANE for attenuator/phase shifter compensation, a blind design feed that corresponds to each interelement phasing is used in the calculations. In the power divider compensation calculations the initial guess produced by the program SANE-PODCON is used. The CPU time data points are calculated from the execution of SANE and SANE-PODCON on IBM 3090 at Va Tech. The number of iterations are calculated for the error in the norm of the nonlinear equations to be less than 1.0E-05.

As it is shown in Fig 9.4-10, SANE requires larger number of iterations to converge to a solution than SANE-PODCON. This is generally true because in SANE generator phase is changed to optimize power efficiency of attenuator/phase shifter compensation network. In this particular example, generator phase was changed from 0° to 170° at

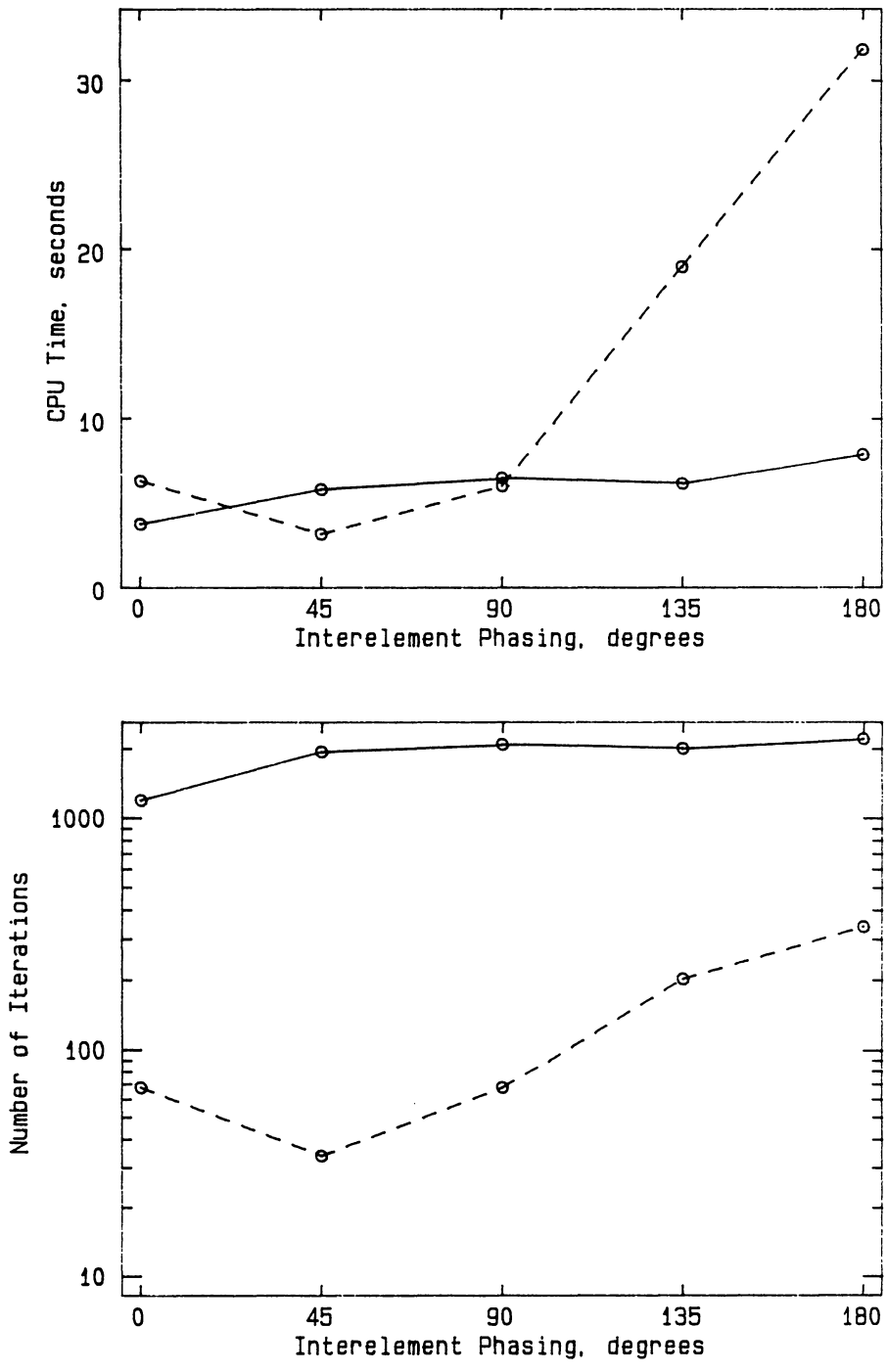

Figure 9.4-10. CPU time and number of iterations required by SANE and SANE-PODCON to converge to a solution as functions of interelement phasing.

10° steps. Thus, in average SANE required only one eighteenth of the total iterations to converge to a solution at each generator phase. Also, it should be noted that though SANE requires more iterations than SANE-PODCON, the required CPU time for this particular array are in the same order of magnitude. SANE requires less CPU time per iteration than SANE-PODCON because the form of nonlinear equations is simpler for attenuator/phase shifter compensation.

It is also apparent in the plots that SANE-PODCON becomes more difficult to converge as the larger interelement phasing is required. For example, the required CPU time for $\alpha = 180°$ (6.32 seconds) is about 5 times longer than for the broadside pattern $\alpha = 0°$ (31.84 seconds). On the other hand, the change in required CPU time for SANE is small for different case of interelement phasing.

The results presented here are only for the 8-element dipole array of Fig. 9.4-1. For an array with larger number of elements, the convergence by SANE-PODCON would be slower than by SANE.

9.4.6 Conclusions from the dipole array study

In this study the latest wire analysis techniques were used in combination with the proposed mutual coupling synthesis methods. This was done for both attenuator/phase shifter compensation and power divider network compensation. The center frequency radiation patterns for the 30 dB eight element parallel dipole array are shown in Figs. 9.4-5 and 9.4-8 for the two compensation networks. Comparison of the blind design and compensated array patterns in both compensation network cases show that in the H-plane the high side lobe level (-15 dB) was reduced to the design value of -30 dB. In the E-plane side lobe level of -15 dB was reduced to -24 dB through compensation. The desired side lobe reduction was not quite achieved in the E-plane due to the varying

shape of individual element pattern for dipole antennas in this elevation plane, whereas the azimuth plane (H-plane) has omnidirectional patterns for all elements.

9.5 An Eight Element Monopole Array Above a Finite Ground Plane

In this section we will consider synthesis of a 30 dB Dolph-Chebyshev pattern using an array of eight monopoles over a finite ground plane. The z-directed monopoles have length $L = 0.233\lambda_0$, radius $a = 0.005\lambda_0$ and are spaced $d = 0.500\lambda_0$ apart along x-axis. The ground plane is a $5.0\lambda_0 \times 5.0\lambda_0$ rectangular plate of a perfect conductor located on xy-plane at $z = 0$. The geometry of the array is shown in Fig. 9.5-1. Y-parameters for the elements are obtained using ESP and then, they are transformed to S-parameters using the steps 1 and 2 discussed in Section 9.3.

The desired pattern is a 30 dB Dolph-Chebyshev pattern with the main beam steered to 30° off broadside. The required element current distribution is the same as the dipole array case in the previous section and is shown in (9.4-1). The same desired pattern was chosen for the comparison with the dipole results.

In Section 9.2, it was shown that ESP may have difficulty in predicting return loss, S_{ii}^{A}, for monopoles over a ground plane. For the array considered in this section, the magnitude of S_{ii}^{A} calculated using ESP are approximately -5 dB. These are unrealistically high return loss which makes blind design radiation pattern worse that what it really should be. Thus, for the blind design analysis the diagonal elements of the array S-matrix are replaced with the S-parameters for the monopoles over an infinite ground plane calculated using MININEC II. The element currents are calculated from the blind design feed network used in Section 9.4 and are shown in Table 9.5-1. The

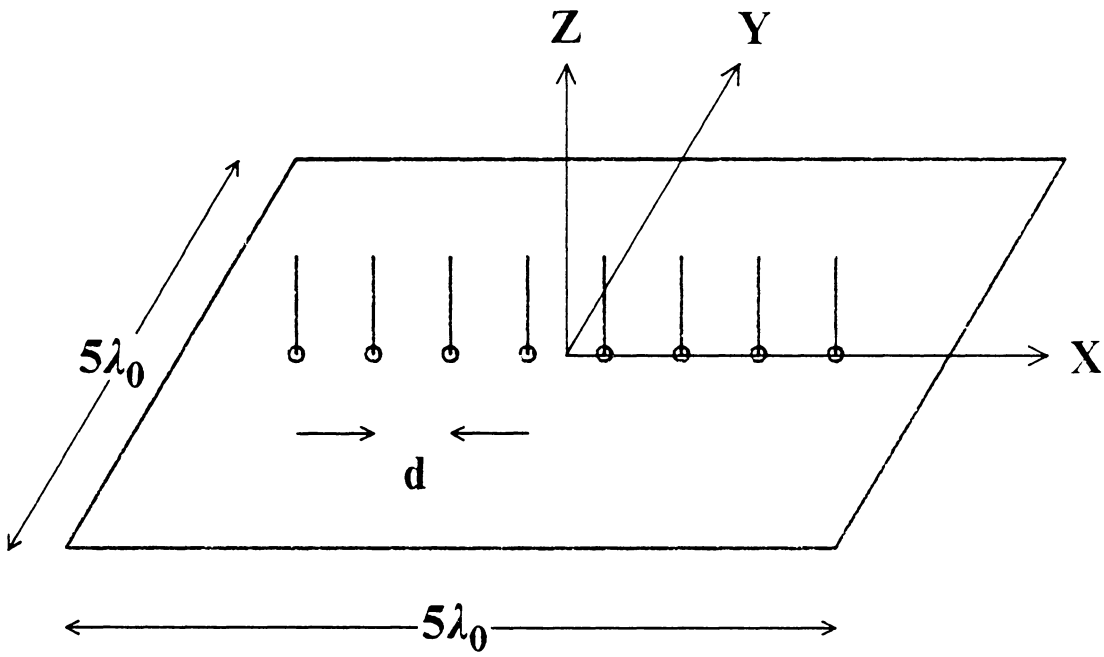

Figure 9.5-1. Geometry of eight element monopole array over a finite ground plane used in the numerical experiment.

corresponding E-plane and H-plane radiation patterns are plotted in Fig. 9.5-2 with dotted curves.

The required compensation network parameters are computed from the ESP calculated element S-parameters and the blind design feed network S-parameters using SANE and SANE-PODCON. The resulting parameters are summarized in Tables 9.5-1 and 9.5-2, respectively. Figure 9.5-2 shows the E-plane and H-plane radiation patterns of the compensated array (solid curves). In the H-plane, the side lobe level of -13 dB was successfully reduced to the desired level of -30 dB. In the E-plane, however, the side lobe was only reduced to -15 dB. Unlike the dipole array case in Section 9.4, the failure to synthesize the desired result comes not only from the shape of element pattern in this plane, but also from the variation in individual element pattern introduced by the finite ground plane. This is similar to result observed in the 35 dB Dolph-Chebyshev microstrip array as discussed in Section 8.4.

Table 9.5-1. Required attenuators and phase shifters for the 30 dB Dolph-Chebyshev monopole array example.

No.	Attenuation	Phase Shift
1	0.000 dB	48.70°
2	4.257 dB	5.39°
3	0.982 dB	41.56°
4	4.319 dB	7.68°
5	1.978 dB	22.00°
6	5.469 dB	3.48°
7	2.735 dB	20.08°
8	5.380 dB	-0.80°
G	2.55183	130.00°

Table 9.5-2. Required variable power dividers and phase shifters for 30dB Dolph Chebyshev monopole array example.

	Blind Design		Compensated Design	
No.	K	Ph. Shift	K	Ph. Shift
1	0.79649	-90.00°	0.07724	-88.48°
2	0.60267	-90.00°	0.06040	-92.17°
3	0.39773	-90.00°	0.03519	-95.22°
4	0.20351	-90.00°	0.01446	-101.29°
5	0.83083	180.00°	0.85802	-168.26°
6	0.16917	180.00°	0.16804	-174.55°
7	0.50000	0.00°	0.52595	4.15°
G	1.99857	-135.00°	1.46877	137.73°

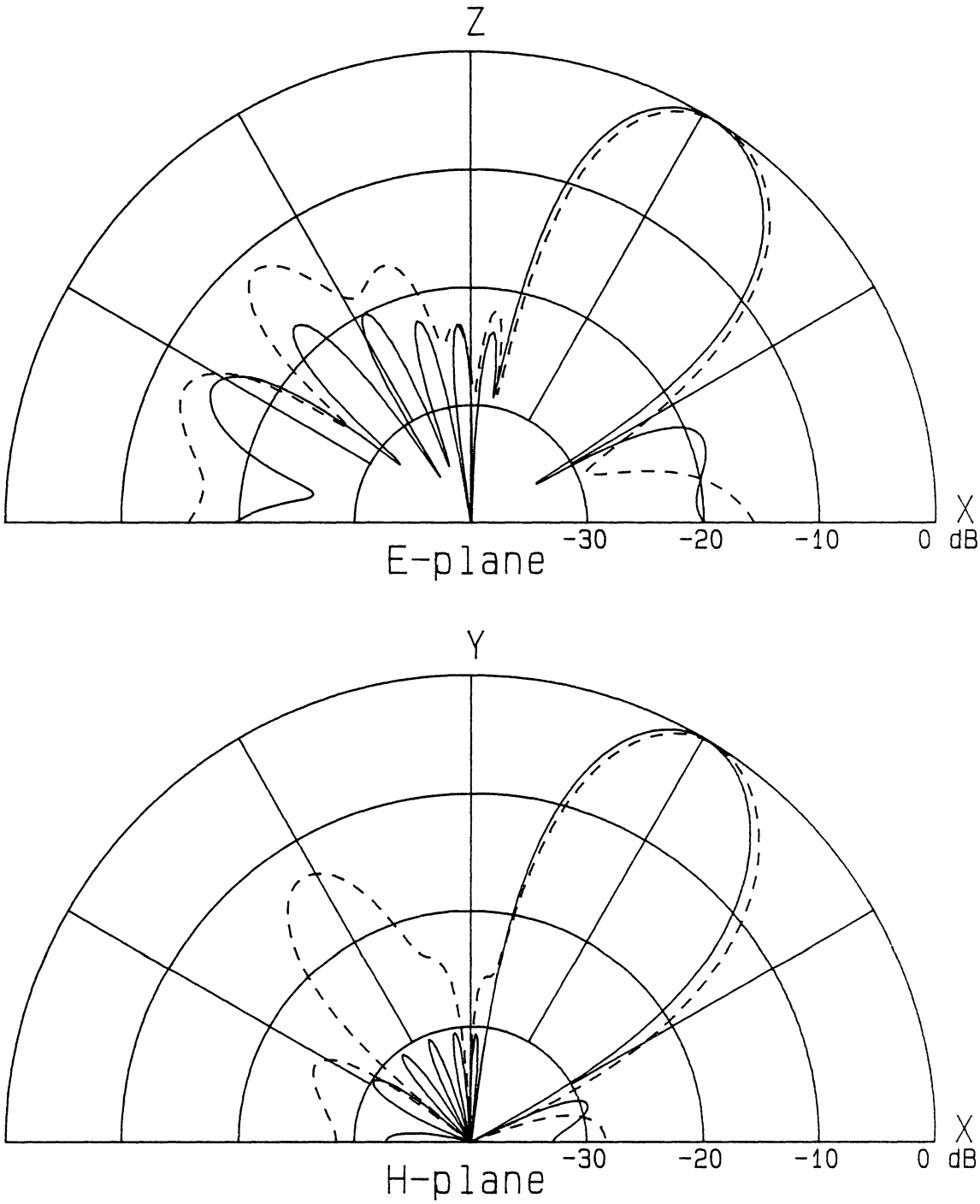

Figure 9.5-2. Comparison of E-plane and H-plane radiation patterns of the array of Fig. 9.5-1 for the blind design (dotted) and compensated design (solid) at 300 MHz.

Table 9.5-3. Element currents used to produce Figure 9.5-2.

Element No.	Blind Design	Atten./Ph. Shifter	Power Divider
1	0.04932/189.96°	0.10274/185.00°	0.17853/177.27°
2	0.32404/85.85°	0.20324/95.00°	0.35319/87.27°
3	0.14857/-9.23°	0.31812/5.00°	0.55281/-2.73°
4	0.78694/261.32°	0.39180/-85.00°	0.68082/267.27°
5	0.27949/159.52°	0.39180/185.00°	0.68085/177.27°
6	0.91869/83.60°	0.31812/95.00°	0.55281/87.27°
7	0.15310/-41.37°	0.20325/5.00°	0.35319/-2.73°
8	0.45119/-88.38°	0.10274/-85.00°	0.17854/267.27°

X. Conclusions

This report reflects four years of study into the effects of mutual coupling on array analysis and synthesis. During this effort several fundamental array issues were addressed as well as new array synthesis techniques. Progress was made in answering several fundamental questions, but much remains. The objective of this study was to develop and verify synthesis techniques for array antennas which include all coupling effects. This was accomplished using an attenuator/phase shifter network and a variable power divider network.

In this chapter the key results are collected and summarized. References are made to the appropriate points in the report for further details. Recommendations for future study are also given in this chapter.

10.1 Summary of Research Results

Fundamental Issues In Array Theory

1. *Scattering Parameter Representation of Arrays with Coupling Effects Included*

The scattering matrix representation for general arrays was developed in Sec. 2.1 and array coupling effects in terms of scattering parameters were discussed in Sec. 2.2, including examples of the coupling effects on radiation patterns (Figs. 2.2-3 and 2.2-4).

2. *Array Pattern Analysis Including Mutual Coupling*

Array pattern analysis techniques in the presence of mutual coupling was developed (Sec. 2.3). It was shown that radiation pattern of an array driven by the feed/generator network can be approximated by (2.3-9) as follows:

$$F(\theta, \phi) \simeq \sum_{n=1}^{N} g_{a,n}(\theta, \phi) I_n e^{j\xi_n} \tag{10.1-1}$$

The element currents, I_n, are obtained using the S-parameter network analysis technique discussed in Section 2.1. $g_{a,n}(\theta, \phi)$ is the pattern of each element in the array environment when all other elements are match loaded. When element patterns are similar in shape and gain, (10.1-1) can be simplified to (2.3-10):

$$F(\theta, \phi) \simeq g_{ae}(\theta, \phi) \sum_{n=1}^{N} I_n e^{j\xi_n} \tag{10.1-2}$$

where $g_{ae}(\theta, \phi)$ is a typical element pattern of the array. These equations need further investigation; see recommendation 4 in the next section.

Computer Aided Microwave Network Analysis To Assist in Array Design

3. *The MCAP program*

MCAP, the Microwave Circuit Analysis Program, originally published in [G-1] was modified by PSL and by Smith during the effort for microstrip array feed analysis and is described fully in Sec. 4.2.

4. *Power Divider Networks*

MCAP was used to study frequency response of a two-way variable power divider (Sec. 4.4.3). The results showed that for a large power ratio the phase difference between two output ports of a quadrature hybrid power divider deviates rapidly from zero for operations off of the design frequency (See plot in Fig. 4.4-4). The two-way power dividers were then used as building block to develop a N-way variable power divider network (Sec. 6.2).

General Array Synthesis Including Mutual Coupling Compensation

5. *Overview of Pattern Synthesis*

It is assumed that the principle of pattern multiplication applies and that the pattern of an array is factorable in the form of (2.3-10) as follows:

$$F(\theta, \phi) = g_{ae}(\theta, \phi) f(\theta, \phi) \tag{10.1-3}$$

where

$$f(\theta, \phi) = \text{normalized array factor} \propto \sum_{n=1}^{N} I_n e^{j\xi_n} \tag{10.1-4}$$

where ξ_n are defined in (2.3-2). For desired pattern $F(\theta, \phi)$ and a known active element pattern $g_{ae}(\theta, \phi)$ we can solve for the corresponding desired array factor using (10.1-3) as

$$f(\theta, \phi) = \frac{F(\theta, \phi)}{g_{ae}(\theta, \phi)} \tag{10.1-5}$$

Then conventional "text book" synthesis techniques that do not account for coupling are used to find the desired currents $\{I_n\}$. The realization of these currents in the presence of coupling effects is the thrust of the proposed methods (see following items). The important assumption here is that the individual active element patterns are sufficiently alike that (10.1-5) holds.

6. *Summary of System of Equations*

Figure 10.1-1 summarizes the solution formulation. A system of nonlinear equations which describes a general array antenna network consisting of antenna elements, a feed network, a compensation network and a generator was developed in (2.4-14) and (2.4-15) and are

$$0 = -a_k^A + \sum_{i=1}^{N} S_{k,i}^C b_i^A + \sum_{i=1}^{M} S_{k,N+i}^C \left[c_i^{F/G} + \sum_{j=1}^{M} S_{i,j}^{F/G} U_j \right] \quad \text{for } 1 \le k \le N \tag{10.1-6}$$

$$0 = -U_{k-N} + \sum_{i=1}^{N} S_{k,i}^C b_i^A + \sum_{i=1}^{M} S_{k,N+i}^C \left[c_i^{F/G} + \sum_{j=1}^{M} S_{i,j}^{F/G} U_j \right] \quad \text{for } N+1 \le k \le N+M \tag{10.1-7}$$

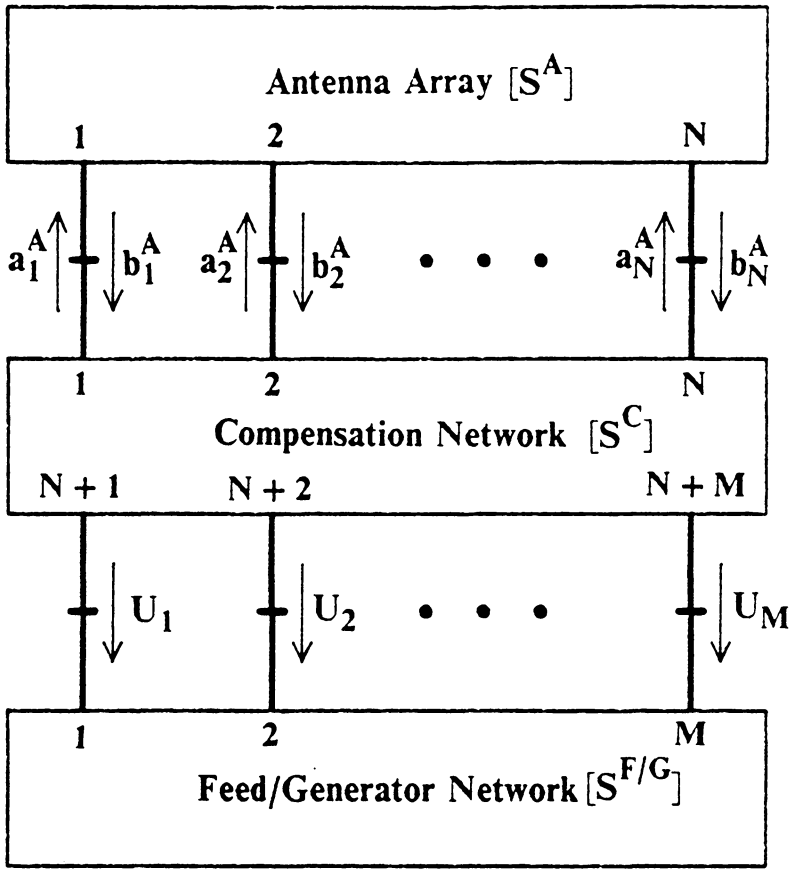

Knowns: Feed/Generator Network $[S^{F/G}]$

Array Excitation $[a^A]$ $[b^A]$

Compensation Network Form $[S^C]$

Unknowns: Reflected Waves from Compensation Network $\{U_i\}$

Compensation Network Parameters $\{X_i\}$ where $S^C = F(X)$

Induced Waves from Generator $\{c_i^{F/G}\}$

Figure 10.1-1. General compensation approach for a N-element array with a M-way feed network.

where $\{a_k^A\}$ and $\{b_i^A\}$ are obtained from (2.4-7) and (2.4-8) using desired element currents $\{I_i^A\}$ and known scattering parameters of the antenna elements $[S^A]$. The feed/generator network has combined S-parameters $[S^{F/G}]$ and the generator induces waves $[c^{F/G}]$ at the feed/generator output ports. The unknown variables $\{X_i\}$ which represent the physical specification for the compensation network are imbedded in the scattering parameters $[S^C]$. The variables $\{U_j\}$ are intermediate unknowns necessary to expand the system of equations in closed form. The equations are nonlinear because of the terms $S^C_{k,N+i}U_j$ which are products of the unknown variables. In the case where the generator value is treated as a unknown, the products $S^C_{k,N+i}c_i^{F/G}$ also contribute to the nonlinear property of the equations.

7. *Mutual Coupling Effect in Symmetric Excitations*

Smith [S-1,Sec 8.4] showed that an ideal N-way power divider could be used to produce a sum pattern which would be insensitive to the presence of mutual coupling. The statement can be extended to any symmetrical excitation. That is, if the feed network produces an array excitation which is symmetric (amplitude and phase symmetric about center of the array) mutual coupling effects (which can be unsymmetric) do not alter the symmetry of the resulting currents. Note that if a linear phase taper is imposed the excitation is unsymmetric and mutual coupling effects alter the current distribution. This property, however, is only applicable to ideal power dividers which have S-parameters as derived by Smith [S-1,(4.4-19)]. The variable power divider network derived in this effort (item 4) has S-parameters different from the N-way power divider derived by Smith. Thus, the property does not apply to the variable power divider network.

A sum pattern feed network that has Smith's form of S-parameters can be realized using 50Ω coaxial T-junctions connected in a corporate feed configuration. Such feed

network would be least effected by mutual coupling. However, the network would have high VSWR at the feed output ports resulting in low power efficiency.

8. *The Decomposition of Element Currents*

The currents in each element of an array can be decomposed into three terms:

$$I = I_{ideal} - I_{antenna\ coupling} + I_{full\ coupling} \tag{10.1-8}$$

This was derived in Sec. 5.4 for an attenuator/phase shifter compensation two element array of matched antennas but should hold with mismatches present as well. In (10.1-8) I_{ideal} is the current that would be present if no mutual coupling were present anywhere in the system. $I_{antenna\ coupling}$ is the contribution to the current in one element induced by the other elements through antenna coupling. This current exists when there is mutual coupling between antenna elements but no coupling through the feed network. $I_{full\ coupling}$ is present when there is a coupling between output ports of the feed network. The coupling through the feed network introduces a feedback loop in the system which makes the currents a nonlinear function of compensation variables; this is discussed in item 9 below.

9. *The Nonlinear Property of Attenuator/Phase Shifter Compensated Arrays*

The nonlinear relation between attenuator/phase shifter compensation network parameters and element currents was demonstrated for a two element array of matched antennas in (5.4-10) and (5.4-11). It was shown that the compensation network can be obtained by solving a system of linear equations when only antenna coupling is considered. When feed network coupling is present the relationship between the element currents and the compensation network parameters becomes a nonlinear function.

10. *The Generator Level Setting Effect*

In solving the system of nonlinear equations for attenuator/phase shifter compensation, it was shown that the constraint in (5.2-6) must be imposed on the unknown variables to ensure that a physically realizable network results. Smith [S-1] showed that the magnitude of generator can be adjusted to meet this constraint. The process, however, is a nonlinear function because of the relation between element currents and generator values. It was shown that the constraint can be used to eliminate an attenuator from the attenuator/phase shifter compensation network.

Specific Solutions

11. *Attenuator/Phase Shifter Compensation Network*

A system of equations for the synthesis of attenuator/phase shifter compensation networks that was derived by Smith [S-1] was summarized in Section 5.2. In addition, our investigation showed that multiple solutions exist and efficiency can be improved by changing the absolute phase of the generator; see Section 5.3. The computer program SANE [S-1] was modified to include this effect in the solution for the system of equations. A description of changes made in SANE is discussed in Appendix A.

12. *Power Divider Compensation Network*

A general system of nonlinear equations for the synthesis of compensation networks (item 6) was modified for power divider networks so that they can be solved numerically; see (6.3-6). Also, the initial guess to the solution of the nonlinear equations which plays an important role in numerical technique was discussed (Sec. 6.4). The computer program SANE-PODCON was written to solve the nonlinear equations using a modified Newton's method; see Appendix B. The code converges much more efficiently than SANE-GECON written by Smith [S-1].

13. *Transmission Line Compensation Network*

Mutual coupling compensation with transmission lines was attempted (Chap. 7). However, except for the case of two element arrays, convergence to a solution for the nonlinear equations was never achieved. This failure seems to come from the physical nature and the specific structure of scattering parameters of the network rather than from the use of inadequate numerical techniques.

Verification

14. *Analysis Experiments with a Microstrip Array*

The S-parameter analysis technique developed in Section 2.1 and the array pattern analysis technique developed in Section 2.3 were applied to an eight element microstrip array in Section 8.2 for sum, difference and endfire excitations. Comparison of measured and calculated patterns (Figs. 8.2-2 through 8.2-4) suggests that the techniques are basically valid. However, close match of measured and calculated patterns were never obtained due to uncertainty in accuracy of measured S-parameters and variation in active element patterns of the microstrip array.

15. *Synthesis Experiment with a Microstrip Array*

Attenuator/phase shifter networks and power divider networks were designed in Section 8.3 to compensated for mutual coupling in the eight element microstrip array for sum, difference and endfire excitation. In Section 8.4 an attenuator/phase shifter compensation network was designed to synthesize a 35 dB Dolph-Chebyshev pattern using the microstrip elements and sum feed network. The compensation network was built and tested at PSL. The measured patterns (Figs. 8.4-1 and 8.4-3) showed reduction in the sidelobe level from -17 dB to -21 dB and improvement in main beam shape. The

desired sidelobe level, however, was not achieved because of the variation in active element patterns.

16. *Wire Antenna Computer Studies*

A 30 dB Dolph-Chebyshev pattern with main beam steered to 30 degrees off broadside was synthesized using an array of eight dipoles and an array of eight monopoles over a finite ground plane. The dipole and monopoles arrays were modeled using the ESP moment method computer code. The required attenuator/phase shifter network and power divider network parameters are given in Tables 9.4-1 and 9.4-2 for the dipole array and in Tables 9.5-2 and 9.5-3 for the monopole array. The calculated E-plane and H-plane patterns of the blind design and and compensated dipole array are shown in Fig. 9.4-5 for attenuator/phase shifter compensation and in Fig. 9.4-8 for power divider compensation. The calculated patterns of the monopole array are shown in Fig. 9.5-2. In both dipole and monopole arrays, complete compensation was achieved in H-plane. However, the sidelobes were not reduced to the desired level in E-plane due to varying shape of individual element pattern in the elevation plane. (See discussion in Sec 9.4.6).

Comparison of Compensation Methods

17. *Accuracy and Convergence*

Attenuator/phase shifter and power divider compensation network parameters were successfully calculated for eight element arrays in Chapters 8 and 9. However, solutions were obtained only for two element array cases using transmission line characteristic impedance network technique (See Chapter 7).

Smith found that convergence of the power divider network equations are very sensitive to the initial guess to the solution. The convergence problem was solved by

using the initial network that would be necessary without considering mutual coupling (See Section 6.4).

18. *Frequency Sensitivity*

Comparison of calculated patterns for the dipole arrays at the center frequency of 300 MHz and side frequencies of 294 MHz and 306 MHz showed that the compensation networks are not extremely sensitive to small variations in the operating frequency. See Figs. 9.4-4 through 9.4-9.

19. *Computer Time*

The required CPU time and number of iterations for the eight element dipole array were compared for different cases of interelement phasing in desired currents in Section 9.4.5. It was shown that SANE for attenuator/phase shifter compensation requires more iterations than SANE-PODCON for power divider compensation because SANE optimizes the compensation network for power efficiency by varying the phase of generator. The required CPU time, however, were similar for both SANE and SANE-PODCON for the particular array considered. It was also shown that convergence to a solution by SANE-PODCON becomes slow as the interelement spacing is increased (See Fig. 9.4-10).

20. *Efficiency of Synthesis Network*

Comparison of power efficiency of attenuator/phase shifter network and power divider network is presented in Table 9.4-5. The power divider network was shown to have very high efficiency.

10.2 Recommendations for Future Work

1. *Experimental Verification*

The next major step necessary in this study is experimental verification of the technique. If the present scattering parameter models for the array can be realized then other types of compensation network can be developed. For example, the technique may be extended to allow series feeding of the elements. Otherwise more rigorous model for the array, feed and compensation networks must be developed.

The present experiments as described in Chapter 8 use measured scattering parameters to compensated for mutual coupling. Such measurements are very difficult for large element array. The Moment methods can be used to approximate for the mutual coupling among antenna elements as shown in Chapter 9. This needs to be verified also through experiments.

2. *Array Factoring*

During the course of this study it was discovered that fundamental questions in basic array pattern formulation remain. For example, a thorough study on (10.1-1), (10.1-2) and the developments in Section 2.3 could be examined with wire antenna moment method computer experiments.

3. *General Study of Sufficient Conditions for Compensation*

In this study we found two network architectures which permit compensation of mutual coupling effects. A worthwhile study would be to find the necessary conditions for compensation in general.

4. *Inclusion of Individual Element Patterns*

The synthesis methods developed here work well only if array factorization as in (10.1-2) holds. A challenging area of study would be to develop synthesis techniques with different individual element pattern as in (10.1-1).

5. *Termination of Synthesis Codes*

The termination condition of the iteration in the computer programs SANE and SANE-PODCON need to be modified. The present programs use error in the element currents as the condition. This should be replaced with the error criterion in radiation pattern.

6. *Extension to Active Devices*

It may be possible to apply this technique to use active component in the compensation network. This will lead to synthesis technique where antenna elements, the feed network and compensation network as well as any other networks such as amplifiers are implemented on the same substrate.

7. *Shaped Beam Synthesis*

The results presented in this report are for narrow beam (or difference) patterns. Synthesis of shaped main beams is also very important. Shaped beam patterns were successfully synthesized using both attenuator/phase shifter and power divider compensation networks for a 16 element dipole array calculated using ESP. Experiments must be conducted using array with larger number of elements.

XI. REFERENCES

[A-1]. John L. Allen, "Gain and impedance variation in scanned dipole arrays," *IRE Trans. on Ant. and Prop.*, vol. AP-10, pp. 566-572, Sept. 1962.

[A-2]. J. Bach Anderson and Jenrik Hass Rasmussen, "Decoupling and descattering network for antennas," *IEEE Trans. on Ant. and Prop.* , vol. AP-24, pp. 841-846, Nov. 1976.

[A-3]. N. Amitay, V. Galindo and and C. P. Wu, *Theory and Analysis of Phased Array Antennas*, Wiley-Interscience: New York, 1972.

[A-4]. L. R. Adkins, H. L. Glass, K. K. Jin, F. S. Stearns, Y. T. Ataiiyn, R. L. Carter, J. M. Owens and D. D. Stancil, "Electronically variable time delays using magnetostatic wave technology," *Microwave Journal*, vol. 29, pp. 109-120, March 1986.

[A-5]. N. Adatin, D. Brain, G. Philippou and P. Rinous, "A theoretical and experimental investigation of multiple-primary feed reflector antenna suitable for contoured beam application," *ICAP 83*, IEE Conf. Pub. no. 219, pp. 6-11, 1983.

[A-6]. Rajendra K. Arora, J. P. Daniel and C. Terret, "Synthesis of linear arrays with unequally spaced element and identical amplitude excitation," *IEEE AP-S 1985 International Symposium*, pp. 103-106, 1985.

[A-7]. J. Bach Andersen, Hans Schjaer-Jacobsen and Henneing A. Lessow, "Coupling between crossed-dipole feed," *IEEE trans. on Ant. and Prop.*, vol. AP-22, pp. 641-646, Sept. 1974.

[A-8]. Ashok K. Agrawal and Gerald F. Mikuchi, "A printed circuit hybrid-ring directional coupler for arbitrary power divisions," *IEEE Trans. on Microwave Theory and Tech.*, vol. MTT-34, pp. 1401-1407, Dec. 1986.

[A-9]. Mohamed D. Abouzahra, "Design and performance of a wideband, multilayer feed network," *Microwave Journal*, vol. 29, pp. 157-164, Nov. 1986.

[A-10]. M. J. Alexander, C. J. Trumpess, J. M. Griffin, M. L. Newton and A. Roederer, "A microstrip patch array for L-band satellite communications," *ICAP 87*, IEE Conf. Pub. No. 274. pp. 285-299, 1987

[A-11]. N. A. Adatia, B. Claydon and D. Brain, "Primary-feed elements for mutiple and contoured beam satellite antennas," *ICAP 81*, IEE Conf Pub. no. 195, pp. 98-103, 1981.

[A-12]. *Anzac catalog*, pp. 204-259.

[B-1]. I. J. Bahl and P. Bhartia, *Microstrip Antennas*, Artech House: Dedham, MA, 1980.

[B-2]. M. C. Bailey, "A Simple Stripline Design for Uneven Power Split," NASA Technical Memorandum 81870, August 1980.

[B-3]. A. K. Bhattacharyya and L. Shafai, "Effect of mutual coupling on the radiation pattern of microstrip phased array antennas," *IEEE 1986 AP-S International Symposium*, pp. 891-893, 1986.

[B-4]. M. C. Bailey and C. W. Bostian, "Mutual coupling in a finite planar array of circular apertures," *IEEE Trans. on Ant. and Prop.*, vol. AP-22, pp. 178-184, March 1974.

[B-5]. Wilfried Bornemann, Peter Balling and William. J. English, "Synthesis of spacecraft array antenna for INTELSAT frequency reuse multiple contoured beams," *Trans. on Ant. and Prop.*, vol. AP-33, pp. 1186-1193, Nov. 1985.

[B-6]. C. R. Boyd, Jr., "On a class of multiple-line directional couplers," *IRE Trans. on Microwave Theory and Techniques*, vol. MTT-10, pp. 287-294, July, 1962.

[B-7]. "Theoretical and experimental investigation of certain basic aspects of patch antennas," Radiation Laboratory, University of Michigan, July 1985.

[B-8]. Allison Babcook, "Analysis of a rectangular microstrip antenna element," March 1985.

[B-9]. C. Balanis, *Antenna Theroy and Analysis and Design*, Harper & Row: New York, 1982.

[C-1]. K. R. Carver, W. L. Stutzman and R. P. Jedlicka, "Analysis and Synthesis of Microstrip Array Antennas Including Mutual Coupling," Jan. 1984.

[C-2]. P. J. Clarricoats, C. G. Parini and S. M. Tun, "Conical horn array feed performance," *ICAP 83*, IEE Int. Conf. Pub. no. 219, pp. 195-199, 1983.

[C-3]. Keith R. Carver and James W. Mink, "Microstrip antenna technology," *IEEE Trans. on Ant. and Prop.*, vol. AP-29, pp. 2-24, Jan. 1981.

[C-4]. K. R. Carver, "Matehmatical modeling of mutual couplign between antennas," *PSL Tech Note, EM 79-1* New Mexico State University, sept. 1979.

[C-5]. Jules A. Cummins, Marcel G. Pelletier and Gilles Y. Delisle, "Network parameter measurements of antenna arrays," *IEEE Trans. on Ant. and Prop.*, vol. AP-25, pp. 760-766, Nov. 1977.

[D-1]. Robert J. Dinger, "Reactively steered adaptive array using microstrip patchantennas at 4 GHz," *IEEE Trans. on Ant. and Prop.*, vol. AP-32, pp. 848-856, August 1984.

[D-2]. Robert J. Dinger, "A planar version of a 4.0 GHz, reactively steered adaptivearray," *IEEE Trans. on Ant. and Prop.*, vol. AP-34, pp. 427-431, March 1986.

[D-3]. D. E. N. Davies, "Mutual coupling compensation for small, circularly symmetric planar arrays," *IEE Proceedings*, vol. 129, part H, pp 281-283, Oct. 1982.

[D-4]. J. E. Dennis, Jr. and R. B. Schnabel, *Numerical Methods for Unconstrained Optimization and Nonlinear Equations*, Prentice-Hall: Englewood Cliffs, New Jersey, 1983.

[D-5]. T. R. Debski and P. W. Hannan, "Complex mutual coupling measured in a large phase array antenna," *Microwave Journal*, vol. 8, pp. 93-96, June 1965.

[D-6]. G. Dubost, *Flat Radiating Dipoles and Applications to Arrays* , Research Studies Press: New York, 1981.

[D-7]. J. P. Daniel and C. Terret, "Mutual coupling between antennas - Optimization of Transistor parameters in active antenna design," *IEEE Trans. on Ant. and Prop.*, vol. AP-23, pp. 513-516, July 1975.

[D-8]. J. P. Daniel and C. Terret, "Experimental verification of reduced mutual coupling between monopoles using appropriate loads," *IEEE Trans. on Ant. and Prop.*, vol. AP-23, pp. 737-739, Sept. 1975.

[D-9]. Dan Davis, "Analysis of array antenna patterns during test," *Microwave Journal*, vol. 21, pp. 67-69, Feb. 1978.

[D-10]. W. A. Davis, D. G. Sweeney and W. L. Stutzman, "MININEC II: an improved version of MININEC for personal computers," *URSI 1987 Radio Science Meeting*, p. 266, June 1987.

[E-1]. R. S. Elliott and G. J. Stern, "The design of microstrip dipole arrays including mutual coupling, part I: theory," *IEEE Trans. on Ant. and Prop.*, vol. AP-29, pp. 757-760, Sept. 1981.

[F-1]. Alan J. Fenn, "Theoretical and experimental study of monopole phased array antennas," *Trans on Ant. and Prop.*, vol. AP-33, pp. 1118-1126, Oct. 1985.

[F-2]. Shoichiro Fukao, Toru Sato, Hiroshi Hojo, Iwane Kimura and Susumu Kato, "A numerical consideration on edge effect of planar dipole phased arrays," *Radio Science*, vol. 21, pp. 1-12, Jan. 1986.

[F-3]. Richard G. Fitzgerrell, "Monopole impedance and gain measurements on finite ground planes," *IEEE Trans. on Ant. and Prop.*, vol. AP-36, pp. 431-438, March 1988.

[G-1]. K. C. Gupta, R. Garg and R. Chadha, *Computer-Aided Design of Microwave Circuit*, Artech House: Dedham, MA, 1981

[G-2]. William F. Gabriel, "Adaptive arrays - An introduction," *Proc. of IEEE*, vol. 64, pp. 239-272, Feb. 1976.

[G-3]. I. J. Gupta and A. A. Ksienski, "Effects of mutual coupling on the performance of adaptive arrays," *IEEE Trans. on Ant. and Prop.*, vol. AP-31., pp. 785-791, Sept. 1983.

[G-4]. Amos E. Gera, "A simplified computational procedure for the analysis of planar arrays," *IEEE Trans. on Ant. and Prop.*, vol. AP-32, pp. 647-650, June 1984.

[G-5]. Gregor Gronau and Ingo Wolff, "Microstrip antennas for satellite broadcast applications," *IEEE 1987 AP-S International Symposium*, pp. 902-905, June 1987.

[G-6]. A. E. Gera, "Mutual coupling easily evaluated," *ICAP 87*, IEE Conf. Pub. No. 274. pp. 385-389, 1987

[G-7]. F. E. Gardiol, "Design and layout of microstrip structures," *IEE Proceedings*, vol. 135, part H, pp. 145-157, June 1988.

[H-1]. P. Henry and R. P. Jedlicka, *A Microwave Circuit Analysis Program (MCAP), Physical Science Laboratory Version*, Physical Science Laboratory, New Mexico, 1985

[H-2]. H. House, Jr., *Stripline Circuit Design*, Artech House: Dedham, MA, 1974.

[H-3]. P. W. Hannan, "Proof that a phased-array can be impedance matched for all scan angles," *Radio Science*, vol. 2, pp. 361-369, March 1967.

[H-4]. P. W. Hannan, D. S. Lerner and G. H. Knittel, "Impedance matching a phased-array antenna over wide scan angles by connecting circuit," *IEEE Trans. on Ant. and Prop.*, vol. AP-13, pp.28-34, Jan. 1965.

[H-5]. Jeffrey S. Herd, "Array element pattern correction in a digital beamforming array: An experimental Study," *1985 North American Radio Science Meeting*, , Canada, p. 26, June 1985.

[H-6]. Victor Fouad Hanna and Jean Jumeau, "A wide-band 12-GHz 12-way planar power divider/combiner," *IEEE Trans. on Microwave Theory and Techniques*, vol. MTT-34, pp. 896-897, Aug. 1986.

[H-7]. Victor Fouad Hanna, Louis Ramboz and Michel Belfort, "Planar power combiner networks providing amplitude and phase control of their 10 ports," *AP-S 1986 International Symposium Digest*, vol. I, pp. 315-318, June 1986.

[H-8]. Peter W. Hannan, "The element gain paradox for a phased array antenna," *IEEE Trans. on Ant. and Prop.*, vol. AP-12, pp. 423-433, July 1964.

[H-9]. John Huang, "Technique for an array to generate circular polarization with linearly polarized elements," *IEEE Trans. on Ant. and Prop.*, vol. AP-34, pp. 1113-1124, Sept. 1986.

[I-1]. Akira Ishimaru, Richard J. Coe, Gary E. Miller and W. Preston Green, "Finite periodic structure approach to large scanning array problems," *IEEE Trans. on Ant. and Prop.*, vol. AP-33, pp. 1213-1220., Nov. 1985.

[I-2]. K. Ito, K. Itoh, and H. Kogo, "Improved design of series-fed circularly polarised printed linear arrays," *IEE Proceedings*, vol. 133, part H, pp. 462-466, Dec. 1986.

[J-1]. R. P. Jedlicka, M. T. Poe and K. R. Carver, "Measured mutual coupling between microstrip antennas," *IEEE Trans. on Ant. and Prop.* vol. AP-29, pp. 147-149, Jan. 1981.

[J-2]. R. P. Jedlicka and K. R. Carver, *Mutual Coupling Between Microstrip Antennas*, Proc. Workshop on Print. Circ. Ant. Tech., Los Cruces, pp. 4.1-4.19, Oct. 1979.

[J-3]. Richard C. Johnson and Henry Jasik, *Antenna Engineering Handbook, Second Edition*, McGraw-Hill: New York, NY, 1980

[J-4]. L. W. Johnson and R. Dean Riess, *Numerical Analysis, 2nd ed.*, Addison Wesley: Reading, MA, 1982.

[J-5]. R. L. Johnston, *Numerical Methods, A Software Approach*, John Wiley and Sons: New York, 1982.

[J-6]. J. R. James, A. Henderson and P. S. Hall, "Micorstrip antenna performance is determined by substrate constants," *MSN*, pp. 73-84, August 1982.

[J-7]. J. R. James, P. S. Hall and C. Wood, *Microstrip Antenna Theory and Design*, Peter Peregrinus Ltd.: New York, 1981.

[J-8]. Immanual Jayakumar, Ramesh Garg, B. K. Sarap and Bhagwan Lal, "A conformal cylindrical microstrip array for producing omnidirectional radiation pattern," *IEEE Trans. on Ant. and Prop.* , vol. AP-34, pp. 1258-1261, Oct. 1986.

[K-1]. Walter K. Kahn, "Impedance-match and element-pattern constraints for finite arrays," *IEEE Trans. on Ant. and Prop.*, vol. AP-25, pp. 747-755, Nov. 1977.

[K-2]. Yoon-Won Kang and David M. Pozar, "Correction of error in reduced sidelobe synthesis due to mutual coupling," *IEEE Trans. on Ant. and Prop.*, vol. AP-33, pp. 1023-1028, Sept. 1985.

[K-3]. P. B. Katehi, "A generalized method for the evaluation of mutual coupling in microstrip arrays," *IEEE 1986 AP-S International Symposium*, pp. 545-548, June 1986.

[K-4]. Walter K. Kahn, "Endfire hybrid array antennas," *IEEE Trans. on Ant. and Prop.*, vol. AP-23, pp. 36-43, Jan. 1984.

[K-5]. C. M. Krowne, "Dielectric and width effect on H-plane and E-plane coupling between rectangular microstrip antennas," *IEEE Trans. on Ant. and Prop.*, vol. AP-31, pp. 39-47, Jan. 1983.

[L-1]. Farzin Lalezari and Clifton David Massey, "mm-wave microstrip antennas," *Microwave Journal*, vol. 30, pp. 87-96, April 1987.

[L-2]. Ajay K. Luthra, "A solution to the adaptive nulling problem with a look-direction constraint in the presnece of coherent jammers," *IEEE Trans. on Ant. and Prop.*, vol. AP-34, pp. 702-710, May 1986.

[L-3]. E. Levine, J. Ashkenazy and D. Treves, "Printed dipole array on a cylinder," *Microwave Journal*, vol. 30, pp. 85-92, March 1987.

[M-1]. A. D. Munger, J. H. Provencher and B. R. Gladman, "Mutual coupling on a cylindrical array of wave guide elements," *IEEE Trans. on Ant. and Prop.*, vol. AP-19, pp. 131-134, Jan. 1971.

[M-2]. George Monser, "Design considerations for broadbanding phase array elements," *Microwave Journal*, vol. 29, pp. 123-130, March 1986.

[M-3]. R. J. Mailloux, J. F. McIvenna and N. P. Kernweis, "Micorstrip Technology," *IEEE Trans. on Ant. and Prop.*, vol. AP-29, pp. 25-37, Jan. 1981.

[M-4]. Giuseppe Mazzarella and Gactano Panariello, "Design of slot arrays for SAR applications," *Alta Frequenza*, vol. 44, pp. 359-364, Nov.-Dec. 1986.

[M-5]. Hitoshi Mizutamari, Yoshihiko Konishi, Hiromasa Nakaguro, Yuji Kobayashi and Takashi Katagi, "Ananlysis method of slot array antenna taking into account mutual coupling," *IEEE 1988 AP-S International Symposium*, pp. 1082-1085, June 1988.

[N-1]. E. H. Newman and P. Tulyathan, "Analysis of microstrip antennas using moment methods," *IEEE Trans. on Ant. and Prop.*, vol. AP-29, pp. 47-53, Jan. 1981.

[O-1]. A. A. Oliner and R. G. Malech, "Mutual coupling in infinite scanning arrays," *Microwave Scanning Antennas*, Ed. R. C. Hansen, vol. II, Academic Press: New York, NY, 1966, Chapter 3.

[P-1]. David M. Pozar, "Input impedance and mutual coupling of rectangular microstrip antennas," *IEEE Trans. on Ant. and Prop.*, vol. AP-30, pp. 1191-1196, Nov. 1982.

[P-2]. David M. Pozar and Daniel H. Schaubert, "Analysis of infinite array of rectangular microstrip patches with idealized probe feed," *IEEE Trans. on Ant. and Prop.* vol. AP-32, pp. 1101-1107, Oct. 1984.

[P-3]. David M. Pozar, "Analysis of finite phased arrays of printed dipoles," *IEEE Trans. on Ant. and Prop.*, vol. AP-33, pp. 1045-1053, Oct. 1985.

[P-4]. David M. Pozar, "Finite phased arrays of rectangular microstrip patches," *IEEE Trans. on Ant. and Prop.*, vol. AP-34, pp. 658-665, May 1986.

[P-5]. E. Penard and J. P. Daniel, "Mutual coupling between microstrip antennas," *Electronics Letters*, vol. 18, no. 12, pp. 520-522, June 1982.

[P-6]. E. Penard and J. P. Daniel, "Mutual coupling between short-circuited microstrip antennas," *Electronics Letters*, vol. 19, pp. 178-180, March 1983.

[P-7]. David M. Pozar, "An update on microstrip antenna theory and design including some novel feeding techniques," *IEEE Ant. and Prop. Society Newsletter*, pp. 5-9, October 1986.

[P-8]. Jose Perini and Kazuhiro Hirasawa, "Antenna pattern synthesis computer program," Technical Report RADC-TR-77-73, Syracuse University, Feb. 1977.

[P-9]. David M. Pozar and Susanne M. Voda, "A rigorous analysis of a microsrip fed patch antenna," *IEEE Ant. and Prop.*, vol. AP-35, pp. 1343-1350, Dec. 1987.

[P-10]. Pyong K. Park and Robert S. Elliott, "Design of collinear longitudinal slot arrays fed by boxed stripline," *IEEE Trans. on Ant. and Prop.*, vol. AP-29, pp. 135-140, Jan. 1981.

[P-11]. David M. Pozar and Daniel H. Schaubert, "Comparison of architectures for monolithic phased array antennas," *Microwave Journal*, vol. 29, pp. 93-104, March 1986.

[R-1]. William F. Richards and Stuart A. Long, "Reactively loaded microstrip antennas," *IEEE Ant. and Prop. Society Newsletter*, pp. 11-17, Oct. 1986.

[S-1]. R. Stephan Smith and Warren L. Stutzman, "Analysis and design of microstrip array antennas including mutual coupling," Virginia Tech Report EE SATCOM 86-1, 1986

[S-2]. W. L. Stutzman and G. A. Thiele, *Antenna Theory and Design*, John Wiley and Sons: New York, 1981.

[S-3]. G. J. Stern and R. S. Elliott, "The design of microstrip dipole arrays including mutual coupling, part II: experiment," *IEEE Trans. on Ant. and Prop.*, vol. AP-29, pp. 761-765, Sept. 1981.

[S-4]. J-C Sureau and A. Hessel, "Element pattern for circular arrays of waveguide-fed axial slits on large conducting cylinders," *IEEE Trans. on Ant. and Prop.*, vol. AP-19, pp. 64-74, Jan. 1971.

[S-5]. A. R. Sindoris and C. M. Krowne, "Calculation of H-plane mutual coupling between rectangular microstrip antennas," *IEEE 1980 AP-S Internatinal Symposium*, pp. 738-742, June 1980.

[S-6]. Hans Steyskal, "Digital Beamforming Antennas: An introduction," *Micorwave Journal*, vol. 30, pp. 107-124, Jan. 1987.

[S-7]. M. Shelley and Kevin Bond, "Invisible antenna takes up less space," *Microwaves & RF*, vol. 25, pp. 93-95, June 1986.

[S-8]. H. K. Schuman and G. A. Bright, "Computer program for designing large phase array radiating elements," *Applied Computational Electromagnetics Conference Proceedings*, March 1986.

[S-9]. Nams Steyskal, Robert A. Shore, Randy L. Haupt, "Methods for null control and their effects on the radiation pattern," *IEEE Trans. on Ant. and Prop.*, vol. AP-34, pp. 404-409, March 1986.

[S-10]. Klaus Solbach, "Phased array simulation using circular patch radiators," *IEEE Trans. on Ant. and Prop.*, vol. AP-34, pp. 1053-1058, August 1986.

[S-11]. L. Shafai and A. K. Bhattacharyya, "Input impedance and radiation characteristics of small microstrip phased arrays including mutual coupling MSAT application," *Electromagnetics*, vol. 5, pp. 333-349, 1986.

[T-1]. J. S. Tanner, "Scattering matrix combination theory and its application to stripline array feeds," *ICAP 83*, IEE Int. Conf. Pub. no. 219, pp. 27-31, 1983.

[T-2]. John C. Tippet and Ross A. Speciale, "A rigorous technique for measuring the scattering matrix of a multiport device with a 2-port network analyzer," *IEEE Trans. on Microwave Theory and Techniques* , vol. MTT-30, pp. 661-666, May 1982.

[T-3]. Alam Tam, "Principles of microstrip design," *RF Design*, vol. 27, pp. 29-34, June 1988.

[V-1]. Emmanuel H. Van Lil and Antoine R. Van De Capelle, "Transmission line model for mutual coupling between microstrip antennas," *IEEE Trans. on Ant. and Prop.*, vol. AP-32, pp. 816-821, August 1984.

[V-2]. Peter Vizmuller, "Broadband miniature power splitter," *RF Design*, vol 26., pp. 49-57, August 1987.

[W-1]. Wasyl Wasylkiwskyj and Walter K. Kahn, "Element pattern and active reflection coefficient in uniform phased arrays," *IEEE Trans. on Ant. and Prop.*, vol. AP-22, pp. 207-212, March 1974.

[W-2]. H. D. Weinschel, "A cylindrical array of circularly polarized microstrip antennas," *IEEE 1975 AP-S International Symposium*, pp. 177-180, June 1975.

[W-3]. T. P. Waldron, S. K. Chin and R. J. Naster, "Distributed beamsteering control of phase array radars," *Microwave Journal*, vol. 29, pp. 133-146, Sept. 1986.

[W-4]. Ernest J. Wilkinson, "An N-way hybrid power divider," *IRE Trans. on Microwave Theory and Tech.*, vol. MTT-8, pp. 116-118, Jan. 1960.

[Y-1]. Leonard H. Yorinks, "Edge effects in low sidelobe phase array antennas," *IEEE 1985 AP-S International Symposium*, pp. 225-228, June 1985.

XII. Appendix A: Program SANE, Version 2.0

This chapter presents a brief description of the modifications to and a user's guide for the program SANE (Synthesis of Array with Network and Element coupling) originally written by Smith [S-1]. SANE is designed to solve the system of nonlinear equations in (5.2-5) for attenuator/phase shifter compensation network parameters given the desired element currents and the S-parameters of the feed network and the antenna elements. SANE can also be used instead of MCAP to analyze the effects of mutual coupling on element currents in an uncompensated array using techniques discussed in Section 2.1. A review of the theory used in SANE is presented in Chapter 5.

12.1 Description of The Code

Two modifications were implemented to SANE (forming Version 2.0) in this effort. The first modification was the addition of a subroutine to handle feed line effects as discussed in Section 2.5. The subroutine PREPRC calculates the S-matrix of antenna elements given the S-matrix of a feed line and the S-matrix of the elements that include

feed lines. This is a FORTRAN implementation of equations (2.5-19) through (2.5-22). Using the S-matrix of elements without feed lines, the desired currents at the elements can be transformed to the desired currents at the input to feed lines by a process similar to (2.5-3).

The second change to SANE was implementation of generator phase variation as discussed in Section 5.3. This is coded as an additional DO loop in the main program to change initial phase value of the generator. This allows users to find an attenuator/phase shifter network that is power efficient. This DO loop can be replaced in future with an optimization routine to find the compensation network with the maximum power efficiency.

12.2 User's Guide to SANE, Version 2.0

The modifications to SANE were implemented in such way that the program can be operated with the same set of input variables as the original SANE. However, the input file format has been changed slightly to accept additional information necessary in SANE 2.0. An user must perform two tasks before SANE can be executed. The first task is to modify the parameter statements in the program. The parameter statements are of the form PARAMETER(NE=n) where n is the number of antenna elements in the array being considered. There are ten parameter statements in SANE, Version 2.0. The parameter statements can be changed using a text editor.

The second task is to prepare an input data file. The data file is set up as a series of alphanumeric character lines which are read through I/O unit 5. The definition and format of the variables in the data file are listed in Table 12.2-1. There are two blocks of variables required in SANE. The first block of numbers controls how SANE runs.

Table 12.2-1. Input file format for SANE.

Variable	Format	Description
FIND	A3	Find Compensation Network
PNTITS	A3	Print iterations
ERROR	E10.3	Maximum error in the nonlinear equations
AERROR	E10.3	Maximum attenuator deviation, ε
MAXIT	I3	Maximum iterations
MAXTRY	I3	Maximum generator tries
CHGPHS	A3	Change generator phase
NPHASE	I3	Number of generator phase changes †
DPHASE	F10.5	Increment in generator phase †
GAMMAG	2F10.5	Reflection coefficient of generator
G	2F10.5	Initial generator value
SF(1,1)	2F10.5	Feed network S-parameter $S^F_{1,1}$
⋮		
SF(N+1,N+1)	2F10.5	Feed network S-parameter $S^F_{N+1,N+1}$
SA(1,1)	2F10.5	Element S-parameter $S^A_{1,1}$
⋮		
SA(N,N)	2F10.5	Element S-parameter $S^A_{N,N}$
REFRNC	A3	Feed lines exist
SFL(1,1)	2F10.5	Feed line S-parameter $S^{FL}_{1,1}$ *
⋮		
SFL(2,2)	2F10.5	Feed line S-parameter $S^{FL}_{2,2}$ *
COORD	A5	Polar or complex format for the desired currents
I(1)	2F10.5	Desired current at element 1
⋮		
I(N)	2F10.5	Desired current at element N
X(1)	2F10.5	Compensation variable X_1 ‡
⋮		
X(N)	2F10.5	Compensation variable X_N ‡

† not necessary if CHGPHS = 'NO'

‡ not necessary if FIND = 'NO'

* not necessary if REFRNC = 'NO'

The first two lines are flags FIND and PNTITS. FIND is 'YES' if a compensation network is to be found and 'NO' otherwise. PNTITS is 'YES' if a summary of the results at each iteration is to be printed. The third line contains the absolute error allowed in norm of the nonliner equations (5.2-5). The allowable deviation of the magnitude of the maximum attenuator value from unity, ε, as defined in (5.2-6) is specified in the fourth line; a tipical value for ε is 0.01 which corresponds to the minimum attenuator of approximately 0.1 dB. The fifth and sixth lines contain the maximum number of iterations for Newton's method and determining the necessary generator magnitude, respectively. The seventh line is a flag CHGPHS which is set to 'YES' if the phase of initial generator is to be changed to find the most power efficient network as discused in Section 5.3. The following two lines are required if CHGPHS is 'YES'. The first of these, NPHASE, contains the number of generator phase changes required, and the second, DPHASE, contains the angle in degrees where generator phase, $\underline{/G}$, will be incremented; typically NPHASE is set to 18 and DPHASE is set to 10.0.

In the second block the array characteristic is specified. The first two lines in the second block are the complex reflection coefficient of the generator (S^G) and the magnitude of the generator excitation ($|c^G|$). The following $(n+1)^2$ lines contain the S-parameters of the feed network, S^F_{ij}. The next n^2 lines contain the S-parameters of the elements, S^A_{ij} . Following these is a flag REFRNC which is 'YES' if feed line effects as discussed in Section 2.5 are to be considered. In this case, S-parameters of a feed line are specified in the four lines following REFRNC. A flag COORD is specified in the next line. COORD is set to 'POLAR' if the required element currents are specified in the magnitude-phase format. COORD is 'COMPLEX' if the required currents are specified in the real-imaginary format. The required element currents are specified in the n lines following the flag COORD. IF the flag FIND is 'NO' then the next n lines contain the value of the compensation network.

As an example consider the eight element microstrip array with the sum feed network as described in Chapter 8. Figure 12.2-1 shows a part of the input data file. The corresponding output file which is written on I/O unit 6 is shown in Figure 12.2-2. Note that these values corresponds to those in Table. 8.3-1.

```
YES                          solve problem
NO                           print iteration
 0.100E-05                   error
 0.500E-05                   attenuator error
020                          max iterations
020                          max tries
YES                          change generator phase
018                          number of changes
  10.00000                   step
   0.00000    0.00000        Gamma G
   1.00000    0.00000        Generator
   0.11700   -0.08800        sum feed 1,1
   0.67500   -0.28600        sum feed 2,1
  -0.23700   -0.03750        sum feed 3,1
  -0.23800   -0.02920        sum feed 4,1
  -0.05110   -0.02490        sum feed 5,1
  -0.04530   -0.02410        sum feed 6,1
  -0.04600   -0.02650        sum feed 7,1
  -0.04840   -0.02470        sum feed 8,1
   0.26800   -0.15500        sum feed 9,1
             •
             •
             •
   0.25100   -0.12800        sum feed 6,9
   0.26700   -0.11900        sum feed 7,9
   0.26300   -0.13400        sum feed 8,9
   0.15700    0.32300        sum feed 9,9
  -0.07940    0.12100        array 1,1
   0.20300   -0.24200        array 2,1
  -0.15800    0.01110        array 3,1
   0.07190    0.08280        array 4,1
   0.00786   -0.08980        array 5,1
  -0.06110    0.03250        array 6,1
   0.04200    0.02940        array 7,1
   0.00065   -0.03710        array 8,1
             •
             •
             •
   0.08210    0.06890        array 5,8
  -0.14000    0.02730        array 6,8
   0.16700   -0.24700        array 7,8
  -0.06270    0.14600        array 8,8
YES                          feed lines
   0.45737   -0.03313        fl 1,1
  -0.06679    0.88615        fl 1,2
  -0.06679    0.88615        fl 2,1
   0.44723    0.10131        fl 2,2
POLAR
   1.00000    0.00000        I1
   1.00000    0.00000        I2
   1.00000    0.00000        I3
   1.00000    0.00000        I4
   1.00000    0.00000        I5
   1.00000    0.00000        I6
   1.00000    0.00000        I7
   1.00000    0.00000        I8
```

Figure 12.2-1. SANE input file for the eight element microstrip array with sum feed network (see Figs. 8.1-1 and 8.1-3).

```
****** SANE ******    version 2.1   Jan. 11, 1988

               ==========> PROGRAM INFORMATION <==========

The maximum runs for SANE is  20
The maximum deviation of the largest attenuation from unity is 0.500E-05

The maximum iterations for Newtons  method is  20
The allowable error for the norm of F(x) is 0.100E-05

The values for the compensation newtwork are to be found

The information on the iterations is not to be printed


               ==========> NETWORK INFORMATION <==========

The network contains    8 elements.
Wave impressed by the generator = (  0.1000E+01,  0.0000E+00)
Reflection coefficient of the generator = (  0.0000E+00,  0.0000E+00)


The S-matrix of the antenna array is:

  (-.079,0.121)(0.203,-.242)(-.158,0.011)(0.072,0.083)(0.008,-.090)(-.061,0.032)(0.042,0.029)(0.001,-.037)
  (0.203,-.242)(-.075,0.077)(0.238,-.257)(-.197,-.006)(0.095,0.109)(0.023,-.101)(-.074,0.026)(0.038,0.032)
  (-.158,0.011)(0.238,-.257)(-.060,0.103)(0.263,-.238)(-.206,-.010)(0.075,0.103)(0.021,-.060)(-.057,0.017)
  (0.072,0.083)(-.197,-.006)(0.263,-.238)(-.020,0.159)(0.213,-.263)(-.182,0.010)(0.072,0.089)(0.018,-.067)
  (0.008,-.090)(0.095,0.109)(-.206,-.010)(0.213,-.263)(-.045,0.074)(0.187,-.278)(-.183,0.022)(0.082,0.069)
  (-.061,0.032)(0.023,-.101)(0.075,0.103)(-.182,0.010)(0.187,-.278)(-.090,0.017)(0.195,-.301)(-.140,0.027)
  (0.042,0.029)(-.074,0.026)(0.021,-.060)(0.072,0.089)(-.183,0.022)(0.195,-.301)(-.106,0.028)(0.167,-.247)
  (0.001,-.037)(0.038,0.032)(-.057,0.017)(0.018,-.067)(0.082,0.069)(-.140,0.027)(0.167,-.247)(-.063,0.146)

The S-matrix for the feed network is:

  (0.117,-.088)(0.675,-.286)(-.237,-.038)(-.238,-.029)(-.051,-.025)(-.045,-.024)(-.046,-.027)(-.048,-.025)(0.268,-.155)
  (0.675,-.286)(0.161,-.121)(-.223,-.038)(-.226,-.035)(-.049,-.024)(-.042,-.022)(-.043,-.026)(-.045,-.024)(0.253,-.152)
  (-.237,-.038)(-.223,-.038)(0.219,-.008)(0.682,-.115)(-.053,-.032)(-.048,-.026)(-.046,-.030)(-.048,-.029)(0.297,-.138)
  (-.238,-.029)(-.226,-.035)(0.682,-.115)(0.223,-.016)(-.052,-.032)(-.047,-.030)(-.047,-.031)(-.050,-.028)(0.297,-.138)
  (-.051,-.025)(-.049,-.024)(-.053,-.032)(-.052,-.032)(0.141,0.046)(0.715,-.116)(-.217,-.053)(-.221,-.038)(0.276,-.147)
  (-.045,-.024)(-.042,-.022)(-.048,-.026)(-.047,-.030)(0.715,-.116)(0.254,0.013)(-.195,-.052)(-.199,-.045)(0.251,-.128)
  (-.046,-.027)(-.043,-.026)(-.046,-.030)(-.047,-.031)(-.217,-.053)(-.195,-.052)(0.172,-.024)(0.727,-.144)(0.267,-.119)
  (-.048,-.025)(-.045,-.024)(-.048,-.029)(-.050,-.028)(-.221,-.038)(-.199,-.045)(0.727,-.144)(0.176,-.054)(0.263,-.134)
  (0.268,-.155)(0.253,-.152)(0.297,-.138)(0.297,-.138)(0.276,-.147)(0.251,-.128)(0.267,-.119)(0.263,-.134)(0.157,0.323)

The S-matrix of feed line is:

  ( 0.457,-0.033)(-0.067, 0.886)
  (-0.067, 0.886)( 0.447, 0.101)
```

Figure 12.2-2. The resulting output from data in Fig. 12.2-1 (see Table 8.3-1).

```
The desired currents at the patch edges are:

   Current    1 = (  0.1000E+01,  0.0000E+00)
   Current    2 = (  0.1000E+01,  0.0000E+00)
   Current    3 = (  0.1000E+01,  0.0000E+00)
   Current    4 = (  0.1000E+01,  0.0000E+00)
   Current    5 = (  0.1000E+01,  0.0000E+00)
   Current    6 = (  0.1000E+01,  0.0000E+00)
   Current    7 = (  0.1000E+01,  0.0000E+00)
   Current    8 = (  0.1000E+01,  0.0000E+00)

The desired currents at the reference plane are:

   Current    1 = ( -0.1734E+00, -0.1317E+01)
   Current    2 = (  0.8961E+00, -0.1274E+01)
   Current    3 = (  0.4078E+00, -0.1178E+01)
   Current    4 = (  0.5357E+00, -0.1079E+01)
   Current    5 = (  0.7464E+00, -0.1268E+01)
   Current    6 = (  0.1070E+01, -0.1404E+01)
   Current    7 = (  0.1028E+01, -0.1505E+01)
   Current    8 = ( -0.1522E+00, -0.1253E+01)


                  =========> RESULTS <=========

The program was successful ( Norm(F)< 0.10E-05 )

**********************************************************************
The solution vector is:
----------------------------------------------------------------------
    X(  1) = (-0.34144 + -0.69717 J ) =  0.77629 exp( 243.90678)
    X(  2) = ( 0.03382 + -0.88312 J ) =  0.88377 exp( -87.80716)
    X(  3) = (-0.20872 + -0.73199 J ) =  0.76116 exp( 254.08504)
    X(  4) = (-0.15367 + -0.72292 J ) =  0.73908 exp( 257.99902)
    X(  5) = (-0.19376 + -0.76665 J ) =  0.79076 exp( 255.81647)
    X(  6) = (-0.18589 + -0.94797 J ) =  0.96603 exp( 258.90552)
    X(  7) = (-0.05258 + -0.99861 J ) =  1.00000 exp( 266.98584)
    X(  8) = (-0.39212 + -0.67021 J ) =  0.77649 exp( 239.66928)

Generator Phase =  40.000 degrees
The necessary generator/feed current ratio is  0.42542E+01 +  0.35697E+01 J
This is      5.5534573 times the inputed value of  0.76604E+00 +  0.64279E+00 J
```

Figure 12.2-2. (Continued)

```
**************************************************************************

                    =========> CURRENT CHECK <=========
The calculated feed currents are:

    CURRENT   1 = (-0.17340 + -1.31656 J) =  1.32793 EXP( 262.49707)   ERROR MAG= 0.00000
    CURRENT   2 = ( 0.89613 + -1.27449 J) =  1.55800 EXP( -54.88782)   ERROR MAG= 0.00000
    CURRENT   3 = ( 0.40783 + -1.17769 J) =  1.24631 EXP( -70.89911)   ERROR MAG= -.00001
    CURRENT   4 = ( 0.53569 + -1.07942 J) =  1.20504 EXP( -63.60599)   ERROR MAG= 0.00000
    CURRENT   5 = ( 0.74644 + -1.26850 J) =  1.47183 EXP( -59.52551)   ERROR MAG= 0.00000
    CURRENT   6 = ( 1.06954 + -1.40400 J) =  1.76497 EXP( -52.70047)   ERROR MAG= 0.00000
    CURRENT   7 = ( 1.02830 + -1.50497 J) =  1.82272 EXP( -55.65645)   ERROR MAG= 0.00000
    CURRENT   8 = (-0.15218 + -1.25282 J) =  1.26203 EXP( 263.07422)   ERROR MAG= 0.00000

The currents at patch edges are:

    CURRENT   1 = ( 1.00000 +  0.00000 J) =  1.00000 EXP(   0.00008)   ERROR MAG= 0.00000
    CURRENT   2 = ( 1.00000 +  0.00000 J) =  1.00000 EXP(  -0.00009)   ERROR MAG= 0.00000
    CURRENT   3 = ( 1.00000 +  0.00000 J) =  1.00000 EXP(   0.00010)   ERROR MAG= 0.00000
    CURRENT   4 = ( 1.00000 +  0.00000 J) =  1.00000 EXP(   0.00000)   ERROR MAG= 0.00000
    CURRENT   5 = ( 1.00000 +  0.00000 J) =  1.00000 EXP(   0.00004)   ERROR MAG= 0.00000
    CURRENT   6 = ( 1.00000 +  0.00000 J) =  1.00000 EXP(   0.00004)   ERROR MAG= 0.00000
    CURRENT   7 = ( 1.00000 +  0.00000 J) =  1.00000 EXP(   0.00003)   ERROR MAG= 0.00000
    CURRENT   8 = ( 1.00000 +  0.00000 J) =  1.00000 EXP(  -0.00004)   ERROR MAG= 0.00000
```

Figure 12.2-2. (Continued)

XIII. Appendix B: Program SANE-PODCON

This chapter presents a brief description and user's guide to the program SANE-PODCON (Synthesis of Array with Network and Element coupling for POwer Divider COmpensation Network). SANE-PODCON solves the system of nonlinear equations (6.3-6) for power divider compensation network parameters given the desired element currents and the S-parameters of the antenna elements. A discussion on the theory used to develop SANE-PODCON is presented in Chapter 6.

13.1 Description of the Code

The program SANE-PODCON consists of five primary blocks: 1) initialization, 2) set up, 3) solve, 4) verify and 5) output, as shown in Fig. 13.1-1. The first block initializes a scaler variable and two array variables. It consists of three subroutines: GETEPS, CALCII, and CALCMX. The subroutine GETEPS calculates machine epsilon of the computer running SANE-PODCON. The machine epsilon is a real number which a computer can distinguish the difference between 1 and $1 + \varepsilon$. It is used

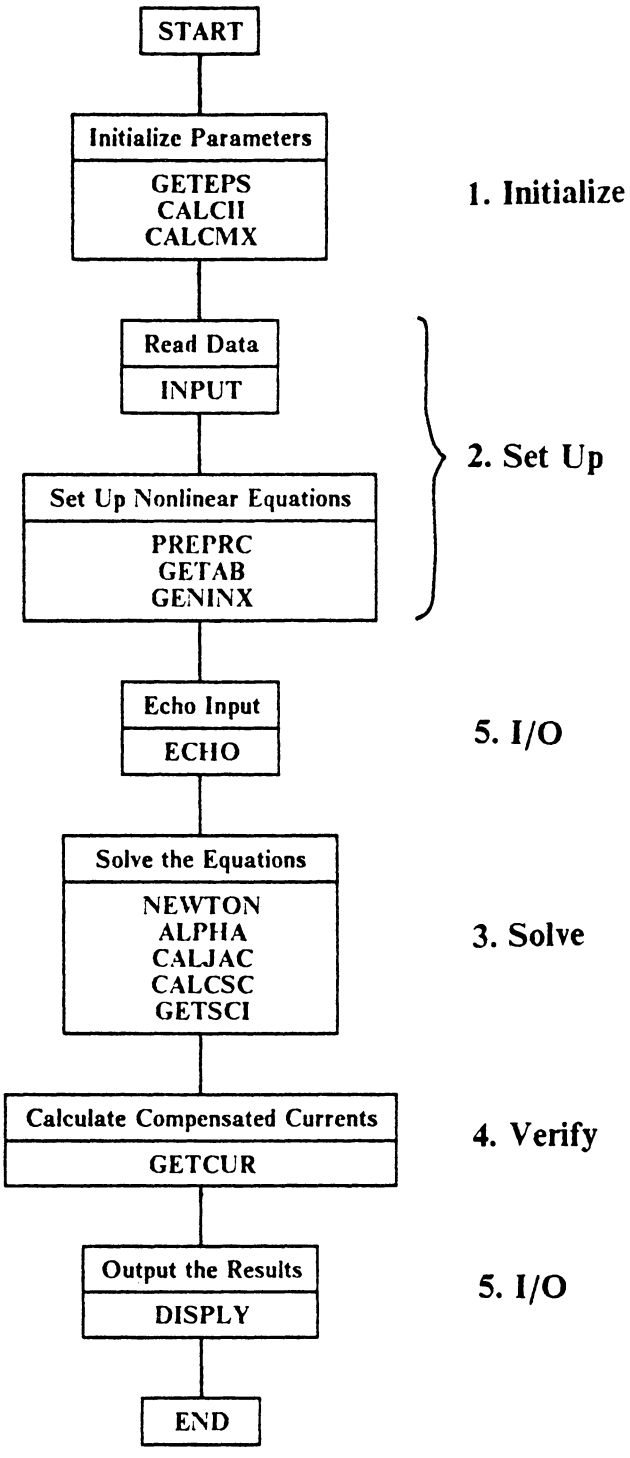

Figure 13.1-1. Block diagram of SANE-PODCON.

in calculation of Jacobian of the nonlinear equations. The subroutines CALCII and CALCMX create indicies used to represent N-way power dividers which are similar to index system as defined in Section 6.2.2.

The second block reads data from a input file and establishes the nonlinear equations. The block contains four subroutines: INPUT, PREPRC, GENAB, and GENINX. The subroutine INPUT reads data from an input file through I/O unit 5. PREPRC is called when S-parameters of the elements contain the feed lines. The process is discussed in Section 2.5. The routine GENAB calculates the incident and reflected wave variables at the elements, $\{a_n^A\}$ and $\{b_n^A\}$ from the desired element currents using (2.4-7) and (2.4-8). The initial guess to the solution from desired element currents are generated in GENINX. This is discussed in Section 6.4.

The third block in SANE-PODCON solves the nonlinear equations set up by the previous block. The block is consists of NEWTON, ALPHA, CALJAC, CALCSC and GETSCI. The subroutine NEWTON is the driver routine that approximates the solutions to the nonlinear equations using Damped Newton's method [D-4]. The damping factor α is calculated in subroutine ALPHA. The subroutine CALJAC calculates the Jacobian of the nonlinear equations at a particular domain represented by $\{X_n\}$. It uses a finite difference method to approximate for the Jacobian [D-4]. The routine calls CALCSC and GETSCI which calculates the S-matrix of the compensation network using equation (6.2-6). In particular, CALCSC calculates the entire S-matrix and GETSCI calculates i-th column of the S-matrix. This was done to increase the computational efficiency since the compensation network S-matrix has many redundant variables.

The forth block calculates the element currents with the compensation network incorporated into the array network. This provides verification that solutions are correct

and are not affected by round off error. The element currents calculations are performed by GETCUR.

The final block contains two routines: ECHO and DISPLY. The subroutine ECHO outputs the input data and other parameters calculated prior to solving the nonlinear equations. DISPLY on the other hand writes the solution of the nonlinear equations. Both ECHO and DISPLY writes output to I/O unit 6. The subroutine DISPLY also writes the resulting S-matrix of compensated feed network through I/O unit 7 in a format compatible with MCAP.

13.2 User's Guide to SANE-PODCON

An user must perform two tasks before SANE-PODCON can be executed. The first task is to modify the parameter statements in the program. The parameter statements are of the form PARAMETER(NE=n) where n is the number of antenna elements in the array being considered. There are eighteen parameter statements in SANE-PODCON. The parameter statements can changed using any text editor.

The second task is to prepare an input data file. The data file is set up as a series of alphanumeric character lines which are read through I/O unit 5. The definition and format of the variables in data file are listed in Table 13.2-1. The first line in the data file is flag PRTITR, which is set to 'YES' if a summary of the results at each iteration is to be printed. The second line contains the maximum number of iterations for Newton's method. The third line contains the absolute error allowed in norm of the nonliner equations (6.3-6); a typical value of ERROR is 1.0E-05. The fourth line is a flag GENINT which is set to 'YES' if the initial guess to the solution vector is to be generated by the program. If GENINT is 'NO' user must supply the initial guess in the

Table 12.2-1. Input file format for SANE-PODCON.

Variable	Format	Description
PRTITR	A3	Print iterations
MAXITR	I4	Maximum iterations
ERROR	F8.5	Maximum error
GENINT	A3	Generate initial guess
X(1)	2F10.5	Initial guess for power divider network 1 †
:		
X(N-1)	2F10.5	Initial guess for power divider network N-1 †
G	2F10.5	Initial generator value
GAMMAG	2F10.5	Reflection coefficient of generator
REFRNC	A3	Feed lines exist
SFL(1,1)	2F10.5	Feed line S-parameter $S^{FL}_{1,1}$ ‡
:		
SFL(2,2)	2F10.5	Feed line S-parameter $S^{FL}_{2,2}$ ‡
SA(1,1)	2F10.5	Element S-parameter $S^{A}_{1,1}$
:		
SA(N,N)	2F10.5	Element S-parameter $S^{A}_{N,N}$
COORD	A5	Polar or complex format for the desired currents
I(1)	2F10.5	Desired current at element 1
:		
I(N)	2F10.5	Desired current at element N

† not necessary if GENINT = 'YES'

‡ not necessary if REFRNC = 'NO'

following n-1 lines. The next two lines are the reflection coefficient of the generator (S^G) and the initial magnitude of generator excitation ($|c^G|$). The following n^2 lines contain the S-parameters of the elements, S^A_{ij}. A flag REFRNC follows next. REFRNC is 'YES' if feed line effects as discussed in Section 2.5 are to be considered. In this case, the four lines following REFRNC are the S-parameters of a feed line. A flag COORD defines the format of the desired currents specified next. COORD is 'POLAR' if the required element currents are specified in magnitude-phase format. COORD is 'COMPLEX' if the required currents are specified in real-imaginary format. The desired element currents are specified in n lines following the flag COORD.

As an example consider the eight element microstrip array for the sum pattern current distribution as described in Chapter 8. Figure 13.2-1 shows a part of the input data file. The corresponding output file which is written on I/O unit 6 is shown in Figure 13.2-2. Note that these values corresponds to those in Table. 8.3-2.

```
NO                                print iterations
0150                              max iterations
00.00010                          max error
YES                               generate initial guess
   0.00000   0.00000              Generator
   0.00000   0.00000              Gamma G
YES                               feed lines
   0.45737  -0.03313              fl 1,1
  -0.06679   0.88615              fl 2,1
  -0.06679   0.88615              fl 1,2
   0.44723   0.10131              fl 2,2
  -0.07940   0.12100              array 1,1
   0.20300  -0.24200              array 2,1
  -0.15800   0.01110              array 3,1
   0.07190   0.08280              array 4,1
   0.00786  -0.08980              array 5,1
  -0.06110   0.03250              array 6,1
   0.04200   0.02940              array 7,1
   0.00065  -0.03710              array 8,1
            •
            •
            •
   0.00065  -0.03710              array 1,8
   0.03750   0.03240              array 2,8
  -0.05690   0.01750              array 3,8
   0.01790  -0.06680              array 4,8
   0.08210   0.06890              array 5,8
  -0.14000   0.02730              array 6,8
   0.16700  -0.24700              array 7,8
  -0.06270   0.14600              array 8,8
POLAR                             current format
   1.00000   0.00000              I1
   1.00000   0.00000              I2
   1.00000   0.00000              I3
   1.00000   0.00000              I4
   1.00000   0.00000              I5
   1.00000   0.00000              I6
   1.00000   0.00000              I7
   1.00000   0.00000              I8
```

Figure 13.2-1. SANE-PODCON input file for the eight element microstrip array with sum pattern excitation (see Fig. 8.1-1).

```
****** SANE-PODCON *****     Version : 1.3.5       April 25, 1988

Iteration dump = NO
Error for the norm of system =  0.10000E-03
Maximum number of iterations =  150
Machine Epsilon =  0.95367E-06
Initial guess were calculated.

     The initial guess for the solution vector
  X( 1) = ( 0.42626E+00, 0.39217E+00) =  0.57922/  42.615
  X( 2) = ( 0.47926E+00, 0.61335E-01) =  0.48317/   7.293
  X( 3) = ( 0.58565E+00, 0.70093E-01) =  0.58983/   6.825
  X( 4) = ( 0.24356E+00,-0.21374E+00) =  0.32405/ -41.269
  X( 5) = ( 0.37342E+00, 0.18703E+00) =  0.41764/  26.604
  X( 6) = ( 0.48094E+00, 0.32526E-01) =  0.48204/   3.869
  X( 7) = ( 0.46211E+00, 0.36075E+00) =  0.58625/  37.977
  X( 8) = ( 0.10000E+01, 0.10000E+01) =  1.41421/  45.000


             ---- Network Parameter ----
The antenna network containes   8 elements
reflection coefficient of the generator = ( 0.00000E+00, 0.00000E+00) =  0.00000/   0.000

The S-matrix of the antenna array
  (-.079,0.121)(0.203,-.242)(-.158,0.011)(0.072,0.083)(0.008,-.090)(-.061,0.033)(0.042,0.029)(0.001,-.037)
  (0.203,-.242)(-.075,0.077)(0.238,-.257)(-.197,-.006)(0.095,0.109)(0.023,-.101)(-.074,0.026)(0.038,0.032)
  (-.158,0.011)(0.238,-.257)(-.060,0.103)(0.263,-.238)(-.206,-.010)(0.075,0.103)(0.021,-.060)(-.057,0.017)
  (0.072,0.083)(-.197,-.006)(0.263,-.238)(-.020,0.159)(0.213,-.263)(-.182,0.010)(0.072,0.089)(0.018,-.067)
  (0.008,-.090)(0.095,0.109)(-.206,-.010)(0.213,-.263)(-.045,0.074)(0.187,-.278)(-.183,0.022)(0.082,0.069)
  (-.061,0.033)(0.023,-.101)(0.075,0.103)(-.182,0.010)(0.187,-.278)(-.090,0.017)(0.195,-.301)(-.140,0.027)
  (0.042,0.029)(-.074,0.026)(0.021,-.060)(0.072,0.089)(-.183,0.022)(0.195,-.301)(-.106,0.028)(0.167,-.247)
  (0.001,-.037)(0.038,0.032)(-.057,0.017)(0.018,-.067)(0.082,0.069)(-.140,0.027)(0.167,-.247)(-.063,0.146)


The S-matrix of initial feed network
  (0.176,-.436)(-.297,0.627)(-.266,0.018)(-.257,-.016)(0.069,-.089)(0.095,-.096)(0.093,-.104)(0.001,-.096)(-.225,0.225)
  (-.297,0.627)(0.242,0.223)(-.244,-.196)(-.210,-.218)(0.130,-.022)(0.158,-.007)(0.163,-.016)(0.077,-.082)(-.373,0.016)
  (-.266,0.018)(-.244,-.196)(0.079,-.166)(-.027,0.809)(0.095,-.045)(0.120,-.040)(0.121,-.048)(0.041,-.080)(-.284,0.094)
  (-.257,-.016)(-.210,-.218)(-.027,0.809)(0.127,-.195)(0.097,-.032)(0.120,-.024)(0.122,-.031)(0.049,-.072)(-.284,0.056)
  (0.069,-.089)(0.130,-.022)(0.095,-.045)(0.097,-.032)(0.112,-.568)(0.072,0.530)(-.370,0.001)(-.192,0.170)(-.350,0.043)
  (0.095,-.096)(0.158,-.007)(0.120,-.040)(0.120,-.024)(0.072,0.530)(0.247,-.331)(-.440,-.051)(-.252,0.175)(-.423,0.001)
  (0.093,-.104)(0.163,-.016)(0.121,-.048)(0.122,-.031)(-.370,0.001)(-.440,-.051)(0.213,-.262)(0.448,0.287)(-.436,0.024)
  (0.001,-.096)(0.077,-.082)(0.041,-.080)(0.049,-.072)(-.192,0.170)(-.252,0.175)(0.448,0.287)(-.628,-.185)(-.216,0.212)
  (-.225,0.225)(-.373,0.016)(-.284,0.094)(-.284,0.056)(-.350,0.043)(-.423,0.001)(-.436,0.024)(-.216,0.212)(0.000,0.000)


The S-matrix of feed lines
  ( 0.457,-0.033)(-0.067, 0.886)
  (-0.067, 0.886)( 0.447, 0.101)
```

Figure 13.2-2. The resulting output from data in Fig. 13.2-1 (see Table 8.3-2).

```
 The desired currents at the reference plane
   I( 1) = (-0.17340E+00,-0.13166E+01) =  1.32793 / -97.503
   I( 2) = ( 0.89613E+00,-0.12745E+01) =  1.55801 / -54.888
   I( 3) = ( 0.40783E+00,-0.11777E+01) =  1.24630 / -70.899
   I( 4) = ( 0.53569E+00,-0.10794E+01) =  1.20504 / -63.606
   I( 5) = ( 0.74644E+00,-0.12685E+01) =  1.47182 / -59.525
   I( 6) = ( 0.10695E+01,-0.14040E+01) =  1.76497 / -52.701
   I( 7) = ( 0.10283E+01,-0.15050E+01) =  1.82272 / -55.656
   I( 8) = (-0.15218E+00,-0.12528E+01) =  1.26203 / -96.926

 The desired currents at the patch edges
   I( 1) = ( 0.10000E+01, 0.00000E+00) =  1.00000 /   0.000
   I( 2) = ( 0.10000E+01, 0.00000E+00) =  1.00000 /   0.000
   I( 3) = ( 0.10000E+01, 0.00000E+00) =  1.00000 /   0.000
   I( 4) = ( 0.10000E+01, 0.00000E+00) =  1.00000 /   0.000
   I( 5) = ( 0.10000E+01, 0.00000E+00) =  1.00000 /   0.000
   I( 6) = ( 0.10000E+01, 0.00000E+00) =  1.00000 /   0.000
   I( 7) = ( 0.10000E+01, 0.00000E+00) =  1.00000 /   0.000
   I( 8) = ( 0.10000E+01, 0.00000E+00) =  1.00000 /   0.000


     ----- Result ------


 Program was successful.  Number of iteration =   63

CPU time =   5.80 seconds

The required power divider specification

     X( 1) = ( 0.43419E+00, 0.34134E+00) =  0.55230 /  38.172
     X( 2) = ( 0.48650E+00, 0.69326E-01) =  0.49141 /   8.110
     X( 3) = ( 0.56410E+00, 0.29745E-01) =  0.56489 /   3.018
     X( 4) = ( 0.28212E+00,-0.88771E-01) =  0.29576 / -17.467
     X( 5) = ( 0.40954E+00, 0.14714E+00) =  0.43517 /  19.762
     X( 6) = ( 0.52584E+00,-0.54481E-01) =  0.52865 /  -5.915
     X( 7) = ( 0.42572E+00, 0.22896E+00) =  0.48339 /  28.272

  Generator = -1.96775, 3.88607 =  4.35587 / 116.856

 The S-matrix of modified feed network
   (0.195,-.430)(-.221,0.631)(-.261,0.028)(-.258,-.009)(0.054,-.100)(0.067,-.111)(0.058,-.142)(0.008,-.099)(-.256,0.256)
   (-.221,0.631)(0.345,0.163)(-.247,-.155)(-.219,-.185)(0.116,-.051)(0.135,-.051)(0.148,-.084)(0.075,-.081)(-.399,0.048)
   (-.261,0.028)(-.247,-.155)(0.154,-.226)(0.042,0.774)(0.079,-.071)(0.094,-.076)(0.096,-.106)(0.039,-.084)(-.306,0.144)
   (-.258,-.009)(-.219,-.185)(0.042,0.774)(0.213,-.201)(0.087,-.058)(0.102,-.061)(0.108,-.090)(0.049,-.077)(-.318,0.098)
   (0.054,-.100)(0.116,-.051)(0.079,-.071)(0.087,-.058)(0.142,-.506)(0.132,0.570)(-.385,0.119)(-.215,0.149)(-.302,0.091)
   (0.067,-.111)(0.135,-.051)(0.094,-.076)(0.102,-.061)(0.132,0.570)(0.221,-.338)(-.445,0.112)(-.254,0.156)(-.349,0.085)
   (0.058,-.142)(0.148,-.084)(0.096,-.106)(0.108,-.090)(-.385,0.119)(-.445,0.112)(0.190,-.227)(0.268,0.441)(-.392,0.163)
   (0.008,-.099)(0.075,-.081)(0.039,-.084)(0.049,-.077)(-.215,0.149)(-.254,0.156)(0.268,0.441)(-.321,-.599)(-.210,0.177)
   (-.256,0.256)(-.399,0.048)(-.306,0.144)(-.318,0.098)(-.302,0.091)(-.349,0.085)(-.392,0.163)(-.210,0.177)(0.000,0.000)
```

Figure 13.2-2. (Continued)

```
**********************************************************************

                ==========> CURRENT CHECK <==========

The currents at reference plane

    I( 1) = (-0.17342 , -1.31661 ) =  1.32798 / 262.49609
    I( 2) = ( 0.89614 , -1.27454 ) =  1.55805 / -54.88885
    I( 3) = ( 0.40781 , -1.17768 ) =  1.24629 / -70.89992
    I( 4) = ( 0.53572 , -1.07949 ) =  1.20511 / -63.60626
    I( 5) = ( 0.74641 , -1.26844 ) =  1.47176 / -59.52562
    I( 6) = ( 1.06957 , -1.40400 ) =  1.76499 / -52.69995
    I( 7) = ( 1.02830 , -1.50500 ) =  1.82275 / -55.65706
    I( 8) = (-0.15218 , -1.25281 ) =  1.26202 / 263.07422

The currents at patch edges

    I( 1) = ( 1.00003 ,  0.00000 ) =  1.00003 /  -0.00020
    I( 2) = ( 1.00002 , -0.00003 ) =  1.00002 /  -0.00177
    I( 3) = ( 1.00003 , -0.00002 ) =  1.00003 /  -0.00109
    I( 4) = ( 1.00000 ,  0.00003 ) =  1.00000 /   0.00186
    I( 5) = ( 0.99999 , -0.00003 ) =  0.99999 /  -0.00172
    I( 6) = ( 0.99998 ,  0.00000 ) =  0.99998 /   0.00013
    I( 7) = ( 1.00002 ,  0.00002 ) =  1.00002 /   0.00138
    I( 8) = ( 1.00001 , -0.00002 ) =  1.00001 /  -0.00095

Total CPU time =   5.88 seconds
```

Figure 13.2-2. (Continued)

13.3 Program Listing

```
c* * * * * * * * * * * * * * * * * * * * * * * * * * * * * * * * * * * * *
c*                                                                       *
c*                            SANE - PODCON                              *
c*                                                                       *
c*      Synthesis of Arrays with Network and Element coupling            *
c*               for POwer Divider COmpensation Networks                 *
c*                                                                       *
c*    Programmer      : Koichiro Takamizawa                              *
c*    Revision        : August 4, 1988                                   *
c*                                                                       *
c*                                                                       *
c* * * * * * * * * * * * * * * * * * * * * * * * * * * * * * * * * * * * *
c* 1.3.6  8/04/88 getcur added                                          *
c* 1.3.5  4/22/88 fixed error in calcsc and getsci                       *
c* 1.3.4 10/25/87 fixed error in geninx                                  *
c* 1.3.3 10/14/87 fixed error in geninx                                  *
c* 1.3.2 10/11/87 fixed bugs in calcsc                                   *
c* 1.3.1 10/10/87 subroutine getsci added to increase the efficiency     *
c* 1.3.0 10/09/87 subroutine calcsc added to replace function sc         *
c* 1.2.2  8/08/87 subroutine preprc added to take care of x-mission      *
c*                lines on the array board                               *
c* 1.2.1  7/01/87 geninx added (creates initial guess solution vector)   *
C* 1.1.0  5/15/87 SANE-PODCON written from SANE-GECON                    *
C*                                                                       *
C* * * * * * * * * * * * * * * * * * * * * * * * * * * * * * * * * * * * *

      program sane_podcon

      parameter (NE=8)
      complex*16 x(NE),jacob(NE,NE),f(NE)
      complex*16 stl(2,2),sa2(NE,NE),curr2(NE),sa(NE,NE),currnt(NE)
      real error
      integer maxitr
      character*3 yes,prtitr,genint,refrnc
      character*26 vers

      common/unknwn/x,jacob
      common/vrsion/vers
      common/option/error,maxitr,prtitr,genint
      common/patch/stl,sa2,curr2,refrnc
      common/antena/sa,currnt
      common/time/itime1,itime2

      call timeon
c
c----version number
c             12345678901234567890123456
      vers = '1.3.6       August 4, 1988'

      yes='YES'
c
c----initialization
c
      call maceps
      call calcii
      call calcmx
c
c----read input variables
c
      call input
c
c----get antenna patch S-matrix
c
      if (refrnc.eq.yes) then
        call preprc
      endif
c
c----set up the nonlinear equations
c
      call genab
c
c----generate initial guess
c
      if (genint.eq.yes) then
```

```
        call geninx
      endif
c
c----print the input variables and the nonlinear equations
c
      call echo

      call timeck(itime1)
c
c----solve the equations
c
      call newton
c
c----print the result
c
      call disply
c
c----varify the compensation network
c
      call getcur
c
c
c
      stop
      end
c
c* * * * * * * * * * * * * * * * * * * * * * * * * * * * * * * * * * * * *
c
      subroutine input
c
c     read input data thru i/o unit 5
c
c* * * * * * * * * * * * * * * * * * * * * * * * * * * * * * * * * * * * *
c
      parameter (NE=8)

      complex*16 x(ne),jacob(ne,ne),sa(ne,ne),currnt(ne)
      complex*16 g,gammag,sa2(ne,ne),curr2(ne),stl(2,2),sn,cn
      real error
      real*8 d2r,mag,ang,cmag,cphase,dang
      integer maxitr
      character*3 yes,prtitr,genint,refrnc
      character*5 polar,compl,coord
      common/unknwn/x,jacob
      common/genrtr/g,gammag
      common/antena/sa,currnt
      common/netwrk/sn,cn
      common/option/error,maxitr,prtitr,genint
      common/patch/stl,sa2,curr2,refrnc

      d2r = 3.141592654 / 180.0
      yes='YES'
      polar = 'POLAR'
      compl = 'RECTA'

c
c----read in the options
c
      read(5,10) prtitr,maxitr,error
   10 format(a3/i4/f8.5)
c
c----initial guess
c
      read(5,30) genint
 30   format(a3)
      if (genint.ne.yes) then
        read(5,40) (x(i),i=1,NE-1)
 40     format(2f10.5)
      endif
c
c----generator
c
      read(5,40) g
      read(5,40) gammag
      sn=gammag
```

```
      cn=(1.0,0.0)
      x(NE) = g
c
c----antenna feed lines
c
      read(5,50) refrnc
   50 format(a3)
      if (refrnc.eq.yes) then
        read (5,40) ((stl(i,j),j=1,2),i=1,2)
      endif
c
c----antenna s-matrix
c
      read(5,40) ((sa(i,j),j=1,NE),i=1,NE)
c
c----desired current
c
      read(5,60) coord
   60 format(a5)
      if(coord.eq.polar) then
        do 100 i=1,NE
          read(5,40) mag,ang
          currnt(i) = dcmplx(mag*dcos(ang*d2r),mag*dsin(ang*d2r))
  100   continue
      else
        read(5,40) (currnt(i),i=1,NE)
      endif
c
c----calculte the initial guess for the Generator
c
      if (cdabs(x(NE)).le.1.0d-05) then
        cmag = cdabs(currnt(1))
        cphase = dble(phase(currnt(1)))* d2r
        dang = 3.141592654/4.0*level-cphase
        x(ne)=dcmplx(cmag*dcos(dang),cmag*dcos(dang))
      endif
      return
      end
c
c* * * * * * * * * * * * * * * * * * * * * * * * * * * * * * * * * * * *
c
      subroutine preprc
c
c    calculate S-matrix of elements without feed lines
c    see Section 2.5
c
c* * * * * * * * * * * * * * * * * * * * * * * * * * * * * * * * * * * *
c
      parameter (NE=8)

      complex*16 sa(ne,ne),sap(ne,ne),currnt(ne)
      complex*16 curr2(ne),sa2(ne,ne),stl(2,2),one
      character*3 refrnc
      common/antena/sa,currnt
      common/patch/stl,sa2,curr2,refrnc

      one=(1.0,0.0)

c
c----make a copy of Antenn S-matrix
c
      do 100 i=1,ne
         do 110 j=1,ne
            sa2(i,j)=sa(i,j)
  110    continue
  100 continue
c
c----iterate from i=1 to NE
c
      do 200 i=1,ne
c
c----calcualte S'(i,i)
c
        sap(i,i) = (sa2(i,i)-stl(1,1))/
     &  (stl(2,2)*(sa2(i,i)-stl(1,1))+stl(1,2)*stl(2,1))
```

```
c
c----calculate S'(i,j) and S'(j,i) for j=1 to NE except j=i
c
        do 210 j=1,ne
          if (j.ne.i) then
            sap(i,j)=sa2(i,j)*(one-stl(2,2)*sap(i,i))/stl(1,2)
            sap(j,i)=sa2(j,i)*(one-stl(2,2)*sap(i,i))/stl(2,1)
          endif
  210   continue
c
c----calculate S'(j,k)
c
        do 220 j=1,ne
          do 221 k=1,ne
            if ((j.ne.i).and.(k.ne.i)) then
     &        sap(j,k)=sa2(j,k)-stl(2,2)*sap(j,i)*sap(i,k)/
              (one-stl(2,2)*sap(i,i))
            endif
  221     continue
c
c----keep a copy of S'
c
  220   continue
        do 230 j=1,ne
          do 231 k=1,ne
            sa2(j,k)=sap(j,k)
  231     continue
  230   continue

  200 continue

      return
      end
c
c* * * * * * * * * * * * * * * * * * * * * * * * * * * * * * * * * * * * *
c
      subroutine geninx
c
c     generate initial guess to the solution
c
c* * * * * * * * * * * * * * * * * * * * * * * * * * * * * * * * * * * * *
c
      parameter (NE=8)
      complex*16 x(NE), jacob(NE),sa(NE,NE),currnt(NE), cdzero
      real*8 cmag(NE),cphase(NE),pmag(NE),pphase(NE),zero,one,dang
      integer level,ct
      common /unknwn/x,jacob
      common /antena/sa,currnt

      zero=0.0
      one=1.0
      cdzero = (0.0,0.0)
c
c----calculate the magnitude and the phase of required current
c
      do 100 i=1,NE
        cmag(i)=cdabs(currnt(i))
        cphase(i)=dble(phase(currnt(i)))*3.141592654/180.0
  100 continue
c
c----calculate the number of levels of power dividers necessary
c
      level = int(log(float(NE))/log(2.0)+0.5)
      ct=0
      do 200 i=1,level
        jend=NE/2**i
        do 210 j=1,jend
c
c----compute the magnitude and phase of initial guess
c
          kcomp1=(j-1)*2**i+1
          kcomp2=j*2**i-2**(i-1)+1
          if (cmag(kcomp2).ne.zero) then
            pmag(j+ct)=one/(one+(cmag(kcomp1)/cmag(kcomp2))**2)
            cmag(kcomp1)=cmag(kcomp1)/dsqrt(one-pmag(j+ct))
```

```
          else
            pmag(j+ct)=zero
          endif
          pphase(j+ct)=cphase(kcomp2)-cphase(kcomp1)
  210   continue
        ct=ct+jend
  200 continue
c
c----convert the initial guess in the rectangular coordinate form
c
      do 600 i=1,ne-1
        x(i)=dcmplx(pmag(i)*dcos(pphase(i)),pmag(i)*dsin(pphase(i)))
  600 continue
      return
      end
c
c* * * * * * * * * * * * * * * * * * * * * * * * * * * * * * * * * * * * *
c
      subroutine maceps
c
c     compute machine epsilon
c
c* * * * * * * * * * * * * * * * * * * * * * * * * * * * * * * * * * * * *
c
      real mcheps, sqreps
      common/macpar/ mcheps,sqreps
      mcheps = 1.0
 100  mcheps = mcheps / 2.0
        if (mcheps+1.0.gt.1.0) goto 100
      mcheps = mcheps * 2.0
      sqreps = sqrt(mcheps)
      return
      end
c* * * * * * * * * * * * * * * * * * * * * * * * * * * * * * * * * * * * *
c
      subroutine genab
c
c     generate a's and b's of antenna array
c     using eqns. (2.4-7) and (2.4-8)
c
c* * * * * * * * * * * * * * * * * * * * * * * * * * * * * * * * * * * * *
c
      parameter (NE=8)

      complex*16 a(NE),b(NE),sa(NE,NE),currnt(NE),g,gammag
      complex*16 tempv(NE),tempm(NE,NE)
      complex*16 sa2(NE,NE),curr2(NE),stl(2,2),ap(NE),bp(NE)
      character*3 refrnc,yes

      common/waves/a,b
      common/genrtr/g,gammag
      common/antena/sa,currnt
      common/patch/stl,sa2,curr2,refrnc

      yes='YES'
c
c----summation of (sa*current)
c
      do 200 i=1,NE
         tempv(i)=(0.0,0.0)
         do 100 j=1,NE
            if (refrnc.eq.yes) then
               tempv(i)=tempv(i)+sa2(i,j)*currnt(j)
            else
               tempv(i)=tempv(i)+sa(i,j)*currnt(j)
            endif
 100     continue
 200  continue
c
c----[I-SA]
c
      do 400 i=1,NE
         do 300 j=1,NE
            if (refrnc.eq.yes) then
```

```
               tempm(i,j)=-sa2(i,j)
             else
               tempm(i,j)=-sa(i,j)
             endif
 300       continue
           tempm(i,i)=tempm(i,i)+(1.0,0.0)
 400   continue
c
c----tempm**(-1)*tempv
c
       call matsol (NE,tempv,tempm)
c
c----a=current+b
c
       do 500 i=1,NE
         b(i)=tempv(i)
         a(i)=currnt(i)+b(i)
         if (refrnc.eq.yes) then
           ap(i)=a(i)
           bp(i)=b(i)
           a(i)=(ap(i)-stl(2,2)*bp(i))/stl(2,1)
           b(i)=stl(1,1)*a(i)+stl(1,2)*bp(i)
           curr2(i)=currnt(i)
           currnt(i)=a(i)-b(i)
         endif
   500 continue
       return
       end
c
c* * * * * * * * * * * * * * * * * * * * * * * * * * * * * * * * * * * * *
c
       subroutine echo
c
c      echo the input file
c
c* * * * * * * * * * * * * * * * * * * * * * * * * * * * * * * * * * * * *
c
       parameter (NE=8)
       complex*16 x(NE),jacob(NE,NE),a(NE),b(NE)
       complex*16 g,gammag,sa(NE,NE),currnt(NE)
       complex*16 sa2(NE,NE),curr2(NE),stl(2,2)
       complex*16 sc(NE+1,NE+1)
       real error
       integer maxitr
       character*3 prtitr,genint,refrnc,yes
       character*26 vers

       common/unknwn/x,jacob
       common/netwrk/sn,cn
       common/waves/a,b
       common/genrtr/g,gammag
       common/antena/sa,currnt
       common/option/error,maxitr,prtitr,genint
       common/macpar/mcheps,sqreps
       common/vrsion/vers
       common/patch/stl,sa2,curr2,refrnc

       yes='YES'
       write(6,10) vers
  10   format(' ****** SANE-PODCON *****     Version : ',A26,//)
       write(6,20) prtitr,error,maxitr
  20   format(' Iteration dump = ',A3/
      &       ' Error for the norm of system = ',E12.5/
      &       ' Maximum number of iterations = ',I4)
       write(6,30) mcheps
  30   format(' Machine Epsilon = ',E12.5)
c
c----initial guess
c
       if (genint.eq.yes) then
          write(6,40)
    40    format(' Initial guess were calculated.')
       else
          write(6,45)
    45    format(' Initial guess were inputted.')
```

```
      endif
      write(6,50)
   50 FORMAT('-     The initial guess for the solution vector')
      write(6,60) (i,x(i),cdabs(x(i)),phase(x(i)),i=1,NE)
   60 format(3X,'X(',I2,') = (',E12.5,',',E12.5,') = ',F8.5,'/',F8.3,/
     &      ,'+',48x,'_________')
      write(6,70) NE,gammag,cdabs(gammag),phase(gammag)
   70 format(//,15X,'---- Network Parameter ----'/
     &       ' The antenna network containes ',I3,' elements'/
     &       ' reflection coefficient of the generator = (',E12.5,',',
     &       E12.5,') = ',f8.5,'/',f8.3/,'+',80x,'_________',//
     &       ' The S-matrix of the antenna array')
      do 85 i=1,NE
         write(6,80) (sa(i,j),j=1,NE)
   80    format(3x,8('(',f5.3,',',f5.3,')  '))
   85 continue

      call calcsc(sc,x)
      write(6,200)
  200 format(//,' The S-matrix of initial feed network')
      do 210 i=1,ne+1
        write(6,220) (Sc(i,j),j=1,ne+1)
  220   format(3x,9('(',f5.3,',',f5.3,')'))
  210 continue
      write(7,230) ((sc(i,j),i,j,j=1,NE+1),i=1,NE+1)
  230 format(2f10.5,'   Power Divider Feed ',il,',',il)
      if (refrnc.eq.yes) then
        write(6,90)
   90   format(//' The desired currents at the patch edges ')
        write(6,100) (i,currnt(i),cdabs(currnt(i)),phase(currnt(i)),
     &  i=1,ne)
  100   format('   I(',i2,') = (',el2.5,',',el2.5,') = ',f8.5,'/',f8.3,/
     &  ,'+',48x,'_________')
        write(6,110)
  110   format(//' The desired currents at the reference plane ')
        write(6,100) (i,curr2(i),cdabs(curr2(i)),phase(curr2(i)),i=1,NE)
      else
        write(6,120)
  120   format(//,' The desired currents')
        write(6,100) (i,currnt(i),cdabs(currnt(i)),
     &  phase(currnt(i)),I=1,NE)
      endif
      return
      end
c
c* * * * * * * * * * * * * * * * * * * * * * * * * * * * * * * * * * * *
c
      subroutine calcf(f,x)
c     calculate the nonlinear equations (6.3-6)
c
c* * * * * * * * * * * * * * * * * * * * * * * * * * * * * * * * * * * *
c
      parameter(NE=8)
      complex*16 f(NE),x(NE),felmt,a(NE),b(NE),sn,cn,zl,sc(NE+1,NE+1)

      common/netwrk/sn,cn
      common/waves/a,b
c
c----get scattering matrix of compensation network
c
      call calcsc(sc,x)
c
c----calculate equation (6.3-6)
c
      do 100 i=1,ne
        zl = 0.0
        felmt = -a(i)
        do 110 j=1,ne
          felmt = felmt + sc(i,j)*b(j)
          zl = zl - sc(ne+1,j)*b(j)
  110   continue
        f(i) = felmt + sc(i,ne+1)*(cn*x(ne)+sn*zl)
  100 continue
      return
      end
```

```
c
c* * * * * * * * * * * * * * * * * * * * * * * * * * * * * * * * * * * * *
c
      function felemt(i,x)
c
c     calculate i-th nonlinear equation
c
c* * * * * * * * * * * * * * * * * * * * * * * * * * * * * * * * * * * * *
c
      parameter (NE=8)

      complex*16 x(NE),a(NE),b(NE),sn,cn,zl
      complex*16 felemt,sc(NE+1,NE+1)
      common/netwrk/sn,cn
      common/waves/a,b

      zl = 0.0
      call getsci(i,sc,x)
      felemt = -a(i)

      do 100 j=1,NE
        felemt = felemt + sc(i,j)*b(j)
        zl = zl - sc(NE+1,j)*b(j)
100   continue
      felemt = felemt + sc(i,NE+1)*(cn*x(NE)+sn*zl)
      return
      end
c
c* * * * * * * * * * * * * * * * * * * * * * * * * * * * * * * * * * * * *
c
      subroutine calcsc(sc,X)
c
c     calculate S-matrix of power divider compensation network
c
c* * * * * * * * * * * * * * * * * * * * * * * * * * * * * * * * * * * * *
c
      parameter (NE=8)
      common/iii/ii,mx
      complex*16 x(NE),sc(NE+1,NE+1),k(NE*2),p(NE*2),one,zero
      complex*16 sctemp,sctmp,plc,pld,piovr2
      integer i,j,l,m,lo,le,level
      integer il,jl,ii(NE,NE),mx(NE,NE)
      real*8 betalc,dzero

      one=(1.0,0.0)
      zero=(0.0,0.0)
      dzero = 0.0
      betalc = 3.141592654 / 4.0
      plc= cdexp(dcmplx(dzero,-betalc))
      pld= cdexp(dcmplx(dzero,-2.0*betalc))
      piovr2 = (0.0,1.0)
c
c----compute power ratio and phase shifts
c
      do 100 l=1,NE-1
        lo = (l-1)*2+1
        le = l*2
        k(le)=cdabs(x(l))
        if (k(le).ne.zero) then
          p(le)=x(l)/k(le)
        else
          p(le)=one
        endif
        k(lo)=one-k(le)
        p(lo)=one
 100  continue
      level=int(log(float(NE))/log(2.0)+0.5)
c
c----input port S-paramter
c
      sc(NE+1,NE+1)=zero
c
c----SCvi and SCv  in (6.2-6)
c
      do 200 i=1,NE
```

```
        sctemp=one
        do 210 l=1,level
          il=ii(i,l)
          sctemp=sctemp*cdsqrt(k(il))*p(il)*plc*piovr2
  210   continue
        sc(i,NE+1)=sctemp
        sc(NE+1,i)=sctemp
  200 continue
c
c----SC(i,i)
c
      do 300 i=1,NE
        sctemp=zero
        do 310 l=1,level
          il=ii(i,l)
          ll=il+mod(il,2)-mod(il+1,2)
          sctmp=k(ll)*p(il)*p(il)*pld
          ll=l-1
          do 320 ll=ll,1,-1
            il=ii(i,ll)
            sctmp=sctmp*k(il)*p(il)*p(il)*plc*plc*(-1.0,0.0)
  320     continue
          sctemp=sctemp+sctmp
  310   continue
        sc(i,i)=sctemp
  300 continue
c
c----SCii and SCiii in (6.2-6)
c
      ibgn=NE/2+1
      iend=NE
      do 400 i=ibgn,iend
        do 410 j=1,NE/2
          sctemp=one
          sctmp=one
          do 420 l=1,level
            il=ii(i,l)
            jl=ii(j,l)
            sctemp=sctemp*k(il)*k(jl)
            sctmp=sctmp*p(il)*p(jl)*plc*plc*(-1.0,0.0)
  420     continue
          sc(i,j)=cdsqrt(sctemp)*sctmp
          sc(j,i)=sc(i,j)
  410   continue
  400 continue
c
c----SCi in (6.2-6)
c
      iend=NE/2-1
      do 500 i=1,iend
        jbgn=i+1
        jend=NE/2
        do 510 j=jbgn,jend
          lbgn=mx(i,j)
          il=ii(i,lbgn)
          jl=ii(j,lbgn)
          sctmp=-cdsqrt(k(il)*k(jl))*p(il)*p(jl)*pld
          mend=lbgn-1
          do 520 m=1,mend
            il=ii(i,m)
            jl=ii(j,m)
            sctmp=sctmp*cdsqrt(k(il)*k(jl))*p(il)*p(jl)*plc*plc*(-1.0,0)
  520     continue
          sctemp=sctmp
          lbgn=lbgn+1
          do 530 l=lbgn,level
            il=ii(i,l)
            ll=il+mod(il,2)-mod(il+1,2)
            sctmp=k(ll)*p(il)*p(il)*pld
            mend=l-1
            do 540 m=1,mend
              il=ii(i,m)
              jl=ii(j,m)
              sctmp=sctmp*cdsqrt(k(il)*k(jl))*p(il)*p(jl)*plc*plc*(-1.0)
  540       continue
```

```
            sctemp=sctemp+sctmp
  530     continue
          sc(i,j)=sctemp
          sc(j,i)=sctemp
  510   continue
  500 continue
c
c----SCiv in (6.2-6)
c
      iend=NE-1
      do 600 i=NE/2+1,iend
        jbgn=i+1
        jend=NE
        do 610 j=jbgn,jend
          lbgn=mx(i-NE/2,j-NE/2)
          il=ii(i,lbgn)
          jl=ii(j,lbgn)
          sctmp=-cdsqrt(k(il)*k(jl))*p(il)*p(jl)*pld
          mend=lbgn-1
          do 620 m=1,mend
            il=ii(i,m)
            jl=ii(j,m)
            sctmp=sctmp*cdsqrt(k(il)*k(jl))*p(il)*p(jl)*plc*plc*(-1.0)
  620     continue
          sctemp=sctmp
          lbgn=lbgn+1
          do 630 l=lbgn,level
            il=ii(i,l)
            ll=il+mod(il,2)-mod(il+1,2)
            sctmp=k(ll)*p(il)*p(il)*pld
            mend=l-1
            do 640 m=1,mend
              il=ii(i,m)
              jl=ii(j,m)
              sctmp=sctmp*cdsqrt(k(il)*k(jl))*p(il)*p(jl)*plc*plc*(-1.0)
  640       continue
            sctemp=sctemp+sctmp
  630     continue
          sc(i,j)=sctemp
          sc(j,i)=sctemp
  610   continue
  600 continue
      return
      end
c
c* * * * * * * * * * * * * * * * * * * * * * * * * * * * * * * * * * * * *
c
      subroutine getsci(i,sc,X)
c
c     get i-th row of compensation network S-matrix
c
c* * * * * * * * * * * * * * * * * * * * * * * * * * * * * * * * * * * * *
c
      parameter (NE=8)
      common/iii/ii,mx
      complex*16 x(NE),sc(NE+1,NE+1),k(NE*2),p(NE*2),one,zero
      complex*16 sctemp,sctmp,plc,pld,piovr2
      real*8 betalc,dzero
      integer i,j,l,m,lo,le,level
      integer il,jl,ii(NE,NE),mx(NE,NE)

      one=(1.0,0.0)
      zero=(0.0,0.0)
      dzero = 0.0
      piovr2 = (0.0,1.0)
      betalc = 3.141592654 / 4.0
      plc= cdexp(dcmplx(dzero,-betalc))
      pld= cdexp(dcmplx(dzero,-2.0*betalc))
c
c----compute power ratio and phase shifts
c
      do 100 l=1,NE-1
         lo = (l-1)*2+1
         le = l*2
         k(le)=cdabs(x(l))
```

```
         if (k(le).ne.zero) then
            p(le)=x(l)/k(le)
         else
            p(le)=one
         endif
         k(lo)=one-k(le)
         p(lo)=one
 100  continue
      level=int(log(float(NE))/log(2.0)+0.5)
c
c---SC(i,NE) and SC(NE,i)
c
      do 200 j=1,ne
        sctemp=one
        do 210 l=1,level
          jl=ii(j,l)
          sctemp=sctemp*cdsqrt(k(jl))*p(jl)*plc*piovr2
  210   continue
        sc(j,ne+1)=sctemp
        sc(ne+1,j)=sctemp
  200 continue
c
c----SC(NE+1,NE+1)
c
      if (i.gt.ne) then
        sc(NE+1,NE+1)=zero
      else
c
c----SC(i,i)
c
        sctemp=zero
        do 300 l=1,level
          il=ii(i,l)
          ll=il+mod(il,2)-mod(il+1,2)
          sctmp=k(ll)*p(il)*p(il)*pld
          ll=l-1
          do 310 ll=ll,1,-1
            il=ii(i,ll)
            sctmp=sctmp*k(il)*p(il)*p(il)*plc*plc*(-1.0)
  310     continue
          sctemp=sctemp+sctmp
  300   continue
        sc(i,i)=sctemp
c
c----SCii and SCiii in (6.2-6)
c
        if (i.ge.ne/2+1) then
          jbgn=1
          jend=NE/2
        else
          jbgn=NE/2+1
          jend=NE
        endif
        do 400 j=jbgn,jend
          sctemp=one
          sctmp=one
          do 410 l=1,level
            il=ii(i,l)
            jl=ii(j,l)
            sctemp=sctemp*k(il)*k(jl)
            sctmp=sctmp*p(il)*p(jl)*plc*plc*(-1.0)
  410     continue
          sc(i,j)=cdsqrt(sctemp)*sctmp
  400   continue
c
c----SCi in (6.2-6)
c
        if (i.le.NE/2) then
          do 500 j=1,NE/2
            if (i.ne.j) then
              lbgn=mx(i,j)
              il=ii(i,lbgn)
              jl=ii(j,lbgn)
              sctmp=-cdsqrt(k(il)*k(jl))*p(il)*p(jl)*pld
              mend=lbgn-1
```

```
              do 510 m=1,mend
                il=ii(i,m)
                jl=ii(j,m)
                sctmp=sctmp*
     &          cdsqrt(k(il)*k(jl))*p(il)*p(jl)*plc*plc*(-1.0)
  510         continue
              sctemp=sctmp
              lbgn=lbgn+1
              do 520 l=lbgn,level
                il=ii(i,l)
                ll=il+mod(il,2)-mod(il+1,2)
                sctmp=k(ll)*p(il)*p(il)*pld
                mend=l-1
                do 530 m=1,mend
                  il=ii(i,m)
                  jl=ii(j,m)
                  sctmp=sctmp*
     &            cdsqrt(k(il)*k(jl))*p(il)*p(jl)*plc*plc*(-1.0)
  530           continue
                sctemp=sctemp+sctmp
  520         continue
              sc(i,j)=sctemp
              sc(j,i)=sctemp
            endif
  500     continue
        else
c
c----SCiv in (6.2-6)
c
          do 600 j=NE/2+1,NE
            if (j.ne.i) then
              lbgn=mx(i-NE/2,j-NE/2)
              il=ii(i,lbgn)
              jl=ii(j,lbgn)
              sctmp=-cdsqrt(k(il)*k(jl))*p(il)*p(jl)*pld
              mend=lbgn-1
              do 610 m=1,mend
                il=ii(i,m)
                jl=ii(j,m)
                sctmp=sctmp*
     &          cdsqrt(k(il)*k(jl))*p(il)*p(jl)*plc*plc*(-1.0)
  610         continue
              sctemp=sctmp
              lbgn=lbgn+1
              do 620 l=lbgn,level
                il=ii(i,l)
                ll=il+mod(il,2)-mod(il+1,2)
                sctmp=k(ll)*p(il)*p(il)*pld
                mend=l-1
                do 630 m=1,mend
                  il=ii(i,m)
                  jl=ii(j,m)
                  sctmp=sctmp*
     &            cdsqrt(k(il)*k(jl))*p(il)*p(jl)*plc*plc*(-1.0)
  630           continue
                sctemp=sctemp+sctmp
  620         continue
              sc(i,j)=sctemp
              sc(j,i)=sctemp
            endif
  600     continue
        endif
      endif
      return
      end
c
c* * * * * * * * * * * * * * * * * * * * * * * * * * * * * * * * * * * * * * *
c
      subroutine calcii
c
c     calculate index system used in power divider network
c
c* * * * * * * * * * * * * * * * * * * * * * * * * * * * * * * * * * * * * * *
c
      parameter (NE=8)
```

```
      common/iii/ii,mx
      integer ii(ne,ne),mx(ne,ne),level

      level=int(log(float(NE))/log(2.0)+0.5)
      icount=(NE-1)*2
      do 100 l=level,1,-1
        do 110 i=1,NE
          ii(i,l)=icount-(ne-i)/(2**(l-1))
  110   continue
        icount=icount-NE/(2**(l-1))
  100 continue
      return
      end
c
c* * * * * * * * * * * * * * * * * * * * * * * * * * * * * * * * * * * * *
c
      subroutine calcmx
c
c     calculate index system used in power divider network
c
c* * * * * * * * * * * * * * * * * * * * * * * * * * * * * * * * * * * * *
c
      parameter (NE=8)

      integer ii(NE,NE),mx(NE,NE),level
      common/iii/ii,mx

      level=int(log(float(NE))/log(2.0)+0.5)

      do 100 k=level,2,-1
        jbgn=2**k/4+1
        jend=2**k/2
        istep=2**(k-1)
        do 110 i=1,ne/2,istep
          lbgn=i
          lend=i+(jend-jbgn)
          do 120 l=lbgn,lend
            do 130 j=jbgn,jend
              mx(l,j+i-1)=k-1
              mx(j+i-1,l)=k-1
 130        continue
 120      continue
 110    continue
 100  continue
      return
      end
c
c* * * * * * * * * * * * * * * * * * * * * * * * * * * * * * * * * * * * *
c
      subroutine caljac
      parameter(NE=8)
c
c     calculate Jacobian of the nonlinear equations
c
c* * * * * * * * * * * * * * * * * * * * * * * * * * * * * * * * * * * * *
c
      complex*16 x(NE),jacob(NE,NE)
      complex*16 f(NE),rtempx(NE),itempx(NE)
      real*8 restep,imstep,retemp,imtemp,rejac,imjac,zero,typx
      real mcheps,sqreps
      common/unknwn/x,jacob
      common/macpar/machep,sqreps

c
c----save current solution
c
      zero=0.0
      typx=0.01
      call calcf(f,x)
      do 1000 i=1,NE
        rtempx(i)=x(i)
        itempx(i)=x(i)
 1000 continue
c
```

```
c----use finite difference in real part
c
      do 2000 j=1,NE
        if (dabs(dreal(x(j))).gt.typx) then
          restep=dreal(x(j))*sqreps
          retemp=dreal(x(j))+restep
          restep=retemp-dreal(x(j))
        else
          restep=dsign(typx,dreal(x(j)))*sqreps
        endif
        rtempx(j)=x(j)+dcmplx(restep)
c
c----use finite difference in imaginary part
c
        if (dabs(dimag(x(j))).gt.typx) then
          imstep=dimag(x(j))*sqreps
          imtemp=dimag(x(j))+imstep
          imstep=imtemp-dimag(x(j))
        else
          imstep=dsign(typx,dimag(x(j)))*sqreps
        endif
        itempx(j)=x(j)+dcmplx(zero,imstep)
c
c----estimate Jacobian
c
        do 2100 i=1,NE
          rejac=(dreal(felemt(i,rtempx)-f(i)))/restep
          imjac=(dreal(felemt(i,itempx)-f(i)))/imstep
          jacob(i,j)=dcmplx(rejac,-imjac)
 2100   continue
        rtempx(j)=x(j)
        itempx(j)=x(j)
 2000 continue
      return
      end
c
c* * * * * * * * * * * * * * * * * * * * * * * * * * * * * * * * * * * * *
c
      subroutine newton
c
c     modifined newton's method driver
c
c* * * * * * * * * * * * * * * * * * * * * * * * * * * * * * * * * * * * *
c
      parameter (NE=8)
      complex*16 x(NE),jacob(NE,NE),deltax(NE),f(NE)
      real error, norm, phase
      integer maxitr, iter
      character*3 yes, prtitr, genint
      logical alphok

      common/unknwn/x,jacob
      common/option/error,maxitr,prtitr,genint
      common/dpinfo/reslop,alphok,deltax,f
      common/result/iret,iter
c
c----initialize
c
      iret=0
      iter=1
c
c----is error less than specified
c
  100 call calcf(f,x)
      checkv=dnorm(f,ne)
      if(checkv.lt.error) goto 999
      if(iter.ne.1.and.prtitr.eq.'YES') then
        write(6,10) iter, checkv, alpha
   10   format(' iteration:',i4,3x,'norm = ',e12.5,3x,'alpha = ',e12.5)
      endif
c
c----get Jacobian
c
      call caljac
c
```

```
c----get next step
c
      do 200 i=1,ne
         deltax(i)=-f(i)
  200 continue
c
c----solve
c
      call matsol(ne,deltax,jacob)
c
c----get damping factor
c
      call damped(alpha)
c
c----compute next estimation to the solution
c
      do 300 i=1,ne
         x(i)=x(i)+alpha*deltax(i)
         if ((i.ne.NE).and.(dcabs(x(i)).gt.1.0)) iret=2
  300 continue
c
c----show the result of this iteration
c
      write(10,20) iter, checkv, alpha
   20 format(' iteration:',i4,3x,'norm = ',e12.5,3x,'alpha = ',e12.5)
      write(10,21) x(ne)
   21 format(2e12.5)
      if (iret.eq.2) then
         write(10,30)
   30    format(' abs(x(i)) > 1.   Program terminated ')
         goto 999
      endif
c
c----is iteration less than max
c
      iter = iter + 1
      if (iter.lt.maxitr) goto 100
      iret=1
  999 return
      end
c
c* * * * * * * * * * * * * * * * * * * * * * * * * * * * * * * * * * * * *
c
      subroutine damped(alpha)
c
c     compute damping factor alpha
c
c* * * * * * * * * * * * * * * * * * * * * * * * * * * * * * * * * * * * *
c
      parameter (NE=8)

      real landa, u, l, minalp, norm, leftsd, rigtsd, lf, insqrt
      logical alphok
      complex*16 x(NE),jacob(NE,NE),xtemp(NE),deltax(NE),f(NE),ftemp(NE)
      complex*16 tempj,inslop

      common/unknwn/x,jacob
      common/dpinfo/reslop,alphok,deltax,f
c
c----initialize
c
      alpha=1.0
      landa=1.0e-02
      u=0.5
      l=0.1
      fo=lf(f)
      alphok=.true.
      it=0
      inslop=(0.0,0.0)
c
c----compute
c
      do 15 i=1,NE
         tempj=(0.0,0.0)
         do 10 j=1,NE
```

```
            tempj=tempj+conjg(f(j))*jacob(j,i)
   10     continue
          inslop=inslop+tempj*deltax(i)
   15   continue
        reslop = real(inslop)
   20   do 30 i=1,NE
          xtemp(i)=x(i)+alpha*deltax(i)
   30   continue
        call calcf(ftemp,xtemp)
        fprev=lf(ftemp)
        if (fprev.lt.fo+alpha*landa*reslop) return
        if (alpha.lt.1.0e-05) then
          alphok=.false.
          return
        endif
        altemp=-reslop/(2*(fprev-fo-reslop))
        alprev=alpha
        f2prev=fprev
        if (altemp.lt.0.1*alpha) then
          alpha=0.1*alpha
        else
          alpha=altemp
        endif
        it=it+1
        if (it.lt.10) goto 20
        alphok=.false.
        return
        end
c
c* * * * * * * * * * * * * * * * * * * * * * * * * * * * * * * * * * * * * *
c
        subroutine getcur
c
c       compute the compensated currents for verification
c
c* * * * * * * * * * * * * * * * * * * * * * * * * * * * * * * * * * * * * *
c
        parameter (NE=8)

        complex*16 x(NE),jacob(NE,NE),sa(NE,NE),currnt(NE)
        complex*16 g,gammag,sa2(NE,NE),curr2(NE),stl(2,2),sc(NE+1,NE+1)
        complex*16 cnt(NE), snt(NE,NE),temps(NE*2,NE*2),tempc(NE*2)
        complex*16 calcur(NE), ap(NE), bp(NE)
        character*3 refrnc, yes

        common/unknwn/x,jacob
        common/genrtr/g,gammag
        common/antena/sa,currnt
        common/patch/stl,sa2,curr2,refrnc

        yes = 'YES'
c
c----initialize tempc and temps to zero
c
        do 100 i=1,NE*2
          tempc(i) = (0.0,0.0)
          do 110 j=1,NE*2
            temps(i,j) = (0.0,0.0)
  110     continue
  100   continue
c
c----get sn and cn of the compensation network
c
        call calcsc(sc,x)
        do 200 i=1,NE
          cnt(i) = x(NE) * sc(i,NE+1)
          do 210 j=1,NE
            snt(i,j) = sc(i,j)+gammag*sc(i,NE+1)*sc(NE+1,j)
  210     continue
  200   continue
c
c----set up the matrix equation describing the entire network
c
        do 300 i=1,NE
          tempc(i) = cnt(i)
```

```
        do 310 j=1,NE
          temps(i+NE,J+NE) = -sa(i,j)
          temps(i,j) = -snt(i,j)
  310   continue
        temps(i,NE+i) = (1.0,0.0)
        temps(NE+i,i) = (1.0,0.0)
  300 continue
      ne2 = NE*2
      call matsol(ne2,tempc,temps)
      do 400 i=1,NE
        calcur(i) = tempc(i+NE)-tempc(i)
  400 continue
      write(6,20)
   20 format(//' The calculated currents at the reference plane ')
      do 500 i=1,NE
        write(6,10) i,calcur(i),dcabs(calcur(i)),phase(calcur(i))
   10   format(3x,'I(',i2,') = (',F10.5,',',F10.5,') = ',
     &          F10.5,' / ',F10.5)
  500 continue
      if (refrnc.eq.yes) then
        do 600 i=1,NE
          bp(i) = (tempc(i)-stl(1,1)*tempc(NE+i))/stl(1,2)
          ap(i) = stl(2,1)*tempc(NE+i)+stl(2,2)*bp(i)
          calcur(i) = ap(i)-bp(i)
  600   continue
        write(6,30)
   30   format(//' The calculated currents at the patch edges ')
        do 700 i=1,NE
          write(6,10) i,calcur(i),dcabs(calcur(i)),phase(calcur(i))
  700   continue
      endif
      return
      end
c
c* * * * * * * * * * * * * * * * * * * * * * * * * * * * * * * * * * * * *
c
      subroutine disply
c
c     output the results
c
c* * * * * * * * * * * * * * * * * * * * * * * * * * * * * * * * * * * * *
c
      parameter (NE=8)

      complex*16 x(NE), jacob(NE,NE),sc(NE+1,NE+1)
      common/unknwn/x,jacob
      common/result/iret,iter
      common/time/itime1,itime2

      write(6,4)
    4 format('1    --- RESULT ----'///)
      if (iret.eq.0) then
         write(6,5) iter
    5    format(' Program was successful.  Number of iteration = ',i4)
      else
         write(6,6) iret
    6    format(' program was unsuccessful.   iret = ',i1)
      endif
      call timeck(itime2)
      rtime = float(itime2-itime1) / 100.0
      write(6,7) rtime
    7 format(/'CPU time = ',f6.2,' seconds ' )
      write(6,10)
   10 format('-The required power divider specification '/)
      write(6,20) (i,x(i),cdabs(x(i)),phase(x(i)),i=1,ne-1)
   20 format(5x,'X(',i2,') = (',e12.5,',',e12.5,') = ',f8.5,'/',f8.3,/,
     &       '+',50X,'_________')
      write(6,40) x(NE),cdabs(x(NE)),phase(x(NE))
   40 format(/'  Generator = ',f8.5,',',f8.5,' = ',f8.5,'/',f8.3,/,
     &        '+',41X,'_________')
      call calcsc(sc,x)
      write(6,200)
  200 format(//,' The S-matrix of modified feed network')
      do 210 i=1,ne+1
        write(6,220) (SC(i,j),j=1,ne+1)
```

```
  220   format(3x,9('(',f5.3,',',f5.3,') '))
  210 continue
      write(8,230) ((sc(i,j),i,j,j=1,NE+1),i=1,NE+1)
  230 FORMAT(2f10.5,'   Power Divider Feed ',il,',',il)
      call timeck(itime2)
      rtime = float(itime2) / 100.0
      write(6,240) rtime
  240 format(///' Total CPU time = ',f6.2,' seconds ')
      return
      end
c
c* * * * * * * * * * * * * * * * * * * * * * * * * * * * * * * * * * * *
c
      real function lf(f)
c
c     norm squared
c
c* * * * * * * * * * * * * * * * * * * * * * * * * * * * * * * * * * * *
c
      parameter (NE=8)

      complex*16 f(NE)
      lf=0.0
      do 10 i=1,NE
         lf=lf+f(i)*conjg(f(i))
   10 continue
      lf=0.5*lf
      return
      end
c
c* * * * * * * * * * * * * * * * * * * * * * * * * * * * * * * * * * * *
c
      real function dnorm (vector,n)
c
c     double percision norm
c
c* * * * * * * * * * * * * * * * * * * * * * * * * * * * * * * * * * * *
c
      complex*16 vector(n)
      real*8 temp

      temp=0.0
      do 100 i=1,n
        temp=cdabs(vector(i))**2+temp
  100 continue
      dnorm=dsqrt(temp)
      return
      end
c
c* * * * * * * * * * * * * * * * * * * * * * * * * * * * * * * * * * * *
c
      subroutine matsol (n,b,pass)
c
c----matrix equation solver
c
c* * * * * * * * * * * * * * * * * * * * * * * * * * * * * * * * * * * *
c
      parameter (NE=8)
      complex*16 pass(4*NE*NE),a(2*NE,2*NE),temp,b(2*NE)
      real di,max
      integer ipivot(2*ne-1),n
c
c----transfers the information in the vector pass to the matrix a
c
      do 100 i=1,n
        do 110 j=1,n
          a(j,i)=pass((i-1)*n+j)
  110   continue
  100 continue
c
c----factor the matrix into an upper triangular matrix using
c    implicit pivoting.
c
      do 200 k=1,n-1
c
```

```
c----perform the implicit pivoting
c
        max=0.0
        do 210 irow=k,n
          di=dcabs(a(irow,k))
          do 211 j=k+1,n
            if (di.lt.dcabs(a(irow,j))) di=dcabs(a(irow,j))
 211      continue
          if (dcabs(a(irow,k))/di.gt.max) then
            ipivot (k)=irow
            max=dcabs(a(irow,k))/di
          endif
 210    continue
c
c----swap the two rows
c
        do 220 i=k,n
          temp=a(k,i)
          a(k,i)=a(ipivot(k),i)
          a(ipivot(k),i)=temp
 220    continue
c
c----zero the k column
c
        do 230 i=k+1,n
          temp=-a(i,k)/a(k,k)
          a(i,k)=temp
          do 231 j=k+1,n
            a(i,j)=a(i,j)+temp*a(k,j)
 231      continue
 230    continue

 200  continue
c
c----establish the corresponding b vector
c
      do 300 k=1,n-1
c
c----pivot the b vector
c
        temp=b(k)
        b(k)=b(ipivot(k))
        b(ipivot(k))=temp
c
c----perform the row multiplications on b
c
        do 310 j=k+1,n
          b(j)=b(k)*a(j,k)+b(j)
 310    continue
 300  continue
c
c----backsolve for the solution vector
c
      b(n)=b(n)/a(n,n)
      do 400 ii=2,n
        i=n+1-ii
        temp=b(i)
        do 410 j=i+1,n
          temp=temp-b(j)*a(i,j)
 410    continue
        b(i)=temp/a(i,i)
 400  continue
      return
      end
c
c* * * * * * * * * * * * * * * * * * * * * * * * * * * * * * * * * * * * *
c
      function phase(x)
c
c     calculate phase of complex variable x in degrees
c
c* * * * * * * * * * * * * * * * * * * * * * * * * * * * * * * * * * * * *
c
      complex*16 x,zero
      real*8 r2d
```

```
      r2d=180.0/3.141592654
      zero=0.0

      if ((dreal(x).eq.zero).and.(dimag(x).eq.zero)) then
         phase=0.0
      else
         phase=sngl(datan2(dimag(x),dreal(x))*r2d)
      endif
      return
      end
c
c* * * * * * * * * * * * * * * * * * * * * * * * * * * * * * * * * * * * * *
c
      real function dcabs(x)
c
c     double percision complex absolute
c
c* * * * * * * * * * * * * * * * * * * * * * * * * * * * * * * * * * * * * *
c
      complex*16 x

      dcabs=sngl(cdabs(x))
      return
      end
```

The vita has been removed from the scanned document